THE
PHYSICAL REVIEW
A Journal of Experimental and Theoretical Physics Established by E. L. Nichols in 1893
VOL. 51, NO. 8 APRIL 15, 1937 SECOND SERIES

On the Structure of Light Nuclei

E. FEENBERG AND M. PHILLIPS*
Institute for Advanced Study, Princeton, New Jersey
(Received January 28, 1937)

Extensive calculations based on the approximation of single particle wave functions (the Hartree method) have been made for the nuclei between He^6 and O^{16} using the general symmetrical interaction operator given by Eq. (1). The Coulomb interaction is treated as a small perturbation. Secular equations are avoided by the construction of space wave functions in the normal state configuration belonging to irreducible representations of the symmetric group. These functions yield an energy matrix which is diagonal in the ordinary and Majorana interaction energies. The contributions of the spin exchange and Coulomb operators to the energy terms are found by a first-order perturbation calculation. Although the general symmetrical operator contains several parameters as yet undetermined, only those parameters which have been fixed by consideration of the two, three and four particle problems are involved in the energy differences within the group of low lying terms belonging to the normal state configuration. These term differences are identical with those recently computed for unsymmetrical interaction operators of the saturation type. New results for mass defects, excitation energies and energy relations between isobars are compared with experimental values.

I. INTRODUCTION

A THEORETICAL description of many nuclear properties is made possible by recent progress in the knowledge of nuclear forces. Extensive calculations based on the approximation of single particle wave functions (the Hartree method) have already been made[1] for the nuclei between He^6 and O^{16}. This method yields results for mass defects, excitation energies, energy relations between isobars, spins and magnetic moments which are on the whole very encouraging. In the present paper we present additional calculations based on the Hartree approximation for the same series of nuclei. Our procedure differs from that of reference 1 in two respects:

1. We employ throughout the general symmetrical interaction operator[2]

$$V=\sum_{i>j} V_{ij}=\sum_{i>j}\{(1-g-g_1-g_2)P_{ij}+gP_{ij}Q_{ij}+g_1 1+g_2 Q_{ij}\}J(r_{ij}), \quad (1)$$

which does not distinguish between like and unlike particle interactions. The Coulomb repulsion between protons is treated separately as a small perturbation. Although the general symmetrical operator contains several parameters as yet undetermined, only those parameters which have been fixed by consideration of the two, three and four particle problems are involved in the energy differences within the group of low lying levels. For the low terms, in fact, the separations are identical with those given by

* Margaret E. Maltby Fellow of the A. A. U. W.
[1] E. Feenberg and E. Wigner, Phys. Rev. **51**, 95 (1937).

[2] G. Breit and E. Feenberg, Phys. Rev. **50**, 850 (1936). The operators in Eq. (1) are defined by the equations

$$P_{ij}\psi(\cdots x_i s_i \cdots x_j s_j \cdots)=\psi(\cdots x_j s_i \cdots x_i s_j \cdots),$$
$$Q_{ij}\psi(\cdots x_i s_i \cdots x_j s_j \cdots)=\psi(\cdots x_i s_j \cdots x_j s_i \cdots).$$

the simple symmetrical Hamiltonian containing only Majorana and Heisenberg forces. From this circumstance it is apparent that the experimental excitation energies cannot be used to reduce the ambiguity which remains in the interaction operator after the restrictions imposed by the two, three and four particle problems have been taken into account.

2. We avoid secular equations by making use of the "correct" space wave functions belonging to the normal state configuration to construct an energy matrix which is diagonal in the ordinary and Majorana interaction energies. Because there is no spin-orbit interaction in Eq. (1) the total spin and the total orbital angular momentum are separately constants of the motion. If the Coulomb and spin exchange forces are neglected (Wigner's "first approximation")[3] the Hamiltonian commutes also with the permutation operators which interchange the space coordinates of two or more particles. Consequently, in this approximation, the space part of an eigenfunction belongs to an irreducible representation of the symmetric group and is characterized by a "partition" quantum number in addition to the orbital angular momentum quantum numbers.

The presence of Coulomb and spin exchange forces spoils the "partition" quantum number by mixing together functions belonging to different partitions. The contributions of the Coulomb and spin exchange energy operators to the energy matrix are small, however, and are given without sensible error by a first-order perturbation calculation in which the "partition" functions are used as zero-order wave functions. Ordinarily there is only one wave function belonging to the normal state configuration with a particular set of partition and angular momentum quantum numbers. Each set of quantum numbers is associated in this approximation with an energy term whose value is the expectation value of the Hamiltonian operator corresponding to the appropriate zero-order wave function. The resulting expressions for the term values are extremely simple. All the excitation energies computed from Eq. (1) can be expressed in terms of two integrals with simple rational (in most cases integral) coefficients.

In reference 1 the sets of functions with definite pairs of spin and orbital angular momentum quantum numbers were used to construct secular equations, often of the second and third order, for the energy terms. The linear combinations of these functions which diagonalize the energy matrix are identical with the partition wave functions so long as the Coulomb and spin exchange forces are neglected. If the contributions from these forces are included in the secular equations the correct linear combinations differ only slightly from the partition wave functions, and the energy values obtained from the two methods of calculation coincide except for negligible corrections.

[3] E. Wigner, Phys. Rev. **51**, 106 (1937).

II. Matrix Elements of the Interaction Energy Within the P Shell

That part of the energy arising from interactions between particles in the p shell can be expressed as a linear combination

$$E_p=\omega L+\gamma K \tag{2}$$

of the two integrals

$$L=\int\cdots\int x_1^2x_2^2R_p(r_1)^2R_p(r_2)^2J(r_{12})d\tau_1d\tau_2,$$
$$K=\int\cdots\int x_1x_2y_1y_2R_p(r_1)^2R_p(r_2)^2J(r_{12})d\tau_1d\tau_2, \tag{3}$$

in which $xR_p(r)$, $yR_p(r)$, $zR_p(r)$ are the normalized single particle wave functions. There exists a useful approximation in which the range of the forces is taken to be large in comparison with the size of the nucleus. In this approximation

$$L=J(0),\quad K=0. \tag{4}$$

Since for a given number of particles in the p shell the coefficient of L in the expression for a term value depends only on the quantum numbers, it is identical with the corresponding coefficient of $J(0)$ in the approximation of long range forces. This latter quantity can be determined directly from the number of particles and the quantum numbers without explicit use of the wave functions. For a nucleus with n particles in the p shell:

$$\begin{aligned}\omega(1)&=\tfrac{1}{2}n(n-1),\\ \omega(P)&=\tfrac{1}{2}n(n-1)\chi(P)/\chi(\mathcal{E}),\\ \omega(Q)&=\tfrac{1}{2}n(n-1)\chi'(Q)/\chi'(\mathcal{E}),\\ \omega(PQ)&=-\tfrac{1}{2}n(n-1)\chi''(R)/\chi''(\mathcal{E}).\end{aligned} \tag{5}$$

Here $\chi(P)$ and $\chi(\mathcal{E})$ are the characters corresponding to a transposition and the identity, respectively, in the irreducible representation of the symmetric group to which the space part of the wave function belongs. This also serves as a definition of the primed symbols if *spin* is substituted for *space;* for the double primed symbols substitute *isotopic spin* for *space*. The antisymmetry of the wave functions in the complete set of space, spin and isotopic spin coordinates[3-5] implies the relation $PQR=-1$ or $PQ=-R$. This relation has been used in writing the last line of Eq. (5).

The derivation of Eq. (5) for ordinary forces is trivial since there are $n(n-1)/2$ interaction terms and each contributes $J(0)$ to the total. For the exchange forces the derivation given in reference 1 (Eqs. (4)–(8)) is applicable to all three types of exchange if $J(r_{12})$ is replaced by $J(0)$ in Eqs. (4) and (5) and the coordinates $x_1, \cdots, x_n$ suitably interpreted as space, spin or isotopic spin coordinates as the case requires.

The values of $\chi(P)/\chi(\mathcal{E})$ for $2\leqq n\leqq 6$ are to be found in Table II, reference 1. To compute $\omega(P)$ for $6<n\leqq 12$ one may use the relation connecting the energy values corresponding to n particles in the p shell with those corresponding to $12-n$ particles. This relation is given by Eq. (9) of the present paper. The coefficients $\omega(Q)$ may be found directly by a straightforward computation:[6]

$$\begin{aligned}\omega(Q)&=\sum_{i>j}Q_{ij}=\tfrac{1}{2}\sum_{i>j}(1+\sigma_i\cdot\sigma_j)\\&=\tfrac{1}{4}n(n-1)-\tfrac{1}{4}\{\textstyle\sum\sigma_i{}^2-(\sum\sigma_i)^2\}\\&=S(S+1)+\tfrac{1}{4}n(n-4).\end{aligned}\tag{6}$$

Similarly

$$\omega(PQ)=\sum_{i>j}P_{ij}Q_{ij}=-T(T+1)-\tfrac{1}{4}n(n-4).\tag{7}$$

Here S is the total spin and T the total isotopic spin. The possible spin and isotopic spin values which can be associated with a given partition in the space coordinates are limited by the exclusion principle. The allowed quantum numbers can be found by a systematic procedure[3] which is merely an extension of the usual one for atomic spectra. This procedure is described in Appendix 2.

The coefficients of K vary from term to term within a partition. There exist, however, two relations connecting the coefficients of L and K which are independent of the quantum numbers:

$$\begin{aligned}\gamma(1)-\gamma(P)&=3\{\omega(1)-\omega(P)\},\\\gamma(Q)-\gamma(PQ)&=3\{\omega(Q)-\omega(PQ)\}.\end{aligned}\tag{8}$$

To prove Eq. (8) we examine the integral

$$\sum_1^3 a_{ij}b_{mn}\int\cdots\int x_{1i}x_{2j}R_p(r_1)R_p(r_2)\times J(r_{12})(1-P_{12})x_{1m}x_{2n}R_p(r_1)R_p(r_2)d\tau_1d\tau_2,$$

in which $x_{\alpha 1}=x_\alpha$, $x_{\alpha 2}=y_\alpha$, $x_{\alpha 3}=z_\alpha$, α takes the values 1 and 2 and the summation extends over i, j, m, n. The general quadratic tensor ($\sum_{ij}a_{ij}x_{1i}x_{2j}$ for example) may be written as the sum of two terms, one symmetric and the other antisymmetric in the subscripts 1 and 2. It is clear that the integral vanishes if either tensor is symmetric, so that the two tensors may be replaced by their antisymmetrical parts and the operator $(1-P_{12})$ by the factor 2. Thus the integral takes the form

$$\text{Constant}\times\int\cdots\int(x_1y_2-x_2y_1)x_1y_2R_p(r_1)^2\times R_p(r_2)^2J(r_{12})d\tau_1d\tau_2=\text{Constant}\times(L-3K).$$

This suffices to prove both parts of Eq. (8) since the presence of a spin exchange operator does not affect the argument.

The energy matrix for a configuration consisting of a closed p shell minus n particles is related to the corresponding matrix for the configuration p^n by the equations

$$\begin{aligned}(i|1|j)_{12-n}&=(j|1|i)_n+(6-n)(11L-18K)\delta_{ij},\\(i|P|j)_{12-n}&=(j|P|i)_n+(6-n)(L+12K)\delta_{ij},\\(i|Q|j)_{12-n}&=(j|Q|i)_n+(6-n)(4L-12K)\delta_{ij},\\(i|PQ|j)_{12-n}&=(j|PQ|i)_n\\&\quad+(6-n)(-4L+12K)\delta_{ij}.\end{aligned}\tag{9}$$

The states designated by the quantum numbers i and j may be any states of a p shell configuration subject to the conditions that their wave

[4] J. H. Bartlett, Phys. Rev. **49**, 102 (1936).
[5] B. Cassen and E. U. Condon, Phys. Rev. **50**, 846 (1936).
[6] P. A. M. Dirac, *Quantum Mechanics* (Oxford University Press, 1930) p. 215.

functions are orthogonal for $i \neq j$ and that the exclusion principle is satisfied.

The complete set of matrix elements of the interaction within the p shell for the "low" partitions together with the spin and isotopic spin quantum numbers is contained in Table I. Table II gives the same quantities for the partitions consisting of fours and two additional addends. The "partition" wave functions used in computing the energy matrix are discussed in Appendix 1.

Very often the matrix elements of Q and PQ can be found without explicit use of the spin functions. The interchange of ordinary and isotopic spin variables in the wave functions simply interchanges the spin and isotopic spin quantum numbers. Therefore the matrix elements of $PQ=-R$ are just the negatives of the corresponding matrix elements of Q with spin and isotopic spin interchanged. The low terms of the configuration p^5 will serve as an example. Since both quantum numbers have the value 1/2

TABLE I. *Matrix elements and quantum numbers within the group of low terms.*

						$\omega L+\gamma K$			
n	PARTITION	T	NUCLEUS	S	STATE	P	1	PQ	Q
2	2	0	Li^6	1	^3S	$L+2K$	$L+2K$	$L+2K$	$L+2K$
					^3D	$L-K$	$L-K$	$L-K$	$L-K$
2	2	1	He^6, Li^6, Be^6	0	^1S	$L+2K$	$L+2K$	$-L-2K$	$-L-2K$
					^1D	$L-K$	$L-K$	$-L+K$	$-L+K$
3	3	1/2	Li^7, Be^7	1/2	^2P	$3L+2K$	$3L+2K$	0	0
					^2F	$3L-3K$	$3L-3K$	0	0
4	4	0	Be^8	0	^1S	$6L+4K$	$6L+4K$	0	0
					^1D	$6L+K$	$6L+K$	0	0
					^1G	$6L-6K$	$6L-6K$	0	0
5	4+1	1/2	Be^9, B^9	1/2	^2P	$5L+9K$	$10L-6K$	$-2L+6K$	$2L-6K$
					^2D	$5L+7K$	$10L-8K$	$-2L+6K$	$2L-6K$
					^2F	$5L+4K$	$10L-11K$	$-2L+6K$	$2L-6K$
					^2G	$5L$	$10L-15K$	$-2L+6K$	$2L-6K$
6	4+2	0	B^{10}	1	^3S	$5L+16K$	$15L-14K$	$-3L+29K/2$	$5L-19K/2$
					$^3D_{\rm I}$	$5L+13K$	$15L-17K$	$-3L+13K$	$5L-11K$
					$^3D_{\rm II}$	$5L+13K$	$15L-17K$	$-3L+53K/5$	$5L-67K/5$
					^3F	$5L+10K$	$15L-20K$	$-3L+10K$	$5L-14K$
					^3G	$5L+6K$	$15L-24K$	$-3L+12K$	$5L-12K$
6	4+2	1	Be^{10}, B^{10}, C^{10}	0	^1S	$5L+16K$	$15L-14K$	$-5L+19K/2$	$3L-29K/2$
					$^1D_{\rm I}$	$5L+13K$	$15L-17K$	$-5L+11K$	$3L-13K$
					$^1D_{\rm II}$	$5L+13K$	$15L-17K$	$-5L+67K/5$	$3L-53K/5$
					^1F	$5L+10K$	$15L-20K$	$-5L+14K$	$3L-10K$
					^1G	$5L+6K$	$15L-24K$	$-5L+12K$	$3L-12K$
7	4+3	1/2	B^{11}, C^{11}	1/2	^2P	$6L+21K$	$21L-24K$	$-6L+18K$	$6L-18K$
					^2D	$6L+19K$	$21L-26K$	$-6L+18K$	$6L-18K$
					^2F	$6L+16K$	$21L-29K$	$-6L+18K$	$6L-18K$
					^2G	$6L+12K$	$21L-33K$	$-6L+18K$	$6L-18K$
8	4+4	0	C^{12}	0	^1S	$8L+28K$	$28L-32K$	$-8L+24K$	$8L-24K$
					^1D	$8L+25K$	$28L-35K$	$-8L+24K$	$8L-24K$
					^1G	$8L+18K$	$28L-42K$	$-8L+24K$	$8L-24K$
9	4+4+1	1/2	C^{13}, N^{13}	1/2	^2P	$6L+38K$	$36L-52K$	$-12L+36K$	$12L-36K$
					^2F	$6L+33K$	$36L-57K$	$-12L+36K$	$12L-36K$
10	4+4+2	0	N^{14}	1	^3S	$5L+50K$	$45L-70K$	$-15L+50K$	$17L-46K$
					^3D	$5L+47K$	$45L-73K$	$-15L+47K$	$17L-49K$
10	4+4+2	1	C^{14}, N^{14}, O^{14}	0	^1S	$5L+50K$	$45L-70K$	$-17L+46K$	$15L-50K$
					^1D	$5L+47K$	$45L-73K$	$-17L+49K$	$15L-47K$
11	4+4+3	1/2	N^{15}, O^{15}	1/2	^2P	$5L+60K$	$55L-90K$	$-20L+60K$	$20L-60K$
12	4+4+4	0	O^{16}	0	^1S	$6L+72K$	$66L-108K$	$-24L+72K$	$24L-72K$

TABLE II. *Matrix elements and quantum numbers for the partitions consisting of 4's and two additional addends.*

						$\omega L+\gamma K$			
n	PARTITION	T	NUCLEUS	S	STATE	P	1	PQ	Q
2	1+1	1	He^6, Li^6, Be^6	1	^3P	$-L+3K$	$L-3K$	$-L+3K$	$L-3K$
2	1+1	0	Li^6	0	^1P	$-L+3K$	$L-3K$	$L-3K$	$-L+3K$
3	2+1	3/2	He^7, Li^7, Be^7, B^7	1/2	^2P	$5K$	$3L-4K$	$-3L+4K$	$-5K$
					^2D	$3K$	$3L-6K$	$-3L+6K$	$-3K$
3	2+1	1/2	Li^7, Be^7	3/2	^4P	$5K$	$3L-4K$	$5K$	$3L-4K$
					^4D	$3K$	$3L-6K$	$3K$	$3L-6K$
3	2+1	1/2	Li^7, Be^7	1/2	^2P	$5K$	$3L-4K$	0	0
					^2D	$3K$	$3L-6K$	0	0
4	3+1	1	Li^8, Be^8, B^8	1	^3P	$2L+7K$	$6L-5K$	$-2L+6K$	$2L-6K$
					^3D	$2L+5K$	$6L-7K$	$-2L+6K$	$2L-6K$
					^3F	$2L+2K$	$6L-10K$	$-2L+6K$	$2L-6K$
4	3+1	1	Li^8, Be^8, B^8	0	^1P	$2L+7K$	$6L-5K$	$-2L+13K/2$	$\frac{1}{2}K$
					^1D	$2L+5K$	$6L-7K$	$-2L+K$	$-5K$
					^1F	$2L+2K$	$6L-10K$	$-2L+4K$	$-2K$
4	3+1	0	Be^8	1	^3P	$2L+7K$	$6L-5K$	$-\frac{1}{2}K$	$2L-13K/2$
					^3D	$2L+5K$	$6L-7K$	$5K$	$2L-K$
					^3F	$2L+2K$	$6L-10K$	$2K$	$2L-4K$
5	3+2	3/2	Li^9, Be^9, B^9, C^9	1/2	^2P	$2L+12K$	$10L-12K$	$-5L+39K/4$	$2L-45K/4$
					^2D	$2L+10K$	$10L-14K$	$-5L+25K/2$	$2L-17K/2$
					^2F	$2L+7K$	$10L-17K$	$-5L+11K$	$2L-10K$
5	3+2	1/2	Be^9, B^9	3/2	^4P	$2L+12K$	$10L-12K$	$-2L+45K/4$	$5L-39K/4$
					^4D	$2L+10K$	$10L-14K$	$-2L+17K/2$	$5L-25K/2$
					^4F	$2L+7K$	$10L-17K$	$-2L+10K$	$5L-11K$
5	3+2	1/2	Be^9, B^9	1/2	^2P	$2L+12K$	$10L-12K$	$-2L+6K$	$2L-6K$
					^2D	$2L+10K$	$10L-14K$	$-2L+6K$	$2L-6K$
					^2F	$2L+7K$	$10L-17K$	$-2L+6K$	$2L-6K$
6	3+3 and 4+1+1	1	Be^{10}, B^{10}, C^{10}	1	^3P	$3L+17K$	$15L-19K$	$-5L+15K$	$5L-15K$
					^3F	$3L+12K$	$15L-24K$	$-5L+15K$	$5L-15K$
6	3+3 and 4+1+1	0	B^{10}	0	^1P	$3L+17K$	$15L-19K$	$-3L+9K$	$3L-9K$
					^1F	$3L+12K$	$15L-24K$	$-3L+9K$	$3L-9K$
7	4+2+1	3/2	Be^{11}, B^{11}, C^{11}, N^{11}	1/2	^2P	$3L+24K$	$21L-30K$	$-9L+87K/4$	$6L-93K/4$
					^2D	$3L+22K$	$21L-32K$	$-9L+49K/2$	$6L-41K/2$
					^2F	$3L+19K$	$21L-35K$	$-9L+23K$	$6L-22K$
7	4+2+1	1/2	B^{11}, C^{11}	3/2	^4P	$3L+24K$	$21L-30K$	$-6L+93K/4$	$9L-87K/4$
					^4D	$3L+22K$	$21L-32K$	$-6L+41K/2$	$9L-49K/2$
					^4F	$3L+19K$	$21L-35K$	$-6L+22K$	$9L-23K$
7	4+2+1	1/2	B^{11}, C^{11}	1/2	^2P	$3L+24K$	$21L-30K$	$-6L+18K$	$6L-18K$
					^2D	$3L+22K$	$21L-32K$	$-6L+18K$	$6L-18K$
					^2F	$3L+19K$	$21L-35K$	$-6L+18K$	$6L-18K$
8	4+3+1	1	B^{12}, C^{12}, N^{12}	1	^3P	$4L+31K$	$28L-41K$	$-10L+30K$	$10L-30K$
					^3D	$4L+29K$	$28L-43K$	$-10L+30K$	$10L-30K$
					^3F	$4L+26K$	$28L-46K$	$-10L+30K$	$10L-30K$
8	4+3+1	1	B^{12}, C^{12}, N^{12}	0	^1P	$4L+31K$	$28L-41K$	$-10L+61K/2$	$8L-47K/2$
					^1D	$4L+29K$	$28L-43K$	$-10L+25K$	$8L-29K$
					^1F	$4L+26K$	$28L-46K$	$-10L+28K$	$8L-26K$
8	4+3+1	0	C^{12}	1	^2P	$4L+31K$	$28L-41K$	$-8L+47K/2$	$10L-61K/2$
					^2D	$4L+29K$	$28L-43K$	$-8L+29K$	$10L-25K$
					^2F	$4L+26K$	$28L-46K$	$-8L+26K$	$10L-28K$
9	4+3+2	3/2	B^{13}, C^{13}, N^{13}, O^{13}	1/2	^2P	$3L+41K$	$36L-58K$	$-15L+40K$	$12L-41K$
					^2D	$3L+39K$	$36L-60K$	$-15L+42K$	$12L-39K$
9	4+3+2	1/2	C^{13}, N^{13}	3/2	^4P	$3L+41K$	$36L-58K$	$-12L+41K$	$15L-40K$
					^4D	$3L+39K$	$36L-60K$	$-12L+39K$	$15L-42K$
9	4+3+2	1/2	C^{13}, N^{13}	1/2	^2P	$3L+41K$	$36L-58K$	$-12L+36K$	$12L-36K$
					^2D	$3L+39K$	$36L-60K$	$-12L+36K$	$12L-36K$
10	4+3+3	1	C^{14}, N^{14}	1	^3P	$3L+51K$	$45L-75K$	$-17L+51K$	$17L-51K$
10	4+3+3	0	N^{14}	0	^1P	$3L+51K$	$45L-75K$	$-15L+45K$	$15L-45K$

TABLE III. *Energy differences within the group of low terms.*

n	NUCLEUS	TRANSITION	ENERGY DIFFERENCE	
2, 10	Li^6, N^{14}	$^3D-^3S$	$-3K$	4.8 mc^2
		$^1S-^3S$	$-G_1(2L+4K)$	6.3
		$^1D-^3D$	$-G_1(2L-2K)$	4.2
	He^6, Li^8, C^{14}, N^{16}	$^1D-^1S$	$-(1-2G_1)3K$	2.7
3, 9	Li^7, Be^7, C^{13}, N^{15}	$^3F-^3P$	$-(1-G_1)5K$	6.3
4, 8	Be^8, C^{12}	$^1G-^1S$	$-(1-G_1)10K$	12.6
		$^1D-^1S$	$-(1-G_1)3K$	3.8
5, 7	Be^9, B^9, B^{11}, C^{11}	$^3G-^3P$	$-(1-G_1)9K$	11.3
		$^3F-^3P$	$-(1-G_1)5K$	6.3
		$^3D-^3P$	$-(1-G_1)2K$	2.5
6	B^{10}	$^3G-^3S$	$-(1-3G_1/4)10K$	13.4
		$^3F-^3S$	$-(1-G_1/4)6K$	9.1
		$^3D\mathrm{I}-^3S$	$-(1-G_1/2)3K$	4.3
		$^3D\mathrm{II}-^3S$	$-(1+3G_1/10)3K$	5.2
		$^1S-^3S$	$-G_1(2L+5K)$	6.6
		$^1D\mathrm{I}-^3D\mathrm{I}$	$-G_1(2L+2K)$	5.6
		$^1D\mathrm{II}-^3D\mathrm{II}$	$-G_1(2L-14K/5)$	3.9
		$^1F-^3F$	$-C_1(2L-4K)$	3.4
		$^1G-^3G$	$-G_1 2L$	4.9
6	Be^{10}, B^{10}, C^{10}	$^1G-^1S$	$-(1-5G_1/4)10K$	11.7
		$^1F-^1S$	$-(1-7G_1/4)6K$	5.9
		$^1D\mathrm{I}-^1S$	$-(1-3G_1/2)3K$	3.2
		$^1D\mathrm{II}-^1S$	$-(1-23G_1/10)3K$	2.4

the matrix elements of Q and R are identical, and

$$\omega(Q)=-\omega(PQ), \quad \gamma(Q)=-\gamma(PQ).$$

According to Eq. (8) and the already determined values of ω, $2\gamma(Q)=6\omega(Q)=12$. Thus the matrix elements of Q and PQ are $2L-6K$ and $-2L+6K$, respectively. In other cases it is convenient to compute the interactions between like and unlike particles separately using the relations

$$\begin{aligned} Q&=-P \\ PQ&=-1 \qquad \text{(like particles)}, \\ Q_{12}&=(1+\sigma_1\cdot\sigma_2)/2 \\ P_{12}Q_{12}&=P_{12}(1+\sigma_1\cdot\sigma_2)/2 \qquad \text{(unlike particles)}. \end{aligned} \tag{10}$$

If the total spin of either group of like particles vanishes the terms in $\sigma_1\cdot\sigma_2$ contribute nothing to the matrix elements. When this happens only the space wave function is needed for the evaluation of the energy matrix.

III. Reduction of the Number of Free Parameters in the Interaction Operator

We interrupt the discussion of the energy matrix to show that the total energies of the low terms involve the exchange parameters g, g_1, g_2 in only two linearly independent combinations and furthermore that only those parameters which have been fixed by consideration of the two, three and four particle problems enter into the expressions for the excitation energies within the group of low terms. Let

$$\begin{aligned} G_1&=g+g_2, \\ G_2&=g-g_2, \\ G_3&=1+g-5g_1-3g_2. \end{aligned} \tag{11}$$

The parameter G_1 determines the singlet-triplet splitting in the deuteron;[2] the binding energy of the deuteron and the scattering cross section of hydrogen for slow neutrons require $G_1\sim 0.22$. The inequality $G_3\geqq 0$ must be satisfied if the theory is to give the binding energy of heavy nuclei proportional to the number of particles.[2] Nothing is known about G_2. By direct substitution we find

$$\begin{aligned} (1-g-g_1-g_2)P+gPQ+g_1 1+g_2 Q \\ =(1-G_1)P+G_1PQ+G_1(1-P)Q/2 \\ +(1-G_1-G_3)(1-P)/5 \\ +G_2(1-P)(4-5Q)/10. \end{aligned} \tag{12}$$

The matrix elements of $\sum_{i>j}(1-P_{ij})(4-5Q_{ij})J(r_{ij})$ vanish for the group of low terms. The truth of this statement is obvious for the contributions from the interactions within the s shell. For the interaction between shells it follows from Eq. (16). Finally the reader can readily verify by the use of Table I that the statement also holds for the interaction within the p shell. Thus, so long as only the low terms are considered, the operator in Eq. (1) may be replaced by an effective interaction operator

$$\begin{aligned} V'=\sum_{i>j}\{&(1-G_1)P_{ij}+G_1P_{ij}Q_{ij} \\ &+\tfrac{1}{5}(1+G_1-G_3)(1-P_{ij})\}J(r_{ij}). \end{aligned} \tag{13}$$

For an s^4p^n configuration the matrix elements of the last term in Eq. (13) depend only on the partition quantum number and can be computed at once from the ω's and Eq. (8). Consequently the separations of the low terms in the Hartree approximation depend only on the simple interaction operator

$$V''=\sum_{i>j}\{(1-G_1)P_{ij}+G_1P_{ij}Q_{ij}\}J(r_{ij}). \tag{14}$$

This symmetrical operator containing only Majorana and Heisenberg interactions has already been discussed in reference 1.

In Table III the separations of the low levels are given in terms of the single parameter G_1. The numerical results are computed from the values of L and K given in Section V.

These results (as deduced from the secular equations) have already been discussed and compared with experiment in reference 1. Some

additional remarks supplementing the earlier discussion will be found in Section VI of this paper.

IV. Remaining Contributions to the Total Energy Matrix

The diagonal matrix elements of the operator V for interactions within the s shell are simply $6(1-G_1)B$ where

$$B=\int\cdots\int R_s(r_1)^2R_s(r_2)^2J(r_{12})d\tau_1d\tau_2, \quad (15)$$

the average value of $J(r)$ in the s shell. From the interaction between a single p particle and the closed s shell we obtain the matrix elements

$$\begin{aligned} &E_{sp}(1)=4C-D, \quad E_{sp}(Q)=2C-2D,\\ &E_{sp}(P)=4D-C, \quad E_{sp}(PQ)=2D-2C, \end{aligned} \quad (16)$$

where

$$\begin{aligned} C&=\int\cdots\int x_1^2R_p(r_1)^2R_s(r_2)^2J(r_{12})d\tau_1d\tau_2,\\ D&=\int\cdots\int x_1x_2R_p(r_1)R_p(r_2)R_s(r_1)\\ &\qquad\times R_s(r_2)J(r_{12})d\tau_1d\tau_2. \end{aligned} \quad (17)$$

The contribution to the energy terms from the interaction between the s and p shells is then

$$E_{sp}(V)=n\{3(1-G_1)D+G_3(D-C)\}. \quad (18)$$

The Coulomb energy matrix can be expressed in terms of the integrals already defined with the interpretation of $J(r_{12})$ as e^2/r_{12}. We shall denote this particular choice of J by adding the subscript c to the symbols used for the general integrals. It is clear that the Coulomb interaction within the s shell gives rise to the energy B_c, and that between the closed s shell and a single p proton to $2C_c-D_c$. The matrix elements of the Coulomb interaction within the p shell are given in Table IV for the group of low terms.

The matrix of the Coulomb interaction is diagonal in the two D states of B^{10}, but not of Be^{10} and C^{10}. For the latter nuclei the nondiagonal matrix element connecting the two D states has the value $(21/20)^{\frac{1}{2}}K_c$, which is small in comparison with the separation of the D states resulting from the spin exchange forces, and can therefore be neglected.

TABLE IV. *Matrix elements of the Coulomb interaction within the p shell.*

STATE				
	Be^6	C^{14}	N^{14}	O^{14}
S	L_c+2K_c	$6L_c-8K_c$	$10L_c-20K_c$	$15L_c-30K_c$
D	L_c-K_c	$6L_c-11K_c$	$10L_c-20K_c$	$15L_c-30K_c$
	Be^7	C^{13}	N^{13}	
P	$L_c+2K_c/3$	$6L_c-28K_c/3$	$10L_c-20K_c$	
F	L_c-K_c	$6L_c-11K_c$	$10L_c-20K_c$	
	Be^8	C^{12}		
S	$L_c+2K_c/3$	$6L_c-28K_c/3$		
D	$L_c+K_c/6$	$6L_c-59K_c/6$		
G	L_c-K_c	$6L_c-11K_c$		
	Be^9	B^9	B^{11}	C^{11}
P	$L_c+2K_c/3$	$3L_c-14K_c/3$	$3L_c-14K_c/3$	$6L_c-28K_c/3$
D	$L_c+2K_c/5$	$3L_c-76K_c/15$	$3L_c-76K_c/15$	$6L_c-48K_c/5$
F	L_c-K_c	$3L_c-14K_c/3$	$3L_c-14K_c/3$	$6L_c-11K_c$
G	L_c-K_c	$3L_c-6K_c$	$3L_c-6K_c$	$6L_c-11K_c$
	Be^{10}	B^{10}	C^{10}	
S	$L_c+3K_c/2$	$3L_c-19K_c/4$	$6L_c-17K_c/2$	
D_I	$L_c+K_c/2$	$3L_c-5K_c$	$6L_c-19K_c/2$	
D_{II}	$L_c-3K_c/10$	$3L_c-23K_c/5$	$6L_c-103K_c/10$	
F	L_c-K_c	$3L_c-5K_c$	$6L_c-11K_c$	
G	L_c-K_c	$3L_c-6K_c$	$6L_c-11K_c$	

The correct kinetic energy operator is the difference between the sum of the single particle operators and the kinetic energy of the center of gravity:

$$\begin{aligned} &-\tfrac{1}{2}\sum\Delta_i+\frac{1}{2(n+4)}(\sum\nabla_i)^2=\\ &\qquad-\tfrac{1}{2}\left(1-\frac{1}{n+4}\right)\sum\Delta_i+\frac{1}{n+4}\sum_{i>j}\nabla_i\cdot\nabla_j. \end{aligned} \quad (19)$$

Here, as in reference 1, the unit of length is $\hbar/(Mm)^{\frac{1}{2}}c$ and the energy is measured in units of mc^2. The last term of Eq. (19) is well known in atomic spectra.[7] It has nonvanishing matrix elements only when i and j refer to like particles having parallel spins and "azimuthal" quantum numbers differing by one unit. The contribution to the energy is therefore one term per particle in the p shell, so that the total effect is proportional to $n/(n+4)$.

V. Numerical Calculations

The numerical analysis is most conveniently carried through using the familiar oscillator functions

$$R_s(r)=ce^{-\alpha\rho r^2}, \quad R_p(r)=c'e^{-\alpha\rho r^2},$$

[7] D. S. Hughes and C. Eckart, Phys. Rev. **36**, 694 (1930). J. H. Bartlett and J. J. Gibbons, Phys. Rev. **44**, 538 (1933).

together with $J(r)=-72e^{-\alpha r^2}$, $\alpha^{-1}=2.25\times10^{-13}$ cm, as in reference 1. A variational calculation using these functions was made for the ground state energies of the series of nuclei Li^6 to O^{16}. In this calculation the terms proportional to G_3 were omitted. The energy has a broad minimum for values of σ and τ ranging from 0.55 to 0.70; no sensible improvement results from varying both σ and τ independently. It thus seems reasonable to take $\sigma=\tau=0.6$ throughout. With this choice of parameters the integrals occurring in the potential energy have the following values:

$$\begin{aligned} B&=-16.53\ mc^2, & B_c&=1.10\ mc^2,\\ C&=-11.37\ \text{“}, & L_c&=0.89\ \text{“},\\ D&=-\ 5.17\ \text{“}, & K_c&=0.055\ \text{“}, \\ L&=-11.04\ \text{“}, & 2C_c-D_c&=1.64\ \text{“}.\\ K&=-\ 1.61\ \text{“}, \end{aligned} \tag{20}$$

The general expressions for these integrals in terms of σ and τ are to be found in reference 1. The kinetic energy is also discussed there, with the exception of the last term in Eq. (19). This term makes only a small contribution to the total energy, being equal to $9.6n/(n+4)\ mc^2$ if $\sigma=\tau=0.6$.

It is, however, not necessary to use separate wave functions for the individual particles within a shell. An attempt was made to improve the energy calculation by the use of functions of a more general character involving a greater number of parameters. A symmetrical linear combination of oscillator functions with different values of τ may be substituted for the simple product functions without affecting the validity of the general analysis. For example, the radial wave function for Li^6 may be

$$e^{-\alpha\sigma(r_1^2+r_2^2+r_3^2+r_4^2)}\{e^{-\alpha\tau(r_5^2+r_6^2)}+\lambda e^{-\alpha\tau'(r_5^2+r_6^2)}\}.$$

A variational calculation for the total energy of Li^6 using this function gave a small improvement, in no case greater than 4 mc^2. This result is in agreement with the work of Inglis[8] who finds that about half the binding energy of Li^6 is accounted for by the effect of excited configurations. It thus appears necessary to consider the interaction with excited configurations to obtain an appreciable increase in the theoretical binding energies. One result of interest which emerged from the calculations with the more general wave function was the essential constancy of the integral K over a wide range of σ, τ, τ' values.

[8] D. R. Inglis, to appear in the Phys. Rev.

VI. Discussion

We add a few remarks here supplementing the discussion in reference 1. The theoretical total energies calculated by the Hartree method are all so small that a direct comparison with the experimental values is useless. To obtain a significant comparison the theoretical values are modified by the addition of a linear function of n chosen to fit the experimental binding energies of He^4 and O^{16}. Results obtained in this way are shown in Fig. 1. The ground state of the most stable nucleus of each mass number is plotted for two values of G_3, namely $G_3=0$ and $G_3=1$, represented by the two solid curves. The curve labeled "coefficient" of G_3 is constructed by subtracting a suitably chosen linear function of n from the actual computed coefficient of G_3. Unquestionably the whole procedure is arbitrary; nevertheless we venture to state the plausible conclusion that G_3 must be small in comparison with unity.

The experimental binding energy differences $(C^{11}-B^{11})$ and $(N^{13}-C^{13})$ are very nearly equal while the corresponding quantities for other adjacent pairs of isobars with odd mass differ appreciably.[9] This fact finds a simple explanation in the Eqs. (21) and (22) which are constructed from the normal state energies listed in Table IV:

$$(N^{13}-C^{13})-(C^{11}-B^{11})=L_c-6K_c, \tag{21}$$

$$\begin{aligned}(O^{15}-N^{15})-(N^{13}-C^{13})&\\ =(C^{11}-B^{11})-(B^9-Be^9)&\\ =L_c+\tfrac{2}{3}K_c.&\end{aligned} \tag{22}$$

In Eq. (21) the Coulomb exchange integral K_c

[9] Reference 1, Table VIII.

Added in proof: All the "experimental" energy differences in Table VIII except that for H^3-He^3 are incorrect. The correct values are 1 mc^2 larger than those given in the table. The discrepancies between the calculated electrostatic and the corrected experimental energy differences average about thirty-five percent. This discrepancy can be reduced by using more concentrated wave functions, but at the expense of exaggerating the four-shell structure and the Li^8-Be^8 energy difference. The corrected experimental energy differences, however, reduce materially the disagreement between the theoretical and observed singlet-triplet separations in the ten and fourteen particle systems.

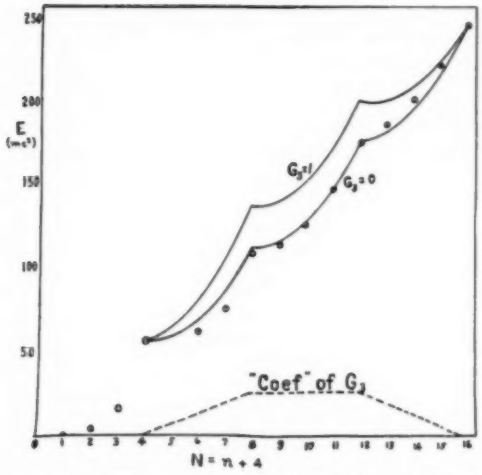

FIG. 1. Binding energy against nuclear mass. The calculated values lie on the solid curves; the circles mark experimental points.

effectively cancels an appreciable part of the ordinary Coulomb repulsion, while in Eq. (22) the exchange integral has the opposite effect. The equality stated in the first line of Eq. (22) is not verified experimentally,[9] but the apparent failure of the theory is probably closely connected with the small binding energy of the particle outside of the two alpha-particle groups in Be^9 and B^9. The small binding energy implies a large volume and consequently an exceptionally small Coulomb energy difference between Be^9 and B^9.

In a recent discussion of the β-ray spectrum of Li^8, Breit and Wigner[10] reach the tentative conclusion that the normal state of Li^8 is $^3P_2$. An examination of the theoretical ^3P, ^1P energy difference reveals that the order of the levels depends primarily on the sign of the parameter g_2. From Eq. (12) and Table II the p shell potential energies are

$$E(^3P)=\tfrac{1}{5}(1-G_1)(14L+23K)-\tfrac{2}{5}(G_2+2G_3)(L-3K),$$
$$E(^1P)=\tfrac{1}{5}(1-G_1)(14L+23K)-\tfrac{1}{2}G_1(2L-7K)+\tfrac{1}{5}(3G_2-4G_3)(L-3K). \quad (23)$$

The triplet-singlet energy difference is

$$E(^3P)-E(^1P)=2g_2(L-3K)-\tfrac{1}{2}G_1K\sim-12.4g_2+0.18. \quad (24)$$

A sufficient condition for the triplet level to lie below the singlet is $g_2>0.015$ or $G_2\leqq0.19$. The necessity of this condition is weakened somewhat by the existence of small spin-orbit interactions which lower the $^3P_2$ level while leaving the singlet level unchanged.[11, 12]

For the $Li^8(^3P)$, $Be^8(^1S)$ mass difference we find

$$-\tfrac{1}{5}(1-G_1)(16L-3K)-\tfrac{2}{5}(G_2+2G_3)(L-3K)-L_c-\tfrac{2}{3}K_c-2C_c+D_c+n^1-H^1\sim25.8\,mc^2+2.5(G_2+2G_3)\,mc^2. \quad (25)$$

This agrees very well with the total energy release of 14 Mev found experimentally, if G_2 and G_3 are small in comparison with unity. The analysis also leads to the equation

$$\{Li^8(^3P)-Be^8(^1S)\}-\{B^{12}(^3P)-C^{12}(^1S)\}=2L_c-21K_c/4\sim1.5\,mc^2. \quad (26)$$

Eq. (26) cannot be expected to hold with great accuracy because L and K are not accurately independent of the number of particles in the nucleus. The observed difference between the total energy released in the 8 and in the 12 particle reactions[13–15] is not known with sufficient accuracy to provide a test for Eq. (26).

The singlet and triplet levels discussed in the preceding paragraph occur also in Be^8, but displaced upward relative to the Li^8 levels by the amount

$$L_c+\tfrac{1}{2}K_c+2C_c-D_c-(n^1-H^1)\sim1.0\,mc^2. \quad (27)$$

There exists a ^3P level which belongs to Be^8 alone ($T=0$, $s=1$), and differs from the normal state of Li^8 by the amount

$$-G_1(L-7K/2)-G_2(L-3K)+(n^1-H^1)-L_c-\tfrac{1}{2}K_c-2C_c+D_c. \quad (28)$$

Both this state and the ^3D belonging to Be^8 alone will fall below $Li^8(^3P)$ if $G_2>0$. In this case radioactive transitions from the ground state of Li^8 to these states of Be^8 should occur. Recently long range alpha-particles have been observed in connection with the radioactive disintegration of Li^8 with about the right energy to come from the

[10] E. Wigner and G. Breit, Phys. Rev. **50**, 1191 (1936).

[11] E. Wigner, private communication.

[12] M. E. Rose and H. A. Bethe, Phys. Rev. **51**, 205 (1937).

[13] W. B. Lewis, W. E. Burcham, W. Y. Chang, Nature **139**, 24 (1937).

[14] L. H. Rumbaugh and L. R. Hafstad, Phys. Rev. **50**, 681 (1936).

[15] W. A. Fowler, L. A. Delsasso, C. C. Lauritsen, Phys. Rev. **49**, 561 (1936).

breaking up of these highly unstable Be^8 nuclei into alpha-particles.[13] The short range alpha-particles which are observed in the same experiment probably result from the disintegration of Be^8 nuclei formed in the ^1D state by the beta decay of Li^8. Additional evidence for a ^1D state in Be^8 with an excitation energy of 2 or 3 Mev is supplied by the short range alpha-particles observed in the disintegration of B^{11} by protons.[16]

It is probably safe to assume that the order of the levels is generally given correctly by the Hartree approximation, but there is some reason for believing that exceptions do occur. The group of low terms in B^{10} contains two D levels which probably interact strongly with each other through excited configurations. For this reason, the possibility that the normal state of B^{10} is ^3D cannot be excluded.

According to the first-order calculation the ground state of N^{14} is ^3S with a magnetic moment equal to that of Li^6 and H^2, 0.85 nuclear magnetons.[12, 17] Experimentally the total angular momentum is unity in agreement with theory, but the magnetic moment appears to be much smaller[18] than 0.85. The assumption that the normal state is ^3D leads to agreement with both the observed total angular momentum and the observed magnetic moment. Because of the spin-orbit interaction the level ^3D splits into three, $^3D_1$, $^3D_2$, $^3D_3$. We expect the inverted order $^3D_3<^3D_2<^3D_1$ in Li^6 (this follows from the theory of Inglis[19] and Furry[20]). The fine structure pattern is therefore normal in N^{14} (two particles missing from a closed shell) with the order $^3D_1<^3D_2<^3D_3$. The magnetic moment has the value

$$\mu=0.5\{J(J+1)+L(L+1)-S(S+1)\}/2(J+1)$$
$$+0.85\{J(J+1)+S(S+1)-L(L-1)\}/2(J+1) \quad (29)$$
$$=0.33 \text{ nuclear magnetons.}$$

These speculative considerations on the order of the levels in B^{10} and N^{14} can be tested by studying the fine structure in the energy distribution of the particles emitted in transmutations in which B^{10} or N^{14} is formed.

A noteworthy property of the term differences within a partition is revealed by Tables I and II. The Majorana and ordinary interactions together give rise to the term differences

$$\tfrac{1}{2}\{l(l+1)-l'(l'+1)\}(1-G_1)K, \quad (30)$$

in which l and l' are the orbital angular momenta of the initial and final states, respectively. The inclusion of the spin exchange forces leaves Eq. (30) still correct for those transitions in which $s=\mathrm{T}=s'=\mathrm{T}'$. The same expression holds also for the arithmetic mean of the energy differences associated with the paired transitions

$$s=s'=0, \quad \mathrm{T}=\mathrm{T}'=1,$$
$$s=s'=1, \quad \mathrm{T}=\mathrm{T}'=0,$$

and also, in the same manner, for the pair

$$s=s'=\tfrac{1}{2}, \quad \mathrm{T}=\mathrm{T}'=\tfrac{3}{2},$$
$$s=s'=\tfrac{3}{2}, \quad \mathrm{T}=\mathrm{T}'=\tfrac{1}{2}.$$

This last statement follows from the relation

$$E(PQ, l, s, \mathrm{T})+E(PQ, l, \mathrm{T}, s)$$
$$=E(PQ, l, s, \mathrm{T})-E(Q, l, s, \mathrm{T}) \quad (31)$$

since the right-hand member of Eq. (31) is independent of l.

It will be necessary to extend the Hartree calculations to the first excited configuration. One level belonging to this configuration is already known, namely an excited state of N^{15} with an excitation energy[15, 21] of 10.5 mc^2. A

[16] P. I. Dee and C. W. Gilbert, Proc. Roy. Soc. **A154**, 279 (1936).

Added in proof: The maximum kinetic energy of the electrons produced by the beta-decay of B^{12} is at least 2 mc^2 greater[15] than the corresponding quantity in the case of Li^8. This fact is noteworthy because the Coulomb interaction reduces the $B^{12}-C^{12}$ mass difference more than the Li^8-Be^8 difference (Eq. 26) and thus would be expected to make the energy available for beta-decay smaller for B^{12} than for Li^8. There is, however, no difficulty if the reactions involved are

$$Li^8(^3P_2)\rightarrow Be^8(^1D_2)+e^-$$
$$B^{12}(^3P_0)\rightarrow C^{12}(^1S_0)+e^-$$

since the $^1D-^1S$ energy difference is at least 4 mc^2. The selection rules for the beta-decay (G. Gamow and E. Teller, Phys. Rev. **49**, 895 (1936)) fix the total angular momentum of the Li^8, B^{12} normal states once the quantum numbers of the decay products are known. The interpretation of the beta-decay in this manner requires that the fine structure pattern in B^{12} be inverted with respect to the pattern in Li^8. An inversion is to be expected from the general theory of "holes" for systems symmetrically situated on opposite sides of the center of the shell. Professor G. Breit has pointed out that the resonance level observed when C^{12} is bombarded with protons (L. R. Hafstad and M. A. Tuve, Phys. Rev. **48**, 306 (1935)) can be identified as the ^3F level of N^{13}. From the masses of C^{12}, N^{13} and H^1 and the kinetic energy (0.0004 mass units) at which resonance occurs we calculate the excitation energy of the resonance level to be 0.0024 mass units or 4.4 mc^2. This value compares favorably with the theoretical value of 6.3 mc^2. There are also indications of a fine structure in the resonance level.

[17] J. H. Manley and S. Millman, Phys. Rev. **51**, 19 (1937).

[18] R. F. Bacher, Phys. Rev. **43**, 1001 (1933).

[19] D. R. Inglis, Phys. Rev. **50**, 783 (1936).

[20] W. H. Furry, Phys. Rev. **50**, 784 (1936).

[21] E. O. Lawrence, E. McMillan and M. C. Henderson, Phys. Rev. **47**, 273 (1935); J. D. Cockcroft and W. B. Lewis, Proc. Roy. Soc. **A154**, 261 (1936).

simple calculation, using the oscillator wave functions with $\sigma=\tau=0.6$, yields the result that the single excitation of a particle in N^{15} should increase the kinetic energy by the amount $14\alpha\sigma/15=9\ mc^2$. This value is in satisfactory agreement with the experimental excitation energy since it leaves some margin for the decrease in potential energy which is to be expected in an excited configuration.

In conclusion we wish to record our indebtedness to Professor E. Wigner for many valuable discussions.

Appendix 1

Construction of functions belonging to irreducible representations of the symmetric group

The single particle wave functions for the p shell may be classified according to the component of orbital angular momentum in an arbitrary direction:

$$(a,\ b,\ c)=\{(x+iy)/2^{\frac{1}{2}},\ z,\ (x-iy)/2^{\frac{1}{2}}\}R_p(r). \tag{32}$$

The set of product functions

$$\phi_k=P_k a(1)\cdots a(n_1)b(n_1+1)\cdots b(n_1+n_2) \times c(n_1+n_2+1)\cdots c(n_1+n_2+n_3), \tag{33}$$

in which the arguments of the various factors designate the space coordinates of the particles and P_k is a permutation operator, subtend the linear manifold $(n_1+n_2+n_3)$ in the total function space of n particles. The total space wave functions for the p^n configuration are then linear combinations of the functions

$$\psi_l=\sum_k c_{lk}\phi_k \tag{34}$$

where the summation extends over all permutations. We wish to determine the coefficients c_{lk} so that the ψ_l's belong to irreducible representations of the symmetric group.

In order to do this we introduce the symmetrical "displacement" operator

$$D_{\alpha\beta}=\sum_{i=1}^{n} D_{\alpha\beta}(i), \tag{35}$$

$D_{\alpha\beta}(1)$: $\alpha(1)\to\beta(1)$, $\beta(1)\to 0$, $\gamma(1)\to 0$, $\alpha,\ \beta,\ \gamma=a,\ b,\ c$ in arbitrary order,

and note that $D_{\alpha\beta}$ commutes with the elements of the permutation group. By means of the displacement operators it is possible to express any manifold as a sum of invariant subspaces, each subtended by a definite set of functions which generates an irreducible representation of the symmetric group.

To illustrate the method we give a complete discussion of the three particle system. The manifold (3+0+0) contains only one function, $\psi_1=a(1)a(2)a(3)$. This function is completely symmetrical and generates the irreducible representation denoted by the partition [3]. The application of the operator D_{ab} to ψ_1 transforms it into the function

$$\psi_2=a(1)a(2)b(3)+a(1)b(2)a(3)+b(1)a(2)a(3)$$

which corresponds to an invariant subspace of the manifold (2+1+0). The complementary invariant subspace (the space of functions orthogonal to the completely symmetrical function) is subtended by

$$\psi_3=a(1)\{a(2)b(3)-a(3)b(2)\},$$
$$\psi_4=a(2)\{a(1)b(3)-a(3)b(1)\}.$$

These functions generate the two dimensional representation [2+1]. Together with ψ_2 they exhaust the manifold (2+1+0). The sum of $D_{ac}\cdot(2+1+0)$ and $D_{bc}\cdot(1+2+0)$ is subtended by the functions

$$\left.\begin{aligned}\psi_5=&a(1)c(2)b(3)+a(1)c(3)b(2)+a(2)c(1)b(3)\\&+a(2)c(3)b(1)+a(3)c(1)b(2)+a(3)c(2)b(1)\end{aligned}\right\}\quad[3],$$

$$\left.\begin{aligned}\psi_6=&b(3)[a(1)c(2)+a(2)c(1)]\\&-b(2)[a(1)c(3)+a(3)c(1)]\\\psi_7=&b(3)[a(1)c(2)+a(2)c(1)]\\&-b(1)[a(2)c(3)+a(3)c(2)]\end{aligned}\right\}[2+1],$$

$$\left.\begin{aligned}\psi_8=&c(3)[a(1)b(2)+a(2)b(1)]\\&-c(2)[a(1)b(2)+a(2)b(1)]\\\psi_9=&c(3)[a(1)b(2)+a(2)b(1)]\\&-c(1)[a(2)b(3)+a(3)b(2)]\end{aligned}\right\}[2+1].$$

The subspace of the manifold (1+1+1) complementary to $D_{ac}\cdot(2+1+0)+D_{bc}\cdot(1+2+0)$ is subtended by the completely antisymmetrical function

$$\psi_{10}=\begin{vmatrix}a(1) & b(1) & c(1)\\ a(2) & b(2) & c(2)\\ a(3) & b(3) & c(3)\end{vmatrix},$$

which generates the representation [1+1+1]. The set of linearly independent functions ψ_5 to ψ_{10} exhaust the manifold (1+1+1). These results may be summarized in the equations

$$\begin{aligned}(3+0+0)&=[3],\\(2+1+0)&=[3]+[2+1],\\(1+1+1)&=[3]+2[2+1]+[1+1+1],\end{aligned} \tag{36}$$

which state the number of times the various irreducible representations appear in the unreduced manifolds. The Eq. (36) and the corresponding equations for other values of n can also be derived directly from the orthogonality and normalization properties of the group characters.

The values of the total orbital angular momentum which appear in the various irreducible representations of the symmetric group may be determined by an inspection of the manifolds and their subspaces. The wave functions describing definite quantized L, M_L values are easily found with the aid of the angular momentum operators $L_x\pm iL_y$.

It is often convenient for the calculation of Coulomb and spin exchange energies to identify the partition functions with linear combinations of products of neutron and proton functions such as are used in reference 1. This can be done by inspection if one constructs the states of reference 1 according to the ordinary methods familiar from the theory of complex spectra. The resulting combinations are identical with those which diagonalize the matrices of the total Majorana and ordinary interactions, as we noted in the introduction.

APPENDIX 2

Determination of the ordinary and isotopic spin values belonging to a definite partition in the space coordinates

The exclusion principle requires that the complete wave function vanish if more than one particle has a given set of orbital angular momentum, spin and isotopic spin quantum numbers. To obtain the total spin and total isotopic spin quantum numbers associated with the different partitions we first make a list, for each manifold separately, of the sets of individual particle quantum numbers compatible with the exclusion principle, classifying them according to Σm_s and Σm_T. Because of the symmetry about the origin, we may restrict ourselves to Σm_s, $\Sigma m_T \geqq 0$. Since $\Sigma m_T = M_T$ and $\Sigma m_s = M_s$, we immediately arrive at the total s and τ necessary to account for these projections. To illustrate the method we again consider the case of three particles:

Manifold		m_s	m_T		m_s	m_T		m_s	m_T	Σm_s	Σm
(3)	a	$\frac{1}{2}$	$\frac{1}{2}$	a	$\frac{1}{2}$	$-\frac{1}{2}$	a	$-\frac{1}{2}$	$\frac{1}{2}$	$\frac{1}{2}$	$\frac{1}{2}$
(2+1)	a	$\frac{1}{2}$	$\frac{1}{2}$	a	$\frac{1}{2}$	$-\frac{1}{2}$	b	$\frac{1}{2}$	$\frac{1}{2}$	$\frac{3}{2}$	$\frac{1}{2}$
		$\frac{1}{2}$	$\frac{1}{2}$		$\frac{1}{2}$	$-\frac{1}{2}$		$-\frac{1}{2}$	$\frac{1}{2}$	$\frac{1}{2}$	$\frac{1}{2}$
		$\frac{1}{2}$	$\frac{1}{2}$		$-\frac{1}{2}$	$\frac{1}{2}$		$\frac{1}{2}$	$\frac{1}{2}$	$\frac{1}{2}$	$\frac{3}{2}$
		$\frac{1}{2}$	$\frac{1}{2}$		$-\frac{1}{2}$	$\frac{1}{2}$		$\frac{1}{2}$	$-\frac{1}{2}$	$\frac{1}{2}$	$\frac{1}{2}$
		$\frac{1}{2}$	$\frac{1}{2}$		$-\frac{1}{2}$	$-\frac{1}{2}$		$\frac{1}{2}$	$\frac{1}{2}$	$\frac{1}{2}$	$\frac{1}{2}$
		$\frac{1}{2}$	$-\frac{1}{2}$		$-\frac{1}{2}$	$\frac{1}{2}$		$\frac{1}{2}$	$\frac{1}{2}$	$\frac{1}{2}$	$\frac{1}{2}$

From the table it is obvious that there is only one pair of s, τ values for the partition [3], namely $s=\frac{1}{2}$, $\tau=\frac{1}{2}$. After the partition [3] has been removed from the manifold (2+1) there remains the three sets of quantum numbers $(s=\frac{3}{2}, \tau=\frac{1}{2})$, $(s=\frac{1}{2}, \tau=\frac{3}{2})$, $(s=\frac{1}{2}, \tau=\frac{1}{2})$, associated with the partition [2+1]. A similar table for the manifold (1+1+1) together with Eq. (36) yields the result that the partition [1+1+1] has only two pairs of spin values, $(s=\frac{3}{2}, \tau=\frac{3}{2})$ and $(s=\frac{1}{2}, \tau=\frac{1}{2})$.

APRIL 15, 1937 PHYSICAL REVIEW VOLUME 51

The Disintegration of Cadmium with Deuterons

J. M. CORK AND R. L. THORNTON
University of Michigan, Ann Arbor, Michigan

(Received February 26, 1937)

The bombardment of a cadmium target by deuterons of energy 6.3 Mev yields certain radioactive isotopes. Chemical analysis of the bombarded metal shows the presence of two radioactive isotopes of cadmium having half-life periods of 4.3 hr and 58 hr, respectively. Both emit negative electrons. The long-period cadmium activity gives rise to a radioactive indium of half-life 2.3 hr. This indium isotope in succession emits negatives resulting in the formation of a stable tin isotope. Successive chemical separations carried out over a period of sixty hours showed the indium to be in equilibrium with the long period cadmium. The existence of radioactive isotopes of half-life periods shorter than about 30 minutes is not precluded.

IT has been observed by Fermi[1] that cadmium is relatively inactive after bombardment with neutrons. Since cadmium is a very effective absorber of slow neutrons its large capture cross section for this process is probably due to the formation of one or more stable isotopes. However, many elements not rendered radioactive by neutrons are readily activated under bombardment with high energy deuterons, and it seemed desirable to investigate the disintegrations of cadmium under such conditions.

Targets of chemically pure metallic cadmium were exposed to a beam of deuterons of energy about 6.3 Mev. Exposures of the order of four microampere-hours rendered the bombarded specimens strongly radioactive. The deuteron beam was obtained by the multiple acceleration of deuterium nuclei in the cyclotron.

In order to determine with what elements the activity was associated, the bombarded specimen was dissolved in nitric acid. To this solution small quantities of solutions of the neighboring elements, silver, palladium, and indium were added.

The silver was first precipitated from this solution as the chloride by the addition of hydrochloric acid. This silver was redissolved in ammonium hydroxide and reprecipitated by the addition of nitric acid. The palladium was next brought down from the original filtrate as palladium dioxime by the addition of dimethylglyoxime to the slightly acid solution. Ammonium hydroxide added to the filtrate next precipitated the indium as indium hydroxide.

[1] E. Amaldi, O. D'Agostino, E. Fermi, B. Pontecorvo, F. Rasetti, and E. Segrè, Proc. Roy. Soc. **149**, 522 (1935).

The remaining cadmium was brought down as the sulphide by the addition of hydrogen sulphide. Each of these precipitates was now placed in turn on a Lauritsen electroscope to detect the presence of radioactivity and to observe the rate of decay should the precipitate prove to be active. It was observed that the silver and palladium precipitates were inactive while both the cadmium and indium precipitates were strongly radioactive.

A plot of the logarithm of the activity of the precipitates as a function of the time should, for a single activity, give a straight line of negative slope. This should correspond to the equation $A_t = A_0 e^{-\lambda t}$ where A_0 is the activity at the beginning of the observation and A_t is the corresponding activity after the time t has elapsed. λ is the decay constant and may readily be expressed as $0.693/T$ where T is the half-life period or the time for the activity to decay to half its original value. As may be observed in Fig. 1 the indium precipitate decayed with a single half-life period of 2.3 hours.

The cadmium precipitate, however, behaved very differently. The activity, instead of getting weaker with time, actually increased for a short period. This seemed to indicate the building up of some short-lived secondary product from a longer-lived primary activity. Since the cadmium precipitate was found to emit only negative electrons when placed in a cloud chamber, it was rational to expect any secondary product formed to be the next heavier element in the periodic table, namely, indium. Accordingly, after the decay had proceeded for a few hours the active cadmium precipitate was redissolved and a small quantity of dissolved indium added. The indium and cadmium were again precipitated separately. Both precipitates were again active as in the beginning, the indium decaying with the 2.3-hour period, short compared to that of the cadmium. This separation of the cadmium was repeated after a few hours and again yielded an active indium precipitate of the same character. To make sure that the indium was built up from the cadmium, and was not due to an incomplete separation in the first attempt, two successive separations of indium were made following one another immediately. In this case the first precipitate was strongly

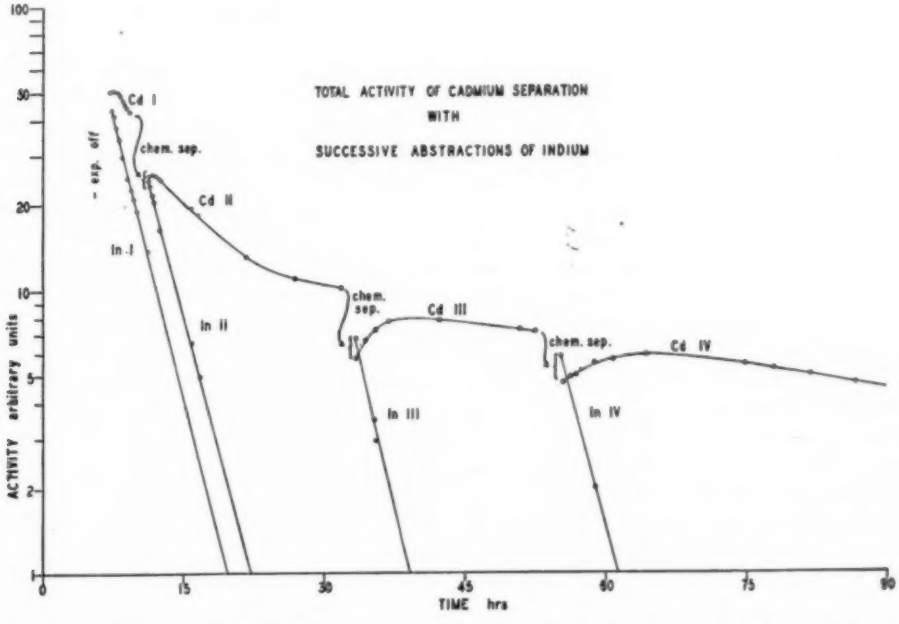

FIG. 1. Showing the continuous building up of indium activity (2.3 hr) from radioactive cadmium (58 hr).

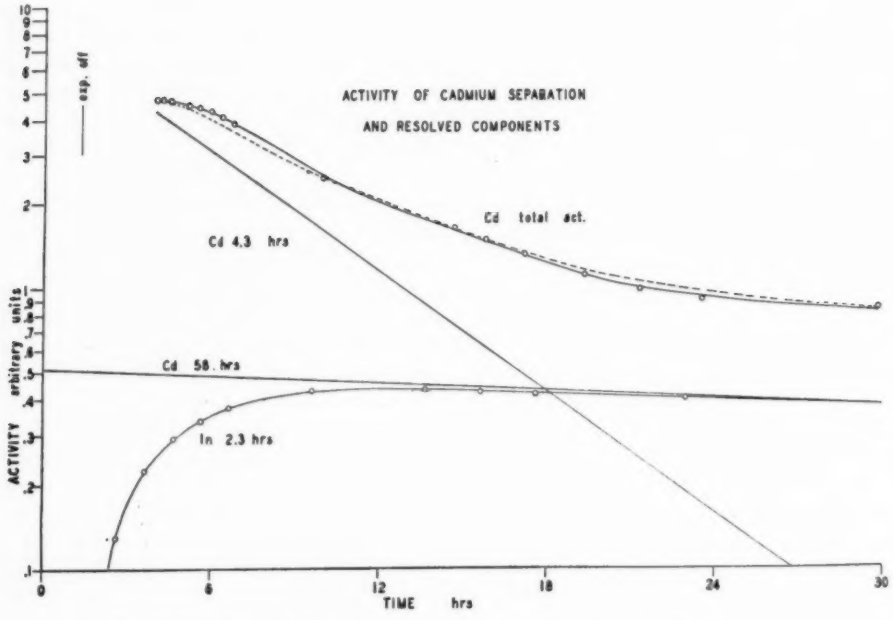

FIG. 2. Showing the resolution of the total cadmium activity into its three components.

active, while the second was completely inactive; yet separations twenty hours later with an identical procedure again yielded a strongly active indium precipitate. Typical decay curves of these successive precipitates are shown in Fig. 1.

Another specimen of bombarded cadmium was subjected to a single chemical separation and the decay curve of the resulting cadmium precipitate was followed for a period of about eighty hours. During this period the specimen was not removed from the electroscope so that errors due to the difficulty of replacing it in exactly the same position were eliminated. The early part of this decay curve is shown as a solid line in the upper part of Fig. 2, the circles being the experimental points. The balance of the decay curve showed a straight line plot corresponding to a half-life of 58 hours.

Now it is evident from the data presented in Fig. 1 that it is this 58-hour period which reaches equilibrium with the 2.3-hour indium activity, since a chemical separation forty hours after exposure showed the precipitated indium to have the same strength as the residual cadmium. Small inequalities may be ascribed to the inevitable geometrical differences for the two samples when placed on the electroscopes. The intensity of the 58-hour activity at the time of the chemical separation (Fig. 2) may be readily obtained, since it corresponds to half the value obtained by extrapolating back the 58-hour straight line portion of the curve to the time of the separation. If to this is added the activity corresponding to the growth into equilibrium of the resulting indium activity, and the curve so obtained is subtracted from that observed, then the experimental points lie along a straight line indicative of a 4.3-hour period. This analysis is shown in the lower part of Fig. 2. The broken line through the experimental points shows the result of the addition of the three postulated curves. The agreement would appear to be quite satisfactory.

The observations may thus be fully explained on the basis of the formation of two radioactive isotopes of cadmium of 4.3 and 58 hours half-life, respectively. The isotope with the longer half-life then decays into a radioactive isotope of indium with a half-life of 2.3 hours.

TABLE I. *Stable and radioactive isotopes of cadmium and neighboring elements.*

ELEMENT	ATOMIC NO.	ISOTOPES
Ag	47	107 109
Cd	48	106 108 110 111 112 113 114 (4.3H) 116 (58H)
In	49	113 (13s) 115 (58m) (2.3H)
Sn	50	112 114 115 116 117 118 119 120 122 124

Since considerable time was required for the chemical separations, the possibility of the existence of active isotopes with shorter periods is not excluded.

The isotopes of the elements in this part of the periodic table are shown in Table I. The following reactions may be postulated to explain the observations.

$$_{48}Cd^{114} + {}_1H^2 \rightarrow {}_{48}Cd^{115} + {}_1H^1$$
$$_{48}Cd^{115} \rightarrow {}_{49}In^{115} + {}_{-1}e \quad (4.3 \text{ hr})$$
$$_{48}Cd^{116} + {}_1H^2 \rightarrow {}_{48}Cd^{117} + {}_1H^1$$
$$_{48}Cd^{117} \rightarrow {}_{49}In^{117} + {}_{-1}e \quad (58 \text{ hr})$$
$$_{49}In^{117} \rightarrow {}_{50}Sn^{117} + {}_{-1}e \quad (2.3 \text{ hr})$$

The failure to observe these radioactive isotopes in the radiative capture of neutrons by cadmium is perhaps surprising. The isotopes involved in their production, Cd^{114} and Cd^{116}, are present to 28.0 and 7.3 percent, respectively.[2] The cross sections for direct neutron capture by these isotopes must therefore be very much lower than those for other cadmium isotopes. Further investigations to ascertain whether these isotopes can be detected after intense neutron bombardment are in progress.

The indium activity is, of course, not identical with either of the periods produced by the bombardment of indium itself with neutrons or deuterons. These half-life periods are known[1] to be 13 sec. and 58 min. and are associated with isotopes In^{114} and In^{116}. Since this new indium activity had a single pure period it was considered worth while to observe its characteristic beta spectrum. Accordingly observations were made of the radii of curvature of about nine hundred tracks photographed with hydrogen in a Wilson cloud chamber. A deflecting magnetic field of about 340 oersteds was employed. Only tracks that clearly originated in the specimen and suffered no collision and traveled at least seven cm in the photographic plane were measured. It was also evident by observing recoil beta-particles from the wall of the Wilson cloud chamber that gamma-rays were emitted during the disintegration process. Since the observed distribution of the beta tracks did not seem to be in accord with a simple plot[3] based on the Konopinski-Uhlenbeck[4] theory of beta emission, further studies of this subject are being made. The maximum value of the beta energies observed was approximately 1.0 Mev ($H\rho = 5000$).

For assistance in carrying out the chemical separations we are indebted to Mr. E. Rosenbaum; the aid of Mr. B. R. Curtis in connection with the cloud chamber observations is also gratefully acknowledged. This work was made possible by a grant from the Horace H. and Mary A. Rackham Fund.

[2] A. O. Nier, Phys. Rev. **50**, 1041 (1936).

[3] F. Kurie, J. Richardson, and H. Paxton, Phys. Rev. **49**, 368 (1936).

[4] E. Konopinski and G. Uhlenbeck, Phys. Rev. **48**, 7 (1935).

Relations Between the Second and Higher Order Processes in the Neutrino-Electron Field Theory

M. H. JOHNSON, JR. AND H. PRIMAKOFF*
Department of Physics, New York University, University Heights, New York City
(Received January 25, 1937)

Without specializing the nature of the interaction between the proton, neutron, electron and neutrino fields both the magnitude and range of the proton-neutron force are deduced. A similar treatment of the proton-proton force shows that the range of this force is certainly less than the range of the proton-neutron force and that there is a simple relationship between the magnitude of this force and the range and magnitude of the proton-neutron force. This relationship together with the relationship between the singlet like and unlike particle forces, deduced from proton-proton and proton-neutron scattering, leads to a value for the range of the proton-neutron force which cannot exceed 0.4×10^{-13} cm. A treatment of an n-tuple process in which a fast proton (or neutron) produces cosmic-ray showers, is also given, and it is found that the same condition on the range is necessary for this process to have an appreciable probability.

INTRODUCTION

ACCORDING to the electron-neutrino field theory[1] there is a finite probability that a neutron makes a transition to a state consisting of a proton, electron and antineutrino while the proton can make an analogous transition to a state consisting of a neutron, positron and neutrino. This probability is governed by an operator F composed of the spin and momentum variables of all four particles which operate on the field scalars of the particles. It is subject to the restriction that the result of the operation shall be a relativistic invariant.

The particles are represented by the quantized amplitudes of their corresponding fields.[2] The quantization of the fields is quite essential, for it gives use to the spontaneous transitions that occur in the β radioactive disintegration of nuclei. Aside from this the formalism of the quantized field is entirely equivalent to speaking of the transitions of the particles among their various states as we shall hereafter do.

If we restrict ourselves to a frame of reference in which the heavy particles are approximately at rest (that is their energies do not differ essentially from their rest energy) the fourth component of the heavy particle momentum energy four vector will be alone important and be equal Mc^2. Further the spin variables can only introduce functions of the angles between the various momenta. Hence to estimate the order of magnitude of the transition probabilities in this frame, we may use

$$F=g\epsilon_p{}^k\epsilon_\eta{}^l,$$

where ϵ_p and ϵ_η are the energy operators for the electron and antineutrino and k and l are the number of times the energy operators of the two light particles appear in F. With units of energy mc^2, units of momentum mc and unit of length $h/2\pi mc$ (m = rest mass of the electron), the probability amplitude of a transition is

$$H=G\int|\mathbf{p}|^k|\mathbf{n}|^l\Phi^*\Psi\psi^*\varphi d\tau, \qquad (1)$$

where G is a dimensionless constant, Ψ, Φ, ψ and φ are the space parts of the relativistic wave functions for proton, neutron, electron and antineutrino, respectively. $\mathbf{p}$ and $\mathbf{n}$ are the ordinary momentum operators of the light particles which we may use in place of the energy upon neglecting the rest mass of these particles. This introduces entirely inappreciable errors in the problems with which we deal. A precisely similar expression holds for the transition of a proton into a neutron, positron and neutrino.

It is known[3] that this theory gives correctly the distribution in momentum of the individual β-ray spectra as well as the dependence of the mean life on the maximum range of the emitted particles with $G=1\times10^{-13}$, $k=0$ and $l=1$ and possibly $k=1$, $l=2$. It is not certain whether

* University Fellow.
[1] E. Fermi, Zeits. f. Physik **88**, 161 (1934).
[2] E. Fermi, reference 1; C. F. von Weizsacker, Zeits. f. Physik **102**, 572 (1936).
[3] Konopinski and Uhlenbeck, Phys. Rev. **48**, 7 (1935); Bethe and Bacher, Rev. Mod. Phys. **8**, 82 (1936).

somewhat higher values of k and l are definitely in contradiction with the β-ray data. Therefore we will not attempt to fix the values of these constants from the spectra but will try to determine them to correlate the high energy phenomena alone. If this is possible and if the values so obtained cannot be fitted to the β-ray data, we may suppose F to be composed of two parts, one with $k=0, l=1$ which will be operative only at low energies, the second with higher values of k and l but with a smaller numerical coefficient which will govern the high energy phenomena.

A serious difficulty arises at once when we attempt to deal with structural questions using (1). Thus the self-energy of a neutron due to the neutrino-electron field is

$$\Delta\epsilon = -\sum_b \frac{H_{ab}H_{ba}}{\epsilon_b - \epsilon_a},$$

where b is the dissolved state of the neutron, ϵ_b is the total energy of this state and the sum is over all possible dissolved states. Using plane waves for all the states we have from (1)

$$H_{ab} = Gp^k\eta^l\delta(\mathbf{N}-\mathbf{P}-\mathbf{p}+\mathbf{n}),$$

where $\mathbf{N}$, $\mathbf{P}$, $\mathbf{p}$, $\mathbf{n}$ are the momenta of neutron, proton, electron and antineutrino, respectively. δ is the Dirac delta function. Further $\epsilon_b - \epsilon_a = p+\eta$, if we omit the rest mass of the electron, the recoil energy of the proton and the mass difference of the proton and neutron, all of which are negligible in the range $p \sim 100$. Then

$$\Delta\epsilon = -G^2\int d\mathbf{p}d\mathbf{n}\frac{p^{2k}\eta^{2l}}{p+\eta} =$$

$$-(4\pi G)^2\int_0^\infty\int_0^\infty \frac{dpd\eta p^{2k+2}\eta^{2l+2}}{p+\eta}. \quad (2)$$

The self-energy is infinite for all values of k and l, a difficulty which is exactly similar to the convergence difficulties of classical electrodynamics. To evade it we must introduce a factor into (1) which will cut out the very high energy components of the neutrino-electron field. For this purpose we use the relativistically invariant expression

$$\exp\left\{-\frac{\alpha}{2}\frac{m}{M}(-\mathbf{N}\cdot\mathbf{p}+\epsilon_N\epsilon_p)\right.$$

$$\left.-\frac{\alpha}{2}\frac{m}{M}(-\mathbf{N}\cdot\mathbf{n}+\epsilon_N\epsilon_\eta)\right\},$$

in which $\mathbf{N}$ and ϵ_N are the momentum and energy operators of the emitting neutron. Neglecting the rest mass of the light particles and remembering that we are using a frame of reference in which the neutron is approximately at rest, the converging factor reduces to $\exp[(-\alpha/2)(p+\eta)]$.

Our expression (2) for the self-energy now contains a factor $e^{-\alpha(p+\eta)}$. The integral is easily evaluated by first evaluating the same integral without the denominator and then integrating the result over α. This gives

$$\Delta\epsilon = -(4\pi G)^2\frac{(2k+2)!(2l+2)!}{2k+2l+5}\alpha^{-2k-2l-5}. \quad (3)$$

Precisely the same result holds for the self-energy of a proton.

Proton-Neutron Force[4]

A force between a proton and a neutron arises through the possibility of the particles changing places by the mechanism of the neutrino-electron field. Let the proton and neutron be originally in the states ρ and σ represented by the wave function Ψ_ρ and Φ_σ and finally are in the states $\Psi_{\rho'}$ and $\Phi_{\sigma'}$. This transition can occur by the following schemes of states:

	I			II	
State	Particles in Field		State	Particles in Field	
a	P_1	N_2	a	P_1	N_2
b	P_1	$P_2e^-n^-$	b	$N_1e^+n^+$	N_2
c	N_1	P_2	c	N_1	P_2

In the first process the neutron emits an electron and antineutrino which are absorbed by the proton. In the second process the proton emits a positron and neutrino which are absorbed by the neutron. These are processes of second order in G.

[4] The magnitude of the proton-neutron force as given by the electron-neutrino field theory has been discussed by: A. Nordsieck, Phys. Rev. **46**, 234 (1934); I. Tamm, Nature **133**, 981 (1934); D. Iwanenko and A. Sokolow Zeits. f. Physik **102**, 118 (1936); C. F. von Weizsacker, reference 2; B. Kahn, Physica **6**, 495 (1936); Bethe and Bacher, reference 3, §44.

Using plane waves for the light particle wave functions, we find from (1) (modified by the converging factor) that the amplitude of this transition is

$$H_{\rho\rho',\sigma\sigma'} = -\sum_b \frac{H_{ab}H_{bc}}{\epsilon_b-\epsilon_a}$$

$$= -\sum_b G^2\left\{\frac{p^{2k}\eta^{2l}}{p+\eta}e^{-\alpha(p+\eta)}\int \Phi_\rho^*(2)\Psi_{\sigma'}(2)\exp\left[i(\mathbf{n}-\mathbf{p})\cdot\mathbf{r}_2\right]d\tau_2\right.$$

$$\left.\int \Psi_\sigma^*(1)\Phi_{\rho'}(1)\exp\left[-i(\mathbf{n}-\mathbf{p})\cdot\mathbf{r}_1\right]d\tau_1+\text{process II}\right\}$$

$$= -\int\int \Phi_\rho^*(2)\Psi_\sigma^*(1)\left[2G^2\sum_b \frac{p^{2k}\eta^{2l}}{p+\eta}e^{-\alpha(p+\eta)}\exp\left[i(\mathbf{n}-\mathbf{p})\cdot(\mathbf{r}_2-\mathbf{r}_1)\right]\right]P_H\Phi_{\rho'}(2)\Psi_{\sigma'}(1)d\tau_1 d\tau_2,$$

where P_H interchange the four coordinates 1, and 2, in $\Phi_{\rho'}$, $\Psi_{\sigma'}$, i.e., P_H is a Heisenberg exchange operator. A proper choice of the operator F, will presumably replace P_H by $(1-g)P_M+gP_H$, where P_M is the Majorana exchange operator, and g is a numerical constant which determines the relative strengths of the Heisenberg and Majorana forces.

The interaction energy in coordinate space now becomes.

$$V_{NP}(r) = -2G^2\int\int \frac{d\mathbf{p}d\mathbf{n}}{p+\eta}p^{2k}\eta^{2l}e^{-\alpha(p+\eta)}\exp\left[i(\mathbf{n}-\mathbf{p})\cdot\mathbf{r}\right]\times P_H.$$

We see at once that $V_{NP}(0)$ is just twice the self-energy of the proton or neutron, due to the electron neutrino field. Effecting the angular integrations:

$$V_{NP}(r) = -2(4\pi G)^2\int_0^\infty\int_0^\infty \frac{dpd\eta}{p+\eta}p^{2k+2}\eta^{2l+2}\frac{\sin pr}{pr}\frac{\sin \eta r}{\eta r}e^{-\alpha(p+\eta)}\times P_H.$$

Now, $\displaystyle\int_0^\infty x^n \sin axe^{-bx}dx = I\left[\int_0^\infty x^n e^{-(b-ia)x}dx\right] = I\left[\frac{n!}{(b-ia)^{n+1}}\right] = \frac{n!}{(b^2+a^2)^{n+1/2}}\sin\left((n+1)\tan^{-1}\frac{a}{b}\right).$

Where $I[\ ]$ means: "the imaginary part of $[\ ]$." We can thus evaluate the integral for $V_{NP}(r)$ if we omit the denominator. Integrating the result over α, from ∞ to α, we obtain after some slight transformations:

$$V_{NP}(r) = -2(4\pi G)^2\frac{(2k+2)!(2l+2)!}{2k+2l+5}\alpha^{-2k-2l-5}G(r/\alpha)P_H \tag{4}$$

with

$$G(r/\alpha) = (2k+2l+5)\int_0^1 \frac{v^{2k+2l+4}dv}{(1+(rv/\alpha)^2)^{k+l+2}}\left[\frac{\sin\{(2k+2)\tan^{-1}(rv/\alpha)\}}{(2k+2)(rv/\alpha)}\frac{\sin\{(2l+2)\tan^{-1}(rv/\alpha)\}}{(2l+2)(rv/\alpha)}\right].$$

$G(r/\alpha)$ is symmetric in k, and l, so we assume, say, $l>k$. For small values of r/α, the denominator and the $[\ ]$ of the integrand are equal to 1, so that $G(r/\alpha)=1$. If we expand in powers of r/α, the next term is in $(r/\alpha)^2$, so that $G(r/\alpha)$ has a horizontal tangent at $r=0$, and the "well" has a flat bottom.

We shall define R_{NP}, the "range" of the proton neutron force, as the value of r, for which $G(r/\alpha)$ first becomes equal to $1/e\sim 1/3$. It is to

be noted that for $r \gg \alpha$, $V_{NP}(r)$ will approach zero as $r^{-2k-2l-5}$. We can obtain explicitly an upper bound $G^+(r/\alpha)$ to $G(r/\alpha)$ [when r/α is so small that the oscillating factors do not pass through zero in the range of integration], by putting $v=3/4$ in the denominator and the [ ] of the integrand, for we overestimate the denominator and the [ ] of the integrand through a region which contributes at least 4/5 of the integral. Similarly we can find the lower bound, $G^-(r/\alpha)$ by putting $v=1$ in the denominator and the [ ] of the integrand. We find that $G^-(r/\alpha) \leqq 1/3$ for $r/\alpha = 1.1/(l+1)$ and $G^+(r/\alpha) \leqq 1/3$ for $r/\alpha = 0.9/(l+1)$. Thus $G(r/\alpha) \leqq 1/3$ for $r/\alpha = 1.0/(l+1)$ and the range of the proton-neutron force is

$$R_{NP} = \alpha/(l+1). \tag{5}$$

Eliminating α, from (4), by using (5), we obtain a purely theoretical relationship between the magnitude and range of the proton-neutron force:[4a]

$$V_{NP}(0) = -2(4\pi G)^2 \times \frac{(2k+2)!(2l+2)!}{(2k+2l+5)(l+1)^{2k+2l+5}} R_{NP}^{-2k-2l-5}. \tag{6}$$

Proton-Proton Force

A force between two protons (or neutrons) arises through the possibility of the simultaneous emission and absorption of neutrinos and positrons by both particles. This process is therefore of the fourth order in G. Let $\Psi_\rho(1)$, $\Psi_\sigma(2)$ represent the initial states of the two protons, and $\Psi_{\rho'}(1)$, $\Psi_{\sigma'}(2)$, represent their final states. The transition can be brought about by the following scheme of states as shown in Table I.

TABLE I. *Process I.*

State	Particles in the Field	
a	P_1	P_2
b	P_1	$N_2 e_2^+ n_2^+$
c	$N_1 e_1^+ n_1^+$	$N_2 e_2^+ n_2^+$
d	$P_1' e_1^+ n_1^+$	N_2
e	P_1'	P_2'

There are three other possible processes obtained by interchanging the order in which the heavy particles emit and absorb the light particles. Using plane waves for all the intermediate states, we find that the amplitude of the transition probability is:

$$H^I_{\rho\rho',\,\sigma\sigma'} = -G^4 \sum_{bcd} (p_2+\eta_2)^{-1}(p_2+\eta_2+p_1+\eta_1)^{-1}(p_1+\eta_1)^{-1} e^{-\alpha(p_1+\eta_1+p_2+\eta_2)} p_1^{2k} p_2^{2k} \eta_1^{2l} \eta_2^{2l}$$
$$\int \Psi_\sigma^*(2) \exp[i(\mathbf{N}_2+\mathbf{p}_2-\mathbf{n}_2)\cdot\mathbf{r}_2] d\tau_2 \int \Psi_\rho^*(1) \exp[i(\mathbf{N}_1+\mathbf{p}_1-\mathbf{n}_1)\cdot\mathbf{r}_1] d\tau_1$$
$$\int \Psi_{\rho'}(3) \exp[i(-\mathbf{N}_1-\mathbf{p}_2+\mathbf{n}_2)\cdot\mathbf{r}_3] d\tau_3 \int \Psi_{\sigma'}(4) \exp[i(-\mathbf{N}_2-\mathbf{p}_1+\mathbf{n}_1)\cdot\mathbf{r}_4] d\tau_4,$$

where we have neglected the recoil energies of the heavy particles. Since $\mathbf{N}_1$ and $\mathbf{N}_2$ appear only in the exponentials, when we integrate over $\mathbf{N}_1$ and $\mathbf{N}_2$ the two delta functions $\delta(\mathbf{r}_2-\mathbf{r}_4)$ and $\delta(\mathbf{r}_1-\mathbf{r}_3)$ are introduced. Upon integrating over r_3 and r_4 we find

$$H^I_{\rho\rho',\,\sigma\sigma'} = -\int\int \Psi_\rho^*(1)\Psi_\sigma^*(2) G^4 \sum_{p_1 p_2 \eta_1 \eta_2} \{(p_2+\eta_2)^{-1}(p_2+\eta_2+p_1+\eta_1)^{-1}(p_1+\eta_1)^{-1} e^{-\alpha(p_1+\eta_1+p_2+\eta_2)}$$
$$\times p_1^{2k} p_2^{2k} \eta_1^{2l} \eta_2^{2l} \exp[i(\mathbf{p}_2-\mathbf{n}_2-\mathbf{p}_1+\mathbf{n}_1)\cdot(\mathbf{r}_2-\mathbf{r}_1)]\} \Psi_{\rho'}(1)\Psi_{\sigma'}(2) d\tau_1 d\tau_2.$$

Upon adding the amplitudes for the other three processes to $H^I_{\rho\rho',\,\sigma\sigma'}$ we find

$$H_{\rho\rho',\,\sigma\sigma'} = -\int\int \Psi_\rho^*(1)\Psi_\sigma^*(2) 2G^4 \sum_{p_1 \eta_1 p_2 \eta_2} \{(p_1+\eta_1)^{-2}(p_2+\eta_2)^{-1} p_1^{2k} \eta_1^{2l} p_2^{2k} \eta_2^{2l} e^{-\alpha(p_1+\eta_1+p_2+\eta_2)}$$
$$\exp[i(\mathbf{p}_2-\mathbf{n}_2-\mathbf{p}_1+\mathbf{n}_1)\cdot(\mathbf{r}_2-\mathbf{r}_1)]\} \Psi_{\rho'}(1)\Psi_{\sigma'}(2) d\tau_1 d\tau_2.$$

[4a] With G taken to fit the β-ray spectrum; $G \leqq 10^{-13}$; and $k=1$, $l=2$, we have: $V_{NP} \leqq 50mc^2$; $R_{NP} \leqq 2 \cdot 10^{-13}$.

Hence the proton-proton interaction in coordinate space is:

$$V_{PP}(r)=-2(4\pi G)^4\left[\int\int\frac{d\mathbf{p}_1 d\mathbf{n}_1}{(p_1+\eta_1)^2}p_1^{2k}\eta_1^{2l}e^{-\alpha(p_1+\eta_1)}\exp\left[i(\mathbf{p}_1-\mathbf{n}_1)\cdot\mathbf{r}\right]\right]$$
$$\times\left[\int\int\frac{d\mathbf{p}_2 d\mathbf{n}_2}{p_2+\eta_2}p_2^{2k}\eta_2^{2l}e^{-\alpha(p_2+\eta_2)}\exp\left[i(\mathbf{p}_2-\mathbf{n}_2)\cdot\mathbf{r}\right]\right]. \quad (7)$$

The expression in the second bracket is just the proton-neutron force, $V_{NP}(r)$. Since one more power of $p+\eta$ appears in the denominator of the expression of the 1st bracket, the expression being otherwise the same as that for $V_{NP}(r)$, we see that the proton-proton force is again a short-range force, the range R_{PP} being in fact, somewhat smaller than the range of the proton-neutron force.

The magnitude of the proton-proton force is:

$$V_{PP}(0)=2(4\pi G)^4\left[\frac{(2k+2)\,!(2l+2)\,!}{2k+2l+5}\alpha^{-2k-2l-5}\right]^2\frac{\alpha}{2k+2l+4}=\tfrac{1}{2}\,|\,V_{NP}(0)\,|^2\frac{\alpha}{2k+2l+4}.$$

Using (5), this becomes:

$$V_{PP}(0)=|\,V_{NP}(0)\,|^2R_{NP}\frac{l+1}{4(k+l+2)}. \quad (8)$$

Thus the electron-neutron field theory relates the magnitude of the proton-proton force to the magnitude and range of the proton-neutron force.

Determination of the Range of the Proton-Neutron (P–N) Force

From the experimentally observed stability of the deuteron, and the cross sections for proton-proton, and neutron-proton scattering it is possible:[5]

a. To find a relation between the magnitude of the triplet P–N force and its range.
b. Determine the relative strengths of the Majorana and Heisenberg interactions in the P–N force.
c. Correllate the magnitude and range of the P–N force with magnitude and range of the P–P force.

We assume the P–N interaction to have the form stated above: $((1-g)P_M+gP_H)V_{NP}(r)$. We have ${}^3V_{NP}(r)=V_{NP}(r)$, ${}^1V_{NP}(r)=(1-2g)V_{NP}(r)$. Then from the stability of the deuteron it follows that:

$$^3V_{NP}(0)R_{NP}{}^2=\frac{\pi^2}{4}\frac{mK}{M}=V_{NP}(0)R_{NP}{}^2, \quad (9)$$

where K is a numerical constant of the order of magnitude unity (always greater than unity) whose exact value depends upon the type of spatial variation of the force, and the definition of the range.

From the scattering cross section of slow neutrons by protons it follows that the deuteron has a virtual singlet state of small energy.[6] From the mere existence of such a state it is possible to estimate g to be about 0.2.[7] The numerical value of g is extremely insensitive to the scattering cross section.

Finally experiments on proton-proton scattering[8] lead to the conclusion that $R^2{}_{NP}{}^1V_{NP}$ is quite accurately equal to $R^2{}_{PP}{}^1V_{PP}$. Since on our theory R_{PP} is certainly somewhat less than R_{NP}, it follows that ${}^1V_{PP}$ is greater than ${}^1V_{NP}$,

$$V_{PP}(0)>{}^1V_{PP}(0)>{}^1V_{NP}(0)=(1-2g)V_{NP}(0). \quad (10)$$

Using our theoretical relationship between $V_{PP}(0)$

[5] Bethe and Bacher, reference 3, Ch. III §12, §13, §18; Breit, Condon and Present, Phys. Rev. **50**, 825 (1936).

[6] Wigner quoted by Bethe and Bacher, reference 3, Ch. III, p. 117.

[7] Feenberg and Wigner, Phys. Rev. **51**, 95 (1937); Present and Rarita, Bull. Am. Phys. Soc. Abstract **46**, Dec. 28–30 (1936).

[8] Breit, Condon and Present, reference 5, Table XIV, p. 842.

TABLE II. *Process A.*

STATE	PARTICLES IN THE FIELD	
1	P_1	N_1
2	$N_2e_1^+n_1^+$	N_1
3	$P_3e_1^+n_1^+e_2^-n_2^-$	N_1
.		
.		
.		
$n+1$	$P_{n+1}e_1^+n_1^+,\cdots,e_n^-n_n^-$	N_1
$n+2$	$P_2\ e_1^+n_1^+,\cdots,e_n^-n_n^-$	N_2

and $V_{NP}(0)$ together with (9) and (10), we get:

$$R_{NP}<\frac{1}{(1-2g)}\frac{\pi^2}{16}\frac{m}{M}\frac{l+1}{k+l+2}K$$

$$<\frac{1}{1-2g}\frac{\pi^2}{16}\frac{m}{M}K\leqq\tfrac{1}{2}10^{-3}K. \quad (11)$$

Therefore the "range" of our proton-neutron force cannot exceed

$$\tfrac{1}{2}10^{-3}K\frac{h}{2\pi mc}\text{cm}=0.2\times10^{-13}K\text{ cm}. \quad (12)$$

The shortest "range" we have been able to find in the literature is that of Present and Rarita[9] who, using an exponential type of force, find that a "range" of 0.86×10^{-13} cm and a correspondingly suitable magnitude for the proton-neutron force, successfully account for all the facts. Now even the utmost liberality cannot permit us to assume K to be more than 2.[10] Thus an absolute maximum for the "range" of the proton-neutron force as given by the electron neutrino field theory is: 0.4×10^{13} cm.

We conclude that the dependence of the second and fourth order processes on the range is such, that to make these processes of the same order of magnitude requires an unreasonably short range.

SHOWER MECHANISM

It has been suggested[11] that the showers of positrons and electrons observed in cosmic-ray Wilson chamber photographs may be due to a multiple process involving the neutrino-electron field. A fast proton or neutron in collision with a nucleus, produces the pairs by a multiple interaction with the field.

Let the proton (or neutron) be originally traveling in the positive x direction with a velocity v. Let $\beta=v/c$, $\xi=(1-\beta^2)^{-\frac{1}{2}}$. We designate by proton frame of reference, the frame in which the proton is at rest before the impact and by laboratory reference frame, the frame in which the pairs are observed. Let $\mathbf{P}_1$ and $\mathbf{P}_2$ be the momentum of the proton before and after the impact and let $\mathbf{N}_1$ and $\mathbf{N}_2$ be the momentum of the nucleus of atomic weight A before and after the impact. We distinguish quantities in the laboratory reference frame by primes. Thus the proton reference frame is characterized by $\mathbf{P}_1=0$ and the laboratory reference frame by $\mathbf{N}_1'=0$. For simplicity we also take $\mathbf{P}_2'=0$.

We must visualize the whole process in the proton reference frame, for it is only in this frame that our approximations in F and the converging factor are valid. The production of pairs can then occur by the scheme of states shown in Table II.

Thus the production of light particles occurs in the first n steps and in the last step the fast nucleus supplies the energy for the entire process and causes the proton to recoil in such a way that $\mathbf{P}_2'=0$. We have put the interaction with the nucleus last for otherwise the proton would obtain a high recoil velocity before the light particle production was completed. We find for the amplitude of the above transitions:

$$H_A^{(n)}=BG^n\prod_{i=1}^{n}\frac{p_i^k\eta_i^l e^{-a/2(p_i+\eta_i)}}{\sum_{j=1}^{i}(p_i+\eta_i)}, \quad (13)$$

where B is the matrix element for the last transition and we have neglected the recoil energies of the heavy particles. The scheme A is only one of many possible schemes obtained by interchanging the order in which given p_i, η_i are produced. If we sum over all possible schemes (summing over all permutations of p_i, η_i with p_j, η_j in (13)) we have:

$$H^{(n)}=BG^n\prod_{i=1}^{n}\frac{p_i^k\eta_i^l e^{-a/2(p_i+\eta_i)}}{p_i+\eta_i}. \quad (14)$$

[9] Present and Rarita, reference 7.
[10] Bethe and Bacher, reference 3, §12, Tables II, III.
[11] W. Heisenberg, Zeits. f. Physik **101**, 533 (1936).

Thus the probability that p_i lie in the range dp_i and the solid angle $d\omega_{pi}$ while η_i lies in the range $d\eta_i$ and the solid angle $d\omega_{\eta i}$ is:

$$dW^{(n)}=B^2G^{2n}\prod_{i=1}^{n}\frac{p_i^{2k+2}\eta_i^{2l+2}}{(p_i+\eta_i)^2}\times e^{-\alpha(p_i+\eta_i)}dp_i d\eta_i d\omega_{pi}d\omega_{\eta i}. \quad (15)$$

So far as the probability factor is concerned the distribution of the light particles is isotropic. We can then easily find the energy absorbed in the production of each light particle:

$$p_a\equiv(p_i)_a=\frac{\int p_i dW^{(n)}}{\int dW^{(n)}}=\frac{2k+3}{\alpha}=\frac{2k+3}{(l+1)R_{NP}}\leqq\frac{1}{R_{NP}},$$
$$\eta_a\equiv(\eta_i)_a=\frac{\int \eta_i dW^{(n)}}{\int dW^{(n)}}=\frac{2l+3}{\alpha}=\frac{2l+3}{(l+1)R_{NP}}\leqq\frac{1}{R_{NP}}. \quad (16)$$

The energy is independent of the direction in which the particles are emitted. Using our previous results for R_{NP}, we have $p_a\leqq\eta_a\leqq 10^3$ so that the production of each pair of light particles absorbs an energy of about 10^3.

We next consider the restrictions imposed by the conservation of energy and momentum. For momentum, we have:

$$\mathbf{N}_1=\mathbf{N}_2+\mathbf{P}_2+\mathbf{Q} \quad \text{with} \quad \mathbf{Q}=\sum_{i=1}^{n}\mathbf{p}_i+\mathbf{n}_i$$

and for energy

$$\xi\frac{MA}{m}=\left(N_1^2+\left(\frac{MA}{m}\right)^2\right)^{\frac{1}{2}}=\left(N_2^2+\left(\frac{MA}{m}\right)^2\right)^{\frac{1}{2}}+(P_2^2+(M/m)^2)^{\frac{1}{2}}-M/m+\sum_{i=1}^{n}(p_i+\eta_i).$$

Since the momentum of the nucleus in the proton frame is very large, to a high degree of accuracy:

$$\left(N_1^2+\left(\frac{MA}{m}\right)^2\right)^{\frac{1}{2}}-\left(N_2^2+\left(\frac{MA}{m}\right)^2\right)^{\frac{1}{2}}\leqq\frac{(\mathbf{P}_2+\mathbf{Q})\cdot\mathbf{N}_1-\frac{1}{2}(\mathbf{P}_2+\mathbf{Q})^2}{(N_1^2+(MA/m)^2)^{\frac{1}{2}}}\leqq(\mathbf{P}_2+\mathbf{Q})\cdot\mathbf{N}_1\frac{m}{\xi MA}.$$

Using the fact that

$$|\mathbf{P}_2|=\frac{\xi\beta M}{m}, \quad |\mathbf{N}_1|=\xi\beta\frac{MA}{m}$$

and that both these vectors are in the negative x direction, the energy equation becomes:

$$\beta Q_{-x}+(1-1/\xi)\frac{M}{m}=\sum_{i=1}^{n}p_i+\eta_i. \quad (17)$$

If β is nearly one and if many particles are produced,

$$Q_{-x}\leqq\sum_{i=1}^{n}p_i+\eta_i$$

from the energy equation, and from the momentum equation, it follows that the light particles are restricted to the backward direction in the proton frame of reference. However, in the laboratory frame, as is easily seen from a Lorentz transformation, the light particles will appear to be restricted pretty well to the forward direction, as seems to be required experimentally.[12]

To find the probability that charged particles be produced in a shower, we must integrate (15) over the region of the momentum space of the light particles permitted by the conservation of energy. Thus

$$W^{(n)}=B^2\left|\frac{1}{(4\pi^2)}\frac{V_{NP}(0)\alpha}{4(k+l+2)}\right|^n\Omega_n, \quad (18)$$

where Ω_n is the solid angle of momentum space in which (17) can be satisfied. The error made in integrating over all magnitudes of p_i, η_i (as we did in deriving (18)) instead of over only those allowed by the conservation of energy, is small because of the exponential decrease of the probability for high values of p_i. To estimate the

[12] P. Auger and P. Ehrenfest, J. de phys. **11**, 473 (1936); Wilson chamber photos in Anderson and Neddermeyer, Phys. Rev. **50**, 263 (1936).

solid angle Ω_n suppose that each particle is confined to a cone about the $-x$ axis, whose solid angle is $(\Omega_i)_a \equiv \Omega$. Then:

$$\left(\frac{[p_i]_{-x}}{p_i}\right)_a = 1 - \frac{\Omega}{4\pi}.$$

Replacing p_i by their average values p_a in (17), we have:

$$\frac{\Omega}{4\pi} = 1 - \frac{1}{\beta} + \frac{1}{\beta}\left(1 - \frac{1}{\xi}\right)\frac{M}{m}\frac{1}{n}\frac{1}{p_a + \eta_a}, \tag{19}$$

which vanishes for

$$n = \frac{(1-1/\xi)(M/m(p_a+\eta_a))}{1-\beta} \leqq \frac{2(1-1/\xi)}{1-\beta}.$$

This value of n is an upper limit to the number of particles that can be produced by a proton of given initial energy, the limiting value occurring when all the light particles are emitted backwards in the proton frame. It is clear from (19) that the solid angle Ω permitted by the conservation laws depends on the number of particles created, becoming larger as n decreases.

Now $$\Omega_n = \int \prod_{i=1}^{n} d\omega_{\eta i} d\omega_{pi} = (\Omega)^{2n}.$$

Hence $$W^{(n)} = B^2\left[\left(\frac{\Omega}{4\pi}\right)^2 \frac{V_{NP}(0)\alpha}{4(k+l+2)}\right]^n. \tag{20}$$

If this probability is to be practically independent of n

$$\frac{V_{NP}(0)\alpha}{4(k+l+2)} > 1,$$

since certainly $\Omega/4\pi < 1$, or using (5), (9)

$$R_{NP} < \frac{\pi^2}{16}\frac{m}{M}\frac{l+1}{k+l+2}K, \tag{21}$$

which is essentially just the condition on the range, found before. We conclude that this theory is capable of providing a shower mechanism, only if the range of the P–N force is less than 0.4×10^{-13} cm, just as it is capable of predicting a singlet P–P force greater than or equal to the singlet P–N force, only if the range of the P–N force is less than or equal to 0.4×10^{-13} cm.

The above computation is open to several objections. In the first place we have neglected the recoil energies of the heavy particles. This can only increase the energy denominators for the intermediate states, the maximum possible effect being to double each denominator. Consequently it can only introduce a factor between 1 and 1/2 into the [ ] of (20). In the second place we have used approximations in F and the converging factor which are only valid if the heavy particle remains approximately at rest. This is certainly not the case for we have seen that the light particles are produced principally in the backward direction in the proton frame. Computations with the complete relativistic converging factor and the relativistic form of F, taking account of all possible orders in which the interactions can occur, become very involved. However, we may imagine a given process viewed from a succession of reference frames in which the heavy particle remains at rest. In this series of reference frames our approximations are valid and the amplitude for a transition at each step is governed by the factor $p^k\eta^l e^{-\alpha/2(p+\eta)}$. We therefore expect that in estimating the total transition probability, the dependence of the probability on α will not be essentially altered and hence (21) will be maintained as a necessary condition. The predictions, with regard to the angular and energy distribution of the pairs may, however, be radically altered in a correct relativistic calculation.

Transmutation Functions at High Bombarding Energies[1]

HENRY W. NEWSON
Radiation Laboratory, Department of Physics, University of California,[2] Berkeley, California

(Received February 16, 1937)

The differential transmutation functions of the reactions,

$$C^{12}+D^2=N^{13}+n^1, \quad (1)$$

$$N^{14}+D^2=O^{15}+n^1, \quad (2)$$

$$O^{16}+D^2=F^{17}+n^1, \quad (3)$$

have been measured at bombarding energies from 2 to 5 Mev. All three curves showed a well marked change of slope at the top of the potential barriers. These points corresponded to potential barrier heights of 2.8, 3.2, and 3.1 Mev for carbon, nitrogen, and oxygen, respectively. These values are slightly more than half those reported for the same elements with alpha-particles. The absolute cross sections for disintegration at the top of the potential barrier are 4.0, 2.8, and 6.0×10^{-26} cm^2 for the elements in order. At bombarding energies greater than the tops of the potential barriers the curves show interesting effects which are probably due to interfering side reactions.

INTRODUCTION

IN a previous paper,[3] work was described on the transmutation functions of carbon and oxygen up to bombarding energies of about three million volts. At that time it was noted that the transmutation function of carbon showed indications of flattening at the highest energies, and this was taken to indicate that the most energetic particles were approaching the top of the potential barrier of the carbon nucleus. When higher energies became available because of improvement of the cyclotron, this problem was reopened in order to study the shapes of the transmutation functions at energies near the tops of the potential barriers, and to study the behavior of the transmutation functions beyond the potential barriers. In order to reach more general conclusions, the three neighboring elements carbon, nitrogen, and oxygen were chosen for the study since they produce radioactive substances by the analogous reactions:

$$C^{12}+D^2=n^1+N^{13}\ (\tfrac{1}{2}\text{ life}=10.3\text{ min.}), \quad (1)$$

$$N^{14}+D^2=n^1+O^{15}\ (\tfrac{1}{2}\text{ life}=\ 2.3\text{ min.}), \quad (2)$$

$$O^{16}+D^2=n^1+F^{17}\ (\tfrac{1}{2}\text{ life}=\ 1.2\text{ min.}). \quad (3)$$

In this way it was hoped that one could detect special behavior of the transmutation functions due to any peculiarity of one of the nuclei. This was a fortunate precaution in as much as the three transmutation functions studied differed in shape very decidedly at bombarding energies greater than the heights of the potential barriers.

EXPERIMENTAL

The principles of the experimental method have been described previously. Briefly, it consists in gathering radioactive recoil atoms at various points along the path of a beam of deuterons as it is retarded while passing through a gas containing the element to be studied. In these experiments the recoil atoms were collected on platinum foils of about 1 cm stopping power, each of which were spaced about three millimeters apart. The platinum foils also served to cut down the range of the beam to a more convenient interval than the range of the beam in air (20 cm). The area of the foils was sufficiently greater than that of the beam so that recoil atoms, projected at an angle from the edge of the beam with a sufficient forward component of range to reach a foil, would strike the foil and not the frame on which it was supported. The spacing of the foils was slightly greater than the maximum forward range of the recoil atoms.

This method leads to a thin target transmu-

[1] A preliminary report on these experiments was given at the Berkeley Meeting, Nov. 28, 1935.
[2] Present address: Department of Chemistry, University of Chicago.
[3] Newson, Phys. Rev. **48**, 790 (1935).

tation function since the target thickness is the average forward range of the recoil atoms which at the maximum energy was only about two millimeters. The transmutation functions are not subject to error due to variations in the intensity of the beam since all the foils are subject to the same fluctuations.

In the experiments, the bombarding chamber of the cyclotron was evacuated and then filled with nitrogen, oxygen, or carbon dioxide at atmospheric pressure. The bombardment was continued for a time greater than the half-life of the resulting radioactivity. The beam had an intensity of about two microamperes. The current was held as constant as possible in order to be able to calculate the absolute cross sections for disintegration. Ten collector foils were used in the experiment. After bombardment the decay of the activity on each foil was measured by measuring the activities of the foils in rotation. About four measurements were made on each foil so that a good decay curve was obtained for the desired activity; and, after the disappearance of this activity, any activity of longer half-life due to contamination could be measured and eliminated. The measurements were made on a Lauritsen type electroscope for which the fiber moved one division for every 10^4 beta-rays which entered.

Corrections

The results of the measurements need to be corrected for two effects which vary with the energy of the deuteron:

First, the stopping power of the platinum foils varies decidedly within the range of energies which were used in this experiment. Corrections were made by using the calculations of Mano.[4] It was necessary to use Mano's formula for energies at which it is not strictly valid. However, these points are below the potential barrier and consequently are of lesser interest in this experiment. Mano's formula has been tested recently by Laslet[5] and found to be valid for deuterons of about the energies used. The stopping powers of the foils were measured originally with the alpha-particles of polonium. The correction of the stopping power found in this way amounted to about twenty-five percent for the highest energies.

Second, the effective target thickness, which is the average forward range of the recoil atoms, varies with the deuteron energy. This quantity is

$$R_t = \tfrac{1}{2}\int_0^{\theta\ \max} (R\cos\theta)F(\theta)d\theta, \qquad \text{(I)}$$

where R is the range of the recoil atom, θ is the angle between the direction of the recoil atom and that of the bombarding particle, $F(\theta)$ is the distribution per unit angle of the recoil atoms, and θ max is the maximum value of θ, which may or may not be 180°. From the work of Blackett and Lees[6] we may take the approximate expression

$$R = \tfrac{3}{4}V_r - 0.2, \qquad \text{(II)}$$

where R is expressed in millimeters and V_r in 10^{-8} centimeters per second. Neglecting the constant term

$$R_t = \tfrac{3}{8}\int_0^{\theta\ \max} V_r\cos\theta F(\theta)d\theta.$$

This expression is more easily integrated in the coordinates of the center of gravity of the system. Let V be the velocity of the moving system, V' be the velocity of the recoil atom in the moving system, and ϕ be the angle between V and V'. Then, the forward component of velocity, $V_r\cos\theta = V + V'\cos\phi$, and, the distribution function, $F(\theta)d\theta = \sin\phi d\phi$ assuming that the distribution is isotropic in the moving system; the integration is to be taken over all values of ϕ. Making the above substitution:

$$R_t = \tfrac{3}{8}\int_0^{\pi} (V + V'\cos\phi)\sin\phi d\phi = \tfrac{3}{4}V. \qquad \text{(III)}$$

Carrying out the integration without neglecting the constant term in Eq. (II) would make a negligible change in Eq. (III). In the case of nitrogen, recoil atoms are projected both forward and backward and the correction should take into account the average backward range which accounts for some of the activity. The correction has been worked out in this way, but the result does not differ essentially from Eq. (III). It is

[4] Mano, J. de phys. **5**, 628 (1934).
[5] Laslet, Phys. Rev. **50**, 391 (1936).
[6] Blackett and Lees, Proc. Roy. Soc. **134**, 658 (1932).

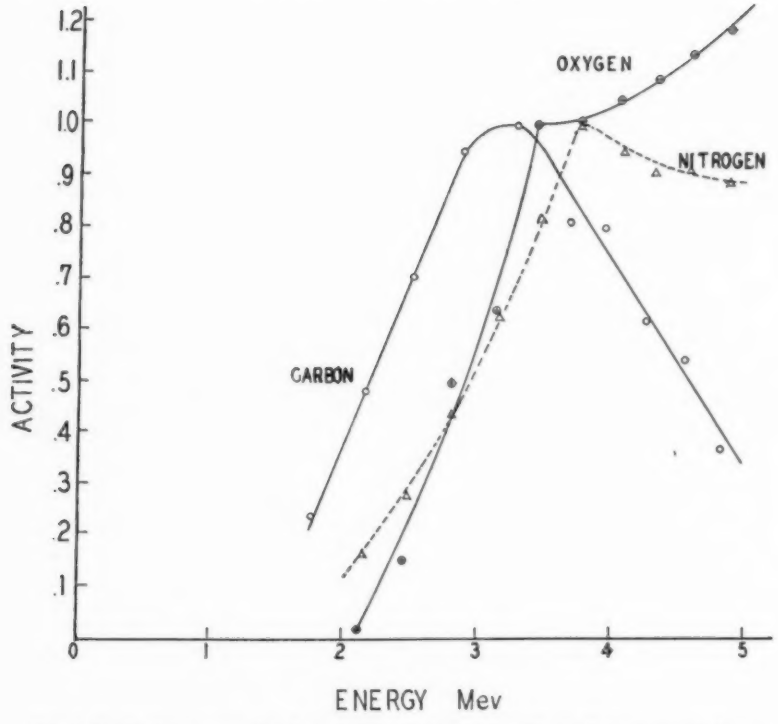

FIG. 1. Excitation curves of carbon, oxygen, and nitrogen. The ordinates are relative to the activity at the top of the potential barrier of each element. The ordinate 1 corresponds to the cross sections 4.0, 6.0, and 2.8×10^{-26} cm² for carbon, oxygen, and nitrogen, respectively.

apparent then, that the effective target thickness is proportional to the velocity of the deuteron, since

$$V=M_D V_D/(M_t+M_D),$$

where V_D and M_D are the velocity and mass, respectively, of the deuteron, and M_t is the mass of the bombarded nucleus.

The residual ranges of the deuterons at the front of each foil was converted into energy by the use of the Cavendish range-energy curve. Fig. 1 shows the transmutation functions in terms of the energy of the deuteron after making all corrections; the activity is plotted relative to the intensity at the top of the potential barrier. The absolute cross sections were calculated from the effective target thickness R_t from Eq. (III). The absolute cross sections at the tops of the potential barriers are 4.0, 2.8, and 6.0 cm²$\times10^{-26}$ for carbon, nitrogen, and oxygen, respectively. These values are probably accurate within a factor of two while their relative accuracy should be considerably better.

RESULTS

All three curves show a very decided change of slope somewhat above three million volts. The almost discontinuous nature of the nitrogen and oxygen curves indicates that the tops of the potential barriers are very well marked. The energies at the points of inflection are 3.3 Mev, 3.7 Mev, and 3.5 Mev for carbon, nitrogen, and oxygen, respectively. Correcting for the motion of the nucleus, the energies at the tops of the potential barriers are 2.8 Mev, 3.2 Mev, and 3.1 Mev.

The value for the top of the potential barrier of nitrogen bombarded by alpha-particles is 5.6 Mev, and for carbon 5.1 Mev, according to Pollard.[7]

[7] Pollard, Phys. Rev. **47**, 611 (1935).

The top of the potential barrier may be considered to be the point at which the attractive force between the two nuclei just balances the Coulomb force of repulsion. If the attractive force, as is frequently assumed, starts at some critical value of the separation and increases extremely rapidly (having a potential curve of nearly infinite slope), the top of the potential barrier for both deuterons and alpha-particles would be located very near to this critical separation and the height for alpha-particles would be twice that for deuterons. It is seen from the above data that this picture is surprisingly close to the truth. However, the two sets of determinations should be repeated under similar experimental conditions before any very definite conclusions can be reached.

The behavior of the transmutation functions beyond the potential barrier is most erratic. The nitrogen curve comes nearest to what one would expect. According to the Gamow formula, the cross section for disintegration, $\sigma = kV^{-1}e^{-s}$, where V is the velocity of the bombarding particle, and s is a function of the bombarding energy. At the top of the potential barrier the exponential term should become constant, and σ should, therefore, be inversely proportional to the velocity. The small decrease beyond the potential barrier in nitrogen is probably due to this cause. There is, however, an interfering reaction which might cause this curve to decrease:

$$N^{14}+D^{2}=C^{13}+He^{3}. \qquad (4)$$

It is impossible, at present, to investigate reaction (4) because the range of the He^3 will always be considerably less than that of the bombarding deuteron.

In the previous paragraph the possibility of a transmutation being affected by side reactions is discussed. However, it is known from the work of Haxel[8] that such interference between two concurrent reactions is possible. Haxel found that the transmutation function of the reaction

$$N^{14}+He^{4}=F^{17}+n^{1} \qquad (5)$$

started with a threshold at 5 Mev; he observed at the same time that the transmutation function of the concurrent reaction

$$N^{14}+He^{4}=O^{17}+H^{1} \qquad (6)$$

dropped sharply at the same point where that of the first reaction started to rise. This showed very definitely the possibility of interference between two such reactions. This is most easily understood on the basis of the theory of the intermediate product put forward by Harkins[9] and by Bohr.[10] On this basis all the alpha-particles which enter the nitrogen nucleus are captured to form an unstable intermediate nucleus, F^{18}, which subsequently breaks up to give the final products of either reaction (5) or (6). Since the number of these intermediates is limited, the sudden increase of reaction (5) beyond its threshold must cause a corresponding decrease in reaction (6).

The slow rise in the transmutation function of oxygen (reaction (3)), after the top of the potential barrier has been reached, must be due to effects which are independent of the penetration of the deuterons into the nucleus. Similarly in the work of Haxel, reaction (5) has a threshold at a bombarding energy near the top of the potential barrier, but, in spite of this, the transmutation function rises with the bombarding energy. Reaction (3) starts from a threshold at 2 Mev so that it is not surprising that its excitation curve should continue to rise beyond the potential barrier.

The sharp drop in the transmutation function of carbon (reaction (1)) is probably due to the reaction:

$$C^{12}+D^{2}=B^{10}+He^{4}. \qquad (7)$$

The transmutation function of this reaction must rise rapidly beyond the potential barrier to cause the decided drop in the intensity of reaction (1). Unfortunately, reaction (7) like reaction (4) cannot be studied directly.

In conclusion, I wish to express my gratitude to Professor Lawrence for the opportunity of using the cyclotron. I am also indebted to my colleagues at the Radiation Laboratory for both helpful discussion and practical assistance. The financial support of the Chemical Foundation and the Research Corporation is gratefully acknowledged.

[8] Haxel, Zeits. f. Physik **93**, 400 (1935).

[9] Harkins, Phys. Rev. **44**, 530 (1933); Science **83**, 533 (1936); Phys. Rev. **51**, 52 (1937); Proc. Nat. Acad. Sci. **23**, 120 (1937).

[10] Bohr, Nature **137**, 344 (1936).

The Radioactivity Induced in Silicon and Phosphorus by Deuteron Bombardment

HENRY W. NEWSON
Radiation Laboratory, University of California,[1] Berkeley, California

(Received February 16, 1937)

Silicon and phosphorus have been bombarded by deuterons and the resulting radioactive substances have been studied.

The two reactions,

$$Si^{30}+D^2=Si^{31}+H^1,$$
$$P^{31}+D^2=P^{32}+H^1,$$

were found to occur. The active substances were identified by the usual chemical tests. The half-life of Si^{31} was found to be 170 ± 10 minutes and that of P^{32}, 14.5 ± 0.3 days. Both substances were found to emit no gamma-rays and advantage was taken of this fact to study the absorption curves of the beta-rays with some care. The absorption curves showed very definite end points from which the maximum energy of the beta-ray spectra was calculated from Feather's empirical formula. The calculated energies were 1.50 ± 0.01 Mev and 1.59 ± 0.03 Mev for Si^{31} and P^{32}, respectively. These values are in satisfactory agreement with the latest direct measurements. The errors in absorption measurements in the presence of gamma-rays are estimated from the shape of the absorption curves.

THE ACTIVATION OF PHOSPHORUS

FROM a consideration of the types of reactions which have been studied heretofore, one may write only two by which radioactive products might be induced in phosphorus under deuteron bombardment:

$$P^{31}+D^2=P^{32}+H^1, \quad (1)$$

$$P^{31}+D^2=P^{30}+H^3. \quad (2)$$

All other reasonable reactions which might be written would lead to stable end products. Reaction (2) appears highly improbable, but it may be easily investigated since the period of P^{30} is known to be about 3 minutes.[2] A target of red phosphorus was bombarded for about five minutes with 3 Mev deuterons and the activity followed for about an hour. The decay curve became flat in about thirty minutes showing that an activity of relatively long period was present. On examining the earlier parts of the decay curve, weak activities with periods of about one minute and ten minutes were found. These are undoubtedly to be attributed to contamination of the target by oxygen and by carbon which give rise to F^{17} (half-life 1.16) and N^{13} (half-life 10.4), respectively. Since no trace was found of any half-life in the neighborhood of 3 minutes, it may be stated definitely that reaction (2) does not occur.

The long period which was found in this experiment is undoubtedly to be attributed to P^{32} formed by reaction (1). This substance has already been prepared in three ways:

$$Cl^{35}+n^1=P^{32}+He^4.$$
$$S^{32}+n^1=P^{32}+H^1,$$
$$Si^{29}+He^4=P^{32}+n^1.$$

The first two reactions were discovered by Fermi[3] and his collaborators while the third has been reported recently by Fallenbrach.[4] The half-life was found to be about two weeks.

In order to check the identity of the active substance obtained in these experiments, the target of red phosphorus was bombarded for an hour and the decay of the activity was followed for several days. As soon as it was apparent that the half-life of the substance was about the same as that reported for P^{32}, the sample was analyzed chemically. The red phosphorus was burned at the bottom of a test tube so that the oxide was condensed on the walls near the mouth of the tube. The deposit was dissolved in water and boiled with nitric acid in order to oxidize any

[1] Present address: Department of Chemistry, University of Chicago.

[2] Curie and Joliot, Comptes rendus **198**, 254 (1934).

[3] Fermi, Amaldi, D'Agostino, Rassetti, and Segrè, Proc. Roy. Soc. **A146**, 483 (1934).

[4] Fallenbrach, Naturwiss. **23**, 288 (1935).

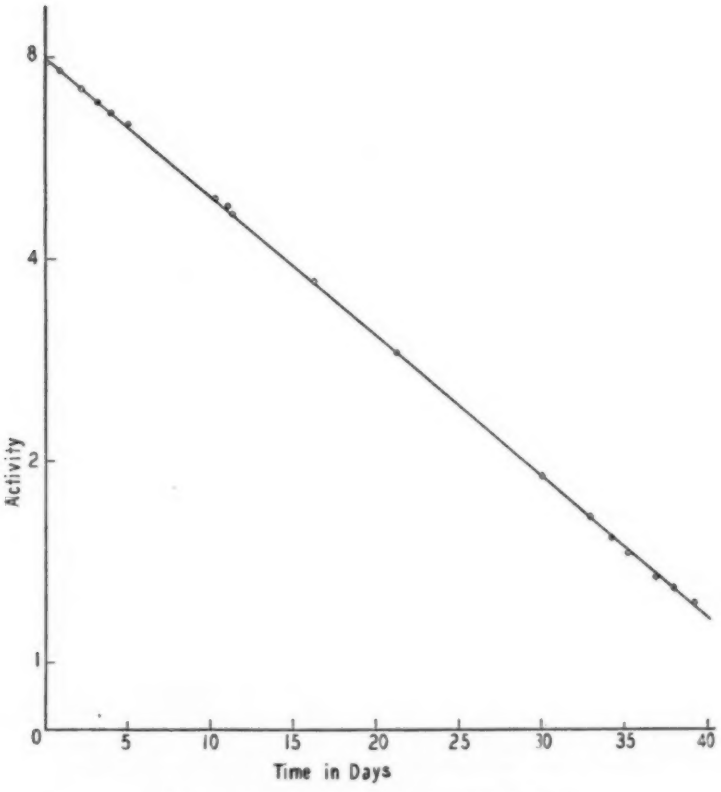

FIG. 1. A logarithmic plot of the decay of P^{32}.

material for which combustion was incomplete. Phosphates were then precipitated with magnesia mixture in the presence of small amounts of sulphates and chlorides. The precipitated $Mg(NH_4)(PO_4)$ showed a large activity. In order to show that the activity was not due to magnesium, aluminum or silicon, the precipitate was dissolved in dilute nitric acid and sodium silicate and aluminum chloride solutions were added. Silicon was then separated by evaporating the acid solution to dryness and filtering out the precipitated silicic acid. This precipitate showed no activity. The phosphates were then separated from aluminum and magnesium by precipitating $(NH_4)_3PO_4 \cdot 13MoO_3$ from dilute acid solution. This precipitate was found to contain all the activity showing that the active substance was an isotope of phosphorus.

In order to measure the half-life of P^{32}, an activated sample of phosphorus was sealed into the ionization chamber of an electroscope and the activity was followed for about three half-lives. The measurements were stopped when the activity was about twenty times the natural leak of the instrument in order that fluctuations in it would not introduce an appreciable error in the measurements. The decay curve so obtained is shown in Fig. 1. Each point on the curve is the average of ten measurements which differed from the mean by less than one percent. The half-life obtained from this curve is 14.5 ± 0.3 days.

The fact that no gamma-rays are given off by P^{32} (see later experiments) is sufficient evidence that the disintegration particles are electrons. However, magnetic experiments also show that the particles are negatively charged. The disintegration equation may then be written:

$$P^{32} = S^{32} + e^{-}.$$

The Activation of Silicon

Radioactive products might be expected to be induced in silicon by deuteron bombardment by the following reactions:

$$Si^{30}+D^2=Si^{31}+H^1, \quad (3)$$

$$Si^{30}+D^2=Al^{28}+He^4, \quad (4)$$

$$Si^{29}+D^2=P^{30}+n^1, \quad (5)$$

$$Si^{28}+D^2=P^{29}+n^1, \quad (6)$$

$$Si^{28}+D^2=Al^{26}+n^1, \quad (7)$$

$$Si^{28}+D^2=Si^{27}+H^3. \quad (8)$$

However, only the products of reactions (3) and (6) may be expected to be easily detectable. Si^{31} is known to have a half-life of about 3 hours[3] so that even though it arises from a rare isotope, the weak activity can be easily detected in the absence of other long periods. However, Al^{28} and P^{30} will be similarly weak and both of them have half-lives of about three minutes so that they will be detected only if other short periods are absent. Al^{26} has a very short half-life (about 7 seconds) and under the conditions of the experiment it probably cannot be detected. Reaction (8) seems very unlikely because the analogous reaction did not occur during the bombardment of phosphorus, and because the energy of the reaction is probably so negative that it could not be excited. The only remaining active substance is P^{29} which should be intense since it arises from the principal isotope of silicon. In the experiments, Si^{31} was easily detected after all of the shorter periods had disappeared. The only short period which was not obviously due to impurities was one of half-life 6–8 minutes and may have been due to P^{29}.

Strong sources of Si^{31} could be prepared by bombarding silicon targets for an hour or more and allowing about an hour for shorter periods to decay. The decay of the active substance could be followed for many half-lives, but owing to the presence of impurities of various substances, the half-lives obtained were not very reproducible. The best value for the half-life which has been obtained so far is 170 ± 10 minutes. This is to be compared with the value 150–180 minutes as found by Fermi[3] and his collaborators for the active substance from the reaction $P^{31}+n^1=Si^{31}+H^1$.

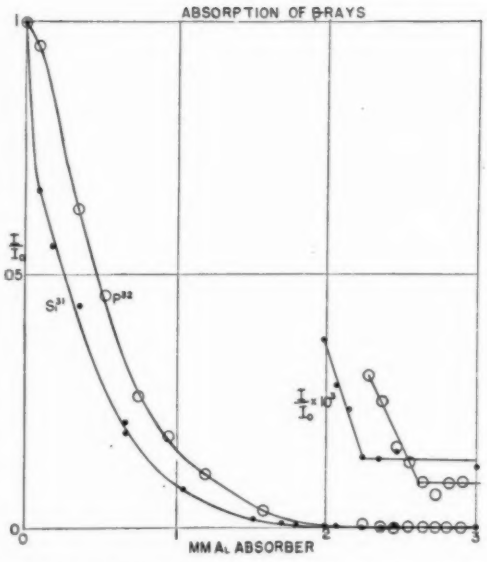

FIG. 2. The absorption of the electrons from Si^{31} and P^{32} in aluminum.

The chemical separation was carried out using the standard method for the analysis of silicon. The target was dissolved in concentrated potassium hydroxide, and silicic acid was precipitated in the presence of aluminum and phosphate ions, filtered in acid solution, and ignited in the usual manner. The activity of the silica which resulted was measured with an electroscope and found to be large. The silica was then treated with hydrofluoric and sulfuric acids to drive out all silicon as SiF_4. The residue was found to be completely inactive. This showed conclusively that the active substance of long life was an isotope of silicon; the filtrate was tested for active aluminium or phosphorus isotopes, but there were none present of long enough half-life to be detected at the end of this rather lengthy separation.

Cloud chamber experiments carried out by Kurie, Richardson, and Paxton showed that the disintegration particles are electrons and the absorption experiments which will be described confirm this result. The disintegration reaction is therefore:

$$Si^{31}=P^{31}+e^-.$$

The Absorption of Beta-Rays

Since both Si^{31} and P^{32} give off no gamma-rays, the absorption of the electrons may be measured accurately. Fig. 2 shows the absorption curves of the two substances in aluminum. From the large scale curves it will be seen that the ionization does not become truly constant until the intensity has been reduced to about one-thousandth of the original activity. This residual ionization, which is equal to about one-fifth of the natural leak of the electroscope, might be ascribed to weak gamma-rays, but experiments by McMillan[5] have shown that they are probably brehmstrahlen or x-rays due to the bombardment of the target material by β-rays. The end points of the absorption curves are very well marked and give maximum ranges in aluminum of 2.67 ± 0.04 mm and 2.51 ± 0.01 mm for P^{32} and Si^{31}, respectively. According to the empirical formula of Feather[6] these values correspond to energies of 1.59 ± 0.05 and 1.50 ± 0.01 Mev, respectively, while use of the range-energy relations of electrons leads to values slightly higher. These values are considerably lower than those obtained from the extrapolation of cloud track data according to the Uhlenbeck-Konopinski theory.[7]

It was thought that this discrepancy might be due to a high order of contact between the absorption curves and the axis as is predicted by the Uhlenbeck-Konopinski theory. To investigate this possibility, the absorption experiment was performed with two samples of Si^{31} where one sample was forty times as strong as the other. The result on the weaker sample gave a maximum energy of 1.44 ± 0.04 Mev as compared with the value for the intense sample previously given. The result showed a very slight increase in the maximum energy which was, however, nearly within the experimental error. It may be concluded, then, that the measured end point of the absorption curve is very close to the true end point. A careful determination of the maximum energy of the beta-rays from P^{32} has been made by Lyman[8] who finds a value of 1.7 Mev. The most recent result on the maximum energy of the beta-rays from Si^{31} has been made by Paxton[9] using cloud chamber data. He obtained a value of 1.65 Mev from the observed maximum energy of the energy distribution curves. The agreement between these two values and the results of the absorption experiments is very satisfactory considering the very different experimental conditions, and the fact that an empirical equation was used to obtain the energies of the electrons from their ranges.

It may be concluded from the above that reliable measurements on the maximum energy of beta-rays may be obtained by absorption measurements in the absence of gamma-rays. However, most artificially radioactive elements give off intense gamma-radiation, so that it is interesting to estimate what errors are introduced by the gamma-rays. If one gamma-ray quantum were given off per disintegration of P^{32}, the ionization due to the gamma would have been about one-fortieth of that due to the beta-rays. If one adds such a background to a logarithmic plot of the absorption of the beta-rays, it is found that, within the error of the instrument, the absorption curve meets the background at about 1.3 Mev instead of 1.6 Mev as found in the absence of gamma-rays.

In conclusion, I wish to express my gratitude to Professor Lawrence for the opportunity of using the cyclotron. I am also indebted to my colleagues at the Radiation Laboratory for both helpful discussion and practical assistance. The financial support of the Chemical Foundation and the Research Corporation is gratefully acknowledged.

[5] McMillan, Phys. Rev. **47**, 801 (1935).
[6] Feather, Phys. Rev. **35**, 1559 (1930).
[7] Kurie, Richardson and Paxton, Phys. Rev. **49**, 368 (1936).
[8] Lyman, Phys. Rev. **51**, 1 (1937).
[9] Paxton, Phys. Rev. **51**, 170 (1937).

Secondary Particles from the Penetrating Component of the Cosmic Radiation

WILLIAM H. PICKERING
Norman Bridge Laboratory of Physics, California Institute of Technology, Pasadena, California

(Received February 24, 1937)

Experiments are described that show that some of the coincidences between three Geiger counters in a vertical line separated by a considerable thickness of lead are not due to the passage of a single ionizing particle through the three counters but rather to secondary particles released in the lead near the counters. The experiments enable an estimate of the magnitude of this effect to be made.

EXPERIMENTS with coincidences between Geiger counters separated by considerable thicknesses of lead have shown the presence of a very penetrating component of the cosmic radiation that can apparently traverse as much as a meter of lead without suffering appreciable deviation from its straight path. The original experiments of Rossi[1] show that such an undeflected radiation is responsible for most of the coincidences, but new experiments that he reported at the London Conference in 1934[2] demonstrate that not all the coincidences are of this type. This paper is concerned with further experiments dealing with coincidences resulting from secondary particles.

The counters used in this work were of the usual copper-sealed-in-glass type, and were filled to a pressure of about 5 cm of mercury with a mixture of 80 percent argon and 20 percent air. Coincidences were selected by a circuit similar to those of Johnson and Rossi.

Three counters were first arranged as shown in Fig. 1. The lead between the counters totalled 15 cm and above the top counter was a lead plate 2.5 cm thick. The number of coincidences per hour was obtained with the lead blocks $a-a'$ in the position shown, and then with these blocks removed. It was found that removing the blocks decreased the counting rate about 7 percent. Obviously the extra coincidences caused by the blocks $a-a'$ must arise either from a bending of the path of the primary ionizing particle, or from a secondary particle generated in the extra lead. From the geometry of the arrangement it is clear that a deflection of a primary particle that had passed through the two top counters would have to be through a large angle and hence this possibility can be excluded as too rare to be significant. This means that the 7 percent more coincidences must be due to secondaries or showers produced in the extra lead beside the bottom counter.

The next experiment is a verification of the fact that secondaries may be formed at intervals along the path of the primary and not just near the end of its range. The same arrangement as Fig. 1 was used but the lead blocks $a-a'$ were removed. The counting rate was then measured with and without the 2.5 cm lead plate above the top counter. It was found that the presence of this lead increased the counting rate about 5.5 percent. This increase can only be ascribed to secondaries produced in the topmost lead.

There are two possible mechanisms by which such secondaries released in the top lead plate could increase the counting rate. First, if the primary is an ionizing particle then secondaries released in this lead could operate the top counter while the primary itself did not pass through this

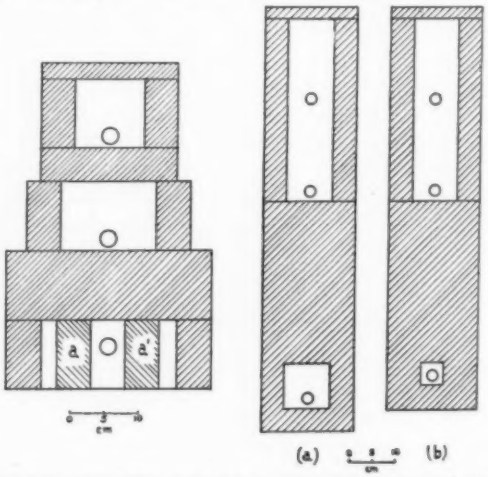

Fig. 1 (left) and Fig. 2 (right). Arrangements of lead about counters.

[1] Rossi, Zeits. f. Physik **82**, 151 (1933).
[2] Rossi, Report at London Conference, 1934.

counter but did operate the other counters. Primaries that passed through the top counter would not be affected by the top lead plate except insofar as the slight additional thickness of lead would cause a slight decrease in the number that reached the bottom counter. Second, if the primary did not ionize then the presence of the lead above the top counter would increase the probability that the primary would be accompanied by an ionizing secondary when it passed through this counter. Hence in this case the lead would cause an increase in the counting rate even with primaries that passed through the top counter.

These two possibilities may be investigated by a simple experiment, namely that of placing a lead block just the size of the geometrical beam defined by the counters, above the top counter. If all the coincidences are due to ionizing primaries then this lead should cause no increase in the counting rate, but rather a slight decrease, provided that there is sufficient lead between the counters to prevent secondaries from reaching the bottom counter. On the other hand, if the coincidences are due to radiation which does not ionize then this lead should cause an appreciable increase in the counting rate, provided that the radiation is not already accompanied by secondaries produced in the air or the roof above the apparatus. This experiment was performed with three counters separated by a total thickness of 20 cm of lead. A lead bar 3.0 cm thick and having a cross section equal to that of the top counter could be placed immediately above this counter. It was found that the lead above the counter increased the counting rate from 30.1 to 30.9 counts per hour with a probable error in each case of about 0.44 count per hour. Thus the effect of the additional lead is small, but these data seem to indicate that there may be a slight increase with the lead above the counters.

A further experiment shows that the secondaries responsible for additional coincidences are not able to penetrate more than a centimeter or two of lead. For this the counters were arranged as shown in Fig. 2, with 36 cm of lead between them and a 2.5 cm lead plate above the top counter. It will be noted that the difference between the two parts of this experiment lies in the arrangement of the lead around the bottom counter. The following results were obtained. In part (a) the lead plate above the top counter increased the counting rate 9 percent with a probable error of about 2 percent. In part (b) no increase could be observed within the limits of error, about 5 percent. The interpretation of the difference between the two cases is as follows: In part (a) secondaries generated in the top plate operate the top two counters while the primary continues through, or more probably, near the bottom counter. Occasionally this primary generates a secondary in the lead a short distance above the bottom counter and the secondary operates this counter and registers a coincidence. In part (b) the only difference is that for secondaries to operate the bottom counter they must be formed in a more restricted area than in part (a), and hence the path of the primary to register a coincidence is restricted to a smaller solid angle and fewer coincidences are observed. It is to be expected that if the experiment had been more accurate a small increase would have been found with arrangement (b). If the range of the secondaries had been more than 5 cm of lead then secondaries formed in the lead near the bottom counter in case (b) would have been able to reach this counter as well in this case as in case (a), and hence there would have been no difference in the two experiments. Since there is a difference the experiment offers good evidence that only secondaries formed within a very few centimeters of the bottom counter are effective in scoring extra coincidences.

The results of these experiments may be summed up as follows: When three Geiger counters are placed in a vertical line with a considerable thickness of lead between them, not all the observed coincidences result from the passage of single ionizing particles through the three counters, but a number which varies with the arrangement of the lead outside the geometrical beam formed by the counters, and which may be as much as 10 percent of the total number of coincidences, result from secondary particles that operate one or more of the counters. The secondaries that are effective in registering coincidences are those that make a large angle with the path of the primary, and accordingly their range is only a centimeter or two of lead.

I wish to thank Dr. R. A. Millikan for many helpful suggestions and discussions during the course of this work.

Structure of the X-Ray *K* Absorption Limits of Bromine, Iodine, and Some of Their Compounds

BERNARD CIOFFARI
Pupin Physics Laboratories, Columbia University, New York, N. Y.
(Received February 23, 1937)

The double crystal spectrometer has been used to investigate the structure, width, and relative positions of the *K* absorption limits of bromine in the vapor, liquid, and solid states; of iodine in the vapor and solid states; and of some compounds of these elements. Curves of these absorption limits are presented. Tables are given of the widths of these limits, of the relative displacements of the limits in compounds, and of the positions of secondary structure. The absorption limit of bromine vapor possesses a pronounced structure near the short wave-length side. This structure does not appear in the absorption limit of either the liquid or solid, or of any of the compounds investigated, except iodine monobromide vapor. The absorption limit of solid iodine shows a faint structure near the short wave-length side. A similar structure is found in the absorption limit of the vapor, but no shift is detected. The iodine *K* absorption limits of the compounds investigated show no measurable shifts.

INTRODUCTION

IN recent years, the double crystal x-ray spectrometer has been used by Barnes,[1] Ross,[2] Richtmyer and Barnes,[3] Zinn,[4] and Stephenson[5] for investigating the structure and width of *K* absorption limits, and by Hull[6] and Semat[7] for *L* absorption limits. The suitability of this instrument for such investigations was previously demonstrated by Bergen Davis and Harris Purks.[8] The effect of physical state and chemical combination on the absorption limits has been studied in the above investigations and also with the single crystal spectrograph by Hanawalt,[9] Coster and Veldkamp,[10] Lindsay,[11] Kawata,[12] and Lindh.[13]

This investigation was undertaken to study the effect of physical state and chemical combination upon the structure, width, and position of an absorption limit. The elements used were bromine in the vapor, liquid, and solid states, and iodine in the vapor and solid states. The compounds used were HBr, CH_3Br, KBr (solid), KBr (solution), IBr (solid), IBr (vapor), bromine water, CdI_2, HgI_2, KI, KIO_3 and SnI_4.

APPARATUS

The double crystal x-ray spectrometer was of the type described by Bergen Davis and Harris Purks.[8] A water-cooled x-ray tube with a tungsten target and a thin glass window was used in this investigation. The tube was operated at 26 kv and 31 ma for the bromine absorption edge, and at 45 kv and 20 ma for the iodine absorption edge. The beam was limited by slits 0.4 cm wide and 1.0 cm high. The ionization chamber was 7 cm long and 2.5 cm in diameter. It was filled with methyl bromide gas at atmospheric pressure for the study of the iodine absorption edge. Methyl iodide was used for the study of the bromine absorption edge. The ionization current was amplified by an FP-54 Pliotron and was read on a Leeds and Northrup type R galvanometer having a sensitivity of 10,000 megohms. The voltage sensitivity was about 10,000 mm/volt. Rates of deflection of the galvanometer were observed.

The cells for the vapors were made of Pyrex. They were 22 cm long, with thin windows at the ends and a side tube at the center. In all cases,

[1] A. H. Barnes, Phys. Rev. **44**, 141 (1933).
[2] P. A. Ross, Phys. Rev. **44**, 977 (1933).
[3] F. K. Richtmyer and S. W. Barnes, Science **77**, 459 (1933); Phys. Rev. **45**, 754 (1934).
[4] W. H. Zinn, Phys. Rev. **46**, 659 (1934).
[5] S. T. Stephenson, Phys. Rev. **44**, 349 (1933); **49**, 495 (1936); **50**, 790 (1936).
[6] H. L. Hull, Phys. Rev. **40**, 676 (1932).
[7] H. Semat, Phys. Rev. **46**, 688 (1934).
[8] Bergen Davis and Harris Purks, Proc. Nat. Acad. Sci. **13**, 419 (1927); Phys. Rev. **32**, 336 (1928).
[9] J. D. Hanawalt, Phys. Rev. **37**, 715 (1931); Zeits. f. Physik **70**, 293 (1931).
[10] D. Coster and J. Veldkamp, Zeits. f. Physik **70**, 306 (1931); **74**, 191 (1932).
[11] G. A. Lindsay, Zeits. f. Physik **71**, 735 (1931); B. Kievit and G. A. Lindsay, Phys. Rev. **36**, 648 (1930).
[12] S. Kawata, Kyoto Coll. Sci. Mem. **14**, 55 (1931); Phys. Math. Soc. Japan Proc. **17**, 89 (1935).
[13] A. E. Lindh, Comptes rendus **172**, 1175 (1921); Dissertation, Lund, 1923.

the amount of material contained in the cell was such that when it was all vaporized, the transmission curve showed optimum contrast. The temperature of the bromine cell was kept at 125°C, which is above the boiling point of bromine; that of the iodine cell was kept at 237°C, which is above the boiling point of iodine. Under these conditions the substances were completely vaporized, hence a small variation in temperature caused no change in the absorption. The temperature of the iodine monobromide cell was kept at 50°C. This was below the boiling point, but it was done to prevent excessive dissociation of the bromide into its elements. The heating coils were so arranged that the regions near the windows were kept at a higher temperature than the rest of the furnace, so as to prevent any condensation of vapor on the windows. The hydrogen bromide cell and the methyl bromide cell were kept at room temperature.

A cell of liquid bromine was made by using Pyrex capillary tubes filled with bromine and sealed off at both ends. These tubes were about 5 cm long and had an outside diameter of 1/10 mm, several hundred of them being used to form a single screen. To insure a reasonably uniform thickness of bromine, two screens were superimposed, each of which was made up of two layers of capillary tubes closely packed together. The cell of solid bromine was obtained by lowering the temperature of the liquid bromine cell by means of carbon dioxide snow. This was done by placing the absorption cell in a copper container provided with thin mica windows and enclosed in a wooden box in which the carbon dioxide snow was placed. The windows were kept clear of frost by blowing warm air over them. The bromine water and the KBr solution were contained in thin-walled paraffin cells. A screen of solid IBr was made by embedding the substance in paraffin. A screen of solid iodine was obtained by spraying an ether solution of iodine upon a microscope cover glass by means of an atomizer. As the ether evaporated, it left behind a fine-grained, uniform deposit of iodine. A similar cover glass was superimposed on the first, and the cell was sealed with paraffin. Substances in powder form were ground as fine as possible and sifted onto cigarette paper coated with a thin layer of castor oil. The thickness of screen used was that which gave maximum contrast in transmitted energy on the two sides of the absorption limit.

The absorbing screens were placed either between the crystals and the x-ray tube, or between the second crystal and the ionization chamber. With the exception of the vapor cells and of the solid bromine cell, the screens were oscillated several times per second in a direction perpendicular to the x-ray beam, in order to smooth out any effects due to nonuniformities in the screens.

In order to make sure that the transmission curves represented changes in energy due to the absorbing material and not fluctuations in the primary radiation, the following procedure was adopted: for each setting of the second crystal, observations were taken of the rates of deflection of the galvanometer, first with the absorber in place, and then with the absorber removed. Each transmission curve is thus accompanied by the corresponding curve of the primary radiation. In a like manner, the relative displacement of the absorption limit of a compound with respect to that of the element was determined by taking observations of the rates of deflection for the unfiltered energy, for the energy transmitted through the element, and for the energy transmitted through the compound, at each setting of the second crystal.

Experimental Results

The structure of the absorption limits of the substances investigated is shown in Figs. 1 to 5. These curves are the results of individual runs; but they are typical of several curves obtained for each substance. Each point on a curve represents the average of about ten readings. The ordinates represent the ratio I/I_0, where I is the x-ray energy transmitted through the absorber, and I_0 is the incident energy; the abscissae represent wave-lengths in x units. The values of the abscissae in volts and in seconds of arc are also indicated. The transmission curves of the compounds, plotted to the same scale as the elements, are shown displaced an arbitrary amount above the curve of the free element. The values of the ordinates correspond-

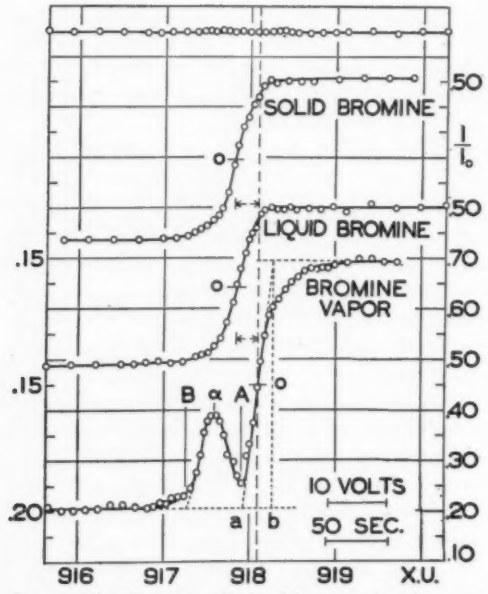

FIG. 1. The absorption limit of bromine for the vapor, liquid, and solid states. The broken vertical line shows the position of the absorption limit of bromine vapor. The center of each limit is marked by the letter *O*. The shift is indicated by the small arrows.

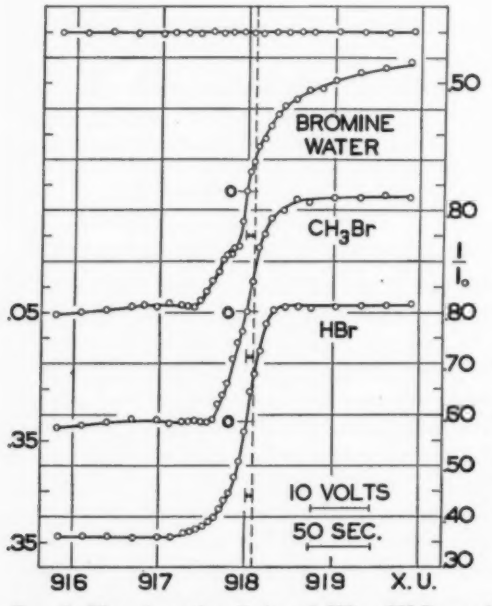

FIG. 2. The absorption limits of HBr, CH_3Br, and bromine water. The broken vertical line shows the position of the absorption limit of bromine vapor. The center of each limit is marked by the letter *O*. The shift is indicated by the small arrows.

ing to each individual curve are shown at the two ends of each curve. The scale units are the same for all curves. At the top of each figure is shown the plot of the incident energy.

The width of the absorption limit was obtained by drawing a straight line tangent to the curve at the point of greatest slope and determining its intersections with the ordinates of maximum and minimum energy. (*a–b* in Fig. 1.) The width of the rocking curve for the crystals

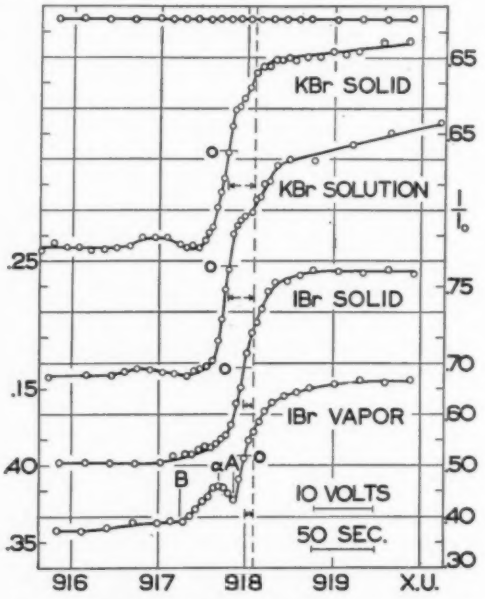

FIG. 3. The absorption limits of IBr vapor, IBr solid, KBr solution, and KBr solid. The broken vertical line shows the position of the absorption limit of bromine vapor. The center of each limit is marked by the letter *O*. The shift is indicated by the small arrows.

in the (1, −1) position was found to be 7.0 seconds. Different corrections for the crystal width have been proposed by Ehrenberg and Mark,[14] Schwarzschild,[15] Ross,[2] Barnes and Palmer,[16] Richtmyer, Barnes and Ramberg,[17] and Parratt.[18] The Ehrenberg-Mark-Schwarzschild equation gives a negligible correction.

[14] W. Ehrenberg and H. Mark, Zeits. f. Physik **42**, 807 (1927).
[15] M. M. Schwarzschild, Phys. Rev. **32**, 162 (1928).
[16] S. W. Barnes and L. D. Palmer, Phys. Rev. **43**, 1050 (1933).
[17] F. K. Richtmyer, S. W. Barnes and E. Ramberg, Phys. Rev. **46**, 843 (1934).
[18] L. G. Parratt, Rev. Sci. Inst. **6**, 387 (1935).

However, the other corrections proposed are quite appreciable. Since there appears to be, as yet, no general agreement regarding the correction to be used, the uncorrected values for the widths of the absorption edges have been given.

The wave-length position of the absorption limit is taken as that of the midpoint of the main edge. No attempt was made to measure this wave-length position, but the center of the limit was fixed on the wave-length scale at the best value given in Siegbahn's *Spektroskopie der Röntgenstrahlen*. The shift is obtained by measuring the displacement of the midpoint of the edge of the compound with respect to that of

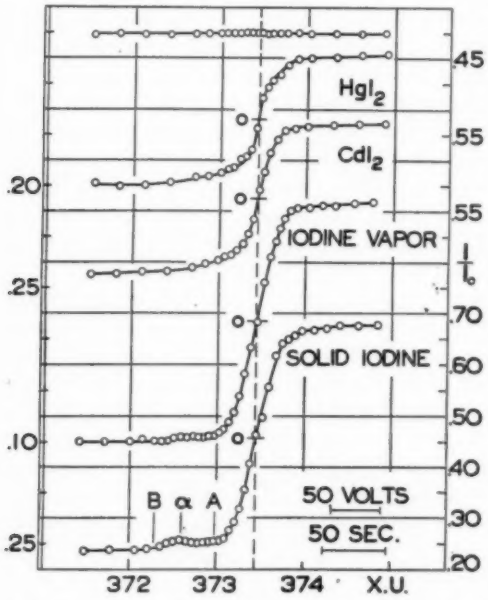

FIG. 4. The absorption limits of solid iodine, iodine vapor, CdI_2, and HgI_2. The broken vertical line shows the position of the absorption limit of iodine vapor. The center of each limit is marked by the letter *O*.

the element. For the bromine curves, all shifts are measured with respect to the absorption limit of the vapor.

Table I gives the widths of the absorption limits in seconds, in x units, and in volts. The values given are the averages obtained from all the curves taken, uncorrected for crystal width. Table II gives the displacements of the absorption limits of the compounds with respect to the absorption limit of the element. All of the shifts are to the short wave-length side of the absorption limit of the element. Table III shows the position, in volts, of the secondary structure with respect to the center of the absorption limit. The convention of Coster and Veldkamp[10] of labeling the minima of the transmission curves by A, B, C, and the maxima by α, β, γ is followed.

DISCUSSION

Secondary structure

The absorption limit of bromine vapor possesses a pronounced structure near the short wave-length side. (See Fig. 1.) The first minimum occurs at 2.7 volts, the first maximum at 6.6 volts, and the second minimum at 13.0 volts from the center of the edge. The structure found for the vapor does not appear either in the absorption limit of the liquid or of the solid. Bromine water does not show this structure, but it does show a break in the curve corresponding very nearly to the first minimum of the absorption limit of the vapor. (See Fig. 2.) Neither HBr nor CH_3Br shows any fine structure. The

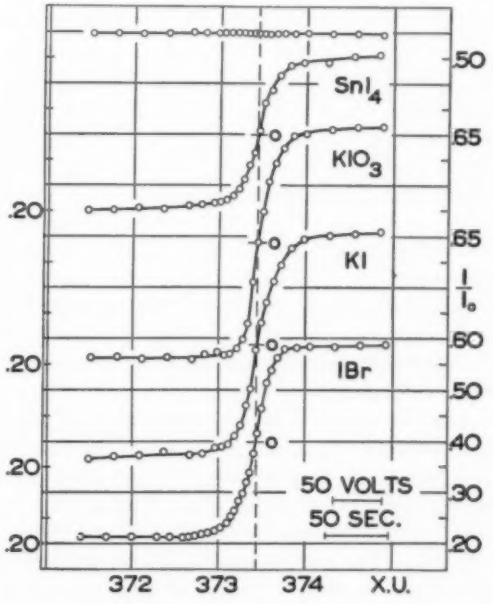

FIG. 5. The absorption limits of IBr, KI, KIO_3, and SnI_4. The broken vertical line shows the position of the absorption limit of iodine vapor. The center of each limit is marked by the letter *O*.

TABLE I. *Width of K absorption limits.*

SUBSTANCE	SECONDS	X.U.	VOLTS
Bromine vapor	24.9±1.0	0.362±0.015	5.3±0.2
Liquid bromine	32 ±3.0	0.46 ±0.04	6.8±0.6
Solid bromine	32 ±3.0	0.46 ±0.04	6.8±0.6
Bromine water	31 ±3.0	0.45 ±0.04	6.6±0.6
HBr	34 ±3.0	0.49 ±0.04	7.2±0.6
CH_2Br	48 ±3.0	0.70 ±0.04	10.2±0.6
KBr (solid)	34 ±3.0	0.49 ±0.04	7.2±0.6
KBr (solution)	33 ±3.0	0.48 ±0.04	7.0±0.6
IBr (solid)	34 ±3.0	0.49 ±0.04	7.2±0.6
IBr (vapor)	27 ±3.0	0.39 ±0.04	5.7±0.6
Solid iodine	35 ±3.0	0.51 ±0.04	45 ±3.9
Iodine vapor	36 ±3.0	0.53 ±0.04	46 ±3.9
CdI_2	26 ±3.0	0.38 ±0.04	34 ±3.9
IBr	31 ±3.0	0.45 ±0.04	40 ±3.9
HgI_2	25 ±3.0	0.37 ±0.04	33 ±3.9
KIO_3	25 ±3.0	0.37 ±0.04	33 ±3.9
SnI_4	30 ±3.0	0.44 ±0.04	39 ±3.9
KI	31 ±3.0	0.45 ±0.04	40 ±3.9

TABLE II. *Displacement of the K absorption limits.*

SUBSTANCE	VOLTS	SUBSTANCE	VOLTS
Bromine vapor	0	CH_2Br	1.3±0.3
Liquid bromine	3.6±0.3	KBr (solid)	4.5±0.3
Solid bromine	3.9±0.3	KBr (solution)	4.2±0.3
Bromine water	1.4±0.3	IBr (solid)	1.7±0.3
HBr	1.2±0.3	IBr (vapor)	1.3±0.3

TABLE III. *Position (in volts) of secondary structure.*

SUBSTANCE	*A*	*α*	*B*
Bromine vapor	2.7	6.6	13.0
KBr (solid)	6.5	13.4	22.4
KBr (solution)	7.5	14.8	21.8
IBr (vapor)	1.7	5.1	11.0
Solid iodine	41	79	103
Iodine vapor	41	75	101

absorption limits of the KBr solution and of the solid are identical within the limits of experimental error. (See Fig. 3.) The vapor IBr is the only one that shows a structure similar to that found for bromine vapor. Solid IBr does not show any structure.

The absorption limit of solid iodine shows a faint structure near the short wave-length side. (See Fig. 4.) The absorption limit of iodine vapor is very nearly the same as that of the solid, both with respect to position and with respect to structure. The compounds of iodine show some indications of fine structure at the base of the edge, but the structure is of the same order of magnitude as the experimental error, hence no attempt was made to investigate it thoroughly. None of the compounds of iodine investigated shows a measurable shift. Since a shift of two seconds of arc could have been detected, it is concluded that if any shifts are present, they must be less than about 2.5 volts.

Ross[2] has examined iodine with the double crystal spectrometer, employing iodine powder with beeswax binder. For the maxima α and β he obtained 77 volts and 120 volts respectively. The first maximum agrees with the value given in Table III. The second maximum was not resolved in this investigation, probably because the intensity was too low. The value of the uncorrected width reported in this paper is a little lower than the value reported by Ross.[2]

Since the absorption limit of bromine vapor was chosen for reference, the number of bromine vapor curves obtained was large, a total of 36. This accounts for the small probable error shown in Table I. Both the bromine vapor and the solid bromine were examined over a region of about 125 volts on the short wave-length side of the absorption limit. No conclusive evidence of any further structure was found. Stephenson[5] finds a structure in the absorption limit of bromine vapor that is very similar to the one reported here, but he finds slightly smaller values, both for the width of the edge and for the position of the secondary structure. An attempt was made to determine whether the structure found for the vapor disappears at higher temperatures. Data on the absorption limit were taken with the vapor held at 180°C and also with the vapor held at 350°C. No noticeable change in the appearance of the structure was observed. This result is to be expected if it is assumed that the structure should disappear for monatomic bromine, for at these temperatures, less than 0.2 percent of the bromine vapor is dissociated.

Structure of the type found for bromine vapor has been found by Prins[19] in the *K* absorption limit of nitrogen vapor and in the chlorine L_{III} absorption limit of CCl_4. It has been found by Lindh[13] in the *K* absorption limit of chlorine. Hanawalt[9] pointed out that polyatomic gases or vapors in general show fluctuations in the absorption coefficient extending to quite a distance from the absorption edge. Coster and

[19] J. A. Prins, Physica **1**, 1174 (1934).

Klamer[20] made accurate measurements of this structure for polyatomic gases. They investigated the *K* absorption limits of Ge and As in the vapors $GeCl_4$ and $AsCl_3$. An interpretation of this structure was given by Kronig[21] on the basis of the wave theory of matter. Hartree, Kronig, and Petersen[22] calculated the *K* absorption coefficient of Ge in $GeCl_4$. The positions of maxima and minima agree very well with the calculated values. However, the first maximum of Coster and Klamer's[20] experimental curve corresponds to the third maximum of the theoretical curve. The explanation given was that the first two theoretical maxima and minima were too close together to be resolved by the single crystal x-ray spectrometer, hence they appeared merely as an irregularity in the slope of the first maximum.

The structure found in the absorption edge of bromine vapor may be explained in a similar manner on the basis of Kronig's theory for polyatomic gases. The observed maximum is the same as the first maximum predicted by theory, for it is very readily resolved by the double crystal spectrometer. The following maxima and minima do not appear in the curve because their intensity is relatively small compared to that of the first, smaller than the experimental error. No attempt was made to calculate the position of the structure for bromine vapor. But an estimate was made of the order of magnitude to be expected, by taking the values found by Hartree, Kronig and Petersen[22] for $GeCl_4$, and calculating the values appropriate to the distance between atoms of the bromine molecule, which is given as 2.28 ± 0.06A by Wierl.[23] This could be readily done, for by Kronig's theory, the distances of the corresponding maxima and minima from the edge are inversely proportional to the square of the atomic distances. The values obtained in this manner were: $A = 0.9$ volt, $\alpha = 6.9$ volts, and $B = 12.0$ volts. These values are of the same order of magnitude as those found experimentally for bromine vapor. (See Table III.)

[20] D. Coster and G. H. Klamer, Physica **1**, 889 (1934).
[21] R. de L. Kronig, Zeits. f. Physik **70**, 317 (1931); **75**, 191 (1932); **75**, 468 (1932).
[22] D. R. Hartree, R. de L. Kronig and H. Petersen, Physica **1**, 895 (1934).
[23] R. Wierl, Ann. d. Physik **8**, 521 (1931).

From x-ray diffraction experiments with water and mercury, Danilow[24] was led to the view that the liquid state approximates in arrangement more closely the solid than the gaseous state. A comparison of the curves for the liquid, solid and vapor states of bromine, in Fig. 1, shows that the results of the present investigation support this conclusion. It is seen that the absorption edge of the liquid is nearly similar to that of the solid, but it is different from that of the vapor, both with respect to structure and to the position of the limit. The absence of structure for the liquid and solid may be explained by assuming that the different interatomic distances in the crystalline structure of the solid and in the closely-packed molecular arrangement of the liquid give rise to maxima and minima which overlap and cannot be resolved. The absorption edge of bromine water was investigated to see whether the pronounced structure found for the vapor appeared for the solution. The faint structure found may be explained by assuming the existence, in the bromine water, of a large fraction of undissociated molecules with a gaseous distribution. No noticeable difference was found between the absorption edges of solid KBr and of the solution; the same structure appeared in both edges. Yost[25] found similar results: he found no detectable difference in the *K* absorption of manganous and chromate ions in crystals and in water solutions. The fine structure found in the chromate edge of the solid salts was also observed in the spectra of the solutions.

The absorption limit of solid IBr does not show any structure. It is similar to that of solid bromine, although it is not displaced quite as much as the latter. The absorption limit of the vapor IBr does show a structure of the type found for bromine vapor, but it is less intense. The presence of this structure may be explained by the fact that there is some dissociation of the IBr vapor into iodine vapor and bromine vapor. No fine structure was found by Hanawalt[9] for molecules containing hydrogen, as AsH_3, HBr and HCl. Petersen[26] explains this as due to the

[24] V. Danilow, Acta Physicochimica **3**, 725 (1935).
[25] D. M. Yost, Phil. Mag. **8**, 845 (1929).
[26] H. Petersen, Zeits. f. Physik **76**, 768 (1932); **80**, 258 (1933); **98**, 569 (1936).

fact that the hydrogen atom scatters very little on account of its small nuclear charge. In this investigation, similar results were obtained for HBr and CH_3Br.

Width of edges

Zinn[4] has presented a curve showing that the volt width of the K absorption limit increases as the fourth power of the atomic number for elements above atomic number 32. The values of the widths of the bromine and of the iodine absorption limits obtained in this investigation fit the curve reasonably well, although in each case the value is somewhat lower than that given by the curve. It is reasonable to expect some fluctuations, in the values of the widths, about the values given by the curve, if consideration is given to the type of transition involved in the absorption, for the width of the edge may be considerably influenced by it. Thus, differences will arise between edges in which the absorption is produced mostly by a transition to a single incomplete level, and those in which the transitions are to any one of a large number of optical levels. The absorption edge of elements which possess either an incomplete outer level or an incomplete inner level seems to be produced mostly by transitions to the incomplete level. Thus, it was shown by Barnes[1] that for the elements Mn to Zn, the initial increase in absorption in the K absorption edge occurs at the same wave-length as the K_{β_2} line of the element, within the limits of experimental error. The K_{β_2} lines of these elements are produced by transitions from the inner incomplete level $M_{IV,V}$ to the K level. This seems to indicate that the absorption limit, in this case, is due to a transition from the K level to the incomplete inner level $M_{IV,V}$. Similarly, Sandström[27] has shown that the wave-length position of many absorption limits is the same as that of certain emission lines. For example, the initial increase in absorption in the K absorption limits of the elements Zn to Br occurs at the same wave-lengths as the K_{β_2} lines of the elements. This seems to indicate that the absorption limit, in this case, is due to a transition from the K level to the incomplete outer level $N_{II,III}$, since the K_{β_2} line is produced by a transition in the reverse direction between the same limits. It appears, then, that an absorption transition to the first incomplete level is more probable than a transition to higher levels of the atom, provided that such a transition is allowed by the selection rules. This allows some latitude to the widths of absorption edges. For in the case where most of the absorption takes place by a transition to an incomplete level, the initial large increase in the absorption is due to such a transition. If the width of the edge is equal to the sum of the widths of the energy levels involved in the transition, then in this case the edge will be relatively narrow, for the K level will supply practically the entire width. This circumstance might explain the narrow width found in bromine. If the width of the edge, measured by the triangle method, were equal to the sum of the widths of the K level and of the combined optical levels, as pointed out by Semat,[7] then the width of the bromine edge should be not less than 12.8 volts, which is the width of the combined optical levels of bromine. Actually, the width of the edge is 5.3 volts. It is thus concluded that the absorption limit represents a transition from the K level to the $N_{II,III}$ level of bromine.

In general, then, it seems that the width of the edge should depend on the type of transition involved in the absorption. If most of the absorption is due to a transition from the K level to the first unoccupied level, the edge will be relatively narrow and its width will be practically the same as the width of the K level. If the transition is from the K level to any one of a large number of optical levels, the width of the edge will be given by the sum of the widths of the K level and of the combined optical levels. The fine structure found in the edge itself, or very close to the edge, is produced by transitions to various permissible unoccupied optical levels, as predicted by Kossel.[28] The secondary structure found at a greater distance from the edge is produced by transitions to crystal lattice levels, as predicted by Kronig's theory.[21]

[27] A. E. Sandström, Nova Acta Regiae Soc. Scient. Upsal., Ser. 4, Vol. 9, No. 11 (1935); Phil. Mag. **22**, 497 (1936).

[28] W. Kossel, Zeits. f. Physik **1**, 119 (1920).

Effect of chemical combination

Chemical combination seems to have very little effect on the width of the K absorption edge. Most of the compounds of iodine investigated show a width nearly equal to that of the element. The compounds of bromine have very nearly the same width. The only exceptions are the IBr vapor, which has a slightly narrower width, and CH_3Br, which has a larger value for its width. The absorption edge of bromine vapor is the narrowest bromine edge found.

The shift found for HBr, 1.2 volts, compares favorably with that found by Hanawalt,[9] 1.5 volts, using photographic methods. The value of the shift found for CH_3Br, 1.3 volts, agrees with the value found by Stephenson,[5] 1.1 volts. The shift found for KBr, 4.5 volts, is of the same order of magnitude as that found by Hanawalt[9] for AgBr, 4.1 volts. Stephenson[5] finds a lower value for KBr and remarks that the effect of chemical combination on the position of the bromine edge seems to be less than that indicated by Hanawalt's data. Our data support Hanawalt's results.

It was thought desirable to check the effect of the thickness of the screen on the position and width of an absorption edge. Data were obtained on three different screens of solid iodine in which the transmission on the long wave-length side of the edge varied from 0.70 to 0.40. It was found that there is no change either in the position of the absorption limit or in its width, as the thickness of the screen is varied between these limits. Richtmyer and Barnes[3] show that the position and the width of an edge should vary with the thickness of the screen, but for the magnitude of variation of the thickness of the screens used for measurements of absorption limits, the change to be expected is too small to measure.

In conclusion, the writer wishes to thank Professor Bergen Davis for suggesting this problem, and for his interest and advice throughout the course of the investigation.

APRIL 15, 1937 PHYSICAL REVIEW VOLUME 51

X-Ray Fluorescence Yields

R. J. STEPHENSON
Ryerson Physical Laboratory, University of Chicago, Chicago, Illinois

(Received February 17, 1937)

The x-ray fluorescence yield for the K shell of atoms has been measured for a number of elements ranging from nickel to tin by an ionization chamber method similar to that developed by A. H. Compton. The results show an increase in the fluorescence yield with atomic number and are compared with those calculated by Massey and Burhop using relativistic wave mechanics and also with those calculated by Burhop from nonrelativistic wave mechanics. The fluorescence yield for the L_{III} shell of lead, thorium and uranium has been determined using suitable exciting radiation. An increase in the yield with atomic number is found.

INTRODUCTION

THE x-ray fluorescence yield, w_K, for the K shell of an assemblage of similar atoms is defined as the ratio of the number of fluorescence K quanta emitted per unit time to the number of atoms ionized in the K shell per unit time. Similar definitions may be applied to any one of the shells of an atom. It might be expected from the simple Bohr atomic theory that every atom ionized in the K shell would necessarily emit a K series quantum of radiation and that therefore this ratio would be unity. However, experiments have shown that this ratio is always less than unity although it increases with increase in the atomic number of the emitting atom. This phenomenon may be explained in either of two ways; first, by assuming that every atom ionized in the K shell emits a K series quantum but that in some of the atoms these quanta are photoelectrically absorbed in the parent atom with the ejection of an electron from an outer shell. The second explanation is

that an atom ionized in the K shell may return to a state of lower energy either by a transition of an outer electron to the K shell with the emission of a K series quantum of radiation, or by a radiationless transition in which the surplus energy available when an outer electron falls into the K shell is transferred to another electron of the atom and this electron thereby ejected from the atom. These ejected electrons are often referred to as Auger electrons since Auger discovered them and explained their origin.

If from a number of similar atoms ionized in the K shell there are n_f fluorescence K quanta emitted per unit time and n_A Auger electrons emitted per unit time the fluorescence yield, w_K, for these atoms is given by:

$$w_K = n_f/n_A + n_f, \tag{1}$$

since $n_A + n_f$ is the number of atoms ionized in the K shell per unit time.

There is another quantity called the *internal conversion coefficient*, I_K, which is often used in relation to this phenomenon. It is defined as the ratio of the number of Auger electrons emitted per unit time to the number of atoms ionized in the K shell per unit time, or

$$I_K = n_A/n_A + n_f. \tag{2}$$

From the definitions of fluorescence yield and internal conversion coefficient it follows that $w_K = 1 - I_K$.

Two methods have been used for experimentally determining the fluorescence yield. In the one introduced by Auger[1] a Wilson cloud chamber is used and electron tracks counted. This method is necessarily limited to gases. A second method adopted by A. H. Compton[2, 3] uses an ionization chamber. This is the method used in this experiment.

The object of this investigation was to determine the variation of fluorescence yield with atomic number. Although many similar investigations have been carried out the somewhat divergent results seemed to justify a repetition of the experiments. Berkey[4] reported a maximum fluorescence yield for molybdenum, atomic number 42. No such maximum has been found in the present work.

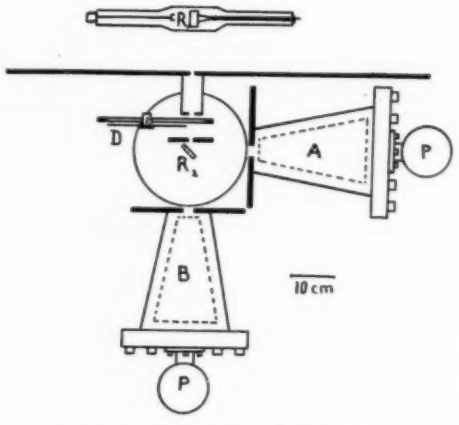

FIG. 1. Arrangement of apparatus.

THEORY

Suppose a beam of monochromatic x-rays of wave-length λ' falls at an angle of 45° on a solid radiator thus exciting K fluorescence radiation of average wave-length λ''. If P' is the power in the primary incident beam and P'' the power emerging from the radiator in a solid angle Ω at a mean angle of 45° with the radiator, then, as is shown elsewhere,[2]

$$w_K = \frac{1}{\Omega} \times \frac{r}{r-1} \times \frac{\mu' + \mu''}{\mu'} \times \frac{\lambda''}{\lambda'} \times \frac{P''}{P'}, \tag{3}$$

where μ' and μ'' are the coefficients of absorption in the radiator of the primary and secondary fluorescence beams respectively and r is the K absorption jump. Eq. (3) is a simplified form of Eq. (7.09) found on page 486 of *X-Rays in Theory and Experiment*. This simplification consists in using average values for the wave-lengths and absorption coefficients. The fraction $r-1/r$ represents the ratio of the amount of the primary beam absorbed in the K shell to that absorbed in the atom as a whole. The solid angle Ω depends on the geometrical arrangement of the apparatus and is equal to $A/4\pi r^2$, where A is the area of the ionization chamber window. (See Fig. 1.)

In the measurement of P' and P'' a correction

[1] P. Auger, Ann. d. Physik **6**, 183 (1926); Comptes rendus **180**, 65 (1925).
[2] A. H. Compton, Phil. Mag. **8**, 961 (1929).
[3] Compton and Allison, *X-Rays in Theory and Experiment* (D. Van Nostrand, 1936) p. 479.
[4] D. K. Berkey, Phys. Rev. **45**, 437 (1933).

must be made for the absorption and for the scattering of these radiations by the gas in the ionization chamber. The fraction f of the x-rays absorbed in the chamber is given by $f=1-e^{-\mu l}$ where μ is the absorption coefficient of the gas for the x-rays of the particular wave-length involved and l is the length of the ionization chamber. Of the fraction f of the x-rays absorbed in the chamber only a portion Rf produces ions. The fraction R is given by the equation[5]

$$R=1-\left(\frac{r-1}{r}e^{-\mu x_0}w_K\frac{\tau_K}{\mu}\frac{\lambda}{\lambda''}\right)_{\text{argon}}-\left(\frac{\sigma}{\mu}e^{-\mu' x}\right)_{\text{argon}}. \quad (4)$$

Comparing Eq. (4) with that given by Allison and Andrew on page 496 of *X-Rays in Theory and Experiment* it will be seen that again average values have been taken for wave-lengths and absorption coefficients. This averaging makes a negligible error and considerably simplifies the calculations. The second term of Eq. (4) represents that part of the incident beam of wave-length λ which produces argon fluorescence radiation of wave-length λ'' which is not absorbed in the chamber. Since the fluorescence yield for argon is small ($w_K=0.07$) and any argon fluorescence radiation produced has such a long wave-length that it is nearly all absorbed in the chamber, it follows that the second term is in this case negligibly small. The third term represents that fraction of the beam which is removed from the chamber by scattering and hence does not produce any ionization current. Since the ratio of scattering to total absorption, σ/μ, increases as the wave-length of the absorbed radiation decreases this term becomes of importance for short wave-length x-rays.

Apparatus

A nearly homogeneous beam of x-rays was obtained by using the fluorescence rays from a radiator R_1 placed just above the window of an x-ray tube, Fig. 1. This beam of x-rays passed through a series of circular holes whose diameter was 0.62 cm and fell on the radiator R_2 whose fluorescence yield was to be determined. The radiator R_2 was placed at the center of the table of an x-ray spectrometer at an angle of 45° to the incident beam. The fluorescence rays from R_2 entered the ionization chamber placed in position A and the resulting ionization current was measured. This was compared with the ionization current obtained with the ionization chamber in position B and the radiator R_2 removed.

Since the power P' of the primary beam which enters the ionization chamber in position B is several hundred times greater than the power P'' of the fluorescent beam entering the chamber in position A some device was necessary to bring the two beams to approximately the same power. At first the power in the primary beam was reduced by using thin absorbers of silver, but this was found unsatisfactory owing to the difficulty of measuring accurately the thickness and the absorption coefficients of the silver absorbers. A rotating disk D with an adjustable radial slot was then tried. This proved a very satisfactory means of reducing the power in the primary beam. The amount transmitted through the radial slot was found to increase uniformly with the angular opening of the slot for angles greater than 1°. When the radial slot was less than 1° the results were not reliable due presumably to edge effects of the slot. Throughout the experiments the slot was fixed at an angular opening of 1° thus reducing the power in the primary beam by 1/360. When further reduction was necessary aluminum absorbing screens were also used. The rotating disk D was placed on an arm so that it could be easily removed when not in use.

When investigating the fluorescence yields of elements of low atomic number up to selenium (34) an x-ray tube having a silver target and a radiator of molybdenum was used. Power for the x-ray tube was furnished by a motor generator set delivering current at 540 cycles to a transformer the high voltage from which was rectified and smoothed out by condensers. This equipment was designed by Professor S. K. Allison for providing constant current and voltage for x-ray use. Suitable ionization currents were obtained when the x-ray tube was operated at 40 kilovolts and 10 milliamperes. For the investigation of elements of higher atomic number from zirconium

[5] S. K. Allison and V. Andrew. Phys. Rev. **38**, 441 (1931).

(40) to tin (50) the silver target x-ray tube was replaced by one having a tungsten target. The radiator R_1 was then silver, tin or barium oxide depending on the element whose fluorescence yield was being investigated. The tungsten target tube was operated at about 65 kilovolts and 7 milliamperes.

The ionization chamber was of a conical shape to receive the divergent beam from R_2. Inside an earthed steel case and separated from it by about 1.5 cm was placed a conical grid of copper wire (shown dotted in Fig. 1) which was kept at about 140 volts and which formed the ionization chamber proper. Inside the conical grid were placed two collecting electrodes connected directly to an FP-54 vacuum tube. The chamber was arranged so that the x-ray beam never struck the collecting electrodes or the side walls of the grid. The window of the ionization chamber was 2.55 cm in diameter and was covered with heavy Cellophane. The length of the chamber was 23.7 cm and its front window was 12.7 cm from the center of the spectrometer.

The rear of the ionization chamber was made of a series of layers of wood, aluminum, iron and copper each about 3 mm thick. This prevented any x-rays which were not absorbed in the chamber from being scattered by the rear wall back into the chamber. The ionization chamber was capable of holding a pressure of 5 atmospheres though the actual pressure of the argon used in it depended on the wave-length of the x-rays being absorbed.

The wave-length λ' and λ'' for the primary and the fluorescence beams were calculated by taking the weighted mean of the α and β lines in accordance with the work of Williams.[6] The values of the K absorption jump r for each element investigated were taken from published data on absorption coefficients on the long and short wave-length side of the K absorption edge.

In determining the power in the primary and fluorescence beams P' and P'', respectively, it was necessary to make a correction both for absorption of the x-rays in the window of the ionization chamber and in the air between the radiator R_2 and the window. An attempt was made to determine if there was any scattered radiation present in the primary and fluorescence beams. This was done by making absorption measurements on the two beams. The results showed the scattered radiation in every case to be small and within experimental error. In the course of the investigation the pressure of the argon in the ionization chamber was changed several times so that the fluorescence yield for any one element was determined at several pressures of gas within the chamber. For a few elements the fluorescence yield was determined using primary radiation of several wave-lengths. No variation in the yield due to this factor was found. This is in accordance with the results of several previous investigators who found that the value of the fluorescence yield is independent of the wave-length of the exciting radiation. (Table I.)

The various primed quantities refer to the primary exciting radiation whereas the double primed quantities refer to the fluorescence radiation.

TABLE I. *Values used in calculations.*

R_1	R_2	λ'	λ''	$\frac{\mu'+\mu''}{\mu'\ \downarrow}$	$\frac{r-1}{r}$	$\frac{R'}{R''}$	$\frac{f'}{f''}$	$\frac{i''}{i'}$	$\frac{P''}{P'}$	ω_K
Mo	Ni28	0.695	1.635	2.25	0.881	0.967	0.431	0.65	0.000162	0.385
Mo	Cu29	.695	1.521	1.875	.879	.969	.435	.96	.00022	.41
Mo	Zn30	.695	1.42	1.87	.875	.970	.438	1.32	.000275	.48
Mo	Se34	.695	1.086	1.45	.866	.977	.507	2.76	.000555	.575
Sn	Zr40	.480	.770	1.525	.852	.95	.496	.464	.000605	.69
BaO	Zr40	.378	.770	1.985	.852	.905	.296	.497	.000368	.69
Sn	Mo42	.480	.695	1.405	.858	.96	.55	.535	.00078	.73
BaO	Mo42	.378	.695	1.77	.858	.91	.328	.595	.000495	.74
BaO	Rh45	.378	.600	1.56	.841	.92	.42	.613	.000664	.77
BaO	Ag47	.378	.545	1.432	.844	.93	.485	.66	.000837	.81
BaO	Cd48	.378	.523	1.39	.842	.936	.504	.668	.000875	.79
BaO	Sn50	.378	.480	1.316	.828	.95	.595	.64	.00101	.81

Discussion of Results

Fig. 2 shows a plot of the collected results of the various authors listed in Table II. The circled dots represent the author's results. The full curve A is that given by Massey and Burhop[7] for the K fluorescence yield and was obtained from theoretical calculations of the K fluorescence yield using relativistic wave mechanics. The dotted curve B shows the earlier nonrelativistic calculations by Burhop of the K fluorescence

[6] J. H. Williams. Phys. Rev. **44**, 146 (1933).
[7] H. S. W. Massey and E. H. S. Burhop. Proc. Roy. Soc. **153**, 661 (1936).

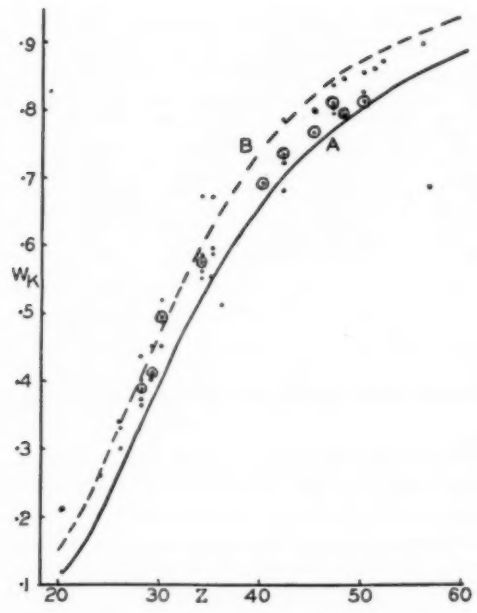

FIG. 2. Values of K fluorescence yields determined by various authors. The results of the present paper are encircled. Dotted curve gives nonrelativistic calculations by Burhop, the full curve gives the calculations of Massey and Burhop who used relativistic wave mechanics.

yields. These calculations are not exact as various approximations have to be made in order to evaluate certain integrals. The nonrelativistic curve* is not that given in this paper but is recalculated on the basis of an error pointed out in a later paper by Burhop.[8]

Thus we see that the data collected to date do not decide in favor of either curve, that is, between that based on the relativistic and that based on the nonrelativistic calculations. The author's results, however, definitely favor the relativistic calculations.

FLUORESCENCE YIELDS FOR THE L_{III} SHELLS OF LEAD, THORIUM AND URANIUM

The procedure in this experiment is the same as that for the determination of the fluorescence yields in the K shells, with the exception that now the radiator R_1 must be chosen so that the radiation which it emits has a wave-length in between the L_{II} and L_{III} absorption edges for the element R_2 under investigation. The radiation from molybdenum is such that it excites the radiation from the L_{III} shell of uranium but not from the L_{II} or any other shells in which the electrons have greater binding energy. In a similar manner suitable radiators were found for exciting the radiation from the L_{III} shells of thorium and lead. The Table III shows the data used in these experiments. The present value given in Table III for the fluorescence yield for the L_{III} shell of uranium is preferred to the author's earlier value[9] where silver absorbers were used to reduce the intensity of the primary beam. The present investigation showed that the

TABLE II. *Collected results of fluorescence yields in the K series.*

ELEMENT	AUGER	MARTIN[a]	COMPTON	HAAS[b]	LAY[c]	ARENDS[d]	BACKHURST[e]	STEPHENSON
18A	0.07							
20Ca				0.15	0.21			
24Cr				0.26	0.265			
26Fe		0.33			0.34	0.30		
28Ni		0.40	0.37		0.436	0.364		0.385
29Cu		0.45				0.401		0.41
30Zn		0.52			0.476	0.45		0.48
34Se		0.67	0.55		0.585	0.55		0.575
35Br		0.67	0.56					
36Kr	0.51							
40Zr								0.69
42Mo			0.68			0.724	0.785	0.735
45Rh							0.801	0.77
46Pd							0.835	
47Ag						0.795	0.838	0.81
48Cd							0.846	0.79
50Sn						0.825	0.855	0.81
51Sb							0.862	
52Te							0.872	
54Xe	0.70							
56Ba							0.900	

[a] L. H. Martin, Proc. Roy. Soc. **A115**, 420 (1927).
[b] M. Haas, Ann. d. Physik **16**, 473 (1932).
[c] H. Lay, Zeits. f. Physik **91**, 523 (1934).
[d] E. Arends, Ann. d. Physik **22**, 281 (1935).
[e] I. Backhurst, Phil. Mag. **22**, 737 (1936).

* Concerning the nonrelativistic curve:

$$I_K = n_A/n_A + n_f, \qquad I_K = 0.42;$$

$n_f = 48.0 \times 10^{-3}$ (data for silver from Burhop's paper). This data gives $n_A = 34.8 \times 10^{-3}$. The error concerned the value of n_f which should have been four times as great as the value given above, i.e., $n_f = 192.0 \times 10^{-3}$. Using this value for n_f and the above value for n_A the calculated value for I_K for silver is 0.154. The relation between I_K and Z, the atomic number of the element, is given by Wentzel and Burhop as $I_K = 1/1 + bZ^4$ where b is a constant. Substituting in this equation $I_K = 0.154$ and $Z = 47$ for silver the constant b is found to be 1.127×10^{-6}. This value for b has been used in calculating the points for the dotted curve in Fig. 2.

[8] E. H. S. Burhop. Proc. Roy. Soc. **148**, 272 (1935).

[9] R. J. Stephenson. Phys. Rev. **43**, 527 (1933).

TABLE III. *Values used in calculating the fluorescence yields from L_{III} shells of atoms.*

R_1	R_2	λL_{II}	λL_{III}	λ'	λ''	$\frac{\mu'+\mu''}{\mu'}$	$\frac{\tau-1}{\tau}$	$\frac{i''}{i'}$	$\frac{P''}{P'}$	ωL_{III}
Rb	Pb82	.8143	.9492	0.908	1.14	1.751	0.58	0.40	0.000214	0.32
Cb	Th90	.6293	.7600	.731	.925	1.796	.56	.97	.00026	.42
Mo	U92	.6913	.7208	.695	.876	1.81	.56	.325	.000274	.44

method of reducing the primary beam by silver absorbers was not capable of giving reliable results. Lay, using a photographic method for determining the power in the primary and fluorescence beams, gives a value of 0.41 for the fluorescence yield from the L_{III} shell of uranium.

The author is indebted to the Museum of Science and Industry of Chicago for the loan of a piece of uranium and to Professor S. K. Allison for many helpful discussions.

APRIL 15, 1937 PHYSICAL REVIEW VOLUME 51

The Energy Distribution of Photoelectrons Emitted by Calcium and Calcium Oxide*

ISRAEL LIBEN
George Eastman Research Laboratory of Physics, Massachusetts Institute of Technology, Cambridge, Massachusetts

(Received February 15, 1937)

Measurements of the energy distribution of the photoelectrons emitted from calcium with the aid of a magnetic velocity analyzer using radiation of wave-length λ2536 have been made. Special care was taken to eliminate contact potentials and to ensure that the emission observed was that from pure calcium. Energy distribution curves were obtained for pure Ca, CaO, and for a number of stages intermediate between the oxide and the pure metal. The theories of Fowler, DuBridge, Mitchell, and Nottingham were found to compare favorably with the data for pure Ca on the high energy side, but to depart from the data at low energies. The photoelectric work function obtained for pure Ca was 3.21 electron volts. The failure of all attempts to fit the above theories to the data for the oxide indicates that the Sommerfeld theory of a metal is not applicable to CaO.

INTRODUCTION

THE appearance of a number of theories of the emission of photoelectrons in recent years has indicated the desirability of developing a method of distinguishing between the various theories and comparing them with the experimental data. Rudberg[1] has shown that the energy distribution curves provide a suitable basis for such a comparison. According to Rudberg, for high energies the energy distribution curves predicted by all the theories are dominated by the Fermi factor

$$1/1+\exp\,(E-E_m)/kT,$$

where E is the energy, E_m is the maximum energy of emission when the temperature T is 0°K, and is defined by

$$E_m=h\nu-\varphi,$$

where φ is the photoelectric work function at the absolute zero of temperature, and ν is the frequency of the incident light. For small values of the energy the distribution function may be approximated by

$$kE^n,$$

where k is a constant. The exponent n differs for each theory and so may be used to differentiate between the theories.

Thus, though the high energy side of the energy distribution curve cannot be used to differentiate between various theories it may be used, in conjunction with the relation for E_m above, to obtain the value of the work function. The behavior of the distribution curve in the neighborhood of the origin determines the exponent n, and so may be used to compare the theories with the data.

A number of attempts have been made to use a uniform magnetic field to measure the energy distribution of photoelectrons. The first of these was by Ramsauer[2] in 1914. Ramsauer

* Submitted to the faculty of the Massachusetts Institute of Technology in partial fulfillment of the requirements for the degree of Doctor of Science.

[1] Rudberg, Phys. Rev. **48**, 811 (1935).

[2] Ramsauer, Ann. d. Physik **45**, 961 (1914); **45**, 1121 (1914).

studied the high energy side in an attempt to test the validity of the Einstein equation. In spite of all his attempts to eliminate reflected and scattered electrons Ramsauer's results were considerably distorted by these sources of error, and he drew the erroneous conclusion that there was no maximum energy of emission. The Fermi-Dirac statistics, of course, predict that for $T \neq 0$ there is really no maximum energy of emission, but, experimentally, at room temperatures an apparent maximum energy should have been found. Klemperer[3] in 1923 repeated Ramsauer's work and reached the conclusion that there was a maximum energy of emission even though his curves were affected by reflected and scattered electrons.

The method which has been used almost exclusively in photoelectric energy analysis work is that of stopping potentials. DuBridge and his co-workers have published a number of researches on energy analysis using stopping potentials, and principal among these we may mention the work of Roehr,[4] and of Brady.[5] However, until recently, these studies have been confined to the high energy side of the distribution curve which permits of an accurate determination of the work function. Quite recently Hill and DuBridge[6] have reported some work on the low energy side of the distribution curve for sodium. They indicate that no theory at present available could predict the energy distribution at low energies.

Theory of the Magnetic Velocity Analyzer

If a semicircle is defined by three slits and a uniform magnetic field H is normal to the plane of the semicircle, then electrons passing through slit 1 of Fig. 1 with a velocity v in a direction normal to the plane of the slit will pass through slit 2 if

$$Hev/c = mv^2/r.$$

Here e is the electronic charge, m the electronic mass, and c the velocity of light. It turns out that electrons passing through slit 1 at neighboring points and making small angles with the normal will converge to a small area at slit 2. It is this focusing property of the 180° deflection in a uniform magnetic field which makes such an arrangement valuable as a velocity analyzer.

The results of a more detailed analysis of the magnetic analyzer may be stated in a few paragraphs. The origin of a right-handed coordinate system is placed at 0 in Fig. 1, so that x and y are as shown, and H is along positive z. At time $t=0$ the electron enters the analyzer through the plane $y=0$. The angles θ and φ are defined as follows: θ is the angle between the velocity vector v at $t=0$ and the z axis, and φ is the angle between y and the projection of v on the xy plane. The initial conditions are:

$$\begin{aligned} x &= x_0, & \dot{x} &= v \sin\theta \sin\varphi, \\ y &= 0, & \dot{y} &= v \sin\theta \cos\varphi, \\ z &= z_0, & \dot{z} &= v \cos\theta. \end{aligned}$$

After deflection through 180° the electron enters the collecting slit with the coordinates x and y as follows:

$$\begin{aligned} x &= x_0 - (2v/a) \sin\theta \cos\varphi, \\ z &= z_0 - ((2\varphi+\pi)v \cos\theta)/a, \\ a &= -eH/mc. \end{aligned}$$

Eliminating θ above we obtain:

$$1 = (x-x_0)^2/(2v \cos\varphi/a)^2 + (z-z_0)^2/(2\varphi+\pi)^2(v/a)^2.$$

This is the equation of an ellipse in the xz plane with its center displaced to x_0, z_0. That is, all the electrons emitted at x_0, z_0 with a given velocity v and angle φ will be collected on an ellipse, so that theoretically the shape of the collecting slit for this case should be elliptical. Actually, however, a rectangular slit is a very good approximation for the values of angle and slit size here involved.

The equation above in x and z may be solved for $mv^2/2$, the energy of the electrons collected in the plane $y=0$ at x, z for given initial con-

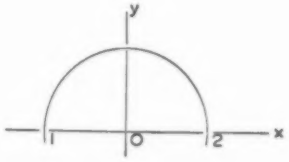

Fig. 1.

[3] Klemperer, Zeits. f. Physik **16**, 280 (1923).
[4] Roehr, Phys. Rev. **44**, 866 (1933).
[5] Brady, Phys. Rev. **48**, 768 (1934).
[6] Hill and DuBridge, Bull. Am. Phys. Soc. Vol. **11**, No. 2.

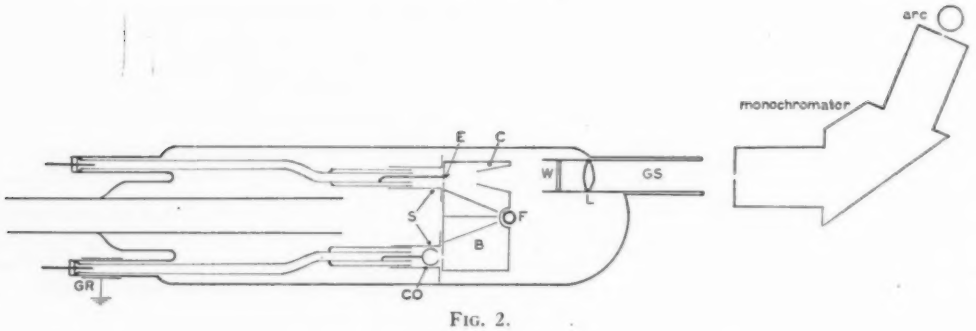

FIG. 2.

ditions. Since the experimental arrangement used allows a fixed, small but finite range of variation for each one of the variables in the relation for the energy, except a, there will be a corresponding spread in the energy of the electrons collected for a given setting of H, that is, for a given a. If E is the energy of the collected electrons, the spread in energy may be written as

$$\delta E=\delta(mv^2/2)=\frac{ma^2}{2}\delta\left[\frac{(x-x_0)^2}{4\cos^2\varphi}+\frac{(z-z_0)^2}{(2\varphi+\pi)^2}\right].$$

The variation on the right is a constant of the apparatus, and since a is proportional to H, the spread in energy of the electrons collected is proportional to H^2, and hence to the energy. Therefore, if the energy distribution of the emitted electrons is given by $dN=f(E)dE$, the current to the collector, for a given setting of H corresponding to an energy E, is proportional to $Ef(E)$. The energy distribution is obtained from the data by plotting the collector current divided by E versus E. If we define the resolving power of the analyzer as $\delta E/E$ it turns out to be 0.07 for the analyzer used.

APPARATUS

The tube used in making the measurements is shown in Fig. 2. All the sheet metal parts in the tube were made of tantalum. The box B was supported on two pieces of 50 mil tungsten wire passing through the four lower corners of the box and sealed to the central tubular support by means of glass rods. This central tube also served as a connection to the exhaust system. The calcium furnace F was supported on a piece of glass rod which ran beneath the box B to the central tube. The leads for the heating current for the furnace and for the thermocouple used to measure the temperature of the furnace, ran along the bottom of the tube to the left and were brought out through a four lead press. The shields S were used to protect the photoelectric emitter E and the collector CO from stray electrons. The emitter was a piece of tantalum 1 cm by 1 mm. The collecting slit was 2 cm by 1 mm. The separation of the centers of the emitter and the collector was 5.99 cm, so that $r=3.00$ cm. GS is a quartz-Pyrex graded seal of 27 mm inside diameter, while W is a quartz window. The collector CO was protected from leakage currents by the guard ring GR and the long leakage path interposed between the shield S and the collector by the double glass sleeves.

The light from the capillary arc[7] was focused on the first slit of the monochromator M by a quartz lens. The monochromator was one built by Bausch and Lomb and has rotating prisms and fixed slits. Light from the second slit of the monochromator was focused by the lens L on the emitter E. The wave-length of the light used was λ2536. With the second slit of the monochromator set at 0.6 mm the wave-lengths λ2536, λ3130, and λ3650 showed no background when photographed by a Hilger quartz spectrograph, model E2, using a 4″×10″ plate. The lens L was placed to give one-to-one magnification of the second slit upon the emitter. The size of the "slit" through which the photoelectrons entered the analyzer was thus 1 cm by 0.6 mm, which corresponds to slit 1 of Fig. 1.

[7] Harries and Hippel, Physik. Zeits. **33**, 81 (1932).

The furnace F sprayed the walls, the emitter, and the inner shields of the box with Ca. The temperature of the furnace was measured with a constantan platinum-iridium thermocouple. Using the data of Rudberg[8] the pressure of the Ca vapor in the furnace could be calculated, and so the rates at which the emitter was being covered with fresh Ca at any temperature.

The purpose of covering the entire inside of the box with Ca at the same time as the emitter and from the same source was to eliminate contact potential fields from the inside of the box. The cone C served to stop stray lines of force from entering the box.

The current to the collector was measured by a Compton electrometer with a high resistance shunt operating at a sensitivity of 5×10^{-15} amp./mm. Since the collector current is proportional to the total emission it was necessary to measure the total emission simultaneously with the collector current as a precaution against error. The total emission was measured with a simple d.c. amplifier using a type '22 tube.

The pressure inside the tube was measured with an ionization gauge built entirely of tantalum. The tube was kept on the pumps continuously and the pressure maintained at 10^{-7} mm of Hg.

The uniform magnetic field used to deflect the electrons through 180° was produced by a pair of Helmholtz coils. Since the applied field varied from zero to 1.5 gauss and thus was comparable with the earth's, it was necessary to eliminate the latter. This was done by another pair of Helmholtz coils adjusted to neutralize the entire local magnetic field.

Data

The total photoelectric emission of a freshly deposited Ca surface was found to decrease with time and eventually reach a constant value. This indicated that the usual technique of depositing a layer of metal and then studying its photoelectric properties could not be employed with Ca. To overcome this change in the Ca surface it was decided to deposit the Ca at the same time as the energy distribution curves were being measured. By varying the temperature of the furnace the rate of deposition of fresh Ca could be controlled, permitting the measurement of a family of energy distribution curves for a number of rates of deposition. Fig. 3 is such a family of curves. The numbers attached to each curve are the rates of coverage of the photoelectric emitting area in atomic layers per minute. The lowest curve is for a Ca surface which was allowed to stand in a vacuum until the total emission was constant. The upper curve is labeled with three rates of coverage, and since these three rates of coverage all gave identically the same curve it was therefore concluded that this curve is characteristic of pure Ca, since its photoelectric emission is independent of a further increase in the rate of coverage. The curves of Fig. 3 represent the average of a number of sets of data.

The exact nature of the surface when fresh Ca is allowed to stand in a vacuum for a number of hours is in doubt, though tentative conclusions may be drawn. The decrease in photo-current observed here has been observed by Brady and Jacobsmeyer[9] for Na on Al, and by Bosworth[10] for Na on W. The former attributed the effect to the formation of aggregates with a resulting decrease in the area exposed to the incident light, while the latter favored the theory that the Na migrated into the base material along the intercrystalline planes. The problem of the aging of Ca in a vacuum has been studied in some detail by

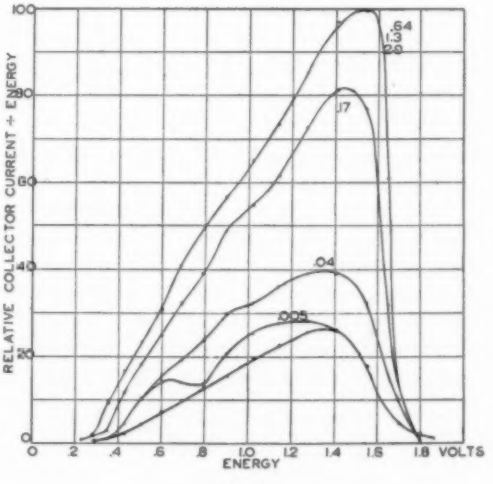

FIG. 3.

[8] Rudberg, Phys. Rev. **46**, 763 (1934).

[9] Brady and Jacobsmeyer, Phys. Rev. **49**, 650 (1936).

[10] Bosworth, Proc. Roy. Soc. **A150**, 56 (1935).

Rudberg.[11] He shot a homogenous beam of electrons at a Ca surface and measured the distribution of energy losses among those that were reflected. He found that the curves changed with time after a fresh Ca surface had been deposited, but the continued renewal of a getter surface of Ca in another part of the tube slowed down the rate of change; this indicated that it was some active gas in the tube which caused the change in the surface. When similar measurements were made on a deposit of CaO in the tube the distribution curves obtained showed characteristic energy losses identical with those for an aged Ca surface. This work on energy losses leads to the conclusion that a surface of Ca upon standing in an evacuated tube changes to CaO.

The high energy portion of the energy distribution curves of Fig. 3 were found to agree quite well with the Fermi factor with a temperature of 300°K and a maximum energy of emission at 0°K of 1.66 electron volts. Since the wave-length of the light used was λ2536 the photoelectric work function is found to be 3.21 electron volts.

A number of measurements of the work function of Ca have been made. Thus the following measurement have been published: Hughes, 3.34 volts;[12] Welch, 2.76 volts;[13] Hamer, 3.08 volts;[14] Pohl and Pringsheim, 1.76 volts;[15] Jamison and Cashman, 2.704 volts;[16] Rentschler and Henry, 3.08 volts.[17] The lowest value of 1.76 volts was obtained from the spectral distribution curve and is obviously too low. The low value is probably due to either the presence of alkali impurities in the Ca or to stray light of shorter wave-length than the desired one. The spread of 0.64 volt of the remaining five values is easily accounted for by variations in the surface.

The curve for CaO cannot be compared with the Fermi factor at high energies if the temperature is assumed to be 300°K. It is necessary to assume a temperature of 1000°K to obtain a fit. The high energy portion of the curve for λ3130, which was also measured as a test, required the assumption of a temperature of 700°K. Since the temperatures that would have to be assumed differed so widely from the true temperature (300°K) and among themselves it was concluded that the Sommerfeld theory of a metal is not applicable to CaO.

Some remarks are appropriate regarding the peculiar shapes of the distribution curves for rates of coverage less than the optimum. The curves might be composites obtained by adding the curves for CaO and Ca, but the separate curves for Ca and CaO indicate that this is not likely. A better guess would probably be that the surface is a composite of oxygen on Ca similiar to the composite surfaces of thorium on W, or caesium on W.

Comparison with Theory

According to Rudberg[1] the energy distribution function for small values of the energy E may be written as

$$f(E)=kE^n,$$

where k is a constant. Those theories which have values of n less than one may be discarded at the outset since they compare very poorly with the data. This leaves the theories of Fowler,[18] DuBridge,[19] Mitchell,[20] and Nottingham.[21]

The theories of Fowler and DuBridge give the same value for $f(E)$, which is

$$f(E)=kE/(1+\exp\,(E-E_m)/kT).$$

The theory of Mitchell, when applied to a magnetic analyzer of this type gives for $f(E)$,

$$f(E)=\frac{kE^{\frac{1}{2}}(E+W_a-h\nu)^{\frac{1}{2}}}{[1+\exp\,(E-E_m)/kT][E^{\frac{1}{2}}+(E+W_a)^{\frac{1}{2}}]}.$$

The theory proposed by Nottingham is semi-empirical in nature and leads to a value of $f(E)$ given by

$$f(E)=\frac{kE[1-\exp\,(-E/\omega)]}{[1+\exp\,(E-E_m)/kT]}\times\left[\frac{(E+W_a-h\nu)}{(h\nu-E)}+\frac{W_a\cos^{-1}((h\nu-E)/W_a)^{\frac{1}{2}}}{(h\nu-E)^{\frac{1}{2}}}\right].$$

[11] Rudberg, Proc. Roy. Soc. **A127**, 111 (1930).
[12] Hughes, Phil. Trans. Roy. Soc. **212**, 205 (1912).
[13] Welch, Phys. Rev. **32**, 657 (1928).
[14] Hamer, J. Opt. Soc. Am. **9**, 251 (1924).
[15] Pohl and Pringsheim, Verh. d. Deutsch. Phys. Ges. **16**, 336 (1914); **15**, 111 (1913); **14**, 546 (1912).
[16] Jamison and Cashman, Phys. Rev. **50**, 624 (1936).
[17] Rentschler and Henry, J. Opt. Soc. Am. **26**, 30 (1926).
[18] Fowler, Phys. Rev. **38**, 45 (1931).
[19] DuBridge, Phys. Rev. **43**, 727 (1933).
[20] Mitchell, Proc. Roy. Soc. **A146**, 442 (1934); **A153**, 513 (1936); Proc. Camb. Phil. Soc. **31**, 416 (1935).
[21] Private communication.

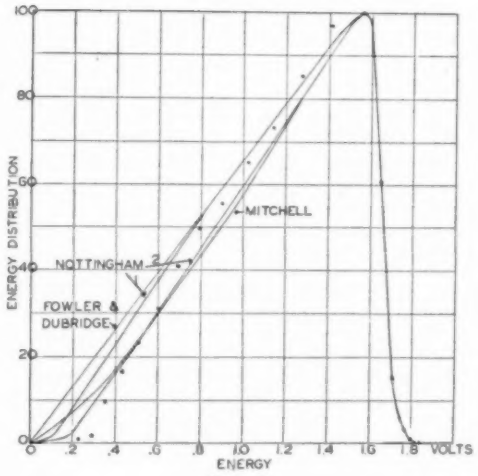

FIG. 4.

ω is a constant found by Nottingham to be 0.192 ev from measurements on W and thoriated tungsten. If we take $\omega = 0.4$ volt a better fit is obtained with the experimental data.

Fig. 4 is a plot of the energy distribution functions given above, while the points represent the experimental data. The curve marked Nottingham 1 is for the case of $\omega = 0.192$ volt and Nottingham 2 is for $\omega = 0.4$ volt.

The theories of Fowler and DuBridge predict the same curve and it is obvious from the figure that they lack some essential factor which would operate at low energies to bring the theory into agreement with the data. The theories of Mitchell and Nottingham appear to have partially overcome this lack of an essential factor.

In his computations Mitchell assumed that the surface potential barrier was a square topped barrier. The effect of this assumption as compared with an image force barrier has been discussed by Myers.[22] He concludes that the image force barrier increases the number of slow electrons. Another assumption made by Mitchell was that the internal potential was constant. The use of a potential varying with the lattice introduces two corrections. The first is equivalent to a change in the number of free electrons per atom, and this has a negligible effect upon the distribution curves, the second correction is the introduction of surface roughness whose effect cannot be entirely evaluated at present. Mitchell assumed that the amplitude of the vector potential of the light wave remained constant in the metal, but Schiff and Thomas[23] have shown that the amplitude of the vector, potential fluctuates rapidly just inside the metal. However, it is difficult to calculate the effect of this fluctuation and so it is as yet indeterminate.

I wish to take this opportunity to express my thanks and appreciation to Dr. Erik G. Rudberg for the unstinted aid and guidance he extended throughout the course of this work. I should also like to thank Mr. James E. Ryan for placing his skill as a glassblower at my disposal.

[22] Myers, Phys. Rev. **49**, 938 (1936).
[23] Schiff and Thomas, Phys. Rev. **47**, 860 (1934).

On Nonadiabatic Processes in Inhomogeneous Fields

JULIAN SCHWINGER
Columbia University, New York, N. Y.
(Received March 1, 1937)

The problem of calculating nonadiabatic transition probabilities is considered. It is shown that the general Güttinger equations are incorrect and lead to erroneous results in any case other than that of the rotating magnetic field, which he considered. The corrected equations are applied in the calculation of the transition probabilities between the various magnetic states of a field precessing with constant angular velocity.

AN atom, or a neutron, moving in an inhomogeneous field is acted on by a time-varying field in the reference system of the particle. If the variation in the field is sufficiently slow, the atom, according to the adiabatic theorem, will remain in the same state with respect to the instantaneous value of the field. The problem of calculating nonadiabatic transition probabilities has been considered by Güttinger,[1] who applied his general equations to the case of a magnetic field rotating with constant angular velocity.

It is the purpose of this paper to point out that Güttinger's equations are incorrect and lead to erroneous results in any case other than that of the rotating field, which he considered. The corrected equations are applied in the calculation of the transition probabilities between the various magnetic states of a field precessing with constant angular velocity.

THE GÜTTINGER EQUATIONS

Consider an atom whose Hamiltonian contains certain time dependent parameters, such as electric or magnetic field strengths. The eigenstate of the system satisfies the equation

$$i\hbar\frac{\partial}{\partial t}\Psi=\mathfrak{H}(t)\Psi. \tag{1}$$

If the system is nondegenerate, Ψ may be expanded in terms of a complete, orthogonal set of eigenstates of $\mathfrak{H}(t)$, *viz.*:

$$\Psi=\sum_m C_m(t)\Psi_m(t), \tag{2}$$

where
$$\mathfrak{H}(t)\Psi_m(t)=E_m(t)\Psi_m(t). \tag{3}$$

[1] P. Güttinger, Zeits. f. Physik **73**, 169 (1931); see also E. Majorana, Nuovo Cimento **9**, 43 (1932); I. I. Rabi, Phys. Rev. **49**, 324 (1936).

It should be emphasized that $E_m(t)$ and $\Psi_m(t)$ are functions of t only in virtue of the time dependence of the parameters contained in $\mathfrak{H}(t)$. The equations which the probability amplitudes $C_m(t)$ satisfy are

$$i\hbar\frac{\partial}{\partial t}C_m(t)-E_m(t)C_m(t)=-i\hbar\sum_{m'}\left(\Psi_m,\frac{\partial\Psi_{m'}}{\partial t}\right)C_{m'}. \tag{4}$$

To put this in a more convenient form, consider $(\partial/\partial t)(\Psi_m,\mathfrak{H}\Psi_{m'})$. Evidently,

$$\begin{aligned}\frac{\partial}{\partial t}(\Psi_m,\mathfrak{H}\Psi_{m'})&=\left(\Psi_m,\frac{\partial\mathfrak{H}}{\partial t}\Psi_{m'}\right)\\&\quad+\left(\frac{\partial\Psi_m}{\partial t},\mathfrak{H}\Psi_{m'}\right)+\left(\Psi_m,\mathfrak{H}\frac{\partial\Psi_{m'}}{\partial t}\right)\\&=\left(\Psi_m,\frac{\partial\mathfrak{H}}{\partial t}\Psi_{m'}\right)+(E_m-E_{m'})\left(\Psi_m,\frac{\partial\Psi_{m'}}{\partial t}\right).\end{aligned} \tag{5}$$

This expression may also be evaluated as $\delta_{m,m'}(\partial E_m/\partial t)$. Therefore,

$$\left(\Psi_m,\frac{\partial\mathfrak{H}}{\partial t}\Psi_{m'}\right)+(E_m-E_{m'})\left(\Psi_m,\frac{\partial\Psi_{m'}}{\partial t}\right)=\delta_{m,m'}\frac{\partial E_m}{\partial t}, \tag{6}$$

whence

$$\left(\Psi_m,\frac{\partial\mathfrak{H}}{\partial t}\Psi_m\right)\equiv\left(m\left|\frac{\partial\mathfrak{H}}{\partial t}\right|m\right)=\frac{\partial E_m}{\partial t}, \tag{7}$$

and

$$\left(\Psi_m,\frac{\partial\Psi_{m'}}{\partial t}\right)=-\frac{(m|\partial\mathfrak{H}/\partial t|m')}{E_m-E_{m'}},\quad m\neq m'. \tag{8}$$

Substituting this latter relation into Eq. (4), we obtain:

$$ih\frac{\partial C_m}{\partial t}-E_mC_m=ih\sum_{m'\neq m}\frac{(m|\partial\mathcal{H}/\partial t|m')}{E_m-E_{m'}}C_{m'}$$
$$-ih\left(\Psi_m,\frac{\partial\Psi_m}{\partial t}\right)C_m. \quad (9)$$

Save for the last term, these equations agree with Güttinger's. Unfortunately, it does not seem possible to find a general expression for this additional term without actually solving Eq. (3). In the next section, we shall solve this equation for a rather general Hamiltonian which includes most of the cases of interest.

Solution of the Eigenstate Equation

In this section, we shall solve Eq. (3) for a Hamiltonian of the form (discarding irrelevant addltive terms):

$$\mathcal{H}(t)=-g\mu_0\mathbf{J}\cdot\mathbf{H}(t), \quad (10)$$

where $\mathbf{J}$ is an arbitrary angular momentum vector in units of h, and μ_0 is the Bohr magneton. This is the appropriate description of a magnetic field $\mathbf{H}(t)$ interacting with (a) the magnetic moment of a neutron; (b) the electronic magnetic moment of an atom with zero nuclear moment; (c) the nuclear moment of an atom with vanishing electronic moment. Referred to a vector coordinate system fixed in space, $\mathbf{H}$ may be written

$$\mathbf{H}(t)=H(\mathbf{i}\sin\vartheta\cos\varphi+\mathbf{j}\sin\vartheta\sin\varphi+\mathbf{k}\cos\vartheta), \quad (11)$$

with H, ϑ, and φ functions of the time. Hence,

$$\mathcal{H}=-g\mu_0HJ_\xi, \quad (12)$$

where

$$J_\xi=\mathbf{J}\cdot\mathbf{H}/H=J_x\sin\vartheta\cos\varphi$$
$$+J_y\sin\vartheta\sin\varphi+J_z\cos\vartheta. \quad (13)$$

An eigenstate Ψ_m of J_ξ, satisfying the equation

$$J_\xi\Psi_m=m\Psi_m, \quad -j\leq m\leq j, \quad (14)$$

will be an eigenstate of $\mathcal{H}$ corresponding to the energy,

$$E_m(t)=-mg\mu_0H(t). \quad (15)$$

The solution of Eq. (4) will, therefore, be a solution of Eq. (3) with the eigenvalue (15).

The substitution, $\Psi_m=e^{-iJ_z\varphi}\Psi_m'$, transforms Eq. (14) into:

$$(\sin\vartheta\cos\varphi e^{iJ_z\varphi}J_xe^{-iJ_z\varphi}+\sin\vartheta\sin\varphi e^{iJ_z\varphi}J_ye^{-iJ_z\varphi}$$
$$+\cos\vartheta J_z)\Psi_m'=m\Psi_m'. \quad (16)$$

Denoting $e^{iJ_z\varphi}J_xe^{-iJ_z\varphi}$, $e^{iJ_z\varphi}J_ye^{-iJ_z\varphi}$, by $A_x(\varphi)$, $A_y(\varphi)$, respectively, we have

$$\frac{dA_x(\varphi)}{d\varphi}=ie^{iJ_z\varphi}(J_xJ_z-J_zJ_x)e^{-iJ_z\varphi}=-A_y(\varphi),$$
$$\frac{dA_y(\varphi)}{d\varphi}=ie^{iJ_z\varphi}(J_zJ_y-J_yJ_z)e^{-iJ_z\varphi}=A_x(\varphi). \quad (17)$$

Therefore,

$$A_x(\varphi)=A_x(0)\cos\varphi-A_y(0)\sin\varphi,$$
$$A_y(\varphi)=A_x(0)\sin\varphi+A_y(0)\cos\varphi, \quad (18)$$

or

$$e^{iJ_z\varphi}J_xe^{-iJ_z\varphi}=J_x\cos\varphi-J_y\sin\varphi,$$
$$e^{iJ_z\varphi}J_ye^{-iJ_z\varphi}=J_x\sin\varphi+J_y\cos\varphi. \quad (19)$$

Utilizing these relations in Eq. (16), we find that Ψ_m' satisfies an equation independent of φ, *viz.*:

$$(\sin\vartheta J_x+\cos\vartheta J_z)\Psi_m'=m\Psi_m'. \quad (20)$$

The further substitution,

$$\Psi_m'=\exp(-iJ_y\vartheta)\Psi_m^{(0)},$$

yields:

$$J_z\Psi_m^{(0)}=m\Psi_m^{(0)}, \quad (21)$$

with the aid of the relations

$$e^{iJ_y\vartheta}J_xe^{-iJ_y\vartheta}=\cos\vartheta J_x+\sin\vartheta J_z,$$
$$e^{iJ_y\vartheta}J_ze^{-iJ_y\vartheta}=-\sin\vartheta J_x+\cos\vartheta J_z. \quad (22)$$

Consequently, $\Psi_m^{(0)}$ is an eigenstate of the z component of angular momentum corresponding to the eigenvalue m. Combining the two substitutions, we obtain, finally:

$$\Psi_m=e^{-iJ_z\varphi}e^{-iJ_y\vartheta}\Psi_m^{(0)}. \quad (23)$$

Having found the eigenstates, we can substitute directly into Eq. (4), without using the

corrected Güttinger equations. One need merely evaluate

$$\left(\Psi_m, \frac{\partial \Psi_{m'}}{\partial t}\right).$$ Now,

$$\frac{\partial \Psi_{m'}}{\partial t} = -i\dot{\varphi} J_z e^{-iJ_z\varphi} e^{-iJ_y\vartheta} \Psi_{m'}{}^{(0)} - i\dot{\vartheta} e^{-iJ_z\varphi} J_y e^{-iJ_y\vartheta} \Psi_{m'}{}^{(0)}, \quad (24)$$

whence we obtain:

$$\left(\Psi_m, \frac{\partial \Psi_{m'}}{\partial t}\right) = -i\dot{\varphi}(\Psi_m{}^{(0)}, e^{iJ_y\vartheta} J_z e^{-iJ_y\vartheta} \Psi_{m'}{}^{(0)}) - i\dot{\vartheta}(\Psi_m{}^{(0)}, J_y \Psi_{m'}{}^{(0)})$$
$$= -i\dot{\varphi} \cos\vartheta (m|J_z|m') + i\dot{\varphi} \sin\vartheta (m|J_x|m') - i\dot{\vartheta}(m|J_y|m'), \quad (25)$$

using the second relation of Eq. (22). The only nonvanishing expressions of this type are:

$$\left(\Psi_m, \frac{\partial \Psi_m}{\partial t}\right) = -i\dot{\varphi} \cos\vartheta m,$$

$$\left(\Psi_m, \frac{\partial \Psi_{m-1}}{\partial t}\right) = (i\dot{\varphi} \sin\vartheta - \dot{\vartheta}) \tfrac{1}{2}((j+m)(j-m+1))^{\frac{1}{2}},$$

$$\left(\Psi_m, \frac{\partial \Psi_{m+1}}{\partial t}\right) = (i\dot{\varphi} \sin\vartheta + \dot{\vartheta}) \tfrac{1}{2}((j-m)(j+m+1))^{\frac{1}{2}}. \quad (26)$$

Hence, the differential equations for the probability amplitudes become:

$$i\hbar \frac{\partial C_m}{\partial t} + mg\mu_0 H C_m = -\hbar\dot{\varphi} \cos\vartheta m C_m + \tfrac{1}{2}\hbar(\dot{\varphi} \sin\vartheta + i\dot{\vartheta})((j+m)(j-m+1))^{\frac{1}{2}} C_{m-1} + \tfrac{1}{2}\hbar(\dot{\varphi} \sin\vartheta - i\dot{\vartheta})((j-m)(j+m+1))^{\frac{1}{2}} C_{m+1}. \quad (27)$$

The Precessing Field

The most general field giving rise to a set of equations for the C_m with constant coefficients satisfies the conditions:

$$\frac{dH}{dt} = 0, \quad \dot{\vartheta} = 0, \quad \dot{\varphi} = \omega = \text{const.}, \quad (28)$$

which is the mathematical description of a field precessing with constant angular velocity ω around the z axis. In this case, Eq. (27) reduces to:

$$i\hbar \frac{\partial C_m}{\partial t} = -m(g\mu_0 H + \hbar\omega \cos\vartheta) C_m + \tfrac{1}{2}\hbar\omega \sin\vartheta((j+m)(j-m+1))^{\frac{1}{2}} C_{m-1} + \tfrac{1}{2}\hbar\omega \sin\vartheta((j-m)(j+m+1))^{\frac{1}{2}} C_{m+1}. \quad (29)$$

To solve this set of equations, let us introduce the eigenstate Φ, defined by

$$\Phi = \sum_m C_m(t) \Psi_m{}^{(0)}. \quad (30)$$

It is easily verified that $\Phi(t)$ satisfies a differential equation of Hamiltonian form, namely:

$$i\hbar \frac{\partial}{\partial t}\Phi = \{-(g\mu_0 H + \hbar\omega \cos\vartheta) J_z + \hbar\omega \sin\vartheta J_x\}\Phi. \quad (31)$$

In terms of the angle Θ, defined by

$$\tan\Theta = \frac{\hbar\omega \sin\vartheta}{\hbar\omega \cos\vartheta + g\mu_0 H}, \quad (32)$$

this may be written

$$i\hbar \frac{\partial}{\partial t}\Phi = -\frac{\hbar\omega \sin\vartheta}{\sin\Theta}(\cos\Theta J_z - \sin\Theta J_x)\Phi. \quad (33)$$

The transformation, $\Phi = e^{iJ_y\Theta}\Phi'$, simplifies this equation to

$$i\hbar \frac{\partial}{\partial t}\Phi' = -\frac{\hbar\omega \sin\vartheta}{\sin\Theta} J_z \Phi', \quad (34)$$

the solution of which is

$$\Phi' = \sum_m C_m' \Psi_m{}^{(0)} e^{-(i/\hbar)E_m' t}. \quad (35)$$

Here, the C_m' are arbitrary integration constants, and

$$E_m' = -m\frac{\hbar\omega \sin\vartheta}{\sin\Theta} = -m(g^2\mu_0^2 H^2 + 2g\mu_0 H\hbar\omega \cos\vartheta + \hbar^2\omega^2)^{\frac{1}{2}}. \quad (36)$$

Therefore,

$$\Phi = e^{iJ_y\Theta} \sum_m C_m' \Psi_m{}^{(0)} e^{-(i/\hbar)E_m' t}, \quad (37)$$

from which we obtain

$$C_m(t) = (\Psi_m^{(0)}, \Phi) = \sum_{m'} (m|e^{iJ_y\Theta}|m')C_{m'}'e^{-(i/\hbar)E_{m'}'t}. \quad (38)$$

The integration constants C_m' are easily evaluated in terms of the initial conditions. By Eq. (38) we have

$$C_m(0) = \sum_{m'} (m|e^{iJ_y\Theta}|m')C_{m'}', \quad (39)$$

whence we obtain

$$\sum_{m'} (m|e^{-iJ_y\Theta}|m')C_{m'}(0) = \sum_{m', m''} (m|e^{-iJ_y\Theta}|m')(m'|e^{iJ_y\Theta}|m'')C_{m''}' = C_m', \quad (40)$$

by the matrix law of multiplication. Hence,

$$C_m(t) = \sum_{m', m''} (m|e^{iJ_y\Theta}|m')e^{-(i/\hbar)E_{m'}'t} \times (m'|e^{-iJ_y\Theta}|m'')C_{m''}(0). \quad (41)$$

$e^{-(i/\hbar)E_{m'}'t}$ is the diagonal matrix element of the operator $e^{(i/\hbar)\gamma tJ_z}$, where γ denotes $(g^2\mu_0^2H^2 + 2g\mu_0H\hbar\omega\cos\vartheta + \hbar^2\omega^2)^{\frac{1}{2}}$. Therefore,

$$C_m(t) = \sum (m|e^{iJ_y\Theta}|m')(m'|e^{(i/\hbar)\gamma tJ_z}|m'') \times (m''|e^{-iJ_y\Theta}|m''')C_{m'''}(0) = \sum_{m'} (m|e^{iJ_y\Theta}e^{(i/\hbar)\gamma tJ_z}e^{-iJ_y\Theta}|m')C_{m'}(0). \quad (42)$$

If the system is initially in a state with magnetic quantum number m, i.e., $C_m(0) = 1$, the probability that the system is in a state m' after a time t is:

$$W(m, m'; t) = |(m'|e^{iJ_y\Theta}e^{(i/\hbar)\gamma tJ_z}e^{-iJ_y\Theta}|m)|^2 = |(m'|e^{(i/\hbar)\gamma t(J_z\cos\Theta - J_x\sin\Theta)}|m)|^2. \quad (43)$$

It is immediately verified that

$$\sum_{m'} W(m, m'; t) = 1. \quad (44)$$

In the simple case of $j = \frac{1}{2}$, the matrix element (43) is easily evaluated. An angular momentum with $j = \frac{1}{2}$ can be considered as a spin and represented in terms of the Pauli matrices, i.e., $\mathbf{J} = \frac{1}{2}\boldsymbol{\sigma}$. Since $(\sigma_z\cos\Theta - \sigma_x\sin\Theta)^2 = 1$, we have

$$W(m, m'; t) = \left|\left(m'\left|\cos\frac{\gamma t}{2\hbar} + i(\sigma_z\cos\Theta - \sigma_x\sin\Theta)\sin\frac{\gamma t}{2\hbar}\right|m\right)\right|^2. \quad (45)$$

Therefore,

$$W(\tfrac{1}{2}, -\tfrac{1}{2}; t) = W(-\tfrac{1}{2}, \tfrac{1}{2}; t) = \sin^2\Theta\sin^2\frac{\gamma t}{2\hbar} = \frac{\hbar^2\omega^2\sin^2\vartheta}{g^2\mu_0^2H^2 + 2g\mu_0H\hbar\omega\cos\vartheta + \hbar^2\omega^2}\sin^2\frac{t}{2\hbar} \times (g^2\mu_0^2H^2 + 2g\mu_0H\hbar\omega\cos\vartheta + \hbar^2\omega^2)^{\frac{1}{2}}. \quad (46)$$

If these transition probabilities are written as $\sin^2\frac{1}{2}\alpha$, it is evident that

$$W(\tfrac{1}{2}, \tfrac{1}{2}; t) = W(-\tfrac{1}{2}, -\tfrac{1}{2}; t) = \cos^2\tfrac{1}{2}\alpha. \quad (47)$$

The uncorrected Güttinger equations result in an *umklappwahrsheinlichkeit* which depends only upon ω^2, namely:

$$W(\tfrac{1}{2}, -\tfrac{1}{2}; t) = \frac{\hbar^2\omega^2\sin^2\vartheta}{g^2\mu_0^2H^2 + \hbar^2\omega^2\sin^2\vartheta}\sin^2\frac{t}{2\hbar} \times (g^2\mu_0^2H^2 + \hbar^2\omega^2\sin^2\vartheta)^{\frac{1}{2}}. \quad (48)$$

A discussion of the measurement of magnetic moments by means of a precessing field, which depends upon the fact that the transition probabilities involve ω explicitly, has been given by Professor Rabi in an accompanying paper.

The evaluation of the matrix element (43) may be carried out, for an arbitrary j, by a method which will not be given here. The results are in complete agreement with those obtained from Majorana's general theorem (see the accompanying paper of Professor Rabi).

In conclusion, the author wishes to express his indebtedness to Dr. Lloyd Motz for pointing out the contradiction between the results obtained by Professor Rabi and those obtained with the Güttinger equations, and to Professor I. I. Rabi for his continued interest throughout the course of this investigation.

Space Quantization in a Gyrating Magnetic Field

I. I. RABI
Columbia University, New York, N. Y.
(Received March 1, 1937)

The nonadiabatic transitions which a system with angular momentum J makes in a magnetic field which is rotating about an axis inclined with respect to the field are calculated. It is shown that the effects depend on the sign of the magnetic moment of the system. We therefore have an absolute method for measuring the sign and magnitude of the moment of any system. Applications to the magnetic moment of the neutron, the rotational moment of molecules, and the nuclear moment of atoms with no extra-nuclear angular momentum are discussed.

IN a previous paper[1] the effect of a rapidly varying magnetic field on an oriented atom possessing nuclear spin and extra-nuclear angular momentum. It appeared that it was possible to deduce the sign of the magnetic moment of the nucleus from the nature of the nonadiabatic transitions which occur if the field rotates an appreciable amount in the time of a Larmor rotation. This effect was applied experimentally[2] with the method of atomic beams to measure the sign of the proton, deuteron, K^{39}, etc. The evaluation of the sign was possible because the experiment decided whether the h.f.s. level was normal or inverted. Since the sign of the electronic moment is known to be negative a normal level meant positive nuclear moment and an inverted level negative moment.

Clearly it is desirable to find another effect which will make it possible to find the sign of the nuclear moment in cases where the normal state of the atom is one in which there is no electronic angular momentum as in the alkaline earths. Spectroscopic methods where applicable will yield this information, but there are numerous important instances in which molecular and atomic beam methods are the only ones available. For example, it would be very desirable to measure the sign of the moment of the neutron directly. Although it would be very difficult to apply atomic beam methods to the neutron, the polarization effect of magnetized iron suggested by Bloch may possibly be useful in this connection as a device for measuring the degree of depolarization caused by the nonadiabatic transitions to be described below. Another example is the sign of the moment arising from molecular rotation which results in a positive contribution from the motion of the nuclei about the centroid and a negative contribution from the electrons.

The following considerations should make it possible to make the same sort of observations with simple systems as are made in the Einstein-de Haas and Barnett experiments: namely, the magnitude and sign of the gyromagnetic ratio.

Consider a simple system such as a neutron with magnetic moment $\mu = -g\mu_0 J$, where g is the Landé g factor, J is the total angular moment due to all causes. If g is positive the total moment is negative as in the spinning electron. If g is negative the moment is positive. In a magnetic field H the system precesses with the Larmor frequency $\nu = g\mu_0 H/h$. If g is positive the precession is in the positive direction and if negative in the negative direction. We shall now consider our system initially quantized with magnetic quantum number m in a field H which is constant in magnitude but rotates with a frequency $\omega/2\pi$ about some direction which is at an angle ϑ with respect to the direction of the field.

This problem was solved by Güttinger[3] for the particular case when the angle is $\pi/2$. He found that transitions will occur to other magnetic levels with quantum number m' when $\omega/2\pi$ is of the order of magnitude of ν. The transition probabilities in this case do not depend on the direction of the field. It will be shown that in the more general case the direction of rotation introduces an asymmetry into the problem and

[1] Rabi, Phys. Rev. **49**, 324 (1936).
[2] Kellogg, Rabi and Zacharias, Phys. Rev. **50**, 472 (1936); Torrey and Rabi, Phys. Rev. **51**, 379A (1937) Millman and Zacharias, Phys. Rev. **51**, 380A (1937).
[3] P. Güttinger, Zeits. f. Physik **73**, 169 (1931); E. Majorana, Nuovo Cimento **9**, 43 (1932).

as a consequence with the same $|\nu|$ and $|\omega|$ the transition probabilities will be different depending on whether g is positive or negative. The Majorana and Güttinger arrangements do not possess this property.

It will suffice to consider only the case where $J=\frac{1}{2}$ since the solution of more general problems depends only on the solution of this simple case. The Schrödinger equation for this case is

$$\begin{aligned} &i\hbar\dot{\psi}=\mathcal{H}\psi, \\ &\mathcal{H}=g(\mu_0/2)(\sigma_1H_1+\sigma_2H_2+\sigma_3H_3). \end{aligned} \tag{1}$$

If we set

$$\psi=C_1\psi_1+C_{-1}\psi_{-1} \tag{2}$$

we obtain from (1)

$$\begin{aligned} dC_1/dt&=(-ig\mu_0/2\hbar)[H_3C_1+(H_1-iH_2)C_{-1}], \\ dC_{-1}/dt&=(-ig\mu_0/2\hbar)[-H_3C_{-1}+(H_1+iH_2)C_1]. \end{aligned} \tag{3}$$

With the substitutions

$$\begin{aligned} &H_1=H\sin\vartheta\cos\varphi, \quad H_2=H\sin\vartheta\sin\varphi, \\ &\qquad\qquad H_3=H\cos\vartheta, \\ &g\frac{u_0}{2}\frac{H}{\hbar}\cos\vartheta=a, \quad g\frac{u_0}{2\hbar}H\sin\vartheta=b, \quad \varphi=\omega t, \end{aligned} \tag{4}$$

which represents a field H constant in magnitude and precessing about the z direction with angular velocity ω, we have

$$\begin{aligned} dC_1/dt&=-iaC_1-ibe^{-i\omega t}C_{-1}, \\ dC_{-1}/dt&=iaC_{-1}-ibe^{i\omega t}C_1. \end{aligned} \tag{5}$$

Therefore

$$d^2C_1/dt^2+i\omega\frac{d}{dt}C_1+(a^2+b^2-\omega a)C_1=0. \tag{6}$$

The solution of this familiar equation is

$$\begin{aligned} C_1&=Ae^{ip_1t}+Be^{ip_2t}, \\ C_{-1}&=-e^{i\omega t}\left[\frac{a+p_1}{b}Ae^{ip_1t}+\frac{a+p_2}{b}Be^{ip_2t}\right], \\ p_1&=-(\omega/2)+\tfrac{1}{2}(\omega^2+4a^2+4b^2-4\omega a)^{\frac{1}{2}}, \\ p_2&=-(\omega/2)-\tfrac{1}{2}(\omega^2+4a^2+4b^2-4\omega a)^{\frac{1}{2}}. \end{aligned} \tag{7}$$

The quantities A and B are determined from the initial conditions and the normalization condition $|C_1|^2+|C_{-1}|^2=1$. If ψ_α and ψ_β are the vectors which correspond to $m=+\frac{1}{2}$, $-\frac{1}{2}$, respectively, in the direction of H we obtain[4]

$$\begin{aligned} &\psi_\alpha=(2\alpha)^{-\frac{1}{2}}(\beta e^{-i\omega t}\psi_1+\alpha\psi_{-1}), \\ &\psi_\beta=(2\gamma)^{-\frac{1}{2}}(-\beta e^{-i\omega t}\psi_1+\gamma\psi_{-1}), \\ &\beta=\sin\vartheta, \quad \alpha=1-\cos\vartheta, \quad \gamma=1+\cos\vartheta, \\ &\alpha^2+\beta^2=2\alpha, \quad \gamma^2+\beta^2=2\gamma. \end{aligned} \tag{8}$$

If $\psi(0)=\psi_\alpha(0)$ at $t=0$ we start with the system quantized in the direction of H with $m=\frac{1}{2}$, and

$$\begin{aligned} &A+B=\beta/(2\alpha)^{\frac{1}{2}}, \\ &-\left(\frac{a+p_1}{b}\right)A-\left(\frac{a+p_2}{b}\right)B=\frac{\alpha}{(2\alpha)^{\frac{1}{2}}}. \end{aligned} \tag{9}$$

Utilizing these values of A and B and setting $n=(\omega^2+4a^2+4b^2-4\omega a)^{\frac{1}{2}}$ we obtain for the probability amplitudes

$$\begin{aligned} C_1&=\frac{1}{(2\alpha)^{\frac{1}{2}}}e^{-(i\omega t/2)}\left[\beta\cos\frac{n}{2}t\right. \\ &\qquad\left.-i\frac{(2\alpha b+2\beta a-\beta\omega)}{n}\sin\frac{n}{2}t\right], \\ C_{-1}&=\frac{1}{(2\alpha)^{\frac{1}{2}}}e^{i\omega t/2}\left[\alpha\cos\frac{n}{2}t\right. \\ &\qquad\left.-i\frac{(2\beta b-2\alpha a+\alpha\omega)}{n}\sin\frac{n}{2}t\right]. \end{aligned} \tag{10}$$

The probability of finding the system in a state with $m=-\frac{1}{2}$ with respect to H is therefore

$$P_{(\frac{1}{2},-\frac{1}{2})}=|\psi_\beta^*\psi|^2=\frac{1}{(4\alpha\gamma)^{\frac{1}{2}}}|-\beta e^{i\omega t}C_1+\gamma C_{-1}|^2 \tag{11}$$

with the values given in Eq. (10)

$$P_{(\frac{1}{2},-\frac{1}{2})}=\frac{\beta^2\omega^2}{n^2}\sin^2\frac{n}{2}t. \tag{12}$$

In terms of the Larmor frequency $\nu=g\mu_0H/h$, the

[4] Dirac, *Quantum Mechanics*, p. 70.

angle ϑ and the frequency of rotation $r=\omega/2\pi$

$$P_{(1,\,-1)}=\frac{\sin^2\vartheta r^2}{\nu^2+\nu^2-2\nu r\cos\vartheta}\sin^2\pi t \times(\nu^2+\nu^2-2\nu r\cos\vartheta)^{\frac{1}{2}}. \quad (13)$$

This result reduces to Güttinger's formula when $\vartheta=\pi/2$. For other values of ϑ it is apparent that the transition probability for given ϑ, H and ω will be quite different depending on whether g is positive or negative since ν appears linearly in the result. Expressed in another way we may say that $P_{(1,\,-1)}$ depends on the direction of rotation of the field for a given sign and magnitude of g.

Since rotating fields are usually realized by allowing the system to pass through a field which changes in direction from point to point, the total change in direction is fixed. If we set $\varphi=2\pi rt$ we obtain from (15) setting $\nu/r=q$

$$P_{(1,\,-1)}=\frac{\sin^2\vartheta}{1+q^2-2q\cos\vartheta}\sin^2\frac{\varphi}{2} \times(1+q^2-2q\cos\vartheta)^{\frac{1}{2}}. \quad (14)$$

If we set $q=\cos\vartheta$ which can be arranged by suitably varying the magnitude and direction of the field,

$$P_{(1,\,-1)}=\sin^2(\tfrac{1}{2}\varphi\sin\vartheta), \quad (15)$$

which can be made as close to unity as one pleases by arranging experimental conditions so that $2\pi>\varphi>\pi$. If one were then to leave everything unchanged but reversed the direction of rotation we would get

$$P_{(1,\,-1)}=\frac{\sin^2\vartheta}{1+3\cos^2\vartheta}\sin^2\left[\frac{\varphi}{2}(1+3\cos^2\vartheta)^{\frac{1}{2}}\right], \quad (16)$$

a very much smaller quantity.

It is clear therefore that from this qualitative difference and a knowledge of the sense of rotation one can infer the sign of the moment. The magnitude may be inferred from the absolute value of the fields and their direction and the angular velocity of its rotation.

It is unnecessary to consider the details of the realization of these rotating fields and the detection of these transitions since similar conditions have already been obtained in the experiments cited above.

To generalize these results we apply the general result of Majorana[2, 3] for any value of J

$$P_{(a,\,m,\,m')}=(\cos\tfrac{1}{2}\alpha)^{4J}(J+m)!(J+m')! \times(J-m)!(J-m')! \times\left[\sum_{\nu=0}^{2J}\frac{(-1)^\nu(\tan\tfrac{1}{2}\alpha)^{2\nu-m+m'}}{\nu!(\nu-m+m')!(J+m-\nu)!(J-m'-\nu)!}\right]^2, \quad (17)$$

where the value of the parameter α is given by

$$\sin^2\tfrac{1}{2}\alpha=P_{(1,\,-1)} \quad (18)$$

and depends only on g and not on m or J.

It may be of interest to note that in cases where we have a coupled system such as a nuclear spin coupled to molecular rotation, in which the coupling is weak and g small, the field required for these transitions can be such that the component systems are completely decoupled. As was shown by Motz and Rose,[5] each system would then make these transitions independently. In particular, if the moments of the two systems are opposite in sign it should be possible to arrange conditions so that only one of these two systems makes these transitions. In this case it should be possible by means of the focusing methods developed in this laboratory to measure directly one moment in the presence of another (rotational and nuclear) with only slight interference.

[5] Motz and Rose, Phys. Rev. **50**, 348 (1936).

The Helium Wave Equation*

T. H. GRONWALL**
Columbia University, New York, N. Y.
(Received February 3, 1937)

This paper represents an attempt to solve the equation $\nabla^2\psi+(1/z)\psi_z+(1/4r)(E-V)\psi=0$, which is the Gronwall form of the wave equation for helium S states. The equation $\nabla^2 u+(1/z)u_z=0$ is separable in polar coordinates (r, β, φ), and has solutions $u_{mk}=r^{2m-k}\sin^k\beta v_{mk}(\sin^2\beta)e^{ik\varphi}=r^{2m-k}w_{mk}(\beta, \varphi)$, where the v_{mk}'s are Jacobi polynomials, and the w_{mk}'s form a complete orthogonal set of surface functions. The function ψ is expanded as $\psi=\sum_{mk}\psi_{mk}(r^{\frac{1}{2}})w_{mk}$, resulting in an infinite system of ordinary linear differential equations for the ψ_{mk}'s.

EDITOR'S INTRODUCTION

AFTER persistent effort, the late T. H. Gronwall of Columbia University succeeded in putting the wave equation for helium S states into a remarkably simple form.[1] He then made an extensive study of the equation in order to learn something about the nature of the solutions. Many calculations had been made when death intervened, and the notes were left behind in an unordered state. Largely owing to the difficulty of arranging them, they were still unpublished in October, 1936, when they came into my hands through the courtesy of Dr. F. Bohnenblust. They have since proved very valuable for my own research, and so it is felt that the essential results should be published. Those results which are to be used in the following paper have been checked, but the unused results, such as the formulae for matrix elements in the Appendix, have not. (The derivation or verification is easy but tedious, and is hence left to any reader who may be sufficiently concerned.) For the sake of clarity and brevity, I have made several insertions, which are indicated by enclosure within curly brackets. Finally, it is a pleasure to express my appreciation of the opportunity to use freely the unpublished work of Gronwall, and to thank Professor E. Hille for permission to publish it.

WAVE EQUATION

The wave equation for S states of the helium atom may be written[1, 2] in the form

$$\nabla^2\psi+\frac{1}{z}\frac{\partial\psi}{\partial z}+\frac{1}{r}\left(\frac{E}{4}+\frac{1}{[2(r+y)]^{\frac{1}{2}}}+\frac{1}{[2(r-y)]^{\frac{1}{2}}}-\frac{1}{2Z(r-x)^{\frac{1}{2}}}\right)\psi=0, \tag{1}$$

where

$$4x=r_1^2+r_2^2-r_{12}^2=2r_1r_2\cos\theta,$$
$$4y=r_1^2-r_2^2,$$
$$4z=4\times\text{area of }\Delta\text{ with sides }r_1, r_2, r_{12}=2r_1r_2\sin\theta,$$
$$4r=4(x^2+y^2+z^2)^{\frac{1}{2}}=r_1^2+r_2^2.$$

Here r_1 and r_2 refer to the electron-nucleus distances, θ denotes the angle between the corresponding radius vectors, and r_{12} denotes the interelectronic distance. Since the range of θ is $0\leq\theta\leq\pi$, the domain of x, y, and z is the upper half-space $z\geq 0$. {It may be noted that $\tan\theta=(z/x)$, so that θ is the angle in the xz plane from the x axis to the projection of the radius vector $\mathbf{r}$ upon this plane. Also, if we let $\alpha=\tan^{-1}(r_2/r_1)$, it follows that 2α is the angle from the y axis to the radius vector. For $\cos 2\alpha=2\cos^2\alpha-1$; $\cos\alpha=[r_1/(r_1^2+r_2^2)^{\frac{1}{2}}]$; and $\cos 2\alpha=[(r_1^2-r_2^2)/(r_1^2+r_2^2)]=(y/r)$.}

* Edited by J. H. Bartlett, Jr., University of Illinois, Urbana, Illinois.
** Dr. T. H. Gronwall died May 9, 1932. This paper together with other manuscripts was then transferred from the physics department of Columbia University where this work was done to the care of Dr. E. Hille of Princeton University.
[1] T. H. Gronwall, Annals of Mathematics **33**, 279 (1932).
[2] The rational units of length and energy of Hylleraas are used. See Zeits. f. Physik **54**, 347 (1929).

The variational problem corresponding to Eq. (1) is

$$\delta\int\left[\psi_x^2+\psi_y^2+\psi_z^2-\frac{1}{r}\left(\frac{E}{4}+\frac{1}{[2(r+y)]^{\frac{1}{2}}}+\frac{1}{[2(r-y)]^{\frac{1}{2}}}-\frac{1}{2Z(r-x)^{\frac{1}{2}}}\right)\psi^2\right]z\,dx\,dy\,dz=0.$$

{In order that this problem have a meaning, the integral must exist. Such a requirement is sufficient to exclude the so-called "second solutions" for hydrogen S states.[3] We shall, therefore, adopt this as a necessary boundary condition on the (univalent) function ψ, which will also be required to be of class C^2, except perhaps on the $(+x)$ and y axes, where ψ might conceivably become infinite.}

Introducing polar coordinates, with the z axis as the pole,

$$x=r\cos\varphi\sin\beta,$$
$$y=r\sin\varphi\sin\beta,$$
$$z=r\cos\beta,$$

we have

$$\delta\int_0^\infty\int_0^{2\pi}\int_0^{\pi/2}\left[\tfrac{1}{4}\psi_s^2+\frac{1}{s^2\sin^2\beta}\psi_\varphi^2+\frac{1}{s^2}\psi_\beta^2-\left(\frac{E}{4}+\frac{f}{s}\right)\psi^2\right]s^5\,ds\sin\beta\cos\beta\,d\beta\,d\varphi=0,$$

where

$$f=[2(1+\sin\varphi\sin\beta)]^{-\frac{1}{2}}+[2(1-\sin\varphi\sin\beta]^{-\frac{1}{2}}-(1/2Z)[1-\cos\varphi\sin\beta]^{-1},\quad\text{and}\quad r=s^2.$$

The corresponding differential equation is

$$\psi_{ss}+(5/s)\psi_s+(4/s^2\sin^2\beta)\psi_{\varphi\varphi}+(4/s^2)(\psi_{\beta\beta}+2\cot 2\beta\psi_\beta)+[E+(4f/s)]\psi=0. \tag{2}$$

Basic Orthogonal Functions

To find an appropriate orthogonal system on the half-sphere, we consider the equation

$$u_{ss}+(5/s)u_s+(4/s^2\sin^2\beta)u_{\varphi\varphi}+(4/s^2)(u_{\beta\beta}+2\cot 2\beta u_\beta)=0. \tag{3}$$

Substituting

$$u=s^{4m-2k}\begin{matrix}\cos\\ \sin\end{matrix}k\varphi g_{mk}(t),\quad t=\sin^2\beta,$$

where m and k are integers, $m\geq k\geq 0$, we find

$$[t(1-t)g'_{mk}]'+\left[\left(m-\frac{k}{2}\right)\left(m+1-\frac{k}{2}\right)-(k^2/4t)\right]g_{mk}=0.$$

Now, writing $g_{mk}(t)=t^{k/2}v(m,k,t)$, the preceding equation gives

$$t(1-t)v_{tt}+[k+1-(k+2)t]v_t+(m+1)(m-k)v=0. \tag{4}$$

{This equation may be recognized as the hypergeometric equation in the usual form.}

The only solution of (4) which is finite both at $t=0$ and $t=1$ is the Jacobi polynomial $F(k-m, m+1, k+1, t)$, $m\geq k\geq 0$ (multiplied by a constant).

Now[4]

$$\int_0^1 t^k F(k-m,m+1,k+1,t)F(k-m',m'+1,k+1,t)dt$$
$$=(1/2m+1-k)[\Gamma(m-k+1)\Gamma(k+1)/\Gamma(m+1)]^2\delta_{mm'}.$$

[3] The editor (J. H. B.) desires to thank Professor R. Courant for informing him of this.

[4] This follows from Jordan, *Cours d'Analyse III*, 242, Eq. (45, 46) upon making $\alpha=\gamma=k+1$ and $n=m-k$.

We also have (Jordan[4])

$$F(k-m, m+1, k+1, t)=[\Gamma(k+1)/\Gamma(m+1)]t^{-k}(d/dt)^{m-k}[t^m(1-t)^{m-k}].$$

Writing

$$v(m\ k\ t)=[\Gamma(m+1)/\Gamma(k+1)\Gamma(m-k+1)]F(k-m, m+1, k+1, t), \quad 0\leq k\leq m,$$

we find

$$N_{mm'k}=\int_0^1 t^k v(m\ k\ t)v(m'\ k\ t)dt=(1/2m+1-k)\delta_{mm'} \tag{5}$$

and

$$v(m\ k\ t)=[1/\Gamma(m-k+1)]t^{-k}(d/dt)^{m-k}[t^m(1-t)^{m-k}]=\sum_{\nu=0}^{m-k}(-)^\nu\frac{(m+\nu)!}{\nu!(k+\nu)!(m-k-\nu)!}t^\nu. \tag{6}$$

From (6)
$$\begin{cases} v(m\ k\ 0)=[m!/k!(m-k)!], \\ v(m\ k\ 1)=(-)^{m-k}, \end{cases} \tag{7}$$

and by (4)
$$\begin{cases} v_t(m\ k\ 0)=-[(m+1)!/(k+1)!(m-k-1)!], \\ v_t(m\ k\ 1)=(-)^{m-k}(m+1)(m-k). \end{cases} \tag{8}$$

Expansion in Terms of Orthogonal Functions

The variational problem in terms of t may be written as

$$\delta\int_0^\infty\int_0^{2\pi}\int_0^1[(1/4)\psi_s^2+(1/s^2t)\psi_\varphi^2+[4t(1-t)/s^2]\psi_t^2-[(E/4)+(f/s)]\psi^2]s^5\,ds\,d\varphi\,dt=0. \tag{9}$$

Expand
$$\psi=\sum_{mk}c_{mk}\psi_{mk}(s)g_{mk}(t)\begin{matrix}\cos\\ \sin\end{matrix}k\varphi, \tag{10}$$

where the cosines belong to the *para* terms and the sines to the *ortho* terms. In the following treatment, we shall consider only the *para* terms.

Setting $\epsilon_k=2$ for $k=0$, and $\epsilon_k=1$ for $k>0$, we obtain

$$\int_0^{2\pi}d\varphi\int_0^1 dt[(1/4)\psi_s^2+(1/s^2t)\psi_\varphi^2+[4t(1-t)/s^2]\psi_t^2]$$

$$=\sum_{mm'k}\pi\epsilon_k c_{mk}c_{m'k}\int_0^1 dt[(1/4)\psi'_{mk}\psi'_{m'k}g_{mk}g_{m'k}+(1/s^2)\psi_{mk}\psi_{m'k}\{(k^2/t)g_{mk}g_{m'k}+4t(1-t)g'_{mk}g'_{m'k}\}]$$

$$=\sum_{mm'k}\pi\epsilon_k c_{mk}c_{m'k}\int_0^1 dt[(1/4)\psi'_{mk}\psi'_{m'k}g_{mk}g_{m'k}+(1/s^2)\psi_{mk}\psi_{m'k}(2m-k)(2m+2-k)g_{mk}g_{m'k}]$$

$$=\sum_{mk}(\pi\epsilon_k c^2{}_{mk}/2m+1-k)[(1/4)(\psi'_{mk})^2+(1/s^2)(2m-k)(2m+2-k)\psi^2{}_{mk}].$$

We have integrated by parts, used the differential equation for g_{mk} and Eq. (5).

The potential energy may be treated in like manner. Let us write

$$\int_0^{2\pi} d\varphi \int_0^1 dt\psi^2[\{2(1+t^{\frac{1}{2}}\sin\varphi)\}^{-\frac{1}{2}}+\{2(1-t^{\frac{1}{2}}\sin\varphi)\}^{-\frac{1}{2}}-(1/2Z)\{1-t^{\frac{1}{2}}\cos\varphi\}^{-\frac{1}{2}}] = \sum_{mkm'k'} a(mkm'k')c_{mk}c_{m'k'}\psi_{mk}\psi_{m'k'}.$$

Then $$a(mk\,m'\,k') = \int_0^{2\pi} d\varphi \int_0^1 dt[\{2(1+t^{\frac{1}{2}}\sin\varphi)\}^{-\frac{1}{2}}+\cdots]g_{mk}g_{m'k'}\cos k\varphi\cos k'\varphi.$$

To simplify, we observe that, n being an integer,

$$\int_0^{2\pi}(1+t^{\frac{1}{2}}\sin\varphi)^{-\frac{1}{2}}e^{in\varphi}d\varphi = e^{3n\pi i/2}\int_0^{2\pi}(1-t^{\frac{1}{2}}\cos\varphi)^{-\frac{1}{2}}e^{in\varphi}d\varphi$$

and

$$\int_0^{2\pi}(1-t^{\frac{1}{2}}\sin\varphi)^{-\frac{1}{2}}e^{in\varphi}d\varphi = e^{n\pi i/2}\int_0^{2\pi}(1-t^{\frac{1}{2}}\cos\varphi)^{-\frac{1}{2}}e^{in\varphi}d\varphi.$$

It follows that

$$a(mk,\,m'k') = (\sqrt{2}\cos(|k-k'|\pi/2)-(1/2Z))I(mk\,m'k';\,|k-k'|) + (\sqrt{2}\cos((k+k')\pi/2)-(1/2Z))I(mk\,m'k';\,k+k'),$$

where $$I(mk\,m'k';\,n) = (1/2)\int_0^{2\pi} d\varphi \int_0^1 dt(1-t^{\frac{1}{2}}\cos\varphi)^{-\frac{1}{2}}g_{mk}g_{m'k'}\cos n\varphi.$$

The variational problem is now, putting $c^2{}_{mk} = (2m+1-k)/\pi\epsilon_k$,

$$\delta\int_0^\infty \{\sum_{mk}[(1/4)(\psi'_{mk})^2+(1/s^2)(2m-k)(2m+2-k)\psi^2{}_{mk}-(E/4)\psi^2{}_{mk}] - \sum_{mk\,m'k'} a(mk\,m'k')\psi_{mk}\psi_{m'k'}c_{mk}c_{m'k'}\}s^5 ds = 0.$$

The corresponding Euler equations are, if we number the functions by setting $n = \frac{1}{2}m(m+1)+k$, and if we set $A(mk\,m'k') = 2\pi c_{mk}c_{m'k'}a(mk\,m'k')$,

$$(1/4)(s^5\psi_n')'-(2m-k)(2m+2-k)s^3\psi_n+(E/4)s^5\psi_n+\sum_{n'}[A(nn')/2\pi]s^4\psi_{n'}=0. \tag{11}$$

{This is an infinite system of ordinary linear differential equations of the second order. We should like to find a solution which is finite everywhere.} Substitute $\psi_n = e^{-(\sqrt{-E})s}f_n(s)$, and let $\rho = 2(-E)^{\frac{1}{2}}s$, obtaining

$$\rho^2 f_n''+(5\rho-\rho^2)f_n'-4(2m-k)(2m+2-k)f_n-(5/2)\rho f_n+\sum_{n'}\frac{A(nn')}{\pi(-E)^{\frac{1}{2}}}\rho f_{n'}=0. \tag{12}$$

(The primes on f denote differentiation *re* ρ.)

Let $$b(nn') = A(nn')/\pi(-E)^{\frac{1}{2}} \quad \text{and} \quad \text{set} \quad f_n = \sum_{\nu=0}^{\infty} c_n{}^{(\nu)}\rho^\nu. \tag{13}$$

The recursion formula is then

$$(\nu-4m+2k)(\nu+4+4m-2k)c_n{}^{(\nu)} = (\nu+\tfrac{3}{2})c_n{}^{(\nu-1)}-\sum_{n'}b_{nn'}c_{n'}{}^{(\nu-1)}. \tag{14}$$

{Gronwall attempted to cut off the series (13) by setting $c_n^{(\nu)}=0$. He calculated $A_{nn'}$ for $n, n'=0, 1, 2$ and solved the equations (14) for $\nu(-E)^{\frac{1}{2}}$. If this procedure were significant, then one might expect to obtain three eigenvalues of helium in this manner. However, it is not clear which three they would be, except that they would be of ^1S type. If it be assumed that they are the three lowest, and if one substitutes the experimentally observed values, then the resulting values of ν do not agree with one another. For this and other reasons, we therefore omit the reproduction of the calculations.

Gronwall also expanded the $c_n^{(\nu)}$ in factorial series of the form

$$c_n^{(\nu)}=\sum_{\mu=0}^{\infty} c_{n\mu}/\Gamma(\nu+\mu+\alpha),$$

and determined relations between the $c_{n\mu}$'s.}

Appendix

1. Recursion formulae for the functions $v(m\ k\ t)$

$$\begin{aligned} tv(m,\ k,\ t) &= -[(m+1)(m+1-k)/(2m+1-k)(2m+2-k)]v(m+1,\ k,\ t) \\ &\quad +\{[2m^2+2m(1-k)+k(k-1)]/(2m-k)(2m+2-k)\}v(m\ k\ t) \\ &\quad -[m(m-k)/(2m-k)(2m+1-k)]v(m-1,\ k,\ t), \end{aligned} \tag{15}$$

$$\begin{aligned} t(1-t)v'(m,\ k,\ t) &= [(m+1)(m-k)(m+1-k)/(2m+1-k)(2m+2-k)]v(m+1,\ k,\ t) \\ &\quad -[k(m+1)(m-k)/(2m-k)(2m+2-k)]v(m\ k\ t) \\ &\quad -[m(m+1)(m-k)/(2m-k)(2m+1-k)]v(m-1,\ k,\ t), \end{aligned} \tag{16}$$

$$tv'(m\ k\ t)+(m+1)v(m\ k\ t)+[(m+1)/(2m+2-k)]v'(m+1,\ k,\ t)-[(m+1-k)/(2m+2-k)]v'(m\ k\ t)=0, \tag{17}$$

$$tv'(m\ k\ t)-(m-k)v(m\ k\ t)-[m/(2m-k)]v'(m\ k\ t)+[(m-k)/(2m-k)]v'(m-1,\ k,\ t)=0, \tag{18}$$

$$v(m,\ k-1,\ t)=[(m+1)/(2m+2-k)]v(m+1,\ k,\ t)-[(m+1-k)/(2m+2-k)]v(m\ k\ t), \tag{19}$$

$$\begin{aligned} tv(m,\ k+1,\ t) &= -[(m-k)/(2m-k)]v(m\ k\ t)+[m/2m-k]v(m-1,\ k,\ t) \\ &= C_k v(m\ k\ t)+D_k v(m-1,\ k,\ t). \end{aligned} \tag{20}$$

2. Expression for $I(m,\ k\ m',\ k',\ n)$ in terms of the v's

Integrate with respect to φ.

$$(1-t^{\frac{1}{2}}\cos\varphi)^{-\frac{1}{2}}=\sum_{\nu=0}^{\infty}\frac{(2\nu)!}{2^{2\nu}\nu!\nu!}t^{\nu/2}\cos^{\nu}\varphi,$$

$$\int_0^{2\pi} e^{in\varphi}\cos^{\nu}\varphi\,d\varphi=\frac{\pi}{2^{\nu-1}}\frac{\nu!}{\mu!(\nu-\mu)!}\delta_{\nu,\ n+2\mu}.$$

Consequently

$$\tfrac{1}{2}\int_0^{2\pi}(1-t^{\frac{1}{2}}\cos\varphi)^{-\frac{1}{2}}e^{in\varphi}d\varphi=\sum_{\mu=0}^{\infty}c_{n\mu}t^{n/2+\mu},$$

where

$$c_{n\mu}=\frac{\pi}{2^{2n+4\mu}}\frac{(2n+4\mu)!}{\mu!(n+\mu)!(n+2\mu)!}.$$

We have

$$\frac{c_{n\mu+1}}{c_{n\mu}}=\frac{\left(\frac{2n+1}{4}+\mu\right)\left(\frac{2n+3}{4}+\mu\right)}{(1+\mu)(n+1+\mu)} \qquad \text{and} \qquad c_{n0}=\frac{\pi}{2^{2n}}\frac{(2n)!}{n!n!},$$

so that

$$\tfrac{1}{2}\int_0^{2\pi}(1-t^{\frac{1}{2}}\cos\varphi)^{-\frac{1}{2}}e^{in\varphi}d\varphi=t^{n/2}F_n(t),$$

where

$$F_n(t)=\frac{\pi}{2^{2n}}\frac{(2n)!}{n!n!}F\left(\frac{2n+1}{4},\ \frac{2n+3}{4},\ n+1,\ t\right).$$

This gives

$$I(m\ k,\ m'\ k';\ n)=\int_0^1 t^{(n+k+k')/2}F_n(t)v(m\ k\ t)v(m'\ k'\ t)dt. \tag{21}$$

For the problem at hand, we require the knowledge of $I(m\ k,\ m'\ k';\ n)$ only for $n=k+k'$ and $n=|k-k'|$.

3. Formula for $I(m, k, 0, 0, k)$

By (21), $$I(m, k, 0, 0, k) = \int_0^1 t^k F_k v(m\ k\ t)dt.$$

But $t^k F_k = [16/(2k+1)(2k+3)][t^{k+1}(1-t)F_k']'$ from the differential equation. Hence

$$(1/16)(2k+1)(2k+3)I(m\ k\ 0\ 0\ k) = \int_0^1 v[t^{k+1}(1-t)F_k']'dt.$$

Integrate by parts and observe that

$$t^{k+1}(1-t)\frac{dF_k}{dt} \to 1/\sqrt{2} \quad \text{as} \quad t \to 1$$

and $$F_k \to \left[\Gamma(k+1)/\Gamma\left(\frac{k}{2}+\frac{1}{4}\right)\Gamma\left(\frac{k}{2}+\frac{3}{4}\right)\right]\log(1-t) \quad \text{as} \quad t \to 1.$$

Then $\int_0^1 v[t^{k+1}(1-t)F_k']'dt = ((-)^{m-k}/\sqrt{2}) + \int_0^1 F_k[t^{k+1}(1-t)v'(m\ k\ t)]'dt = ((-)^{m-k}/\sqrt{2}) - (m+1)(m-k)\int_0^1 t^k F_k v(m\ k\ t)dt.$

Therefore, $$I(m\ k\ 0\ 0\ k) = [8\sqrt{2}(-)^{m-k}]/(4m-2k+1)(4m-2k+3). \tag{22}$$

4. Formula for $I(m\ k\ 1\ 0\ k)$

$$I(m\ k\ 1\ 0\ k) = \int_0^1 t^k F_k v(m\ k\ t)v(1\ 0\ t)dt = \int_0^1 t^k F_k v(m\ k\ t)(1-2t)dt = I(m\ k\ 0\ 0\ t) - 2\int_0^1 t^{k+1} F_k v(m\ k\ t)dt.$$

But $tv(m\ k\ t) = Av(m+1, k\ t) + Bv(m\ k\ t) + Cv(m-1, k\ t)$. (Cf. Eq. (15)) and hence

$$I(m\ k\ 1\ 0\ k) = (1-2B)I(m\ k\ 0\ 0\ t) + AI(m+1, k\ 0\ 0\ t) + CI(m-1, k\ 0\ 0\ t). \tag{23}$$

5. Formulae for $I(m\ k, m'\ m'; n)$

First we may note that $v(m'\ m'\ t) = 1$. Then

$$I(m\ k\ m'\ m', k+m') = \int_0^1 t^{k+m'} F_{k+m} v(m\ k\ t)dt.$$

Consider $m' = 1$. $$tF_{k+1} = \{4kF_k - (2k-1)F_{k-1}\}/(2k+1).$$

Then, applying formula (20)

$$\int_0^1 t^{k+1} F_{k+1} v(m\ k\ t)dt = (4k/2k+1)\int_0^1 t^k F_k v(m\ k\ t)dt - [(2k-1)/(2k+1)]\int_0^1 t^{k-1} F_{k-1} t v(m\ k\ t)dt$$

$$= [4k/(2k+1)]I(m\ k\ 0\ 0\ k) - [(2k-1)/(2k+1)]\int t^{k-1} F_{k-1}[C_{k-1}v(m, k-1, t) + D_{k-1}v(m-1, k-1, t)]dt$$

and

$$I(m\ k, 1\ 1\ k+1) = (4k/2k+1)I(m\ k\ 0\ 0\ k) - [(2k-1)/(2k+1)][C_{k-1}I(m, k-1, 0\ 0, k-1) + D_{k-1}I(m-1, k-1, 0\ 0\ k-1)], \tag{24}$$

$$I(m\ m, m'\ m', m+m') = 8\sqrt{2}/(2n+1)(2n+3), \qquad n = m+m'. \tag{25}$$

If $I(m\ m, m'\ m', m-m') = J(m', n)$, $n = m-m'$, then

$$\left(m' + \frac{2n+1}{4}\right)\left(m' + \frac{2n+3}{4}\right)J(m', n) = (1/\sqrt{2}) + m'(m'+n)J(m'-1, n), \tag{26}$$

so that the successive J's may be found. In particular,

$$J(0, n) = 8\sqrt{2}/(2n+1)(2n+3), \tag{27}$$

$$J(1, n) = [16/(2n+5)(2n+7)]\{(1/\sqrt{2}) + 16(n+1)/\sqrt{2}(2n+1)(2n+3)\}. \tag{28}$$

6. Recursion formula for $I(m\ k\ m'\ k'\ n)$

One may derive the following:

$$(2n+1)/2m+1-k)[(m+1)I(m+1, k+1, m', k', n+1) - (m-k)I(n, k+1, m', k', n+1)]$$
$$= 4nI(m, k, m', k', n)$$
$$-[(2n-1)/(2m+1-k)][mI(m-1, k-1, m', k', n-1) - (m-k+1)I(m, k-1, m', k', n-1)]. \tag{29}$$

{Gronwall actually computed only the first few I's. It might be useful to know their asymptotic properties in general (for large values of the indices) for the solution of the system (12).}

The Helium Wave Equation

J. H. BARTLETT, JR.
University of Illinois, Urbana, Illinois
(Received February 3, 1937)

This paper is a sequel to the preceding one by Gronwall. In Part I it is shown that the ground state eigenfunction, if it exists, cannot have the form $\psi=\sum_{p,k=0}^{\infty} s^{p+\gamma}a^{p,k}(\beta)\cos k\varphi$, where $s=r^{\frac{1}{2}}=(r_1^2+r_2^2)^{\frac{1}{2}}$, and γ is some constant. In Part II, it is assumed that the solution of Gronwall's infinite system of ordinary differential equations (see preceding abstract) is to be found by extrapolation from a finite system. Arguments are given to show that if the wave function is finite everywhere except at the origin, then the expansion about the origin is of the form $\psi=\sum_{k=0}^{\infty} c^{(k)}(s,\beta,\varphi)(\log s)^k$, where the $c^{(k)}$-s are ascending power series in s.

RESEARCHES on hyperfine structure and on isotope shift by the writer[1] and his co-workers have demonstrated that extremely good wave functions are required for significant quantitative results. The chief bar to the finding of accurate solutions of the wave equation is its nonseparability. This has not prevented, however, the construction of a serviceable atomic model, and this is due to the predominant influence of the nucleus. In particular, isotope shifts are very small. Inside the nucleus the situation is quite different, according to our present ideas, for the elementary particles all have approximately equal masses, and the nonseparable terms responsible for "isotope shift" are not at all negligible. It is, therefore, of considerable importance for the development of a satisfactory theory of the nucleus that one study these nonseparable wave equations.

The equation which has received most attention so far has been the helium wave equation, since there are but three particles involved. The mathematical theory of partial differential equations with singularities, of which this is one, is as yet undeveloped, so that we cannot even say whether or not quadratically integrable solutions exist. (The present paper is devoted to this question, and we shall give arguments to show why a large class of quadratically integrable functions cannot be solutions of the helium wave equation.) So far, physicists have assumed that the Schrödinger wave equation is soluble in general. The procedure has then been to guess at the form of an approximating function, and to apply the modified Ritz variational method. This furnishes us with an upper bound to the lowest eigenvalue. Hylleraas[2] has made extensive calculations to determine this upper bound for the ground state of helium, and has shown that the least upper bound attainable with his form of function agrees very closely with the experimentally determined eigenvalue. Nevertheless, this is not completely conclusive by itself. One must be able to find lower bounds, and to show that the approximating functions converge to a solution of the wave equation.

Suppose that φ is an approximating function, and denote $(H\varphi)/\varphi$ by ϵ. If we take the weighted average over configuration space, we have

$$\epsilon_a=\int\varphi^2(H\varphi/\varphi)d\tau=\int\varphi H\varphi d\tau.$$

The mean square deviation is

$$[(\epsilon-(\epsilon)_a)^2]_a=(\epsilon^2)_a-(\epsilon^2)_a,\quad\text{where}\quad(\epsilon^2)_a=\int\varphi^2(H\varphi/\varphi)^2d\tau=\int(H\varphi)^2d\tau.$$

[1] See, for example, Bartlett and Gibbons, Phys. Rev. **44**, 538 (1933), and Bartlett, Gibbons and Watson, Phys. Rev. **50**, 315 (1936).
[2] E. A. Hylleraas, Zeits. f. Physik **54**, 347 (1929); **65**, 209 (1930).

We have calculated[5] the root-mean-square deviation of ϵ for the six-term wave function of Hylleraas and found it to be 3.5 electron volts. It is our opinion that this is a large deviation, although it might be argued[3] that the difference between the approximating function and the exact wave function might be small but yet have large second derivatives, so that this difference would be oscillatory over a considerable portion of space.

Weinstein[4] has suggested a method[5] for obtaining lower bounds. According to this, the lower bound is $\epsilon_a - \{[(\epsilon-\epsilon_a)^2]_a\}^{\frac{1}{2}}$, so that the spread between upper and lower bounds for the helium ground state is 3.5 ev. Romberg[6] has developed an empirical method, which gives $-(\epsilon^2)_a^{\frac{1}{2}}$ as the "lower bound." The "lower bound" is then -1.45310, as compared with an upper bound of -1.45162, giving a spread of only 0.08 volt. Now we must have $(\epsilon^2)_a \geq \epsilon_a^2$, and hence if the "lower bounds" keep increasing steadily with improving wave functions, they will converge to the eigenvalue. So far, these "lower bounds" have increased for the helium ground state, but, in the absence of a convergence proof, there is no guarantee that they would continue to do so.

Even granting that a function φ had been found which made $[(\epsilon-\epsilon_a)^2]_a$ very small, which would mean that ϵ were close to a true eigenvalue over most of space, we still would not know how closely the function φ approximated the exact eigenfunction, and it is this information which we should like to have.

In this paper, we attempt to construct functions which will be valid solutions of the wave equation everywhere. As will be shown, great difficulties are encountered, one result being that the continuity assumptions usually made in perturbation theory cannot be true if the helium wave equation is to have a solution.

Since the work of Gronwall[7] is our starting-point, we shall assume that this paper is read in conjunction with his, and shall accordingly refer the reader to that paper for the definition of the symbols used.

The wave equation is

$$\psi_{ss}+(5/s)\psi_s+(4/s^2\sin^2\beta)\psi_{\varphi\varphi}+(4/s^2)(\psi_{\beta\beta}+2\cot 2\beta\psi_\beta)+[E+(4f/s)]\psi=0. \tag{1}$$

(One might suppose that it would be of advantage to convert this into an homogeneous integral equation by means of a Green's function. The problem is then to solve this integral equation, and this is the sticking point. The Fredholm method is impractical, but one might attempt the method of successive approximations. In order to use a Green's function such as $1/R$, one is (practically) forced to expand it in a Laplace series. The function ψ will then be in an expanded form, which we might just as well have assumed at the start. Again, the second approximation will usually be of the wrong functional type, especially if the first approximation is taken as a Hylleraas function. We have, therefore, avoided the integral equation method.)

PART I

Let us now try to find a solution of (1) of the form

$$\psi=\sum_{p=0}^{\infty} a^{(p)}s^{p+\gamma}, \quad a^{(p)}=a^p(\varphi,\beta). \tag{2}$$

---

[3] This possibility was pointed out to me by Professor Birkhoff, whom I wish to thank for friendly discussions of the equation.

[4] D. H. Weinstein, Phys. Rev. **40**, 737 (1932); **41**, 839 (1932); Proc. Nat. Acad. Sci. **20**, 529 (1934).

[5] Bartlett, Gibbons and Dunn, Phys. Rev. **47**, 679 (1935). In this paper, we said that the methods of Weinstein (reference 4) and MacDonald seemed "difficult to justify rigorously." Since then we have had a lengthy correspondence with Dr. Weinstein, from which it developed that the argument depends essentially on the validity of the inequality $\int[(H-V)\xi]^2 d\tau \geq (W_i-V)^2$, (see Nat. Acad. paper, p. 530, Eq. (4)). This we have not been able to deduce without assuming expansibility in terms of orthogonal functions.

[6] W. Romberg, Physik. Zeits. Sowjetunion **8**, 516 (1935); **9**, 546 (1936).

[7] T. H. Gronwall, Phys. Rev. **51**, 655 (1937). We shall refer to this as "G."

Formal solutions of this type would be expected to exist, because the above equation involves s in the manner of the ordinary confluent hypergeometric equation. If then, we substitute the series in the equation and compare coefficients of like powers of s, we find for the recursion formula

$$(p+\gamma+2)(p+\gamma+6)a^{p+2}+(4/\sin^2\beta)a^{p+2}{}_{\varphi\varphi}+4(a^{p+2}{}_{\beta\beta}+2\cot 2\beta a^{p+2}{}_{\beta})+Ea^p+4fa^{p+1}=0. \quad (3)$$

For $p=-2$, $\quad \gamma(\gamma+4)a^0+(4/\sin^2\beta)a^0{}_{\varphi\varphi}+4(a^0{}_{\beta\beta}+2\cot 2\beta a^0{}_{\beta})=0.$

Expand $a^0=\sum_{k=0}^{\infty}a^{0k}\cos k\varphi$, and write $a^{0k}=t^{k/2}v$. Then

$$t(1-t)v_{tt}+[k+1-(k+2)t]v_t+\left[\frac{\gamma(\gamma+4)}{16}-\frac{k}{2}-\frac{k^2}{4}\right]v=0. \quad (4)$$

This equation is similar to Eq. G(4). Exact correspondence may be achieved by making $\gamma=4m-2k$. The solution of the above equation is

$$F\left(\frac{k}{2}-\frac{\gamma}{4},\ \frac{k}{2}+\frac{\gamma}{4}+1,\ k+1,\ t\right).$$

This is of the form $F(a, b, c, t)$ with $c-a-b=0$, and we wish to know its behavior as $t\to 1$. Lindelof,[8] among others, has shown that in this case

$$F(a, b, c, t)=P(t)-[\Gamma(c)/\Gamma(a)\Gamma(b)]\log(1-t)$$

where P(1) is finite. A glance at G(9) shows that the variational integral will not exist unless the coefficient of $\log(1-t)$ is zero. This will only be so if either a or b is a negative integer or zero. We thus have two possibilities: (1), $(k/2)+(\gamma/4)+1=-n$, $(n=0, 1, 2\cdots)$, implying $\gamma=-4n-4-2k$; and (2), $(k/2)-(\gamma/4)=-n$, or $\gamma=2k+4n$. Now the exponent γ must be the same no matter what the magnitude of the term representing the electronic interaction. If this term were not present, the solution of the wave equation would be

$$\psi=e^{-(1/2)(r_1+r_2)}=e^{-\frac{1}{2}[2(r-v)]^{\frac{1}{2}}+[2(r+v)]^{\frac{1}{2}}]}.$$

For this solution $\gamma=0$, so that $k=0$ and $n=0$. A second exponent $\gamma=-4$ is also possible for these values of n and k. The exponent difference is integral, so that the second solution would involve logarithms. It may be ruled out according to our general boundary condition (existence of the variational integral).

For $\gamma=0$, the solution is $a^0=a^{00}=F(0, 1, 1, t)=\text{const}$. We may therefore put $a^0=1$. Now set $p=-1$ in the recursion formula.

$$5a^1+(4/\sin^2\beta)a^1{}_{\varphi\varphi}+4(a^1{}_{\beta\beta}+2\cot 2\beta a^1{}_{\beta})+4fa^0=0. \quad (5)$$

This is an inhomogeneous equation for a^1. The homogeneous equation would correspond to (4) with $\gamma=1$, which is not an eigenvalue of (4). Consequently, any solution of (5) which satisfies the boundary condition will be unique.[9] Such a solution is

$$a^1=-(1/2)^{\frac{1}{2}}\{(1-\sin\varphi\sin\beta)^{\frac{1}{2}}+(1+\sin\varphi\sin\beta)^{\frac{1}{2}}\}+(1/2Z)(1-\cos\varphi\sin\beta)^{\frac{1}{2}}. \quad (6)$$

This reduces, when $Z\to\infty$, to the solution above for the separable case. If (6) be substituted in (5), then (5) is seen to be linear in $1/2Z$, so that one need only verify that the coefficient of $1/2Z$ vanishes. This is done in the Appendix.

[8] E. Lindelof, Acta. Soc. Scient. Fennicae **19**, 22 (1893).
[9] See Courant, *Methoden der Math. Physik*, edition I, p. 277.

The recursion formula with $p=0$ is

$$12a^2+(4/\sin^2\beta)a^2_{\varphi\varphi}+4(a^2_{\beta\beta}+2\cot 2\beta a^2_\beta)+E+4fa^1=0. \tag{7}$$

The homogeneous part of this equation corresponds to (4) with $\gamma=2$, and this is an eigenvalue. In order, therefore, that a solution satisfying the boundary conditions exist, it is necessary[9] that the inhomogeneity corresponding to the self-adjoint form of (4) be orthogonal to the eigenfunction of (4). Expand (7) in Fourier series, obtaining

$$12a^{2k}-(4k^2/\sin^2\beta)a^{2k}+4(a^{2k}_{\beta\beta}+2\cot 2\beta a^{2k}_\beta)=-\frac{1}{\epsilon_k\pi}\int\cos k\varphi(E+4fa^1)d\varphi. \tag{8}$$

Now, if $\gamma=2$, then $k=1$ and $n=0$, so that the solution of (4) is $F(0, 2, 2, t)=\text{const}$. The self-adjoint form of (4) is

$$[t^2(1-t)v']'+\left[\frac{\gamma(\gamma+1)}{16}-\frac{3}{4}\right]tv=0.$$

Substitute $a^{2,1}=t^{\frac{1}{2}}w$, find the equation for w and multiply this by t, and the result is

$$[t^2(1-t)w']'+\left[\frac{\gamma(\gamma+1)}{16}-\frac{3}{4}\right]tw=-(t^{\frac{1}{2}}/16\pi)\int 4fa^1\cos\varphi\,d\varphi. \tag{9}$$

We have already noted that $w=\text{const}$, so that if (9) has a "proper" solution, the equation

$$\int_0^1 t^{\frac{1}{2}}dt\int_0^{2\pi}\cos\varphi fa^1d\varphi=0$$

must be true. We show in the Appendix that this is not so, so that *the ground state solution of (1), if it exists, is not of the form (2)*. Indeed, it would be an accident if there were a solution of (9) of the required type, for everything which enters is predetermined.

Part II

Since the above assumption as to the radial behavior of the wave function has been shown not to yield a proper solution, one must relax the restrictions. As a preliminary, it is convenient to consider a new system of polar coordinates, which we shall call the H system, while the system of Gronwall will be termed the G system. The H system will be defined by the transformation

$$\begin{aligned} x&=r\cos\theta, & 0\le\theta\le\pi,\\ y&=r\sin\theta\cos\varphi, & 0\le\varphi\le\pi,\\ z&=r\sin\theta\sin\varphi, \end{aligned}$$

so that the x axis is the polar axis. In this system, the wave equation is

$$\psi_{ss}+(5/s)\psi_s+(4/s^2\sin^2\theta)(\psi_{\varphi\varphi}+\cot\varphi\psi_\varphi)+(4/s^2)(\psi_{\theta\theta}+2\cot\theta\varphi_\theta)$$
$$+\left\{E+\frac{4}{s[2(1+\sin\theta\cos\varphi)]^{\frac{1}{2}}}+\frac{4}{s[2(1-\sin\theta\cos\varphi)]^{\frac{1}{2}}}-\frac{2}{Zs(1-\cos\theta)^{\frac{1}{2}}}\right\}\psi=0.$$

The corresponding variational problem is

$$\delta\int[\tfrac{1}{4}\psi_s^2+(1/s^2\sin^2\theta)\psi_\varphi^2+(1/s^2)\psi_\theta^2-\tfrac{1}{4}(E-V)\psi^2]s^5\,ds\sin^2\theta\,d\theta\sin\varphi\,d\varphi=0.$$

We are particularly interested in the behavior of ψ near the singularity $\theta=0$, which corresponds to coincidence of the two electrons. Suppose ψ is expansible as an ascending power series in θ at this point, i.e.,

$$\psi=\sum a^{(m)}(s\varphi)\theta^{m+\gamma}.$$

Substituting in the wave equation, we have

$$a^m{}_{ss}+(5/s)a^m{}_s+(4/s^2)(a^{m+2}{}_{\varphi\varphi}+\cot\varphi a^{m+2}{}_\varphi)+(4/s^2)(m+\gamma+2)(m+\gamma+3)a^{m+2}$$
$$+\left(E+\frac{8}{s\sqrt{2}}\right)a^m-\frac{4}{Zs\sqrt{2}}a^{m+1}+\cdots=0.$$

For $m=-2$, $a^0{}_{\varphi\varphi}+\cot\varphi a^0{}_\varphi+\gamma(\gamma+1)a^0=0$.

If $\psi\theta^{-\gamma}$ has a definite value at $\theta=0$, no matter from what direction the axis is approached, then a^0 is independent of φ, and $\gamma=0$, -1. This means that ψ is finite[10] at $\theta=0$ (except perhaps for $s=0$).

Along the y axis, one should expect the solution for small electronic interaction to be not very different from that for no interaction, or in other words to be finite. The magnitude of the interaction is determined by the value of the atomic number Z, which may be varied continuously in the above equation, so that we should expect the wave function along the y axis to be finite in general.

If the wave function is finite and sufficiently continuous except at $s=0$, then a development of the type G(10) is probably valid, since this is analogous to a Laplace series, for which corresponding theorems are true. Let us therefore assume such a development and rewrite G(11) as follows:

$$\psi_n''+(5/s)\psi_n'-(4/s^2)(2m-k)(2m+2-k)\psi_n+E\psi_n+\sum_{n'}\frac{2A(nn')}{\pi s(-E)^{\frac{1}{2}}}\psi_{n'}=0. \tag{10}$$

Make the substitution $\psi_n=(F^n/s^{5/2})$ and abbreviations $B(nn')=(2/\pi)[A(nn')/(-E)^{\frac{1}{2}}]$; $\alpha_n=(2m-k)\times(2m+2-k)$, obtaining

$$F^n{}_{ss}-(4\alpha_n/s^2)F^n+[E-(15/4s^2)]F^n+\sum_{n'}[B(nn')/s]F^{n'}=0. \tag{11}$$

This system may be reduced to one of the first order by the usual device of taking F^n, as a new dependent variable, which we denote as p^n.

Then

$$(dF^n/ds)=p^n,\quad (dp^n/ds)=[(4\alpha^n+(15/4))/s^2]F^n-EF^n-\sum[B(nn')/s]F^{n'}. \tag{12}$$

Infinite systems such as this do not seem to have been studied to any great extent. One would expect that solutions could be found by regarding (12) as the limit of a finite system. That one would obtain in this way all analytic solutions is, however, open to question, in view of the work of Ritt.[11, 12] We shall limit ourselves here to the extrapolation from the finite system (thus making the argument to this extent nonrigorous). Such a system can be solved readily, according to the work of Pierce.[13]

It is convenient to change the notation so that the equations have the same form as those of Pierce. Set $p^i=x^{2i}$ and $F^i=x^{2i-1}$, $i=1, 2\cdots N$.

Then $(dx^{2i-1}/ds)=x^{2i}$, $(dx^{2i}/ds)=[(4\alpha^i+(15/4))/s^2]x^{2i-1}-Ex^{2i-1}-\sum_j[B(2i-1, 2j-1)/s]x^{2j-1}$. (13)

[10] The exponent $\gamma=-1$ gives an infinite variational integral, and must hence be excluded.
[11] J. F. Ritt, Trans. Amer. Math. Soc. **18**, 27 (1917).
[12] See also the summary of work in this field by R. D. Carmichael, Bull. Amer. Math. Soc. **42**, 193 (1936).
[13] J. Pierce, Amer. Math. Monthly **43**, 530 (1936).

This can be written as

$$(dx^k/ds)=\sum_l(\theta_{kl}/s^2)x^l, \quad (k, l=1, 2\cdots 2N), \tag{14}$$

where

$$\theta_{2i-1,\,2i}=s^2,$$
$$\theta_{2i,\,2i-1}=4\alpha^i+(15/4)-Es^2-B_{2i-1,\,2i-1}s,$$
$$\theta_{2i,\,2j-1}=-B_{2i-1,\,2j-1}s \quad (j\neq i),$$
$$\theta_{2i-1,\,2i-1}=0.$$

According to Pierce, the solution of the system (14) is expressible as a series of definite integrals, as follows:

$$x^i=\sum_{h=1}^{\infty}y_{ih}, \tag{15}$$

where

$$y_{ih}=\int_{s_0}^{s}\sum_j(\theta_{ij}/t^2)y_{j,\,h-1}dt, \tag{16}$$

and the integration is to avoid the origin. One is also to start by setting $y_{i1}=c_i$, which are arbitrary constants. For purposes of visualization, it is perhaps best to write down the matrix

$$(\theta_{ij})=\begin{pmatrix} 0 & s^2 & 0 & 0 & 0 & 0 & \cdots \\ \theta_{21} & 0 & \theta_{23} & 0 & \theta_{25} & 0 & \cdots \\ 0 & 0 & 0 & s^2 & 0 & 0 & \cdots \\ \theta_{41} & 0 & \theta_{43} & 0 & \theta_{45} & 0 & \cdots \end{pmatrix}.$$

The equations (16) may be set down in more detail:

$$y_{1h}=\int_{s_0}^{s}y_{2,\,h-1}dt \quad (\text{since } \theta_{ij}=\theta_{12}\delta_{2j}), \tag{16a}$$

$$y_{2h}=\int_{s_0}^{s}\sum_{j=1}^{N}(\theta_{2,\,2j-1}/t^2)y_{2j-1,\,h-1}dt, \tag{16b}$$

$$y_{3h}=\int_{s_0}^{s}y_{4,\,h-1}dt, \quad \text{etc.} \tag{16c}$$

The coefficients $\theta_{2,\,2j-1}$ are

$$\theta_{21}=(4\alpha_1+(15/4))-B_{11}s-Es^2$$
$$\theta_{23}=\qquad\qquad -B_{13}s \qquad\qquad , \text{ etc.}$$

Then

$$y_{2j-1,\,2}=\int_{s_0}^{s}(\theta_{2j-1,\,2i}/t^2)y_{2i,\,1}dt=\int_{s_0}^{s}c_{2j}dt=c_{2j}(s-s_0), \tag{17}$$

$$y_{2j,\,2}=\int_{s_0}^{s}[\theta_{2j,\,1}c_1+\theta_{2j,\,3}c_3+\theta_{2i,\,5}c_5+\cdots](dt/t^2)$$

$$=\int_{s_0}^{s}[(4\alpha^j+(15/4)-Et^2)c_{2j-1}-\sum_{i=1}^{N}B_{2j-1,\,2i-1}tc_{2i-1}](dt/t^2)$$

$$=\left[-(4\alpha^j+(15/4))\left(\frac{1}{s}-\frac{1}{s_0}\right)-E(s-s_0)\right]c_{2j-1}-\left(\log\frac{s}{s_0}\right)\sum_{i=1}^{N}B_{2j-1,\,2i-1}c_{2i-1}, \tag{18}$$

$$y_{2j-1,\,3}=\int_{s_0}^{s}(\theta_{2j-1,\,2j}/t^2)y_{2j,\,2}dt=\int_{s_0}^{s}y_{2j,\,2}dt, \tag{19}$$

$$y_{2j,\,2}=\int_{s_0}^{s}(\theta_{2j,\,1}y_{12}+\theta_{2j,\,2}y_{22}+\cdots)(dt/t^2). \tag{20}$$

The general formulae are

$$y_{2j-1,\,i}=\int_{s_0}^{s}y_{2j,\,i-1}dt, \tag{21}$$

$$y_{2j,\,i}=\int_{s_0}^{s}[(4\alpha^j+(15/4)-Et^2)y_{2j-1,\,i-1}-\sum_{k=1}^{N}B_{2j-1,\,2k-1}ty_{2k-1,\,i-1}](dt/t^2). \tag{22}$$

By applying first (22) and then (21), we may proceed from $y_{2k-1,\,i-1}$ to $y_{2j-1,\,i+1}$ or from $y_{2k-1,\,i}$ to $y_{2j-1,\,i+2}$. By mathematical induction, then, we can find the form of all the y_{ik}'s. From formula (19), we see that $y_{2j-1,\,3}=a^j+b^j\log s+c^js+d^js^2$, where a^j, b^j, c^j, and d^j are constants. Applying (22), we have

$$y_{2j,\,4}=\frac{A^j}{s}+\frac{B^j\log s}{s}+C^j\log s+D^j(\log s)^2(+\text{ascending power series in } s).$$

The application of (21) now gives $y_{2j-1,\,5}$ and this is of the same form as $y_{2j-1,\,3}$ except for higher powers of s and $\log s$. In a similar fashion, one may find from $y_{2j-1,\,2}$ the expressions for $y_{2j,\,3}$ and $y_{2j-1,\,4}$. The same results hold, so that the x^{ij} in (15) will be ascending power series in t (or s), except for logarithmic terms. This would imply that the wave function is of the form $\sum_{k=0}^{\infty}c^{(k)}(s,\beta,\varphi)\,(\log s)^k$, where the $c^{(k)}$'s are of the same nature as the ψ of Eq. (2). This conclusion is legitimate subject to two assumptions: (1) that ψ can be expanded in a series of the type G(10), and (2) that the infinite system of equations has qualitatively the same behavior as any finite system.

Discussion

If, at the origin, the solution of the equation with a small electronic interaction were not very different from the corresponding solution of the unperturbed (separable) equation, then we should expect that a solution of the form (2) would be possible. Since this does not appear to be so (Part I), we must conclude that, if a solution of (1) exists, it differs essentially from the separable solution at the origin. Hence we see that the ordinary continuity assumption of perturbation theory cannot be generally legitimate, at least at such a singular point.

Even though the eigenfunctions may exist, the continuity property does not always need to hold. Rellich[14] gives an example in which the eigenvalues vary continuously when a small perturbation is introduced, but the eigenfunctions do not.

For the present, then, we see that there are serious difficulties in the way of finding a solution to the helium wave equation, if such exists. If the properties of continuity in the parameter are to be preserved, then no solution can exist. If a solution does exist, then the continuity requirement must be abandoned, at least in certain regions of phase space. It is conceivable that retention of the continuity

[14] F. Rellich, Math. Annalen **113**, 600 (1936). I am indebted to Professor Weyl for referring me to this paper.

requirement except at the singularities may allow one to find a solution quadratically integrable over all space. This is beyond the scope of the present paper, but is worthy of further investigation.

This research has been carried out at the Institute for Advanced Study, and the writer deeply appreciates the opportunity to avail himself of its facilities. He wishes to thank the University of Illinois for the granting of a sabbatical leave. Furthermore, he is grateful to Professor E. P. Wigner for reminding him of Gronwall's form of the wave equation, and to Professor S. Bochner for fruitful suggestions which led to Part I of this paper. The problem has also been discussed with many others, to whom thanks are extended for their interest and encouragement.

Appendix

1. Solution of Eq. (5), verification

Given: $a^1=a_0^1+(1/2Z)(1-\cos\varphi\sin\beta)^{\frac{1}{2}}$, where a_0^1 satisfies (5) if $Z=\infty$.
To show: a^1 satisfies (5) for any Z.
Demonstration: Let $b^1=a^1-a_0^1$.

$$b^1{}_\beta=-(1/2Z)\tfrac{1}{2}\cos\varphi\cos\beta(1-\cos\varphi\sin\beta)^{-\frac{1}{2}};\qquad b^1{}_\varphi=(1/2Z)\tfrac{1}{2}\sin\varphi\sin\beta(1-\cos\varphi\sin\beta)^{-\frac{1}{2}},$$

$$b^1{}_{\beta\beta}=-(1/2Z)\tfrac{1}{2}\cos\varphi\left\{\frac{1}{2}\frac{\cos\varphi\cos^2\beta}{(1-\cos\varphi\sin\beta)^{\frac{3}{2}}}-\frac{\sin\beta}{(1-\cos\varphi\sin\beta)^{\frac{1}{2}}}\right\},$$

$$b^1{}_{\varphi\varphi}=(1/2Z)\tfrac{1}{2}\sin\beta\left\{-\frac{1}{2}\frac{\sin^2\varphi\sin\beta}{(1-\cos\varphi\sin\beta)^{\frac{3}{2}}}+\frac{\cos\varphi}{(1-\cos\varphi\sin\beta)^{\frac{1}{2}}}\right\},$$

$$(b^1{}_{\varphi\varphi}/\sin^2\beta)+b^1{}_{\beta\beta}=(1/4Z)\left\{-\frac{1}{2}\frac{\sin^2\varphi+\cos^2\varphi\cos^2\beta}{(1-\cos\varphi\sin\beta)^{\frac{3}{2}}}+\frac{\cos\varphi(1+\sin^2\beta)}{\sin\beta(1-\cos\varphi\sin\beta)^{\frac{1}{2}}}\right\},\tag{23}$$

$$2\cot 2\beta b^1{}_\beta=-(1/4Z)(\cos^2\beta-\sin^2\beta)(\cos\varphi/\sin\beta)(1-\cos\varphi\sin\beta)^{-\frac{1}{2}},\tag{24}$$

$$(23)+(24)=(1/4Z)[1-\tfrac{1}{2}(1+\cos\varphi\sin\beta)+3\sin\beta\cos\varphi](1-\cos\varphi\sin\beta)^{-\frac{1}{2}},$$

$$fa^0=(1/4Z)[-2(1-\cos\varphi\sin\beta)^{-\frac{1}{2}}],$$

$$(23)+(24)+fa^0=(1/4Z)[-\tfrac{3}{2}(1-\cos\varphi\sin\beta)^{\frac{1}{2}}]=-\tfrac{3}{4}b^1.$$

Since (25) is the same as (5), the verification is complete. As stated in the text, we have needed only to compare the terms involving Z.

2. Computation of $\int_0^1 t^{\frac{1}{2}}dt\int_0^{2\pi}\cos\varphi fa^1d\varphi$

$$f=[2(1+t^{\frac{1}{2}}\sin\varphi)]^{-\frac{1}{2}}+[2(1-t^{\frac{1}{2}}\sin\varphi)]^{-\frac{1}{2}}-(1/2Z)(1-t^{\frac{1}{2}}\cos\varphi)^{-\frac{1}{2}},$$

$$a^1=-(1/\sqrt{2})\{(1+t^{\frac{1}{2}}\sin\varphi)^{\frac{1}{2}}+(1-t^{\frac{1}{2}}\sin\varphi)^{\frac{1}{2}}\}+(1/2Z)(1-t^{\frac{1}{2}}\cos\varphi)^{\frac{1}{2}},$$

$$fa^1=-1-(1/2Z)^2+(1/2Z\sqrt{2})\{(1-t^{\frac{1}{2}}\cos\varphi)^{\frac{1}{2}}[(1+t^{\frac{1}{2}}\sin\varphi)^{-\frac{1}{2}}+(1-t^{\frac{1}{2}}\sin\varphi)^{-\frac{1}{2}}]$$
$$+(1-t^{\frac{1}{2}}\cos\varphi)^{-\frac{1}{2}}[(1-t^{\frac{1}{2}}\sin\varphi)^{\frac{1}{2}}+(1-t^{\frac{1}{2}}\sin\varphi)^{\frac{1}{2}}]\}.$$

Now, if $h(\varphi)$ is a function of period 2π,

$$\int_0^{2\pi}h(\varphi)d\varphi=-\int_{2\pi}^0h(2\pi-\varphi)d\varphi=\int_0^{2\pi}h(-\varphi)d\varphi.$$

In particular,
$$\int_0^{2\pi}\cos\varphi d\varphi\left(\frac{1-t^{\frac{1}{2}}\cos\varphi}{1+t^{\frac{1}{2}}\sin\varphi}\right)^{\frac{1}{2}}=\int_0^{2\pi}\cos\varphi d\varphi\left(\frac{1-t^{\frac{1}{2}}\cos\varphi}{1-t^{\frac{1}{2}}\sin\varphi}\right)^{\frac{1}{2}}.$$

Also,
$$\int_0^{2\pi}\cos\varphi d\varphi\left(\frac{1-t^{\frac{1}{2}}\cos\varphi}{1-t^{\frac{1}{2}}\sin\varphi}\right)^{\frac{1}{2}}=\int_0^{2\pi}\cos(\varphi+\pi/2)d(\varphi+\pi/2)\left(\frac{1-t^{\frac{1}{2}}\cos(\varphi+\pi/2)}{1-t^{\frac{1}{2}}\sin(\varphi+\pi/2)}\right)^{\frac{1}{2}}$$
$$=\int_0^{2\pi}-\sin\varphi d\varphi\left(\frac{1+t^{\frac{1}{2}}\sin\varphi}{1-t^{\frac{1}{2}}\cos\varphi}\right)^{\frac{1}{2}}=\int_0^{2\pi}\sin\varphi d\varphi\left(\frac{1-t^{\frac{1}{2}}\sin\varphi}{1-t^{\frac{1}{2}}\cos\varphi}\right)^{\frac{1}{2}}.$$

Therefore

$$I=\int_0^{2\pi}fa^1\cos\varphi d\varphi=(1/Z\sqrt{2})\int_0^{2\pi}(\cos\varphi+\sin\varphi)d\varphi\left(\frac{1-t^{\frac{1}{2}}\sin\varphi}{1-t^{\frac{1}{2}}\cos\varphi}\right)^{\frac{1}{2}}.$$

The quickest and most convenient procedure is to evaluate $I(t)$ numerically. It is also useful to know how I behaves near the end points $t=0$ and $t=1$.

(a) For $t=0$, expand the integrand in a Taylor's series.

$$\sqrt{2}ZI=\int_0^{2\pi}(\cos\varphi+\sin\varphi)d\varphi[1-\tfrac{1}{2}t^{\frac{1}{2}}\sin\varphi-\tfrac{1}{8}t\sin^2\varphi-\tfrac{1}{16}t^{\frac{3}{2}}\sin^3\varphi-\cdots][1+\tfrac{1}{2}t^{\frac{1}{2}}\cos\varphi+\tfrac{3}{8}t\cos^2\varphi+\tfrac{5}{16}t^{\frac{3}{2}}\cos^3\varphi+\cdots]$$
$$=\int_0^{2\pi}(\cos\varphi+\sin\varphi)d\varphi[1+\tfrac{1}{2}t^{\frac{1}{2}}(-\sin\varphi+\cos\varphi)+t(\tfrac{3}{8}\cos^2\varphi-\tfrac{1}{4}\cos\varphi\sin\varphi-\tfrac{1}{8}\sin^2\varphi)$$
$$+t^{\frac{3}{2}}(\tfrac{5}{16}\cos^3\varphi-\tfrac{3}{16}\cos^2\varphi\sin\varphi-\tfrac{1}{16}\cos\varphi\sin^2\varphi-\tfrac{1}{16}\sin^3\varphi)+\cdots].$$

Only the odd powers of $t^{\frac{1}{2}}$ will have nonvanishing coefficients. The coefficient of $t^{\frac{1}{2}}$ itself is zero, and if we consider values of t for which $t^2 \ll 1$, then

$$\sqrt{2}ZI \leqq t^{\frac{1}{2}}\int_0^{2\pi} (\cos\varphi + \sin\varphi)d\varphi(\tfrac{5}{16}\cos^3\varphi - \tfrac{3}{16}\cos^2\varphi\sin\varphi - \tfrac{1}{16}\cos\varphi\sin^2\varphi - \tfrac{1}{16}\sin^3\varphi)$$
$$= t^{\frac{1}{2}}\int_0^{2\pi} d\varphi(\tfrac{5}{16}\cos^4\varphi + \tfrac{1}{8}\cos^3\varphi\sin\varphi - \tfrac{1}{8}\cos^2\varphi\sin^2\varphi - \tfrac{1}{8}\cos\varphi\sin^3\varphi - \tfrac{1}{16}\sin^4\varphi)$$
$$= \pi/8t^{\frac{1}{2}}.$$

(b) As $t \to 1$, I becomes infinite, as may be seen from inspection. The infinity is due to the behavior of the integrand near $\varphi = 0$, and it is therefore obvious that I becomes infinite in the same way as

$$J = \int_0^{2\pi} \cos\varphi d\varphi(1 - t^{\frac{1}{2}}\cos\varphi)^{-\frac{1}{2}} = \text{const.}\, t^{\frac{1}{2}}F(\tfrac{3}{4}, \tfrac{3}{4}, 2, t). \qquad \text{(See "G".)}$$

If $t \to 1$, J behaves as $-t^{\frac{1}{2}}\log(1-t)$, which is positive.

(c) Numerical integration yields positive values of I for values of t between 0 and 1. The following values of cI (c a constant) show the run of the function:

$t = 0.09$, $cI = 0.15$; $t = 0.25$, $cI = 0.80$; $t = 0.64$, $cI = 5.5$; and $t = 0.95$ $cI = 23$.

It is therefore to be concluded that I is positive throughout the interval $0 \leqq t \leqq 1$, and that the integral $\int_0^1 t^{\frac{1}{2}}dtI(t)$ cannot possibly vanish.

APRIL 15, 1937 PHYSICAL REVIEW VOLUME 51

On the Connection Formulas and the Solutions of the Wave Equation

RUDOLPH E. LANGER
Department of Mathematics, University of Wisconsin, Madison, Wisconsin

Part 1 gives a general discussion of asymptotic representations of the solutions of the one-dimensional wave equation. The forms ordinarily used in the so-called W. K. B. method are multiple valued and consequently necessitate a consideration of the Stokes' phenomenon, in any region about a turning point, i.e., a point in which the kinetic energy changes sign. Except under restrictive hypotheses they give no description of the solutions near the turning points. The author's method for representing the solutions of such differential equations by means of single valued functions is discussed, and the formulas applicable to the wave equation are given. These formulas are usable over the whole of an interval which includes a turning point. The Stokes' phenomenon is not involved. It need be considered only if expressions of the older type are desired, and then the connection formulas of the W. K. B. method are immediately evolved. An appropriate formal development of the solutions of the wave equation as power series in $\hbar$ is given.

Part 2 deals with the radial wave equation for motion in a central field of force. Both the attractive and repulsive Coulomb field are considered. It is shown that the application of the W. K. B. analysis to this equation as it has generally been made is uncritical and in error. The solution commonly identified thereby as the wave function is in fact not the wave function. The "failure" of the W. K. B. formulas, and the apparent necessity for modifying them by replacing the number $l(l+1)$ by $(l+\frac{1}{2})^2$, has been noted by many investigators. This is traced to the misapplication of the theory. When correctly applied the theory naturally yields the formulas which have been found to be called for on other grounds.

Finally the case is discussed in which a turning point lies too near the point $r = 0$ for the W. K. B. method to be effectively applicable. It is shown how the solutions are describable in this case, the formulas given specializing, when the field is an attractive field and the energy is zero, to formulas which were given for that special case by Kramers.

PART 1. THE ONE-DIMENSIONAL WAVE EQUATION

THE wave equation for a mechanical system of one degree of freedom is familiarly of the form

$$d^2u/dx^2 + Q^2(x)u = 0, \qquad (1)$$

with

$$Q^2(x) = \frac{2m}{\hbar^2}\{E - V(x)\}.$$

m, E and $V(x)$ representing respectively the mass, the total energy and the potential energy,

and $\hbar$ standing for $h/2\pi$, where h is Planck's constant. With the exception of a few special functions $V(x)$ the equation is not explicitly solvable. In general, therefore, its solutions must be studied through the medium of representative functions which in a specific sense approximate them. A well-known procedure for obtaining such representations[1] consists in effect of substituting into the differential equation a series in powers of $\hbar$. With proper adjustments the coefficients of such a series may be successively determined, at least theoretically, whenever x is restricted to an interval upon which the function $Q^2(x)$ is bounded from zero. The series so obtained, still with x restricted as noted, represent the solutions in the sense that they are approximations to them which take on an asymptotic character with respect to $\hbar$ when this symbol is regarded as an arbitrary small parameter. Retaining only the first terms of the series one finds in this way, if $Q^2(x)$ is positive the real functions

$$W_+(x;\gamma,\delta)=\delta Q^{-\frac{1}{2}}(x)\cos\left\{\int_{x_1}^{x}Q\,dx+\gamma\right\}, \quad (2)$$

and if $Q^2(x)$ is negative the real functions

$$W_-(x;\alpha,\beta)=|Q(x)|^{-\frac{1}{2}}\left\{\alpha\exp\left[\int_{x_1}^{x}|Q|\,dx\right]+\beta\exp\left[-\int_{x_1}^{x}|Q|\,dx\right]\right\}. \quad (3)$$

The letters α, β, γ, δ stand for entirely arbitrary constants, while x_1 may, in each case, be any constant for which the integral concerned is convergent.

Upon any interval on which $Q^2(x)$ is positive, the form (2) with each choice of its constants represents some solution of the equation (1). If there is also an interval upon which $Q^2(x)$ is negative that same solution is represented thereon by a form (3), with specific constants. The property that they represent one and the same solution thus correlates each form (2) with a form (3) and *vice versa*, the correlation being fixed by the association of their respective constants. It is easily seen that to determine this association much more is necessary than, for instance, the mere substitution of $i|Q|$ in the place of Q and the transcription of (2) into the form (3). For, in the first place, each of the forms (2) or (3) becomes infinite at any point where $Q^2(x)$ is zero, and hence neither form can be retained during the transit from one to another interval between which $Q^2(x)$ changes sign. In the second place the differential equation of which the functions (2) and (3) are solutions is

$$d^2W/dx^2+\{Q^2(x)-\omega(x)\}W=0 \quad (4)$$

with

$$\omega(x)=3[Q'(x)]^2/4Q^2(x)-Q''(x)/2Q(x).$$

For this equation any point where $Q^2(x)$ vanishes is obviously a singular point. The functions (2) and (3) are, therefore, multiple valued in the region about such a point (i.e., a so-called turning point) whereas the solutions of the equation (1) are single valued. Since the approximation of a single valued function by a multiple valued one can maintain only in a restricted region, it is clear, that the mere existence of a pair of relations

$$\begin{aligned} u(x)&\sim W_+(x;\gamma,\delta),\\ u(x)&\sim W_-(x;\alpha,\beta), \end{aligned} \quad (5)$$

valid, respectively, in intervals on opposite sides of a turning point, cannot be used as a basis for inferring that the right-hand members are one and the same solution of the equation (4) simply because the left-hand members are the same solution of the equation (1). The contrary is in fact the case; the so-called Stokes' phenomenon.

The possibility of inferring either of the relations (5) from the other depends, therefore, upon the so-called "connection formulas," which associated the values α, β with the γ, δ, and which are, therefore, the quantitative analysis of the Stokes' phenomenon. Such formulas have been deduced from various considerations. Thus they have been obtained for such cases as permit the assumption that in a suitable interval including the turning point the function $Q^2(x)$ is representable with a sufficient degree of accuracy by a linear function.[2] They have also been found for

[1] J. Horn, Math. Annalen **52**, 271 (1899); G. D. Birkhoff, Trans. Amer. Math. Soc. **9**, 219 (1908); O. Blumenthal, Archiv. d. Math. u. Physik **19**, 136 (1912); G. Wentzel, Zeits. f. Physik **38**, 518 (1926).

[2] H. A. Kramers, Zeits. f. Physik **39**, 829 (1926); also H. Jeffreys, Proc. London Math. Soc. (2) **23**, 428 (1923); also H. A. Kramers and G. P. Ittmann, Zeits. f. Physik **58**, 217 (1929); and for an extension of the method, S. Goldstein, Proc. London Math. Soc. (2) **28**, 81 (1929).

such cases as permit the assumption of a suitable mode of passage around the turning point through the complex plane.[3] This latter method unfortunately leads to no description of the solutions in the immediate neighborhood of the turning point. The problem can, however, be dealt with, and with greater effectiveness, by a method which eliminates completely the whole source of the difficulty,[4] namely the approximation of a single valued function by means of multiple valued ones.

If in an equation of the form (1) x_1 is a turning point at which the function $Q^2(x)$ has a zero, which may be of any order, say ν, the functions

$$U(x;\alpha,\beta)=S(x)\{\alpha\xi^{\mu}J_{-\mu}(\xi)+\beta\xi^{\mu}J_{\mu}(\xi)\} \quad (6)$$

are solutions of the differential equation

$$\frac{d^2U}{dx^2}+\{Q^2(x)-\theta(x)\}U=0 \quad (7)$$

with

$$\theta(x)=S''(x)/S(x). \quad (8)$$

The symbols J in (6) stand for the Bessel functions usually so denoted, while

$$\mu=\frac{1}{\nu+2},\quad \xi=\int_{x_1}^{x}Qdx,\quad S(x)=Q^{-\frac{1}{2}}(x)\xi^{\frac{1}{2}-\mu}. \quad (9)$$

The differential equation (7) resembles the equation (1) on any range of values for which the function $\theta(x)$ is small relatively to $Q^2(x)$. It can be shown that this includes any range on which representation of the solutions of (1) by forms (2) or (3) is possible. Beyond that, however, the range need not exclude the turning point x_1, for in the neighborhood of this point, as may easily be verified, the function $S(x)$ is bounded from zero. Since the turning point is, therefore, an ordinary, nonsingular point for the equation (7), the functions (6) are single valued, and are thus evidently suited with a distinct advantage over such functions as (2) or (3), for instance, for the rôle of approximations to the single valued solutions of the equation (1). They are not restricted to yield representations of the solutions of (1) in intervals on the one or the other side of the turning point, but are adapted to do so in the whole interval including the turning point. The term "representation" is used to signify, as heretofore, the leading term of an expression which is asymptotic with respect to $\hbar$.

As is evident the representations (6) are explicitly relative to the point x_1. At any other turning point they are to be replaced by those relative to it, which are again obtainable from the formulas (6) with only the obvious modifications. It is a necessary restriction, then, that the interval may not extend across or even completely up to another turning point. Except for this it may extend even to infinity, provided in such case that the integral

$$\int|\theta(x)/Q(x)|\,dx \quad (10)$$

converges, when extended over the interval, with the permissible exception of a neighborhood of x_1.

Since the representation of a solution of Eq. (1) by a form (6), if it holds at all thus holds to the left, to the right and at the turning point, no question of connection formulas arises in association with it. The Stokes' phenomenon is therefore obviated, unless, to be sure, representations in terms of the more familiar functions (2) or (3) are desired. In that case it is merely necessary to replace the Bessel functions in (6) by their appropriate asymptotic expressions which are available from the literature of the Bessel functions. If that is done the connection formulas associating the forms (2) and (3) appear automatically and without resort to additional restrictions.

In the usual case the wave equation (1) involves a function $Q^2(x)$ which has a simple zero at x_1. With the positive direction of the x chosen so that $(x-x_1)$ has the same sign as $Q(x)$, the form (6) becomes more explicit, the general solution of the equation (1) being represented by the formula

$$u(x)\sim\left\{\frac{8\pi\xi}{3Q}\right\}^{\frac{1}{2}}\left\{\cos\left(\frac{\pi}{3}+\eta\right)J_{1/3}(\xi)+\cos\left(\frac{\pi}{3}-\eta\right)J_{-1/3}(\xi)\right\} \quad (11a)$$

with $\xi=\int_{x_1}^{x}Qdx$, and η an arbitrary constant on

[3] A. Zwaan, *Dissertation* (Utrecht, 1929), see also E. C. Kemble, Phys. Rev. **48**, 549 (1935).

[4] R. E. Langer, Trans. Am. Math. Soc. **33**, 29 (1931), also **34**, 447 (1932), also Bull. Am. Math. Soc. **37**, 397 (1935).

the range $-\pi/2<\eta\leqq\pi/2$. This form is real when $(x-x_1)$ is positive or zero. When $(x-x_1)$ is negative it may be rewritten so as again to avoid the use of imaginaries in the form

$$u(x)\sim\left\{\frac{8|\xi|}{\pi|Q|}\right\}^{\frac{1}{2}}\left\{\pi\sin\eta\cdot I_{1/3}(|\xi|)+2\cos\left(\frac{\pi}{3}-\eta\right)K_{1/3}(|\xi|)\right\} \quad (11b)$$

with $|\xi|=\int_x^{x_1}|Q|dx$. These formulas describe $u(x)$ over a whole interval including x_1. In subintervals lying completely on one or the other side of x_1 the Bessel functions admit of asymptotic representations, the substitution of which results in the formulas

$$\begin{aligned}&\text{(a)}\quad u(x)\sim 2Q^{-\frac{1}{2}}(x)\cos\{\xi-(\pi/4)+\eta\},\\ &\text{(b)}\quad u(x)\sim|Q(x)|^{-\frac{1}{2}}\{2\sin\eta\cdot e^{|\xi|}+\cos\eta\cdot e^{-|\xi|}\},\end{aligned} \quad (12)$$

which are appropriate, respectively, when $(x-x_1)$ is positive or negative. It is clear that in (12b) the term in the negative exponential is negligible relatively to the other, except when η is numerically very small.

The formulas (12) clearly involve the connection formulas appropriate to (2) and (3), for if the phase of the solution $u(x)$ dictates for η in (12a) a value differing appreciably from zero, this value substituted in (12b) leads to the connection formula

$$|Q(x)|^{-\frac{1}{2}}\left\{2\sin\eta\cdot\exp\left[\int_x^{x_1}|Q|dx\right]+\cos\eta\cdot\exp\left[-\int_x^{x_1}|Q|dx\right]\right\}\rightarrow 2Q^{-\frac{1}{2}}(x)\cos\left\{\int_{x_1}^{x}Qdx-\frac{\pi}{4}+\eta\right\}, \quad (13)$$

$$\eta\neq 0.$$

The case in which there is no other turning point to the left of x_1 requires special mention. For in that case the wave function, i.e., the solution $u(x)$ which remains bounded for all x can be given by (12b) only with $\eta=0$. This value in (12a) evidently leads to the connection formula

$$|Q(x)|^{-\frac{1}{2}}\exp\left[-\int_x^{x_1}|Q|dx\right]\rightarrow 2Q^{-\frac{1}{2}}(x)\cos\left\{\int_{x_1}^{x}Qdx-\frac{\pi}{4}\right\}, \quad (14)$$

which is central in the so-called W.K.B. method of dealing with the equation (1). Near the turning point the descriptions of the solutions to which either (13) or (14) apply are obtainable from the formulas (11a) or (11b) with appropriate values of η.

It must be born in mind that the formulas here in question are all in a sense approximate, and not exact. On that account it is essential that inference of the one representation from the other in the relations (13) or (14) be made only in the directions indicated by the arrows. A comparison of formula (12a) with experimental or other data can suffice only to determine the value of η *approximately*. This fact is of dominating importance when the distinction between "η equals zero" or "η *nearly* equals zero" is in question, for in the former case the first term in (12b) is absent, while in the latter it is present and then necessarily of dominant importance when x is sufficiently remote from x_1. The arrow in (14), therefore, may not be reversed. On the other hand, since an arbitrary multiplicative constant factor may be inserted in or removed from $u(x)$, the value of η is identifiable from (12b) only when the second term is not entirely overshadowed by the first, namely when $\eta=0$. Hence one may not reverse the arrow in (13).[5]

The deduction of power series in $\hbar$ which are asymptotic to $u(x)$, and of which the forms (2) or (3) are the leading terms is familiar, as has already been mentioned. It is to be noted that such series with the forms (6) as leading terms may also be formally derived. Let the expression

$$U'(x)A(x,\hbar^2)+U(x)B(x,\hbar^2),$$

[5] The case in which two turning points lie too close together for application of the formulas (13) and (14) requires independent consideration. Cf. S. Goldstein, Proc. London Math. Soc. (2) **33**, 246 (1932); W. Voss, Zeits. f. Physik **83**, 581 (1933); R. E. Langer, Trans. Am. Math. Soc. **36**, 90 (1934), and Bull. Am. Math. Soc. **40**, 574 (1934).

in which

$$A(x, \hbar^2)=\sum_{j=0}^{\infty}\alpha_j(x)\hbar^{2j},$$

$$B(x, \hbar^2)=\sum_{j=0}^{\infty}\beta_j(x)\hbar^{2j},$$

be substituted for $u(x)$ in the equation (1). It is found then, if

$$Q^2(x)=\frac{1}{\hbar^2}q_1{}^2(x)+q_0(x),$$

that

$$U(x)\left\{\left(2\theta-\frac{2q_1{}^2}{\hbar^2}-2q_0\right)A'+\left(\theta-\frac{q_1{}^2}{\hbar^2}-q_0\right)'A+B''+\theta B\right\}+U'(x)\{2B'+A''+\theta A\}=0.$$

If the coefficient of each power of $\hbar^2$ which multiplies either $U(x)$ or $U'(x)$ is set equal to zero, the choice $\alpha_0=0$, $\beta_0=1$, is seen to be permissible, while the subsequent coefficients must satisfy the relations

$$2q_1{}^2\alpha_j'+2q_1q_1'\alpha_j=\beta_{j-1}''+\theta\beta_{j-1}+(2\theta-2q_0)\alpha_{j-1}'+(\theta'-q_0')\alpha_{j-1},$$

$$2\beta_j'=-\alpha_j''-\theta\alpha_j, \qquad j=1, 2, 3, \cdots.$$

Thus, one obtains formally the expansion

$$u(x)=U(x)+U'(x)\sum_{j=1}^{\infty}\alpha_j(x)\hbar^{2j}+U(x)\sum_{j=1}^{\infty}\beta_j(x)\hbar^{2j}, \quad (15)$$

in which the coefficients are given in succession by the formulas

$$\alpha_j(x)=\frac{1}{2q_1(x)}\int^x\frac{2(\theta-q_0)\alpha_{j-1}'+(\theta'-q_0')\alpha_{j-1}+\beta_{j-1}''+\theta\beta_{j-1}}{q_1}dx, \quad (16)$$

$$\beta_j(x)=-\frac{1}{2}\int^x(\alpha_j''+\theta\alpha_j)dx,$$

with any chosen constants as the lower limits of integration. It is to be noted that the formulas (16) are convergent even when x is the turning point.

Part 2. The Radial Wave Equation

In the case of motion in a central field of force the general wave equation in spherical polar coordinates permits a separation of the variables.[6] If the radial component of the motion is designated by $\psi(r)/r$, the wave equation for $\psi(r)$ is thus found to be

$$d^2\psi/dr^2+Q_0{}^2(r)\psi=0 \quad (17)$$

with

$$Q_0{}^2(r)=\frac{2m}{\hbar^2}\left\{E+\frac{Ze^2}{r}\right\}-\frac{l(l+1)}{r^2}. \quad (18)$$

With the customary interpretation of the symbols the formula (18) implies the field to be an attractive field, since the potential energy is given by the term $-Ze^2/r$. The case of a repulsive field may be included in the discussion by the simple expedient of admitting for the charge Z negative values as well as positive ones. The variable r representing radial distance is, of course, restricted to be positive.

Structurally, the equation (17) bears evident features of resemblance to the equation (1). Insofar as the writer is aware, the degree of this resemblance has hitherto been regarded without exception as sufficient for assuming the out-and-out applicability to the equation (17) of the formulas deduced in the foregoing discussion, especially of the formula (14). The first point at which $Q_0{}^2(r)$ is zero is found directly to be

$$\text{(a)}\quad \rho_1=\frac{l(l+1)\hbar^2}{mZe^2\left\{1+\left(1+\frac{2El(l+1)\hbar^2}{mZ^2e^4}\right)^{\frac{1}{2}}\right\}}, \quad \text{if } Z>0,\ l\neq 0,\ E\gtreqless 0, \quad (19)$$

$$\text{(b)}\quad \rho_1=\frac{Ze^2}{-2E}\left\{1+\left(1+\frac{2El(l+1)\hbar^2}{mZ^2e^4}\right)^{\frac{1}{2}}\right\}, \quad \text{if } Z<0,\ E>0.$$

[6] Cf., for instance, T. Sexl, Zeits. f. Physik **99**, 751 (1936).

the range $-\pi/2<\eta\leqq\pi/2$. This form is real when $(x-x_1)$ is positive or zero. When $(x-x_1)$ is negative it may be rewritten so as again to avoid the use of imaginaries in the form

$$u(x)\sim\left\{\frac{8|\xi|}{\pi|Q|}\right\}^{\frac{1}{2}}\left\{\pi\sin\eta\cdot I_{1/3}(|\xi|)+2\cos\left(\frac{\pi}{3}-\eta\right)K_{1/3}(|\xi|)\right\} \quad (11b)$$

with $|\xi|=\int_x^{x_1}|Q|dx$. These formulas describe $u(x)$ over a whole interval including x_1. In subintervals lying completely on one or the other side of x_1 the Bessel functions admit of asymptotic representations, the substitution of which results in the formulas

$$\begin{aligned}&\text{(a)}\quad u(x)\sim 2Q^{-\frac{1}{2}}(x)\cos\{\xi-(\pi/4)+\eta\},\\&\text{(b)}\quad u(x)\sim|Q(x)|^{-\frac{1}{2}}\{2\sin\eta\cdot e^{|\xi|}+\cos\eta\cdot e^{-|\xi|}\},\end{aligned} \quad (12)$$

which are appropriate, respectively, when $(x-x_1)$ is positive or negative. It is clear that in (12b) the term in the negative exponential is negligible relatively to the other, except when η is numerically very small.

The formulas (12) clearly involve the connection formulas appropriate to (2) and (3), for if the phase of the solution $u(x)$ dictates for η in (12a) a value differing appreciably from zero, this value substituted in (12b) leads to the connection formula

$$\begin{aligned}|Q(x)|^{-\frac{1}{2}}&\left\{2\sin\eta\cdot\exp\left[\int_x^{x_1}|Q|dx\right]\right.\\&\left.+\cos\eta\cdot\exp\left[-\int_x^{x_1}|Q|dx\right]\right\}\\&\rightarrow 2Q^{-\frac{1}{2}}(x)\cos\left\{\int_{x_1}^{x}Qdx-\frac{\pi}{4}+\eta\right\},\end{aligned} \quad (13)$$

$$\eta\neq 0.$$

The case in which there is no other turning point to the left of x_1 requires special mention. For in that case the wave function, i.e., the solution $u(x)$ which remains bounded for all x can be given by (12b) only with $\eta=0$. This value in (12a) evidently leads to the connection formula

$$|Q(x)|^{-\frac{1}{2}}\exp\left[-\int_x^{x_1}|Q|dx\right]\rightarrow 2Q^{-\frac{1}{2}}(x)\cos\left\{\int_{x_1}^{x}Qdx-\frac{\pi}{4}\right\}, \quad (14)$$

which is central in the so-called W.K.B. method of dealing with the equation (1). Near the turning point the descriptions of the solutions to which either (13) or (14) apply are obtainable from the formulas (11a) or (11b) with appropriate values of η.

It must be born in mind that the formulas here in question are all in a sense approximate, and not exact. On that account it is essential that inference of the one representation from the other in the relations (13) or (14) be made only in the directions indicated by the arrows. A comparison of formula (12a) with experimental or other data can suffice only to determine the value of η *approximately*. This fact is of dominating importance when the distinction between "η equals zero" or "η *nearly* equals zero" is in question, for in the former case the first term in (12b) is absent, while in the latter it is present and then necessarily of dominant importance when x is sufficiently remote from x_1. The arrow in (14), therefore, may not be reversed. On the other hand, since an arbitrary multiplicative constant factor may be inserted in or removed from $u(x)$, the value of η is identifiable from (12b) only when the second term is not entirely overshadowed by the first, namely when $\eta=0$. Hence one may not reverse the arrow in (13).[5]

The deduction of power series in $\hbar$ which are asymptotic to $u(x)$, and of which the forms (2) or (3) are the leading terms is familiar, as has already been mentioned. It is to be noted that such series with the forms (6) as leading terms may also be formally derived. Let the expression

$$U'(x)A(x,\hbar^2)+U(x)B(x,\hbar^2),$$

[5] The case in which two turning points lie too close together for application of the formulas (13) and (14) requires independent consideration. Cf. S. Goldstein, Proc. London Math. Soc. (2) **33**, 246 (1932); W. Voss, Zeits. f. Physik **83**, 581 (1933); R. E. Langer, Trans. Am. Math. Soc. **36**, 90 (1934), and Bull. Am. Math. Soc. **40**, 574 (1934).

in which

$$A(x, \hbar^2)=\sum_{j=0}^{\infty}\alpha_j(x)\hbar^{2j},$$

$$B(x, \hbar^2)=\sum_{j=0}^{\infty}\beta_j(x)\hbar^{2j},$$

be substituted for $u(x)$ in the equation (1). It is found then, if

$$Q^2(x)=\frac{1}{\hbar^2}q_1{}^2(x)+q_0(x),$$

that

$$U(x)\left\{\left(2\theta-\frac{2q_1{}^2}{\hbar^2}-2q_0\right)A'+\left(\theta-\frac{q_1{}^2}{\hbar^2}-q_0\right)'A+B''+\theta B\right\}+U'(x)\{2B'+A''+\theta A\}=0.$$

If the coefficient of each power of $\hbar^2$ which multiplies either $U(x)$ or $U'(x)$ is set equal to zero, the choice $\alpha_0=0$, $\beta_0=1$, is seen to be permissible, while the subsequent coefficients must satisfy the relations

$$2q_1{}^2\alpha_j'+2q_1q_1'\alpha_j=\beta_{j-1}''+\theta\beta_{j-1}+(2\theta-2q_0)\alpha_{j-1}'+(\theta'-q_0')\alpha_{j-1},$$

$$2\beta_j'=-\alpha_j''-\theta\alpha_j, \qquad j=1, 2, 3, \cdots.$$

Thus, one obtains formally the expansion

$$u(x)=U(x)+U'(x)\sum_{j=1}^{\infty}\alpha_j(x)\hbar^{2j}+U(x)\sum_{j=1}^{\infty}\beta_j(x)\hbar^{2j}, \quad (15)$$

in which the coefficients are given in succession by the formulas

$$\alpha_j(x)=\frac{1}{2q_1(x)}\int^x\frac{2(\theta-q_0)\alpha_{j-1}'+(\theta'-q_0')\alpha_{j-1}+\beta_{j-1}''+\theta\beta_{j-1}}{q_1}dx, \quad (16)$$

$$\beta_j(x)=-\frac{1}{2}\int^x(\alpha_j''+\theta\alpha_j)dx,$$

with any chosen constants as the lower limits of integration. It is to be noted that the formulas (16) are convergent even when x is the turning point.

Part 2. The Radial Wave Equation

In the case of motion in a central field of force the general wave equation in spherical polar coordinates permits a separation of the variables.[6] If the radial component of the motion is designated by $\psi(r)/r$, the wave equation for $\psi(r)$ is thus found to be

$$d^2\psi/dr^2+Q_0{}^2(r)\psi=0 \quad (17)$$

with

$$Q_0{}^2(r)=\frac{2m}{\hbar^2}\left\{E+\frac{Ze^2}{r}\right\}-\frac{l(l+1)}{r^2}. \quad (18)$$

With the customary interpretation of the symbols the formula (18) implies the field to be an attractive field, since the potential energy is given by the term $-Ze^2/r$. The case of a repulsive field may be included in the discussion by the simple expedient of admitting for the charge Z negative values as well as positive ones. The variable r representing radial distance is, of course, restricted to be positive.

Structurally, the equation (17) bears evident features of resemblance to the equation (1). Insofar as the writer is aware, the degree of this resemblance has hitherto been regarded without exception as sufficient for assuming the out-and-out applicability to the equation (17) of the formulas deduced in the foregoing discussion, especially of the formula (14). The first point at which $Q_0{}^2(r)$ is zero is found directly to be

$$\text{(a)}\quad \rho_1=\frac{l(l+1)\hbar^2}{mZe^2\left\{1+\left(1+\frac{2El(l+1)\hbar^2}{mZ^2e^4}\right)^{\frac{1}{2}}\right\}}, \quad \text{if } Z>0,\ l\neq 0,\ E\gtreqless 0, \quad (19)$$

$$\text{(b)}\quad \rho_1=\frac{Ze^2}{-2E}\left\{1+\left(1+\frac{2El(l+1)\hbar^2}{mZ^2e^4}\right)^{\frac{1}{2}}\right\}, \quad \text{if } Z<0,\ E>0.$$

[6] Cf., for instance, T. Sexl, Zeits. f. Physik **99**, 751 (1936).

When $Z<0$, $E<0$, $Q_0^2(r)$ does not vanish at all, and when $Z>0$, $E<0$, it vanishes a second time, namely at the point which is given precisely by (19b). The case $l=0$ for an attractive field stands out as exceptional, for the pole of $Q_0^2(r)$ at $r=0$ is then of a different sort than otherwise, while the zero otherwise given by (19a) is then entirely absent. With the point ρ_1 used in the place of x_1, and with r and $Q_0(r)$ replacing x and $Q(x)$ the relation (14) has been commonly regarded as applicable to the equation (17), and to describe the wave function for that case.[7] This procedure, however, soon leads to a difficulty. The resulting formulas were found by Kramers to give an incorrect phase for the solution unless the number $l(l+1)$ is replaced by $(l+\frac{1}{2})^2$, a modification which is tantamount to raising the potential barrier. Young and Uhlenbeck found the same modification requisite, both if the Balmer formula is to be obtained, and if the wave function is to vanish to the proper degree at $r=0$. This "failure" of the W.K.B. method, i.e., to the extent that the change in question is requisite, has been generally verified both in studies of attractive and repulsive fields. No explanation of it seems to have been given, though that can be done very simply to the following effect. The fault lies not in the method but in the application of it. The commonly accepted assumption that the equation (17) is of the form (1) as it stands is, namely, incorrect. The formula (14) is at best only restrictedly applicable to the equation (17), and when it is applicable it describes a solution which is not bounded, i.e., which is not the wave function.

The functions which constitute the several members of the relations (14) and (13) are solutions of the differential equation

$$d^2\Psi/dr^2+\{Q_0^2(r)-\omega_0(r)\}\Psi=0 \tag{20}$$

with

$$\omega_0(r)=\frac{3[Q_0'(r)]^2}{4Q_0^2(r)}-\frac{Q_0''(r)}{2Q_0(r)}. \tag{21}$$

The resemblance between this equation and the equation (17), and hence the possibility of representing the solutions of the latter by means of those of the former, fails, of course, near the points where $Q_0^2(r)$ becomes zero. It fails also, though this seems to have been overlooked, near $r=0$, for at that point the function $\omega_0(r)$ becomes infinite similarly to $Q_0^2(r)$. The relation (14), therefore, though it can represent a solution of the equation (17) in suitable intervals, cannot do so in an interval which actually reaches up to the point $r=0$. It follows at once from this that the vanishing of the left-hand member of (14) at $r=0$, gives no ground for concluding that the solution of (17) which is elsewhere represented by (14) also vanishes at $r=0$. That is in fact not so. The solution elsewhere represented by (14) becomes infinite at $r=0$, and so is not the wave function.

Let the variables in the equation (17) be changed by the substitution

$$r=e^x, \quad \psi=e^{x/2}u. \tag{22}$$

The domain of the variable becomes then $-\infty<x<\infty$, and the resulting equation is found to be

$$d^2u/dx^2+Q^2(x)u=0, \tag{23}$$

with

$$Q^2(x)=\frac{2m}{h^2}\{E\cdot e^{2x}+Ze^2\cdot e^x\}-(l+\tfrac{1}{2})^2. \tag{24}$$

Now this equation is obviously of the form (1). Its turning points computed from (24) but expressed in terms of r, are found to be

$$\text{(a)}\quad r_1=\frac{(l+\frac{1}{2})^2h^2}{mZe^2\left\{1+\left(1+\dfrac{2E(l+\frac{1}{2})^2h^2}{mZ^2e^4}\right)^{\frac{1}{2}}\right\}}, \quad \text{if } Z>0,\ E\gtreqless 0, \tag{25}$$

$$\text{(b)}\quad r_1=\frac{Ze^2}{-2E}\left\{1+\left(1+\frac{2E(l+\frac{1}{2})^2h^2}{mZ^2e^4}\right)^{\frac{1}{2}}\right\}, \quad \text{if } Z<0,\ E>0,$$

there being no turning point if $Z<0$, $E<0$, and a second one given by (25b) if $Z>0$, $E<0$. The formulas (22) and (24) are found, moreover, to

[7] H. A. Kramers, Zeits. f. Physik **39**, 836 (1926); L. A. Young and G. E. Uhlenbeck, Phys. Rev. **36**, 1158 (1930); E. C. Kemble, Phys. Rev. **48**, 560 (1935); F. L. Yost, J. A. Wheeler and G. Breit, Phys. Rev. **49**, 180 (1935); T. Sexl, Zeits. f. Physik **99**, 771 (1936).

give the identities

$$e^{x/2}Q^{-\frac{1}{2}}(x)\equiv Q_1^{-\frac{1}{2}}(r),$$
$$\int_{x_1}^{x}Q(x)dx\equiv\int_{r_1}^{r}Q_1(r)dr, \tag{26}$$

in which

$$Q_1^2(r)=\frac{2m}{\hbar^2}\left\{E+\frac{Ze^2}{r}\right\}-\frac{(l+\frac{1}{2})^2}{r^2}. \tag{27}$$

The formulas (11), (13) and (14) are directly applicable to the equation (23). If they are so applied, and the original variables are reintroduced, the results are found to be those which are formally obtainable by the direct substitution of r, ψ for u and x, and of the r_1 and $Q_1^2(r)$ of (25) and (27), for x_1 and $Q^2(x)$. The difference between this procedure and the incorrect one of substituting the ρ_1 and $Q_0^2(r)$ of (19) and (18) for x_1 and $Q^2(x)$, is seen to amount formally to precisely the replacement of $l(l+1)$ by $(l+\frac{1}{2})^2$. It will be noted, moreover, that for the formula (25a) the case $l=0$ is not exceptional as it was for (19a).

Since the applicability of the formulas as described right up to the point $r=0$ depends upon their applicability to the equation (23) over the infinite interval to $x=-\infty$, the validity of the procedure is still questionable. It is, however, easily established, for from the formulas (24), (8) and (9) it is seen that as $x\to-\infty$

$$Q(x)=O(1),\quad \theta(x)=O(x^{-2}).$$

Thus the integrand in (10) is of the order of x^{-2}, and for such the integral to $x=-\infty$ converges. The formulas relative to the right-hand turning point (which may, of course, be the only turning point) are similarly seen to be applicable even to $x=+\infty$, for from the formulas (24), (8) and (9) it is seen that as $x\to+\infty$

$$Q(x)=O(e^{-x}),\quad \theta(x)=O(1),$$

whence the integrand in (10) is of the order of e^{-x}, and the integral to $x=+\infty$ is convergent.

Whenever the number l is small the turning point (25a) lies very near to the point $r=0$, and this is true also in the case of the turning point (25b) whenever the energy is very large. The use of the formulas (13) or (14) under such circumstances is questionable, and is generally less satisfactory than otherwise. The formulas are of course entirely inapplicable when there is no turning point at all, namely when $E<0$ with a repulsive field. In such cases the following analysis of the wave equation may be resorted to.

The change of variables

$$r=s^2,\quad \psi=s^{\frac{1}{2}}v, \tag{28}$$

gives to the equation (17) the form

$$(d^2v/ds^2)+\{\lambda^2\varphi^2(s)+(\tfrac{1}{4}-\beta^2)/s^2\}v=0 \tag{29}$$

with
$$\lambda^2=8mZe^2/\hbar^2,\qquad \beta=2l+1,\qquad \varphi^2(s)=1+Es^2/Ze^2 \tag{30}$$

The solutions of an equation of this type are known,[8] however, to be represented by the functions

$$\left\{\frac{\int_0^s\varphi ds}{\varphi(s)}\right\}^{\frac{1}{2}}C_\beta\left(\lambda\int_0^s\varphi ds\right), \tag{31}$$

the symbol C_β signifying any Bessel function of the order $\pm\beta$. The representations are valid from $s=0$ over an interval which does not reach up to a zero of the function $\varphi^2(s)$.

In the case of an attractive field ($Z>0$) the value λ^2 is positive. The choice of C_β successively as J_{2l+1} and Y_{2l+1} yields respectively the representations, which in terms of the original variables are

$$\psi_1(r)\sim\left\{\frac{\int_0^r Q_2dr}{Q_2(r)}\right\}^{\frac{1}{2}}J_{2l+1}\left(\int_0^r Q_2dr\right),$$
$$\psi_2(r)\sim\left\{\frac{\int_0^r Q_2dr}{Q_2(r)}\right\}^{\frac{1}{2}}Y_{2l+1}\left(\int_0^r Q_2dr\right) \tag{32}$$

with
$$Q_2^2(r)=\frac{2m}{\hbar^2}\left\{E+\frac{Ze^2}{r}\right\}. \tag{33}$$

Clearly $\psi_1(r)$ is the solution which vanishes at $r=0$, while $\psi_2(r)$ is a specific one which is unbounded there. Upon substituting for the

[8] R. E. Langer, Trans. Amer. Math. Soc. **37**, 397 (1935).

Bessel functions their familiar asymptotic representations, the formulas become alternatively

$$\psi_1(r)\sim\left(\frac{2}{\pi}\right)^{\frac{1}{2}}Q_2^{-\frac{1}{2}}(r)\cos\left\{\int_0^r Q_2dr-(l+\tfrac{3}{4})\pi\right\},$$
$$\psi_2(r)\sim(2\pi)^{\frac{1}{2}}Q_2^{-\frac{1}{2}}(r)\sin\left\{\int_0^r Q_2dr-(l+\tfrac{3}{4})\pi\right\}. \tag{34}$$

These formulas are usable in intervals which extend across and include the first turning point (25a). When $E<0$ there is a second turning point which limits the intervals of the present formulas, and relative to which the analysis given previously may be applied. In the special case in which $E=0$ the formulas (32) and (34) for the solution $\psi_1(r)$ reduce to formulas which were obtained for that case by Kramers.[9]

In the case of a repulsive field ($Z<0$) the value λ^2 is negative and hence the choices

$$I_{2l+1}\left(|\lambda|\int_0^s \rho ds\right), \quad \text{and} \quad K_{2l+1}\left(|\lambda|\int_0^s \varphi ds\right)$$

for the Bessel functions in (31) will avoid the introduction of imaginaries. The resulting formulas, in terms of the original variables, are then found to be

$$\psi_1(r)\sim\left\{\frac{\int_0^r|Q_2|dr}{|Q_2(r)|}\right\}^{\frac{1}{2}}I_{2l+1}\left(\int_0^r|Q_2|dr\right),$$
$$\psi_2(r)\sim\left\{\frac{\int_0^r|Q_2|dr}{|Q_2(r)|}\right\}^{\frac{1}{2}}K_{2l+1}\left(\int_0^r|Q_2|dr\right). \tag{35}$$

The interval upon which they are usable extends from $r=0$ outward, but when $E<0$ it must not include or extend up to the turning point which then exists. The substitution of asymptotic forms gives the alternative representations

$$\psi_1(r)\sim\frac{1}{(2\pi)^{\frac{1}{2}}}|Q_2(r)|^{-\frac{1}{2}}\exp\left[\int_0^r|Q_2|dr\right],$$
$$\psi_2(r)\sim-\left(\frac{\pi}{2}\right)^{\frac{1}{2}}|Q_2(r)|^{-\frac{1}{2}}\exp\left[-\int_0^r|Q_2|dr\right]. \tag{36}$$

Finally, the substitutions

$$\rho=\frac{(2mE)^{\frac{1}{2}}}{h}r, \quad k=\frac{-Z}{h}\left(\frac{2me^2}{E}\right)^{\frac{1}{2}},$$

reduce the equation (17) to

$$\frac{d^2\psi}{d\rho^2}+\left\{1-\frac{k}{\rho}-\frac{l(l+1)}{\rho^2}\right\}\psi=0.$$

Analyses of the equation in this form, both with $l=0$ and $l\neq0$, have been given.[10] By comparison with them the present analysis and its consequent formulas may be found to have at least the advantages of simplicity and of generality of method.

[9] H. A. Kramers, Zeits. f. Physik **39**, 837 (1926).

[10] T. Sexl, Zeits. f. Physik **56**, 72 (1929); F. L. Yost, J. A. Wheeler and G. Breit, Phys. Rev. **49**, 174 (1935).

LETTERS TO THE EDITOR

Prompt publication of brief reports of important discoveries in physics may be secured by addressing them to this department. Closing dates for this department are, for the first issue of the month, the eighteenth of the preceding month, for the second issue, the third of the month. Because of the late closing dates for the section no proof can be shown to authors. The Board of Editors does not hold itself responsible for the opinions expressed by the correspondents.

Communications should not in general exceed 600 words in length.

Note on the Mathematical Foundation of the Thermodynamical Equation of State

Starting from the resolution of the differential equation for the volume deviation Δv

$$T\left(\frac{\partial(\Delta v)}{\partial T}\right)_p - \Delta v = \varphi(T, p)$$

we shall show that the thermodynamical equation of state may be given in the general form

$$vp = RT + pT\left\{\int \frac{\varphi}{T^2} dT + \theta\right\},$$

where $\varphi(T, p)$ denotes the function of the Joule-Thomson effect and θ depends on pressure alone.

Any equation of state can be represented in the form

$$vp = RT + p\Delta v \tag{1}$$

where Δv (the "volume deviation") may be regarded as a definite function of the independent variables: pressure p or volume v and absolute temperature T; R is the gas constant.

The thermodynamical expression for the Joule-Thomson effect μ_y as a function of T and p gives

$$\varphi(T, p) = \frac{\mu_y C_p}{A} = T\left(\frac{\partial v}{\partial T}\right)_p - v, \tag{2}$$

where C_p and A are, respectively, the specific heat at constant pressure and the thermal equivalent of mechanical energy.

Substituting $(\partial v/\partial T)_p$ and v in Eq. (2) from Eq. (1), we get

$$T(\partial(\Delta v)/\partial T)_p - \Delta v = \varphi(T, p). \tag{3}$$

From the differential Eq. (3), there follows the equation for Δv in the integral form

$$\Phi(p)\Delta v - T \exp\left(\int \frac{\varphi}{\Delta v}\frac{d\psi}{\psi}\right) = 0, \tag{4}$$

which can be resolved in the following way. From Eq. (4) we get

$$lg\frac{\Phi(p)\Delta v}{T} = \int \frac{\varphi}{\Delta v}\frac{dT}{T}$$

or differentiating and simplifying

$$\left(\frac{\partial(\Delta v/T)}{\partial T}\right)_p = \frac{\varphi}{T^2}. \tag{5}$$

Hence integrating

$$\Delta v = T\left\{\int \frac{\varphi}{T^2} dT + \theta\right\}, \tag{6}$$

where θ is the arbitrary function of pressure p alone.[1]

Eq. (3) can be therefore regarded as a satisfactory mathematical foundation for finding the exact and general form of the thermodynamical equation of state.

But while the function φ of the Joule-Thomson effect is not yet satisfactorily known for any body, nevertheless the general resolution (6) and especially (4) are of great importance in limiting the arbitrariness of functional constructions of equations of state and in finding the adequate form by concrete mathematical operations.

The volume v satisfies the same Eq. (2). Hence analogously,

$$v = T\left\{\int \frac{\varphi}{T^2} dT + \theta, (p)\right\}. \tag{7}$$

From Eq. (7) in connection with Eq. (1) and Eq. (6) follows

$$\theta_1 = \theta + R/p, \tag{8}$$

where θ is due to the expression for the volume deviation alone.

Eq. (8) shows that for finding the equation of state the consideration of the volume deviation Δv is more convenient than the direct operation with the volume v, since thus the large and regularly varying term RT/P is eliminated from the calculations.

WITOLD JACYNA

Institute of Metrology,
Leningrad, U.S.S.R.,
February 5, 1937.

[1] The Eq. (3) may also be resolved otherwise. For the case that $\varphi = 0$, we have

$$T\partial(\Delta v_1)/\partial T - \Delta v_1 = 0 \quad \text{and} \quad \Delta v_1 = T\omega(P).$$

The application of Lagrange's method of variation of arbitrary function suggests the resolution of the Eq. (3) where $\varphi \neq 0$, in the form

$$\Delta v = T\Omega(T, p) \tag{a}$$

with the new unknown function Ω. Thus

$$\partial(\Delta v)/\partial T = \Omega + T\partial\Omega/\partial T \tag{b}$$

and substituting in Eq. (3) from Eq. (a) and Eq. (b) we get

$$T^2\partial\Omega/\partial T = \varphi.$$

Hence $\Omega = \int \frac{\varphi}{T^2} dT + \phi(p)$ and finally $\Delta v = T\left\{\int \frac{\varphi}{T^2} dT + \theta\right\}$.

The application of Lagrange's method in the case is due to Professor R. O. Kuzmin in Leningrad.

On the Nuclear Transformation with the Absorption of the Orbital Electron

According to the present theory of β disintegration, the nucleus of atomic number Z transforms into its isobar $Z-1$ with the emission of a positron and a neutrino, if the difference ΔW of proper energies of these isobars is larger than $mc^2 + \mu c^2$, where m and μ are the masses of the electron and the neutrino, respectively. On the contrary, the isobar

TABLE I.

Z	αZ	τ(Fermi)	τ(K-U)
1	1/137	2740 $(\Delta w+1)^{-2}$ years	1860 $(\Delta w+1)^{-4}$ years
2	2/137	170 $(\Delta w+1)^{-2}$ years	120 $(\Delta w+1)^{-4}$ years
14	0.1	200 $(\Delta w+1)^{-2}$ days	130 $(\Delta w+1)^{-4}$ days
27	0.2	25 $(\Delta w+1)^{-2}$ days	16 $(\Delta w+1)^{-4}$ days
69	0.5	12 $(\Delta w+0.87)^{-2}$ hours	8 $(\Delta w+0.87)^{-4}$ hours

$Z-1$ transforms into Z with the emission of an electron and an antineutrino, if ΔW is smaller than $-mc^2-\mu c^2$. The isobar Z can transform into $Z-1$ also by absorbing one of the orbital electrons and emitting a neutrino at the same time, if ΔW is larger than $-E+\mu c^2$, where E is the total energy of the orbital electron.

Thus, two isobars with consecutive atomic numbers are both stable, only if ΔW lies between $-mc^2-\mu c^2$ and $-mc^2+\mu c^2$. This condition can be fulfilled very rarely, if the neutrino mass is small compared with the electron mass. Since the existence of several such pairs of stable nuclei was confirmed by experiment recently,[1] it will be worthwhile to give a brief account of the results of our previous calculations on this subject.[2] It will be interesting, moreover, to determine the ratio of the probabilities of the positron emission and the electron absorption above considered, when ΔW is larger than $mc^2+\mu c^2$.

First, the mean lifetime τ of the nucleus Z due to the absorption of either of two K electrons with $E=mc^2(1-\alpha^2Z^2)^{\frac{1}{2}}$ was calculated for the allowed transition, where α was the fine structure constant. If the neutrino mass is assumed to be zero, τ is approximately proportional to

$$(\alpha Z)^{2\gamma+1}/(\Delta w+\gamma)^2 \quad \text{or} \quad (\alpha Z)^{2\gamma+1}/(\Delta w+\gamma)^4,$$

according as the coupling scheme of Fermi or Konopinski-Uhlenbeck is adopted, where

$$\Delta w=\Delta W/mc^2, \qquad \gamma=(1-\alpha^2Z^2)^{\frac{1}{2}}.$$

The numerical values for several cases are shown in Table I.[3]

The apparent discrepancy between these results and the existence of stable pairs of heavy nuclei can be removed, only if we assume (i) the difference of nuclear spins to be large in every case, or (ii) the neutrino mass to be comparable with the electron mass, or (iii) the wave functions of the electron in the neighborhood of the nucleus to be much smaller than those calculated by Dirac's theory.

The extreme case $Z=1$ in Table I, which corresponds to the transformation of the hydrogen atom into the neutron, will not occur actually according to the recent data of mass defects, whereas the case $Z=2$ has some practical importance indicating the spontaneous transformation of He^3 into H^3 by absorbing one of the K electrons.

TABLE II.

Z	αZ	Δw	σ(Fermi)	σ(K-U)
14	0.1	2	2.9	0.15
14	0.1	5	250.	36.
27	0.2	2	0.2	0.022
27	0.2	5	21.	3.1
82	0.6	2	0.8×10^{-3}	2.5×10^{-5}
82	0.6	5	0.1	0.016

Next, the ratio σ of the probabilities of the positron emission and the K electron absorption was calculated on similar assumptions as above, when ΔW is larger than $mc^2+\mu c^2$, the numerical results for $\mu=0$ being summarized in Table II.

Thus, for ordinary radio elements emitting positrons, for which Z is small and Δw is about 5 or more, the ratio σ is so large that the order of the mean lifetime calculated by assuming the positron emission alone is not changed by the additional contribution of the absorption of the orbital electron. On the contrary, for large values of Z, the latter process will occur far more frequently than the former as long as Δw is not too large compared with 1. It will be possible to test these conclusions by experiment.

HIDEKI YUKAWA
SHOICHI SAKATA

Department of Physics,
Osaka Imperial University,
Osaka, Japan,
February 18, 1937.

[1] Brainbridge and Jordan, Phys. Rev. **50**, 282 (1936).
[2] Proc. Phys.-Math. Soc. Japan **17**, 467 (1935); **18**, 128 (1936). Extension of the calculation to the case of forbidden transitions was made by Lamb, Phys. Rev. **50**, 388 (1936). (Abstract). See also Bethe and Bacher, Rev. Mod. Phys. **8**, 82 (1936). Similar calculations were made recently by Møller, Phys. Rev. **51**, 84 (1937).
[3] For the numerical calculation in the case of K-U, the same coupling constant as that of Bethe and Bacher (reference 2, p. 193) was employed.

On the Nature of the Superconducting State

Most attempts to explain superconductivity encounter the difficulty that they have to introduce an enormous number of different quantum states in order to represent the infinite number of possible currents, different as to their direction and intensity; it seems difficult to explain how the interaction between these electronic states and the lattice could be sufficiently weak for no transitions between them to be possible and no energy and velocity of the electrons to be dissipated over the lattice.

It has recently been shown,[1] however, that quantum kinematics furnishes a possibility of describing superconductivity in such a manner, that for a simply connected superconductor even one single electronic state is sufficient for representing the electromagnetic behavior of a superconductor with all its various possible currents. It would be sufficient to show that this state has the following properties:[2]

(1) Its energy is separated by a finite interval from that of the ordinary Bloch states and lies lower than those.

(2) Its eigenfunction is nondegenerate and in a weak magnetic field it undergoes no stronger perturbation than one proportional to H^2.

$$\psi=\psi_0+H^2\psi_1 \qquad (\psi_0=\text{eigenfunction for } H=0).$$

There may be several states of this kind below the Bloch states. Transitions between them would not produce a dissipation of current.

The properties (1) and (2) characterize the electromagnetic behavior of the superconductor as being the same as that of a single big diamagnetic atom. The variety of currents which can be produced in the one ground state of a diamagnetic atom by suitably varying the orientation and intensity of the external magnetic field corresponds, in

this description, to an analogous variety of currents in the superconductor. It could be shown that this description provides just as many possible currents as are required in order to satisfy uniquely the macroscopic boundary conditions for current and field. All currents observed in the conductivity experiments can be conceived as produced by the magnetic field. The new relation between current J and magnetic field H derived on this basis is

$$\text{rot } \Lambda J = -H,$$

where Λ is a constant characteristic of the superconductor.

This mechanism of conduction is entirely different from that discussed in customary theories of conductivity: The transport of electricity is not based, as usually, on *progressive* waves (or wave packets) but on *stationary* waves. By these a transport of electricity can only be effected *in the presence of a magnetic field* and just this is our assertion as to the nature of the supercurrents.

Though in such a way a serious difficulty could be removed which seemed hitherto to render impossible any theory of superconductivity, the problem remained yet unsolved as to *which kind of interaction* could be made responsible for the appearance of such separated diamagnetic states.

In a paper just published by Slater[3] attention has been drawn to a mechanism which seems to be able to explain the appearance of such a separation of the lowest Bloch eigenvalues as characterized by (1) and it is therefore of interest to examine whether this mechanism is able to fill up the gap still left in the theory of superconductivity. Actually, Slater seems not to have thought of the particular possibility, mentioned above, of a magnetic interpretation of the phenomena of conductivity. In any case, he did not undertake to make plausible a property like that formulated under (2). Instead he refers rather to the notorious difficulties in dealing with the resistance problem at low temperatures. It appears doubtful, indeed, whether such a proof of the superconductivity of the model can be given. Moreover, proof of an infinitely high conductivity would not imply the fact that a superconductor, when formed in a magnetic field, has a magnetic induction zero. The reference in Slater's paper to the parallelism between specific heat and resistance seems to be rather misleading: there are superconductors with a high specific heat in the normal phase and nevertheless a high critical temperature (e.g., *Ta* has a high specific heat and a critical temperature of 4.4°).

The construction of such isolated states is certainly of greatest interest, and perhaps the indications given here may be found useful for discussing this or similar models.

F. LONDON

Institut Henri Poincaré,
Paris, France,
March 7, 1937.

[1] F. and H. London, Proc. Roy. Soc. **A149**, 71 (1935); Physica **2**, 341 (1935). M. v. Laue, F. and H. London, Zeits f. Physik **96**, 539 (1935). F. London, Proc. Roy. Soc. **A152**, 25 (1935). E. Schrödinger, Nature **137**, 824 (1936). H. London, Proc. Roy. Soc. **A152**, 650 (1935); **155**, 102 (1936). F. London, Physica **3**, 450 (1936). Nature **137**, 991 (1936). For a general review see F. London, *Une conception nouvelle de la supraconductibilité*. Actualités scientifiques et Industrielles No. **458** Paris (Hermann & Cie) 1937.

[2] See e.g., Proc. Roy. Soc. **A152**, 31–33 (1935).

[3] J. C. Slater, Phys. Rev. **51**, 195 (1937).

On the Probability of Detecting Nebulae Which Act as Gravitational Lenses

Recently various authors[1, 2] have again[3] considered the possibility of observing the image of a distant star A whose light is bent around some nearer star B. For reasons discussed by these authors, the probability that the mentioned effect will ever be observed with *stars* is vanishingly small. The general feeling therefore was that the idea of gravitational lenses affords "perfect tests of general relativity that are unavailable," as Professor H. N. Russell[2] puts it.

The problem in question, however, takes on a radically different aspect, if, instead of in terms of stars we think in terms of *extragalactic nebulae*.[4] Provided that our present estimates[5] of the masses of *cluster nebulae* are correct, the probability that nebulae which act as gravitational lenses will be found becomes practically a *certainty*. The reasoning which leads to this optimistic view is as follows.

Let us consider only the least probable but perhaps most spectacular case in which the straight line which joins the observer in O with the gravitational center of the lens-nebula B passes through a distant nebula A. What is the probability that for a specified nebula B this "coincidence condition" is satisfied? Clearly, if all of the distant nebulae whose apparent magnitude is brighter than m cover a total solid angle ω_m, the probability p for OB to intersect one of these nebulae is $p = \omega_m/4\pi$. Consequently, among $n = 1/p$ nearby nebulae B, one satisfies on the average the coincidence condition.

On limiting exposures with the 100-inch telescope about 1/400 of the photographic plate is on the average covered by nebular images. Thus for a limiting magnitude of about $m = 21.5$ we have approximately $n = 400$. With gravitational focusing, nebulae considerably fainter than $m = 21.5$ will be observable. Thus around one in about one hundred nebulae B the ring-like image of a distant nebula should be expected, *provided* that the chosen nebula B has an apparent angular radius ρ smaller than the angles γ through which light is deflected on grazing the surface of this nebula. Present estimates of masses and diameters of cluster nebulae are such that the observability of gravitational lens effects among the nebulae would seem insured. In any case, whatever the outcome, the search for such effects will provide us with valuable information regarding the masses of nebulae.

In searching through actual photographs, a number of nebular objects arouse our suspicion. It will, however, be necessary to investigate certain composite objects spectroscopically, since differences in the red shift of the different components of such objects will immediately betray the presence of gravitational lens effects. Until such tests have been made, further discussion of the problem in question may be postponed.

F. ZWICKY

California Institute of Technology,
Pasadena, California,
March 18, 1937.

[1] A. Einstein, Science **84**, 506 (1936).

[2] H. N. Russell, Scientific American, p. 76, Feb. (1937).

[3] Dr. G. Strömberg of the Mt. Wilson Observatory kindly informs me that the idea of stars as gravitational lenses is really an old one. Among others, E. B. Frost, late director of the Yerkes Observatory, as early as 1923 outlined a program for the search of such lens effects among *stars*.

[4] F. Zwicky, Phys. Rev. **51**, 290 (1937).

[5] F. Zwicky, Helv. Phys. Acta **6** 124 (1933).

Electric Breakdown Field Intensity of Water and Aqueous Solutions

Many theories of breakdown phenomena of liquid dielectrics have been proposed, and Nikuradse's[1] is one of the well-known theories. His theory rests on the current-voltage curve up to breakdown, and the current is represented by the following equation,

$$I = I_0 e^{\alpha\delta},$$

where I_0 = saturation current,
α = ionization constant,
δ = distance between electrodes.

He discussed the electric breakdown phenomena according to this equation nearly in the same manner as is done in Townsend's theory of electric discharge in gases. In gases, the current at the beginning of the current-voltage curve is due to electrons from the cathode, and the avalanche current at the last part of the curve is caused by ionization by collision of electrons. Therefore, the electric discharge in gases from beginning up to the end is an electronic phenomenon.

However, in the case of liquid dielectrics, the initial part of the current-voltage curve is due to ionic conduction, and the last part may be due to electronic phenomena.

Though the characteristic form of the current-voltage curve in liquid dielectrics and in gases bear some resemblance to each other, their physical meaning is different. The theory of electric discharge in gases may not be applied to that in liquid dielectrics without restatement.

When the breakdown voltage of insulating oil is measured in vacuum, sparkover may sometimes happen at the range of saturation current. It may therefore be concluded that the current has no direct relation to the breakdown voltage, and there is no direct relation between conductivity of the liquid dielectrics at low field intensity and the breakdown field intensity.

As extreme examples of liquid dielectrics, we measured the breakdown voltage of distilled water and aqueous solutions using impulse voltage chopped at the tail of the impulse wave.

The experimental results are shown in Fig. 1. As seen in the figure, the breakdown voltage varies according to the kinds of solutions. In the case of a solution of NH_4OH the breakdown voltage is larger than that of distilled water, but the conductivity of the solution is about 7.5 times greater than that of water.

In short, though the conductivity of liquid dielectrics increases very much, the breakdown field intensity does not decrease at the same rate. Moreover, on the contrary, the breakdown voltage of the solution of NH_4OH is larger than that of distilled water in spite of the much increased conductivity. It appears then that there is no direct relation between the current-voltage characteristic and the breakdown field intensity of liquid dielectrics, and that breakdown is an electronic phenomenon, and the conduction through liquid dielectrics is ionic.

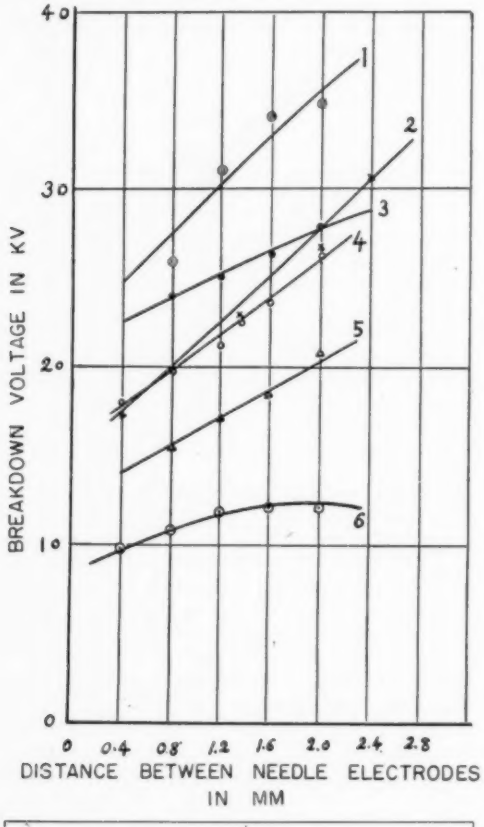

Aqueous Solution	Conductivity
1. NH_4OH (0.05N)	10.5 $\times 10^{-4}$ Ω^{-1} cm^{-1}
2. Distilled water	1.43 × " " "
3. $BaCl_2$ (0.05N)	560 × " " "
4. NaCl (0.04N)	1248 × " " "
5. NaOH (0.05N)	1660 × " " "
6. HCL (0.05N)	3156 × " " "

Fig. 1.

Y. Toriyama
U. Shinohara

Laboratory of High Voltage Engineering,
Hokkaido Imperial University, Sapporo, Japan,
February 17, 1937.

[1] A. Nikuradse, Physik. Zeits. **19**, (1928).

Proceedings of the American Physical Society

Minutes of the North Carolina Meeting, February 19–20, 1937

THE 212th regular meeting of the American Physical Society was held on Friday, February 19, 1937 at Durham, North Carolina and on Saturday, February 20, 1937 at Chapel Hill, North Carolina, in affiliation with the Southeastern Section of the American Physical Society and the American Association of Physics Teachers. The presiding officers were Professor H. M. Randall, President of the Physical Society, Professor W. L. Kennon, Chairman of the Southeastern Section, and Professor F. K. Richtmyer, President of the American Association of Physics Teachers. There were about three hundred in attendance at the meetings.

There were two symposia of invited papers of the Physical Society. The symposium on *Nuclear Physics* was held on Friday at ten A.M. and consisted of two papers (1) "Energy Partition of Nuclear Degrees of Freedom" by Professor Niels Bohr, University of Copenhagen, and (2) "Nuclear Reactions and Angular Momentum" by Professor Hans A. Bethe, Cornell University. The second symposium, held on Saturday at nine forty-five o'clock, was on *Applied Physics* with the following papers (1) "The Structure of the Cotton Fiber" by Dr. Wanda K. Farr, Boyce-Thompson Institute for Plant Research, Yonkers, New York, (2) "Moisture in Textiles" by Dr. A. C. Walker, Bell Telephone Laboratories, Inc., New York, N. Y., (3) "The Place of Statistics in Textile Research" by Mr. J. P. Elting, Kendall Mills, Paw Creek, N. C., and (4) "The Physical Basis of Color Measurement" by Professor A. C. Hardy, Massachusetts Institute of Technology.

On Saturday morning at nine forty-five o'clock the American Association of Physics Teachers held a symposium of invited papers on *Some Problems of Physics Teaching* which consisted of the following: (1) "Some Aspects of Physics Teaching in the South" by Dean L. L. Hendren, University of Georgia, (2) "What College Physics Expects of Pre-College Education" by Professor Thomas D. Cope, University of Pennsylvania, and (3) "Graduate Training for a Career in Physics" by Professor G. P. Harnwell, Princeton University.

Duke University gave a complimentary luncheon at the University Union to all registered members of the societies at one-fifteen P.M. Thursday. At two-fifteen P.M. Dr. Saul Dushman, assistant director of research, General Electric Company, addressed members and friends of Sigma Pi Sigma on "The Physicists Training for Industry." At four-thirty P.M. Professor Niels Bohr gave a public address on "Causality in Atomic Physics" in the Page Auditorium.

On Friday evening a joint dinner of the societies was held at the University Union. President H. M. Randall and President W. P. Few of Duke University presided. They called upon President Frank P. Graham of the University of North Carolina, President F. K. Richtmyer of the American Association of Physics Teachers, Professor W. L. Kennon, Chairman of the Southeastern Section, and Dean George B. Pegram of Columbia University and Treasurer of the Physical Society.

At the close of the Saturday morning session Professor John R. Dunning of Columbia University was requested to repeat his address with demonstrations on "The Neutron and Atomic Transmutations" which he had given on Thursday evening at Chapel Hill before the Society of Sigma Xi.

Meeting of the Council. At the meeting of the Council held on Friday afternoon at Durham at four o'clock the Secretary reported the deaths of one fellow (John Bradshaw Taylor) and two members (Albert C. Erickson and Robert S. Prescott), and the resignations of two members (Frederick L. Hunter, Jr. and Waldo Truesdell). One candidate was elected to fellowship, two candidates were transferred from membership to fellowship, and forty-three candidates were elected to membership. *Elected to fellowship:* G. W. Potapenko. *Transferred from membership to fellowship:* Walter M. Nielsen and Lyman G. Parratt. *Elected to membership:* Orrick H. Biggs, James E. Boyd, Claude W. Bruce, John T. Burwell, Jr., W. Y. Chang, John Chesna, Marvin I. Chodorow, George K. T. Conn, C. J. Craven, Baldwin R. Curtis, Carl Darnell, Curtice Davis, Willem de

Groot, Clair L. Farrand, James E. Forbes, Lorence W. Fraser, Wilbur H. Goss, Louis C. Green, Sister M. Laetitia Hill, Harold J. Hoge, Lloyd R. Jackson, Wilhelm Jorgensen, Hans Klemperer, H. W. Knerr, Walter L. Krahl, Kenji Kusumoto, S. E. Madigan, Arthur C. Menius, Jr., H. E. Morgan, Lawrence N. Morscher, Jr., John A. Osteen, Carlyle V. Parker, L. Donald Payne, William H. Pickering, Irven B. Prettyman, Nicholas M. Smith, Jr., Arthur H. Snell, G. Steensholt, Roger A. Sykes, Sister Mary Therese, E. Dale Trout, C. K. Wu, and Hiroshi Yoshinaga.

The regular scientific program of the Society consisted of forty-seven contributed papers of which number 38 was read by title. The abstracts of these papers are given in the following pages. An *Author Index* will be found at the end.

W. L. SEVERINGHAUS, *Secretary*

ABSTRACTS

1. Calculations on Beta-Ray Spectra. W. G. POLLARD, *The University of Tennessee.*—Calculations have been made on beta-ray spectra using $\psi^*\varphi$, $\psi^*\vec{\alpha}\varphi$ for the Fermi interaction and $\psi^*\beta\partial\varphi/\partial t$, $c\psi^*\beta$ grad φ for the Konopinski-Uhlenbeck form. Special features of these calculations are: (1) The "vector" parts of the interaction are included and all matrix elements evaluated by assuming the heavy particle wave functions to be solutions of Dirac's equation in a square hole. (2) The depth of the hole is calculated for heavy elements by means of Van Vleck's potential in the form

$$U_\nu = 2(1-\tfrac{1}{2}g)\int_0^{p_\pi} d\vec{p}a(\vec{p}_\nu-\vec{p}) + 2(1-2g)\int_0^{p_\nu} d\vec{p}a(\vec{p}_\nu-\vec{p})$$

with $g=0.21$, the coefficients a adjusted to give the Fourier integral of Feenberg's and Knipp's interaction, and p_ν determined from the boundary conditions. (3) For the width of the hole Bethe's extended radius 13×10^{-13} cm was used. (4) The potentials U_ν or U_π were introduced into the wave equation so as to reduce the rest energy instead of the total energy as suggested by Furry. (5) The author's improved approximations to the electron wave functions were used. Kurie plots on Lyman's RaE spectrum have been made for $1p\rightarrow1s$, $2p\rightarrow1s$, $2s\rightarrow1p$, and $2p\rightarrow2s$ transitions for both F and KU interactions. The KU: $1p\rightarrow1s$ plot is quite straight with only a slight lowering at the end. The results on light elements indicate that the use of the spectral distribution function for permissible transitions in making Kurie plots of forbidden spectra is justifiable within 2 or 3 percent. This is of course in agreement with experimental evidence.

2. Range of High Speed Electrons. ARTHUR BRAMLEY, *Swarthmore, Pa.*—Comparison of theoretical energy losses for cosmic-ray electrons indicates that losses arising from existence of Fermi interaction between light particles and nuclei are comparable with or even greater than losses predicted by the radiation theory.[1] Cross section for radiation is $\sigma=(6Z^2/137)(e^2/mc^2)^2\cdot\Phi/6$ where $5\leq\Phi\leq18$. Energy losses suffered by electrons of energy W as consequence of Fermi interaction may be divided thus: (1) Capture[2] of electron with creation of neutrino, $\sigma\sim10^{-30}(W/mc^2)^4$. (2) Collision with creation of two neutrinos, (a) $\sigma\sim10^{-46}(W/mc^2)^6$, for capture of electron in virtual level;[3] (b) $\sigma\sim10^{-31}(W/mc^2)^6$ through excitation of β-field of nucleus by electromagnetic field of colliding electron. Alternative process with comparable cross section dissipates energy as radiation rather than by neutrinos. These cross sections are valid for energies $\sim137\ mc^2$, where Fermi constant g has maximum.[4] Cross sections become negligible for electronic energies $\gg137\ mc^2$. For energies $<137\ mc^2$, only process (2b) retains large cross section. Since these processes favor large energy losses, comparison of experimental large losses[5] with predicted losses would establish the nature of Fermi's g-factor for high speed electrons.

[1] Bramley, Abs. 67, Atlantic City Meeting.
[2] Bethe and Bacher, Rev. Mod. Phys. **8**, 2 (1936).
[3] Bronstein, Zeits. d. Sowjetunion **9**, 537 (1936).
[4] v. Weizsacker, Zeits. f. Physik **102**, 572 (1936).
[5] Anderson and Neddermeyer, Phys. Rev. **50**, 263 (1936); Klarmann and Bothe, Zeits. f. Physik **101**, 489 (1936).

3. Stable States of Two Deuterons. HERMAN PARKER, *University of North Carolina.*—Previous studies of the binding energies of the light nuclei have been made, using a simple variational wave function of an exponential form, containing one or more parameters. A different type of wave function is suggested by the point of view which regards the alpha-particle as composed of two deuterons; on this basis we should start out with a wave function made up of the product of the internal wave functions of the two deuterons and a function U depending upon their separation. Thus

$$\Psi = U((1+3)/2-(2+4)/2)S(1,3;2,4)\varphi(3-1)\varphi(4-2) - U((1+4)/2-(2+3)/2)S(1,4;2,3)\varphi(4-1)\varphi(3-2), \quad (1)$$

where
$$U(x)=U(-x), \quad (2a)$$

$$S=6^{-\frac{1}{2}}\{2^{-\frac{1}{2}}[\alpha(1)\beta(3)+\alpha(3)\beta(1)]2^{-\frac{1}{2}}[\alpha(2)\beta(4)+\alpha(4)\beta(2)] - \alpha(1)\alpha(3)\beta(2)\beta(4)-\alpha(2)\alpha(4)\beta(1)\beta(3)\} \quad (2b)$$

and
$$\varphi(3-1)=C_\lambda\exp[-\lambda(3-1)^2] \quad (2c)$$

has been adopted as such a tried function, where the function of separation U gives effectively an infinite number of parameters to be adjusted to give the best wave function. (1) is capable, to a certain approximation, of describing the system, not only in the ground state, but in the other discrete and continuous states as well. A differential-integral equation (derived by Dr. J. A. Wheeler) determines U. λ and the strength of the like and unlike particle forces were fixed by applying the usual variation procedure to fit the binding energies of ^{2}H and ^{3}H using the wave functions

$\phi^2_H = \alpha(1)\alpha(3)C_\lambda \exp[-\lambda(3-1)^2]$,
$\phi^3_H = 2^{-\frac{1}{2}}\alpha(2)[\alpha(3)\beta(4)-\alpha(4)\beta(3)]C_{\mu\nu} \exp[-\mu\{(2-3)^2 + (2-4)^2\} - \nu(3-4)^2]$.

U has been calculated for the ground state of the alpha-particle and the corresponding binding energy is compared with what one gets using the two-parameter function employed by Feenberg. Application of the same treatment to alpha-particle levels having spin $S=2$ (deuterons with parallel spin) gives no stable levels. Further investigations are planned, taking into account the improved description of the four-particle system using a superposition of the wave functions representing $^2H+^2H$, $^3H+^1H$, and $^2H_e+^1n$.

4. Photoelectric Cross Section of the Deuteron. KATHARINE WAY AND JOHN A. WHEELER, *University of North Carolina.*—Several writers have pointed out that for Majorana forces the area under the photoelectric cross section curve $\int\sigma(\nu)d(h\nu)$ is not equal to $\pi e^2h/2Mc$ as it is for ordinary forces. A general formula for this deviation from the f-sum rule is derived and it is shown that for three special types of exchange forces

$$\int\sigma(\nu)d(h\nu) \geqq (\pi e^2h/2Mc)(1+a\alpha),$$

where a is the range of the interaction and α is defined by $\hbar^2\alpha^2/M=\epsilon$, the binding energy of the deuteron. Photoelectric cross-section curves for three different types of neutron-proton interactions are compared to see if experimental determination of the cross section for any value of $h\nu$ would furnish a criterion for deciding in favor of one of them. The three different types are (1) square hole Majorana, (2) bell-shaped Majorana, $V=V_0e^{-r^2/a^2}$, and (3) a velocity dependent interaction defined by $J_0=-(2B/a)e^{-(r+\rho)/a}$. The ranges and depths of the interactions chosen are those which have been shown to be best for accounting for the binding energies of H^2, H^3, and He^4. It is found that the cross-section curves for (2) and (3) are very similar but that they differ considerably from (1). The addition of a short depth, long range repulsive force to the velocity dependent interaction is shown to decrease the cross section for this type of interaction considerably.

5. Resonating Group Structure in the Nucleus. JOHN A. WHEELER, *University of North Carolina.*—By regarding the neutrons and protons in a given nucleus, ^{7}Li for example, as resonating between different possible configurations, such as ^{4}He(normal)+^{3}H(normal), ^{5}He(excited) +^{2}H(normal), etc., one obtains a description of nuclear structure in which by far the largest part of the energy of the compound nucleus is already accounted for by the internal binding of the separate groups. Use from the beginning of this saturation property of nuclear binding gives an improved treatment of nuclear collisions and transmutations. In applying the method of "resonating group structure," the wave function is written as a sum of properly anti-symmetrized parts corresponding to the most important configurations, each part involving a different unknown function, F, of the inter-group separations. The condition that the F's shall give the best possible wave function of this form (in the sense of the variation principle) gives simultaneous integro-differential equations for the F's. With the help of a generalized Green's function these equations are transformed to integral equations. The condition that the Fredholm determinant of this set of equations shall vanish determines energy levels, scattering phase shifts, and transmutation probabilities. The method gives very satisfactory results when applied to the interaction between two alpha-particles, and is being employed in the treatment of other collision problems.

6. On the Structure of Light Nuclei. E. FEENBERG AND M. PHILLIPS,* *Institute for Advanced Study.*—Extensive calculations based on the approximation of single particle wave functions (the Hartree method) have been made for the nuclei between He^6 and O^{16} using the general symmetrical interaction operator[1]

$$V=\sum_{i<j}\{(1-g-g_1-g_2)P_{ij}+gP_{ij}Q_{ij}+g_1 1+g_2Q_{ij}\}J(r_{ij}). \quad (1)$$

The Coulomb interaction is treated as a small perturbation. Secular equations are avoided by the construction of space wave functions in the normal state configuration belonging to irreducible representations of the symmetric group. These functions yield an energy matrix which is diagonal in the ordinary and Majorana interaction energies. The contributions of the spin exchange and Coulomb operators to the energy terms are found by a first order perturbation calculation. Although the general symmetrical operator contains several parameters as yet undetermined, only those parameters which have been fixed by consideration of the two-, three- and four-particle problems are involved in the energy differences within the group of low lying terms belonging to the normal state configuration. These term differences are essentially identical with those recently computed[2] for unsymmetrical interaction operators of the saturation type. Results for mass defects, excitation energies, energy relations between isobars, spins and magnetic moments are on the whole very encouraging.

* Margaret E. Maltby Fellow of the A.A.U.W.
[1] G. Breit and E. Feenberg, Phys. Rev. **50**, 850 (1936).
[2] E. Feenberg and E. Wigner, Phys. Rev. **51**, 95 (1937).

7. Transitions Between States of Space Quantization in a Rotating Magnetic Field. I. I. RABI, *Columbia University.*—A calculation of the nonadiabatic transition which a system with angular momentum $J=\frac{1}{2}$ and magnetic moment $-g\mu_0J$ makes in a magnetic field H rotating with frequency ω about an axis inclined at an angle ϑ to the field gives for the transition probability

$$P_{(1,\,-1)}=\frac{\sin^2\vartheta\omega^2}{\nu^2+\omega^2-2\nu\omega\cos\vartheta}\sin^2\pi t(\nu^2+\omega^2-2\nu\omega\cos\vartheta)^{\frac{1}{2}},$$

where ν is the Larmor frequency $g\mu_0H/h$. The generalization for any value of J follows immediately from Majorana's formula. It is evident that the effect depends on the sign of the magnetic moment of the system through the sign of ν. We thus have an absolute method of measuring the sign and magnitude of the magnetic moment of any system. Applications to the moment of the neutron, the rotational moment of molecules and the nuclear moment of atoms with no extra nuclear angular momentum will be discussed.

8. The Molecular Volumes and Lattice Forces of Liquid Normal- and Para-Hydrogen. R. B. SCOTT AND F. G. BRICKWEDDE, *National Bureau of Standards.*—The volumes between 14° and 20.4°K were measured with a quartz dilatometer, the mass of hydrogen being determined from the pressure of the gas in a calibrated flask whose temperature was measured. The results are represented by the equations:

$$V(n-H_2)\ \text{cm}^3\text{mol}^{-1} = 24.747 - 0.08005T + 0.012716T^2,$$
$$V(p-H_2)\ \text{cm}^3\text{mol}^{-1} = 24.902 - 0.0888T + 0.013104T^2.$$

At the normal boiling point of $n-H_2$(20.38°K), $V(n-H_2) = 28.397 \pm 0.010$ and $\Delta V(p-n) = 0.138 \pm 0.010$. The expansivity of $p-H_2$ is only slightly greater than that of $n-H_2$. For H_2, the nonrotating variety ($p-H_2$) has a larger energy and volume than the rotating variety ($o-H_2$). This is opposite to the direction of the difference observed for other substances whose molecules are oriented at low temperatures. The uncertainty principle shows that the nonrotating state of $p-H_2$ is fundamentally like that of free rotation in other substances. The difference between the lattice forces of condensed $p-H_2$ and $n-H_2$ arises from the difference in the average electron distribution of the molecules. The average angular distribution of the orientations of the axis of an H_2 molecule, which determines the average electron distribution, is given by the Legendre polynomials of the ψ-function for a rotator.

9. The Nuclear Separation of the Te_2 Molecule by Electron Diffraction. LOUIS R. MAXWELL AND V. M. MOSLEY, *Bureau of Chemistry and Soils, Washington, D. C.*—Electron diffraction photographs obtained from tellurium vapor show an interference pattern which can be explained by electron scattering from the diatomic tellurium molecule. Visual measurements were taken on the second, third, fourth and fifth interference maxima which are found to occur at $(1/\lambda)\sin\frac{1}{2}\theta = 0.422$, 0.618, 0.815 and 1.018 respectively. These values lead to a Te−Te separation of 2.59 ± 0.02A, where the variation given represents the average deviation. This distance is considerably less than the accepted band spectra value of 2.85A for the nuclear separation of the ground state of the Te_2 molecule.* Additional electron diffraction data have been obtained from I_2 giving an I−I distance of 2.66 ± 0.01A which is exactly equal to the band spectra value for the internuclear distance in the normal state of I_2.* Further agreement has already been obtained by various workers between electron diffraction and band spectra for the molecules Br_2 and Cl_2. On the basis of the above information we conclude that at least part of the rotational constants computed for Te_2 from band spectra data must be in error.

* See for instance *Report on Band Spectra of Diatomic Molecules* by W. Jevons.

10. Response of Synthetic Rubber to Temperature Changes. MILTON L. BRAUN, *Catawba College.*—From a sheet of DuPont synthetic rubber about 2 mm in thickness was cut a double hairpin shape band of approximately square cross section and about 7 cm in length. From the band, in a closed cabinet, was suspended a kilogram load which produced an immediate stretch of nearly 50 percent. The length of the band was observed at numerous intervals under various temperature sequences within an extreme range of 16 to 48°C, and over a duration of about ten months. The band showed a drift quite comparable to that in ordinary vulcanized rubber. Superimposed on this drift, the rate of change of length with temperature was found to vary between −0.010 and −0.027 cm per degree. A similar control band without load showed practically no change in length with temperature, and in this respect it differed from a slight positive rate ordinarily found for unloaded vulcanized bands. The present elongation is about 400 percent, nearly one-half of which is accounted for by the drift effect, the other half by a sudden rise in the drift curve probably due to a plastic give when the temperature one time reached the neighborhood of 48°.

11. Measurement of Permeability of Porous Media by a Radial Flow Method. O. T. KOPPIUS AND W. G. HOLTON, *University of Kentucky.*—A theory and method is presented by which the permeability of a consolidated medium to gas and to liquid flow may be determined. The specimens used were diamond drill cores from oil sands. The fluid flow in the sample was radial, and the flow was confined entirely to the region of viscous flow where D'Arcy's law applies. The permeabilities of the sample were found to be different for gas flow from that for liquid flow, being 9.64 millidarcies for air and 4.00 millidarcies for furnace oil. This difference between the permeability of the sample for gas and liquid flow is at variance with the results obtained by other observers using a linear flow method and materials whose permeabilities for air were about 120 times as great. The question is raised as to whether the constant in D'Arcy's equation, $C = k/\mu$, is of such simple form when this equation is applied to materials having as small a permeability as the sample used here. No "plugging" action of the sample for liquid flow was observed.

12. A Spark Timer Actuated by Thermionic Tubes, C. T. RAZOR, *The Citadel.*—A strip of sensitized paper is clamped to a drum driven at constant speed by a synchronous motor. The paper is marked by a spark discharge from an electrode near the drum. The spark is produced by the action of a grid glow tube circuit which resets itself within a few milliseconds to produce another spark, without the use of mechanical relays or contacts. The spark discharge may be controlled by successive sound pulses through a microphone and amplifier. The time between any of a series of low frequency voltage pulses may be determined. Any mechanical action which can be made to close two electrical contacts in succession may be timed.

13. A Study of the Thyratron Inverter. MARVIN SLEDD AND J. B. PEEBLES, *Emory University.*—By the use of the operational calculus, considerable progress can be made in the effort to predict mathematically the behavior of the self-excited, parallel-type, single-phase inverter with static loads. The frequency can be calculated within 5 percent of the observed value, and a fair approximation of the wave shape of the output voltage can be obtained. Several parts of the inverter circuits often seen can be omitted, and the

apparatus will continue to function. Perhaps the most interesting example of this statement is the fact that, by proper adjustment of the grid circuit, the separate commutating condenser can be dispensed with. And after this is done, the inverter will continue to deliver load to an output circuit consisting of inductance and resistance only. By a proper adjustment of the circuit, a sine wave of voltage can be obtained in the load in which no harmonic exceeds 3 percent of the fundamental.

14. Electrolytic Polarization with Alternating Current. SCHUYLER M. CHRISTIAN, *Agnes Scott College.*—A comprehensive investigation of this phenomenon is outlined, the resistance and capacitance of the electrodes being measured. The effects of the following factors have been studied: (1) frequency, (2) distance between electrodes, (3) current density, (4) temperature, (5) nature of solution, (6) nature of electrodes, (7) superimposed d.c., (8) superimposed a.c. Of these effects, the first is most definitely established: the resistance and capacitance vary inversely as the square root of the frequency, within the limits of experimental error. The best theory to account for the observed facts is based on the diffusion of ions from the electrodes; though incomplete, this is more satisfactory than the concept of a gaseous film surrounding the electrodes.

15. Measurements of the Verdet Constant of Crystalline Nickelous Sulphate. F. G. SLACK, R. T. LAGEMAN AND NEWTON UNDERWOOD, *Vanderbilt University.*—The Verdet constant of "Baker's Analyzed" nickelous sulphate crystals, $NiSO_4 \cdot 6H_2O$, has been measured for light passing normal to the natural cleavage plane of the crystal. The set up consists of a special drilled core Leybold electromagnet which fits between the polarizer and analyzer of a Lippich half-shade polarimeter. The sample is oriented, by means of a goniometer head, in the narrow gap between the pole pieces. Light from an automobile bulb passing through a B. & L. monochromator serves as a source. Measurements between 4500A and 6000A show the Verdet constant to vary inversely as the square of the wave-length. Temperature measurements over the range $-10°C$ to $30°C$ show a temperature variation in the Verdet constant proportional inversely to the absolute temperature.

16. An Infrared Study of Alcohol-Acetate Mixtures. E. S. BARR, *Tulane University.*—The infrared spectra of methyl and ethyl alcohols and of their acetates, as well as mixtures of these, have been obtained in the region from 4μ to 8μ. Anhydrous materials were used to prevent confusion due to hydrolysis and hydration effects. The ethyl alcohol-methyl acetate and methyl alcohol-ethyl acetate mixtures were refluxed for thirty-six hours and left undisturbed for six months, to facilitate any possible exchange reactions. The spectrum of the methyl alcohol-ethyl acetate mixture showed no indication of either ethyl alcohol or methyl acetate. Likewise, the ethyl alcohol-methyl acetate spectrum showed only bands due to its original constituents. This is taken as an indication that no exchange reaction takes place in the absence of water. Furthermore, the absence of new bands or marked modifications of the combined spectra of the mixtures indicates that there is very little, if any, interaction. As a check on this supposition, calculations based upon the assumption of no interaction were used to plot curves for a mechanical mixture of the substances. These curves were found to be in excellent agreement with the observed curves.

17. The Infrared Spectra of Binary Mixtures of Certain Organic Liquids. DUDLEY WILLIAMS AND WALTER GORDY, *University of Florida and Baylor College.*—The spectra of methyl alcohol-ethyl formate and methyl alcohol-ethyl acetate mixtures were studied in the region between 2μ and 10μ. The presence of the esters was found to shift the OH band of methyl alcohol to shorter wave-lengths and to increase its intensity. On the other hand the CO band of the esters was shifted to longer wave-lengths by the alcohol. These results are interpreted as arising from the effects of association between the components of the mixture. The possibility of a type of association involving the formation of proton bonds is discussed.

18. Infrared Absorption of Strong and Weak Acid Solutions, E. K. PLYLER, *University of North Carolina at Chapel Hill.*—A study has been made of infrared absorption spectra of aqueous solutions of HCl and HBr. The solution strengths were varied from 1 N to 8 N, and in the region of 5.4μ intense absorption was observed. As this absorption band is not due to water or the acid molecule, it was concluded that it is produced by the hydrated ion or molecule. Solutions of propionic and acetic acids were also studied and they showed strong absorption in the region of 5.75μ, which is also due to hydration. Several other acids have been studied and it is found in all cases that strong acids in solution produce a band at 5.4μ, and weak acids in solution produce a band at 5.75μ. This difference in the position of the hydration band is explained by attributing the absorption at 5.4μ to the hydrated ion, and the absorption at 5.75μ to the hydrated acid molecule.

19. The Infrared Absorption of Various Solutions of Acetic Acid. WALTER GORDY, *Mary Hardin-Baylor College and the University of North Carolina.*—The characteristic vibrational band associated with the C=O group of acetic acid has been studied as a function of concentration of acetic acid in benzene, in carbon tetrachloride, and in iso-propyl ether. The effects of benzene and carbon tetrachloride on the band were approximately the same. In both solvents the band became sharper, its intensity was increased, and its center was shifted to the longer wave-lengths. For concentrations of acetic acid as low as 6 percent the shift amounted to 0.15μ. Although in iso-propyl ether solution there was a measurable shift of the band to the longer wave-lengths, the shift was small compared to that observed for benzene and carbon tetrachloride solutions. It is suggested that the changes in the C=O acetic acid band are likely due to variations in the polymerization of the acetic acid as the concentration is varied. However, the position of the band does not approach that for the vapor state in any of these solvents. Ethyl acetate was also studied in benzene and in iso-propyl ether; no variations could be detected in the C=O band.

20. Spirals in Paraffin Crystals. CHARLES M. HECK, *North Carolina State College of Agriculture and Engineering.*—Some two hundred spirals formed in tabular paraffin crystals have been photographed. They have the following characteristics: (a) the convolutions follow accurately the pinacoidal diamond shape of the exterior of a perfect crystal; (b) they always have their axes parallel to the axes of the crystal; (c) though generally concentric with the crystal, they may appear in any part of it; (d) more than one spiral may be present in a single crystal: generally this occurs when internal lines and external configuration indicate a form of twining. Generally the directions of the windings in two contiguous spirals in the same crystal are opposite; (e) spirals are more often perfect when the heavier fractions of Pennsylvania paraffin are crystallized from a liquid composed of the lighter members of the paraffin series; (f) spirals tend to lose their angles and become circular as the degree of crystallinity of the paraffin is diminished or the solution from which it is crystallized poisons them.

21. A Simple Demonstration in Sound. J. C. MOUZON, *Duke University.*—The existence of harmonics in a tuning fork and the suppression of certain harmonics by a closed resonating air column may be beautifully demonstrated through the medium of an oscilloscope. A microphone is coupled to the oscilloscope and a vibrating tuning fork mounted on a resonating box (one end closed) is presented to the microphone. The pattern on the oscilloscope screen usually indicates a complex wave form. When, however, the open end of the resonating box is presented to the microphone a very nice sine wave is seen on the screen of the oscilloscope. It is evident then that the majority of the distortion of the wave is due to the even harmonics of the fork. The second harmonic is usually audible if the fork is not struck with extreme care. It, of course, cannot exist in the closed resonating box.

22. A Quantitative Study of the Doppler Effect in Sound Waves, NEWLAND F. SMITH, *The Citadel.*—A whistle, built into the end of a long tube, is rotated by a motor at constant speed. The sound of the whistle is impressed upon a microphone in the plane of rotation of the whistle, and the resulting current is amplified. A photographic record of the amplified current is obtained by means of an oscillograph. From this photograph, the frequency of the note is determined when the source is approaching and receding from the microphone with a known velocity. Theoretical and observed values of the changes in frequency are compared. The sound may be recorded on a phonograph disk and a permanent record made.

23. New Values of the Change of Resiliency with the Velocity of Impact, JOHN B. DERIEUX, *North Carolina State College of the University of North Carolina.*—Golf balls were selected as suitable bodies with which to make the study. The change in velocity was obtained by dropping the balls from heights varying from three to sixty feet onto a large stone slab, and the corresponding resiliency was determined from the height of rebound. The velocities could not be computed from $V=\sqrt{2gh}$, however, because of the resistance of the air. The resistance at different velocities had first to be determined, and this was done by placing the balls in a wind tunnel and measuring the drag of the air at different speeds. The equation of resistance against velocity was determined from these data, and incorporating it in an equation between height and velocity an infinite series was obtained by which the correct velocities were computed. The values of the resiliency showed a decided decrease with increase of velocity of impact. This being the case, it is proposed that the standard values of resiliency should be those with zero velocity. This value can be determined from the graph of the finite values against velocity extended to zero velocity, or from the equation of resiliency against velocity when zero is substituted as a velocity.

24. The Distribution in a Horizontal Plane of Light from a Point Source, W. L. BRENNER, *The Citadel.*—A Weston photronic cell with attached galvanometer is placed on a horizontal surface. A concentrated filament lamp, free to move vertically, is varied in height. Readings of the galvanometer are taken for each position of the lamp, and a curve plotted showing the relation between lamp height and the horizontal distance from the cell to the point immediately below the lamp. From this curve, the height of the lamp giving maximum illumination on the cell is determined. This point can also be determined from theoretical considerations involving the inverse square law and Lambert's law. The above procedure correlates in the student's mind the laws of illumination and the calculus treatment of maxima in a single experiment. The entire apparatus may be housed in a black box and, since the galvanometer may be placed outside, the experiment may be performed in a lighted room.

25. Diffraction Patterns by Polarized Light. A. W. DICUS, *Tennessee Polytechnic Institute.*—To obtain these patterns, a diffraction tube, about thirty feet in length and nine inches in diameter, was used. One end was fitted with a spring clamp to receive a plate holder and on the other end of the tube was fastened a metal plate containing four or five small holes to be used as apertures. Near the center of the tube was an opening to permit the insertion of objects of which patterns were to be made. The box shaped opening was covered with a light-tight lid. The source of light was a carbon arc. The light was filtered through blue glass and then focused on the Nicol prism of a polariscope tube. To the opposite end of this tube was fastened a Polaroid disk to be used as an analyzer. This beam of plane polarized light was then focused on a small aperture in the end of the diffraction tube. The plane of polarization was horizontal. Patterns were taken with a number of objects and in each case the diffraction was equally evident in both horizontal and vertical directions. Following is a list of patterns: 1. Screen-wire as an object, monochromatic nonpolarized light. 2. Same object as No. 1 but monochromatic polarized light was used. 3. Razor blades as object, monochromatic nonpolarized light. 4. Razor blades as object, monochromatic polarized light. 5. Razor blades as object, mono-

chromatic polarized light. The Nicol prism was removed and the Polaroid disk used as a polarizer. 6. Razor blades as an object, monochromatic polarized light. Both the Nicol prism and Polaroid disk removed and the disk was placed inside the diffraction tube, thus polarizing the light after passing through the aperture.

26. Observation of Spectra—An Experiment for the Elementary Laboratory. PAUL E. SHEARIN, *University of North Carolina.*—We have recently introduced into our elementary laboratory an experiment on the observation of spectra. Four different types of spectroscopes are used, each with a different kind of source. Wave-lengths of line spectra are measured. Selective absorption of certain liquids is used as a simple method of chemical analysis.

27. An Elementary Laboratory Experiment Dealing with the Relationship $I = Q/t$. J. H. HOWEY, *Georgia School of Technology.*—The calibration of a condenser by the tuning fork method has long been a standard experiment in physics, but it is not commonly included in elementary laboratory courses. By considering the experiment as a calibration of a galvanometer using a known capacity, the experiment has been adapted for use in an elementary laboratory course. As such, it possesses a number of desirable features. It can be scheduled earlier in the course than most other experiments in electricity because the necessary theoretical background is covered early in the course, if the usual logical order is followed in class work. The required apparatus is inexpensive except for the galvanometer which is already available in most laboratories. Finally the principles involved are fundamental relationships in electricity with which every student should be made thoroughly familiar. The advent of radio and other branches of electronics has made it more imperative than ever that the principles involved in this experiment be emphasized.

28. Laboratory Demonstration Experiments in Modern Physics. D. S. ELLIOTT, *Tulane University.*—This paper outlines the methods developed at this university for giving the junior student definite perceptual knowledge of the principal phenomena of modern physics, as addenda to the traditional half-year course in electricity and magnetism.

29. The First Courses in Physics in American Colleges. CHARLES W. EDWARDS, *Duke University.*—A statistical analysis is made of current practices in American colleges with a brief discussion of the relation of the Preliminary Physics, the General Physics, and the Intermediate Physics courses to the type of student body served in different sections of the country, and to the different objectives of the students in each type of institution. An exhibit is made of the great variety of procedures which are being employed by teachers of physics to reach a common goal. (Lantern slides.)

30. A Description of the Physical and Astronomical Equipment at the University of Mississippi Prior to 1860. W. L. KENNON, *University of Mississippi.*—A description, supplemented by slides, photographs, and exhibits, of a remarkable collection of physical and astronomical equipment acquired by the University of Mississippi between 1850 and 1860. Apparatus purchased in 1851 from John Millington, first professor of natural philosophy in the university, brought to Mississippi by Millington from the Royal Institution (London); among other pieces of historic interest it includes a unit from the famous battery which furnished current for Davy, and for Faraday, for their classic experiments. An elaborate collection of the highest grade research equipment mostly by Lerébours et Secrétan (Paris), which comprised a complete replica of the apparatus described and illustrated in *Jamin's Cours de Physique.* A collection of 80 oil paintings by Atélier Clichy (Paris), large four prism spectroscope by Steinheil, complete set of Koenig's original manometric flame apparatus, and replicas of practically all classic apparatus of the period. The oil paintings appear to have been the originals from which were made the beautiful color plates in *Les Phénoménes de la Physique par Amédée Guillemin* (Paris), 1869. As a part of the astronomical equipment might be mentioned the undelivered nineteen inch Dearborn Objective ground by Alvin Clark to the order of the University.

31. Quizzes and Examinations in Physics. NEWTON S. HEROD, *Georgia School of Technology.*—Quizzes and examinations are discussed as an integral part of a teaching program. This makes it necessary to discuss the adaptation of questions to the group dealt with, the method of rating various types of questions, and the treatment that follows the return of papers after they are graded.

32. Recording Machines as a Means of Teaching and Advertising Physics. L. E. MCALLISTER, *Berry College.*—In order that physics may have its rightful place in an educational institution it must touch in a practical way the lives of as many individuals as possible. At Berry College that is done in many ways. Among them is the use of recording machines for making phonograph records. Advanced students in physics learn the theory and operation of the machines by study and by assisting in their operation. This includes a knowledge of sound itself, the microphone and amplifiers as well as the actual recording. Records are made for individuals in the form of personal greetings, songs, poems, etc., to send home at Christmas and Easter time. The music and public speaking departments make records for teaching purposes. Choirs and other ensembles make records of their productions before presentation to note mistakes that should be corrected. Individuals, singing or speaking, have a chance to hear themselves as others hear them. Their teachers say the students learn more from one record than from a dozen lessons. Actually it benefits other departments but at the same time it gives students more respect for and interest in the subject matter of physics.

33. Present Tendencies and Status of Physics in the High Schools of the South. C. R. FOUNTAIN, *George Peabody College for Teachers.*—Preliminary reports from various southern states indicate that physics is not being given in as large a percentage of the high schools, nor is it being elected by as many students where given as it was

twenty years ago. Among the many suggestions offered as possible causes for this changing attitude may be mentioned: (1) General belief by students, parents and school executives that physics is useful only for students planning for some field of engineering. (2) That physics taught in the high schools is being ignored by colleges and universities. (3) Budget cutting is most effective when applied to physics equipment. (4) Physicists do not advertise their accomplishments. (5) Courses in physics have been too hard and too formal. (6) Laboratory apparatus has been too complicated and unfamiliar. To offset this tendency we should: (1) Show that physics is the easiest of all the subjects with which to learn to think. In no other subject is it so easy to see the effect of changing just one factor or to check one's reasoning. (2) Show that we use physics in every move we make, in athletic games and in our daily work. (3) Show that physics helps us judge most of the materials and the machines we buy.

34. The Effect of an Electric Field on the Diffraction Pattern of Liquids. A. A. BLESS, *University of Florida.*—The negative results obtained by F. C. Todd (Phys. Rev. **44**, 787 (1933)) on the effects of an electric field on the x-ray diffraction pattern of nitrobenzene are not altogether conclusive for the following reasons: 1. Temperature changes were prevented by using the liquid in the form of a stream running through a tube. The disturbances thus introduced may have been counteracting the effects of the field. 2. The ionization chamber method employed is not suitable if the action of the field is such as to produce a pseudo-crystalline state in the liquid. To overcome these objections experiments were made on the effects of an electric field on the diffraction pattern using the photographic method with the fluid in a container which could be kept at any desired temperature. No changes were observed in the diffraction pattern produced in nitrobenzene and in methyl alcohol by white or Mo $K\alpha$ radiation with fields up to 10 kv/cm, applied parallel to the direction of the x-ray beam as well as perpendicular to it.

35. The Physical Constants of the Ossicles of the Human Ear. OTTO STUHLMAN, JR., *University of North Carolina.*—Data represent mean values from nine complete sets of human ossicles. Experimental data obtained from 26X models made from the average data indicated.

Malleus: mass 22.9 mg. Over-all length 8.5 to 9.00 mm, from end of lateral process to end of manubrium 5.5 to 6.00 mm, angle between head and manubrium 145°, angle between head and lateral process 70°. Center of gravity in neck at corda tympani. Tensor tympani attached just below this point, lever arm to center of gravity 1.0 mm, manubrium lever arm 6.5 mm. Angle between axes of head and manubrium 145°, lateral process and manubrium 70°.

Incus: mass 27.4 mg. Over-all height along axis of long crus 7.0 mm, at right angles from short crus to facet 5.0 mm, height of facet 3.5 mm. Axis of short crus set at 35° to axis of long crus. Angle between long and short crus 85° to 90°. Center of gravity 5.0 mm above lenticular process. Long crus lever arm 5.0 mm from center of lenticular process to center of articulation facet.

Stapes: mass 3.5 mg. Over-all vertical height to foot plate 4.00 mm. Foot plate, length 3.2 mm, width at middle 1.4 mm. Area 3.2 sq. mm. Posterior crus compression member, anterior crus tension member for hinged vibration around posterior end of foot plate. Resultant tension supplied by stapedius muscle. Superior arch Gothic, inferior arch parabolic. Gothic arch tension, parabolic arch compression for hinged vibration around inferior edge of foot plate. Cross sections through crura U-shaped.

Fenestra ovalis to fenestra rotunda areas ratio 3 to 2. Conical depression at center of membrana tympani subtends 135°.

36. The Striking Potential of the High Frequency Discharge in Hydrogen as Conditioned by Frequency. SHERWOOD GITHENS, JR., *University of North Carolina and Wake Forest College.*—Having developed a high frequency oscillator (described in Feb. 1937 R. S. I.) which inherently measures the potential it generates, the striking potential of hydrogen was observed using polished brass electrodes, 3.7 cm in diameter, 1.4 cm apart, in the center of a spherical 5-liter Pyrex flask, over the range of frequency from 5 to 10.5 megacycles, with pressures varying from 0.01 to 130 mm Hg. The curves which will be shown reveal, among other things, the existence of a "critical spark length" for the h.f. discharge, analogous to that observed using spherical brass electrodes in air and an induction coil. At pressures below the critical pressure, which depends upon both the electrode separation and the frequency of the applied e.m.f., the glow emerges from between the electrodes, being maintained, and apparently having been struck, over a distance greater than the electrode separation. A considerably higher potential is required to strike the discharge in this pressure range. The data indicate that the h.f. "critical spark length" decreases progressively with increase in frequency in the ranges examined.

37. Improved Scale-of-Eight Recording Circuits. FOREST E. BRAMMER AND ARTHUR E. RUARK, *University of North Carolina.*—Shepherd and Haxby (R. S. I. Nov. 1936) have described a scale-of-eight counter using tubes between the stages to prevent blowing out the arc by negative impulses on the grids. We have constructed and tested two simplified circuits in which these coupling tubes are eliminated by employing only a fraction of the pulse available at the output of one stage to excite the next. In one of these circuits grid batteries are also eliminated. Uniform pulses are fed to the circuits by a choked multivibrator of the type described by Evans (R. S. I. Dec. 1936).

38. Fluctuations in the Counts of Geiger Counters. RAYMOND L. DRISCOLL AND ARTHUR E. RUARK, *University of North Carolina.*—Before a previous meeting of the Society one of us (R. L. D.) described an apparatus for automatically recording all counts occurring in a Geiger counter and also all intervals between adjoining counts which are longer than a chosen time T. Improvements in the apparatus and results obtained with it will be described.

39. Time Delay Circuits for Operating Wilson Cloud Chambers. CREIGHTON C. JONES, *University of North Carolina.*—Circuits have been developed in which grid glow tubes with time delay inputs perform all the switching operations necessary to operate a Wilson cloud chamber and its accessory mechanisms. The cycle of operations can be initiated either at regular intervals (by a motor and reduction gear) or by coincidences in Geiger counters placed above and below the chamber. Change over from one mode of operation to the other is very simple, being effected by a double pole double throw switch.

40. Theory of the Three Regions of the Ionosphere. E. O. HULBURT, *Naval Research Laboratory.*—The ionization of the upper atmosphere in thermodynamic equilibrium with solar radiation is calculated by the theory of Saha as modified by Pannekoek to refer to the atmosphere of the earth. Assuming that oxygen and nitrogen are atomic for the sun overhead, maximum electron densities of 1.8×10^6 and 1.3×10^5 are found at 230 and 290 km, respectively, in fair agreement with the observed F_1 and F_2 regions, F_1 being due to O and F_2 to N. Assuming that for large solar zenith angles and at night oxygen and nitrogen revert to the molecular state the calculated changes in F_1 and F_2 agree with those observed. A third maximum due to He of 900 electrons cm^{-3} is found at 60 km, which does not agree well with the observed E region. In this respect the theory is incomplete.

41. Cosmic-Ray Shower Production in Large Thicknesses of Lead and Iron. KARL Z. MORGAN, *Lenoire Rhyne College,* AND W. M. NIELSEN, *Duke University.*—A study has been made of twofold coincidences associated with various thicknesses (up to about 600 g/cm^2) of lead and iron above the counters. The usual maxima in the curves are observed at thicknesses of approximately 20 g/cm^2 and 50 g/cm^2 for lead and iron, respectively. If the right-hand side of the Rossi transition curve be interpreted as indicating the absorption of the shower producing radiation the data may be interpreted as indicating a soft and hard component, the absorption coefficients of which are for lead, 0.030 cm^2/g Pb and 0.0006 cm^2/g Pb, respectively. These coefficients are very nearly the same as those observed by Auger, LePrince-Ringuet and Ehrenfest (J. de phys. **7**, 58 (1936)) for the absorption of cosmic rays with three counters in a vertical line. In the case of iron the corresponding absorption coefficients are 0.007 cm^2/g Fe and 0.00044 cm^2/g Fe. Coincidences due to the hard component obtained by extrapolating the estimated soft component into the region of larger thicknesses show a maximum for lead at a thickness of about 225 g/cm^2. For iron there is an indication of a maximum at about 550 g/cm^2.

42. Cosmic-Ray Shower Production in Lead of Various Thicknesses. WALTER M. NIELSEN, *Duke University,* AND KARL Z. MORGAN, *Lenoire Rhyne College.*—Measurements have been made of showers consisting of a minimum of two, three, and four particles produced in various thicknesses of lead up to 240 g/cm^2. The ratios between doubles, triples and quadruples at the larger thicknesses (at about 240 g/cm^2) were not significantly different from the corresponding ratios at smaller thicknesses near the maxima of the Rossi transition curves. The results also indicate that the thickness corresponding to the first maximum in the transition curve occurs at a larger thickness for quadruples than for doubles.

43. The Influence of Temperature on the Reaction of Hydrogen Atoms with the Wall. GERTRUD KORNFELD. (Introduced by Frances G. Wick, *Vassar College.*)—Hydrogen and chlorine combine with each other at 220°C by a chain reaction very similar to the chain mechanism underlying the photochemical reaction at room temperature. In both reactions the atoms of hydrogen and chlorine are the chain carriers, but at 220°C the chains are much more frequently stopped by collisions of the atoms with the wall. The absolute value of the rate of reaction gives the number of these collisions and by calculating approximately the number of collisions occurring with the wall it can be shown that at 220°C nearly every collision of a hydrogen atom with the wall is effective. The reaction at room temperature yields quite different results and this difference is further discussed.

44. An Axial Magnetic Suspension. F. T. HOLMES, *University of Virginia.*—A vertical magnetic needle suspended by the coaxial field of a solenoid has theoretically the properties of infinitesimal friction and restoring torque. Such a needle can be made macroscopically steady by using a variable magnetic field and appropriate damping devices. In the present arrangement two suspending solenoids are used. A steady current flows through one and a variable current through the other. The variation is produced by the partial interruption of a beam of light striking a photo-cell by a vane mounted on the needle. The same photo-cell controls a third coaxial solenoid which supplies, by virtue of a stage of transformer-coupled amplification, damping forces opposing and roughly proportional to the vertical velocity of the needle. A copper disk just below the lower end of the needle provides sufficient transverse damping in some cases. Torsional sensitivity obviously depends on symmetry of all mechanical and magnetic items.

45. An Inverted Ultracentrifuge. J. W. BEAMS AND F. W. LINKE, *University of Virginia.*—An air-driven "vacuum" type of ultracentrifuge is described in which the large rotor or "centrifuge" is mounted upon a flexible shaft (rod or tube) extending upward from the turbine rather than downward as in the original design.[1] The turbine is situated below the vacuum tight chamber which surrounds the centrifuge. The small flexible shaft connecting the turbine and the centrifuge lies in their vertical axis of rotation and passes through an air-tight oil gland which seals the vacuum chamber. The rotating parts are supported on an air cushion below the turbine and are driven by air jets which impinge upon the flutings of the turbine. The motion of the centrifuge is very stable and smooth and the maximum rotational speed is set only by the strength of the centrifuge.

[1] Beams and Pickels, R. S. I. **6**, 299 (1935).

46. A Steam-Driven Ultracentrifuge. L. G. HOXTON AND J. W. BEAMS, *University of Virginia.*—An ultracentrifuge similar in design to one previously described[1] but driven by steam instead of air has been constructed. The rotating parts consist of (1) a steam-driven, air or steam supported turbine, (2) a large rotor (centrifuge) which spins in a vacuum tight chamber, and (3) a small flexible shaft that extends vertically downward from the turbine above the chamber through a vacuum tight oil gland to the centrifuge which it drives and supports. The maximum rotational speed is limited by the bursting strength of the centrifuge. The centrifuge and the vacuum tight chamber, which surrounds it, are maintained at a constant temperature by circulating water around the chamber. The steam is generated electrically.

[1] Beams and Pickels, R. S. I. 6, 299 (1935).

47. The Sensitiveness of Paraffin Crystal Formation to the Physical and Chemical Conditions Under Which They Crystallize.* CHARLES M. HECK, *North Carolina State College of Agriculture and Engineering.*—The progressive modifications of shape and internal structure of paraffin crystals have been photographed and are found to be related to the physical and chemical conditions under which they are formed. The normal pinacoidal diamond-shaped tabular crystals are found to have certain points of their exterior outline more sensitive to changes in these conditions than others. A number of series of progressive variations are shown and classified with respect to the type of physical or chemical variation assumed to be causing the change. Variations in the form of parallel striations across the crystal face are also related to the changes in these conditions during formation.

* To be called for after Paper No. 20.

AUTHOR INDEX TO ABSTRACTS OF NORTH CAROLINA MEETING

Barr, E. S.—No. 16
Beams, J. W.—see Hoxton, J. G.
—— **and F. W. Linke**—No. 45
Bless, A. A.—No. 34
Bramley, Arthur—No. 2
Brammer, E. and Arthur Ruark—No. 37
Braun, Milton L.—No. 10
Brenner, W. L.—No. 24
Brickwedde, F. G.—see Scott, R. B.

Christian, Schuyler M.—No. 14

Derieux, John B.—No. 23
Dicus, A. W.—No. 25
Driscoll, Raymond L. and Arthur E. Ruark—No. 38

Edwards, Charles W.—No. 29
Elliott, D. S.—No. 28

Feenberg, E. and M. Phillips—No. 6
Fountain C. R.—No. 33

Gilhens, Sherwood, Jr.—No. 36
Gordy, Walter—No. 19
—— see Williams, Dudley

Heck, Charles M.—No. 20
—— No. 47
Herod, Newton S.—No. 31
Holmes, F. T.—No. 44
Holton, W. G.—see Koppius, O. T.
Howey, J. H.—No. 27
Hoxton, L. G. and J. W. Beams—No. 46
Hulburt, E. O.—No. 40

Jones, Creighton C.—No. 39

Kennon, W. L.—No. 30
Koppius, O. T. and W. G. Holton—No. 11
Kornfeld, Gertrud—No. 43

Lageman, R. T.—see Slack, F. G.
Linke, F. W.—see Beams, J. W.

Maxwell, Louis R. and V. M. Mosley—No. 9
McAllister, L. E.—No. 32
Morgan, Karl Z.—see Nielsen, Walter M.
—— **and W. M. Nielsen**—No. 41
Mosley, V. M.—see Maxwell, Louis
Mouzon, J. C.—No. 21

Nielsen, Walter M. and Karl Z. Morgan—No. 42
Nielsen, W. M.—see Morgan, Karl Z.

Parker, Herman—No. 3
Peebles, J. B.—see Sledd, Marvin
Phillips, M.—see Feenberg, E.
Plyler, E. K.—No. 18
Pollard, W. G.—No. 1

Rabi, I. I.—No. 7
Razor, C. T.—No. 12
Ruark, Arthur—see Brammer, E.
—— see Driscoll, Raymond L.

Scott, R. B. and F. G. Brickwedde—No. 8
Shearin, Paul E.—No. 26
Slack, F. G., R. T. Lageman and Newton Underwood—No. 15
Sledd, Marvin and J. B. Peebles—No. 13
Smith, Newland F.—No. 22
Stuhlman, Otto, Jr.—No. 35

Underwood, Newton—see Slack, F. G.

Way, Katharine and John A. Wheeler—No. 4
Wheeler, John A.—No. 5
—— see Way, Katharine
Williams, Dudley and Walter Gordy—No. 17